CLASSIFICATION CHANGE
To UNCLASSIFIED
By authority of GDS-GP-4
Changed by L. Shirley Date 11-75
Classified Master Control Station, NASA
Scientific and Technical Information Facility

~~CONFIDENTIAL~~

NASA-MSC-G-R-67-1
Supplemental Report 2

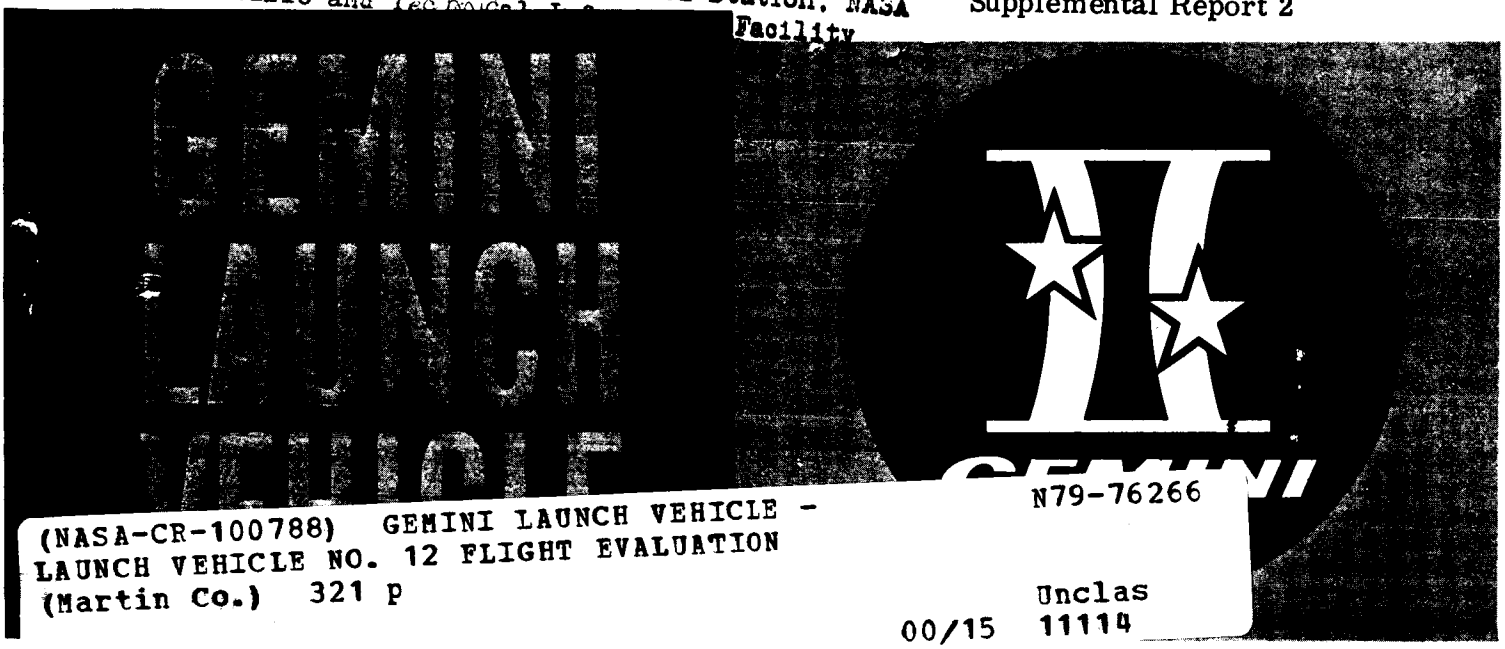

(NASA-CR-100788) GEMINI LAUNCH VEHICLE - LAUNCH VEHICLE NO. 12 FLIGHT EVALUATION (Martin Co.) 321 p

N79-76266

Unclas
00/15 11114

FF No. 602(D)
321 (PAGES) None (CODE)
CR-100788 (NASA CR OR TMX OR AD NUMBER) (CATEGORY)
[redacted]

Issued as: Supplemental Report 2
To: Gemini Program Mission Report
Gemini XII
MSC-G-R-67-1
By: Gemini XII Mission Evaluation Team
National Aeronautics and Space Administration
Manned Spacecraft Center
Houston, Texas

LAUNCH VEHICLE NO. 12 FLIGHT EVALUATION (U)

Engineering Report 13227-12

MARTIN COMPANY

UNDER CONTRACT NUMBER
AF 04(695)-394
PRIORITY DX-A2

SPACE SYSTEMS DIVISION
AIR FORCE SYSTEMS COMMAND
UNITED STATES AIR FORCE . . . Los Angeles, California

This document is subject to special export controls and each transmittal to foreign governments or foreign nationals may be made only with prior approval of Headquarters Space Systems Division (AFSC), Air Force Unit Post Office, Los Angeles, California (90045), Attn: Gemini System Program Office (SSVL)

December 1966

~~CONFIDENTIAL~~

[redacted]

This document contains information affecting the National Defense of the United States within the meaning of the Espionage Laws, Title 18, U.S.C., Sections 793 and 794, the transmission or revelation of which in any manner to an unauthorized person is prohibited by law.

Group 3
Downgraded at 12 year intervals; declassified after 12 years. DOD DIR 5200.10.

Copy No. _____

[redacted]

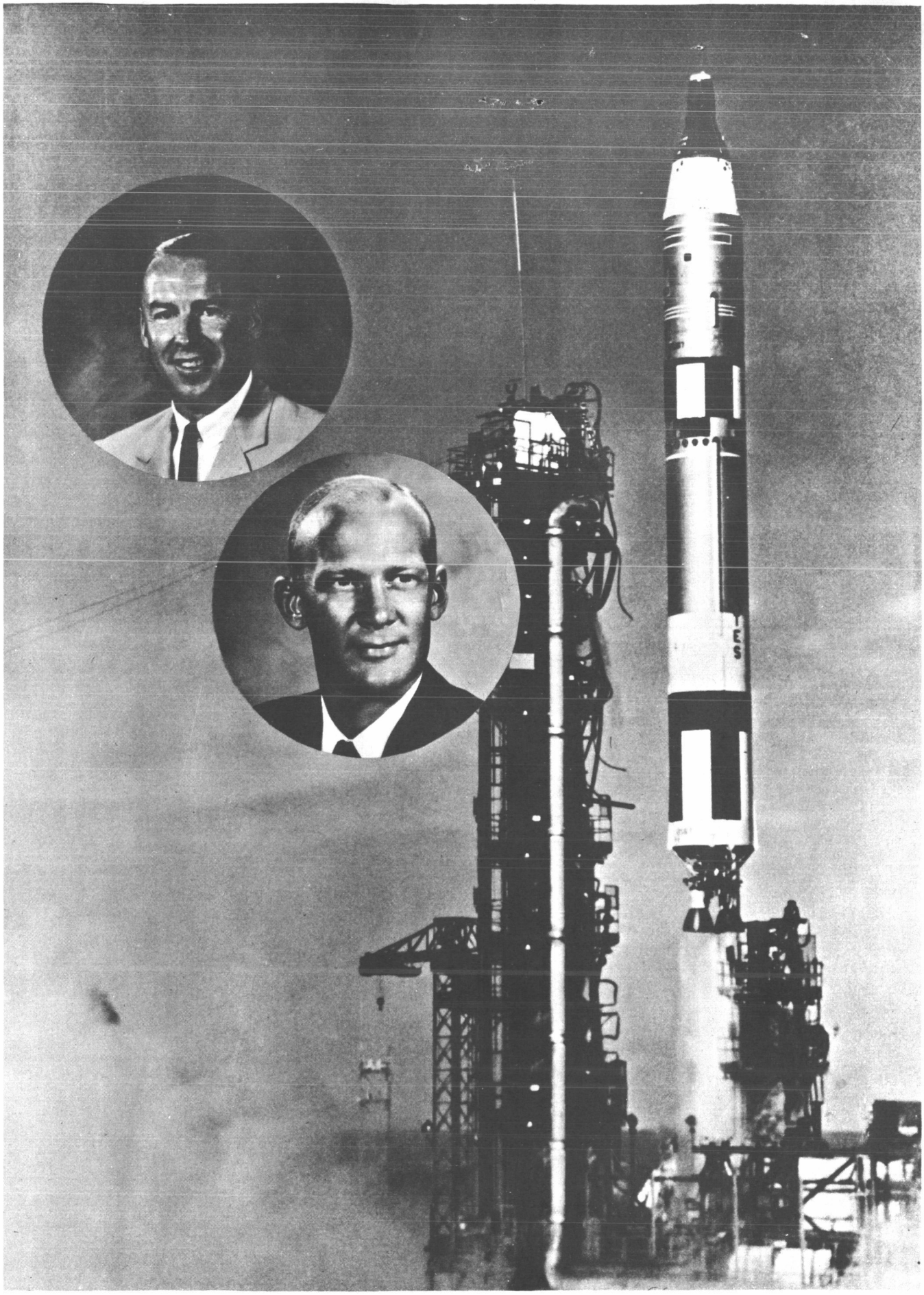

C 67-8749

ER 13227-12

[redacted]

December 1966
NASA-MSC-G-R-67-1
Supplemental Report 2

Issued as:
Supplemental Report 2
To:
Gemini Program Mission
Report Gemini XII
By:
Gemini XII Mission
Evaluation Team
National Aeronautics
and Space Administration
Manned Spacecraft Center
Houston, Texas

LAUNCH VEHICLE NO.12
FLIGHT
EVALUATION (U)

NOTICE - THIS DOCUMENT CONTAINS INFORMATION AFFECTING THE NATIONAL DEFENSE OF THE UNITED STATES WITHIN THE MEANING OF THE ESPIONAGE LAWS, TITLE 18, U.S.C., SECTION 793 AND 794, TRANSMISSION OR REVELATION OF ITS CONTENTS IN ANY MANNER TO AN UNAUTHORIZED PERSON IS PROHIBITED BY LAW.

Approved by

E J Walsh
E. J. Walsh
Assistant Technical Director

J. C. Curlander
J. C. Curlander
Technical Director

This document is subject to special export controls and each transmittal to foreign governments or foreign nationals may be made only with prior approval of Headquarters Space Systems Division (AFSC), Air Force Unit Post Office, Los Angeles, California (90045), Attn: Gemini System Program Office (SSVL)

Prepared by

MARTIN COMPANY, BALTIMORE DIVISION
Baltimore, Maryland 21203

Under CONTRACT AF 04(695)-394
PRIORITY DX-A2

For

SPACE SYSTEMS DIVISION
AIR FORCE SYSTEMS COMMAND

UNITED STATES AIR FORCE
Los Angeles, California

[redacted]

GROUP 4
Downgraded at 3 year
intervals; declassified
after 12 years

UNCLASSIFIED

FOREWORD

This report has been prepared by the Gemini Launch Vehicle Program Test Evaluation Section of the Martin Company, Baltimore Division. It is submitted to the Space Systems Division, Air Force Systems Command, in compliance with Contract AF04(695)-394.

UNCLASSIFIED

CONTENTS

		Page
	Foreword	ii
	Summary	vii
I.	Introduction	I-1
II.	System Performance	II-1
	A. Trajectory Analysis	II-1
	B. Payload Capability	II-39
	C. Staging	II-41
	D. Weight Statement	II-41
III.	Propulsion System	III-1
	A. Engine Subsystem	III-1
	B. Propellant Subsystem	III-17
	C. Pressurization Subsystem	III-59
IV.	Flight Control System	IV-1
	A. Stage I Flight	IV-1
	B. Stage II Flight	IV-8
	C. Post-SECO Flight	IV-9
V.	Hydraulic System	V-1
	A. Stage I	V-1
	B. Stage II	V-5
VI.	Guidance Systems	VI-1
	A. Radio Guidance System Performance	VI-1
	B. Spacecraft Inertial Guidance System Ascent Performance	VI-6

CONTENTS (continued)

		Page
VII.	Electrical System Analysis	VII-1
	A. Configuration	VII-1
	B. Countdown and Flight Performance	VII-1
VIII.	Instrumentation System	VIII-1
	A. Airborne Instrumentation	VIII-1
	B. Landline Instrumentation	VIII-1
IX.	Range Safety and Ordnance	IX-1
	A. Command Control Receivers	IX-1
	B. MISTRAM	IX-1
	C. Ordnance	IX-3
X.	Malfunction Detection System	X-1
	A. Configuration	X-1
	B. System Performance	X-1
XI.	Crew Safety	XI-1
	A. Prelaunch Winds Operations	XI-1
	B. Slow Malfunction Monitoring	XI-5
	C. Staging Anomaly	XI-11
XII.	Airframe System	XII-1
	A. Structural Loads	XII-1
	B. POGO	XII-10
XIII.	AGE and Facilities	XIII-1
	A. Mechanical AGE	XIII-1

CONTENTS (continued)

		Page
	B. Master Operations Control Set	XIII-1
	C. Facilities	XIII-2
XIV.	Reliability	XIV-1
XV.	Range Data	XV-1
	A. Launch Data Distribution	XV-1
	B. Film Coverage	XV-6
XVI.	Prelaunch and Countdown Operations	XVI-1
	A. Prelaunch	XVI-1
	B. Launch Countdown Summary	XVI-1
XVII.	Configuration Summary	XVII-1
	A. Launch Vehicle Systems Description	XVII-1
	B. Major Components	XVII-2
XVIII.	References	XVIII-1
	Appendix A	A-1

SUMMARY

On 11 November 1966, Gemini-Titan No. 12 (GT-12) was launched successfully and on schedule from Complex 19, Cape Kennedy, Florida. Launch vehicle/spacecraft separation was completed 366.7 seconds after liftoff. Spacecraft re-entry was accomplished after completion of 63 orbits.

The GT-12 240-minute countdown was picked up at 1143 EST on 11 November and progressed smoothly, with astronaut ingress at approximately T-115 minutes. The Atlas-Agena was successfully launched at T-95 minutes (1407 EST). The countdown continued normally, and the programmed hold was initiated automatically at T-3 minutes for 3.5 minutes to adjust for proper liftoff time. The countdown resumed at T-3 minutes, and liftoff occurred on schedule at 1546 EST. The spacecraft was inserted into an elliptical orbit with a perigee of 87.3 nautical miles and an apogee of 151.5 nautical miles. All test objectives for the launch and flight were achieved.

Stages I and II engines operated satisfactorily throughout powered flight. Stage I burning time was 158 seconds, with shutdown initiated by fuel exhaustion. Stage II engine operation was terminated by a guidance command after 188.8 seconds of burning.

The flight control system (FCS) maintained satisfactory vehicle stability during Stages I and II flight. The primary FCS was in command throughout the flight. Vehicle rates during Stage I flight did not exceed 1.7 deg/sec, and the maximum attitude error was 1.26 degrees. The maximum rate and attitude error that occurred during staging did not exceed 4.3 deg/sec and 1.3 degrees, respectively.

Performance of the radio guidance system (RGS) was satisfactory. Pitch and yaw steering signals and SECO discrete commands were properly executed.

IGS pitch, yaw and roll performance during the entire flight appeared normal. The dispersions between IGS and primary system attitude errors remained within acceptable limits during powered flight.

The hydraulic system operated satisfactorily during the 240-minute countdown and both stages of flight. There were no significant pressure perturbations at liftoff or during flight.

The electrical system functioned as designed throughout the launch countdown and flight. Power transfer to vehicle batteries was smooth.

All channels of the PCM instrumentation system except Meas 0514 functioned properly throughout the flight. The landline instrumentation system also functioned satisfactorily prior to and up to liftoff. All

airborne instrumentation hold functions monitored in the blockhouse remained within specification throughout the countdown.

The ordnance system umbilical dropweight release, propulsion system prevalves, explosive launch nuts and stage separation nuts operated satisfactorily.

The performances of the command control receivers and the MISTRAM transponder were satisfactory.

Malfunction detection system (MDS) performance during preflight checkout and flight was satisfactory. There were no switchover commands during the flight.

The flight environment encountered by GT-12 was within design requirements. Flight loads were well within the structural capabilities of the launch vehicle. The most critical loading (which occurred at pre-bECO, aft of Station 320) reached 87.3% of design limit load in compression.

The longitudinal oscillation (POGO) on GT-12 reached a maximum value at spacecraft/launch vehicle interface of 0.14 g zero-to-peak at a frequency of 11.2 cps at LO + 126.1 seconds.

A review of film from ground tracking and ALOTS indicates that the GLV-12 staging event appeared similar to that noted on GLV-10. After stage separation a large reddish cloud appeared at the top of the Stage I oxidizer tank, followed by a white cloud at the Stage I fuel tank. This staging event posed no hazards to crew safety and did not jeopardize mission success.

Crew safety monitoring, which was conducted at NASA-MSC, was active during prelaunch and the launch. All guidance monitor parameters were nominal, and no corrective action was required during the flight.

All electrical umbilicals disconnected in the planned sequence and within 0.83 second. Engine blast and heat damage to the launch stand was minor.

The simulated flight test (SFT) was successfully performed on 2 November 1966. The precountdown tests, for the launch scheduled for 9 November 1966, were not started due to a secondary flight control system 26-volt 800-cycle power failure. The launch was subsequently rescheduled for 10 November 1966. After replacement packages for the autopilot were installed and successfully tested, a secondary Stage II rate gyro SMRD no-go was observed for approximately 45 seconds. The secondary autopilot was replaced, and the launch was rescheduled for 11 November 1966. The precountdown tests were successfully completed at 1530 EST on 10 November.

Propellant loading to specified load and temperature limits was completed within a span of 3 hours 20 minutes.

GLV-12 Test Objectives and Results

Objective		Results	
Primary			
P-1	Demonstrate satisfactory boost by the Gemini launch vehicle system of a manned Gemini spacecraft into the prescribed orbital insertion conditions.	P-1	Orbit insertion was within the predicted tolerances for V, h and γ.
P-2	Demonstrate performance of GLV subsystems during powered flight, relative to mission success and crew safety.	P-2	All systems performed satisfactorily throughout flight. The POGO oscillation was 0.14 g zero-to-peak at a frequency of 11.2 cps at spacecraft-launch vehicle interface.
Secondary			
S-1	Demonstrate ability to load propellants to weight and temperature limits imposed by payload and vehicle requirements.	S-1	Tanks were loaded within the required tolerances of weight and temperature.
S-2	Demonstrate effectiveness of combined GLV and GAATV countdown and launch operations, including necessary ground/range support systems to achieve prescribed rendezvous mission launch requirements.	S-2	Atlas/Agena was successfully launched at T-95 minutes, followed by the GT-12 liftoff on schedule. A 3.5 minute hold to adjust for proper liftoff time was required.

I. INTRODUCTION

This report presents an engineering evaluation of Gemini Launch Vehicle No. 12 (GLV-12) systems performance during the countdown, launch and powered flight phase of the Gemini 12 mission.

The GT-12 vehicle was launched on schedule from Complex 19, Cape Kennedy, Florida at 1546 hours EST on 11 November 1966.

Gemini 12 was the twelfth mission and the tenth manned flight of the program, with astronauts James A. Lovell, Jr., and Edwin E. Aldrin, Jr. aboard the spacecraft. The mission, which included a rendezvous and docking with the Agena Target Vehicle (ATV), was completed on 15 November 1966.

The GT-12 vehicle was comprised of the two-stage GLV-12 (similar to GLV-11) and the Gemini 12 spacecraft. The spacecraft was injected into an elliptical orbit having a perigee of 87.3 nautical miles and an apogee of 151.5 nautical miles.

Significant events and tests for GLV-12 at ETR are summarized in Fig. I-1.

UNCLASSIFIED

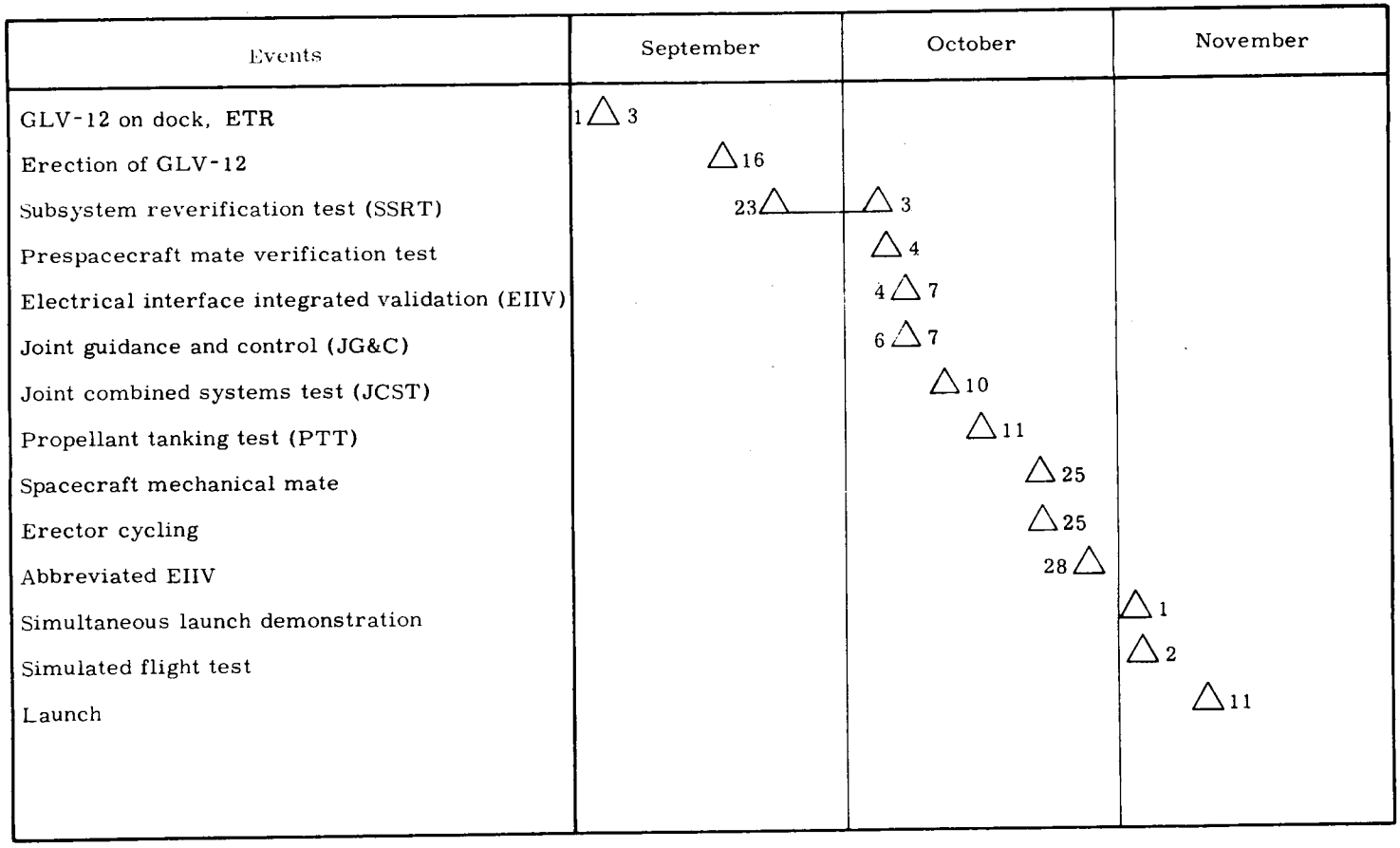

Fig. I-1. Significant Events and Tests for GLV-11

UNCLASSIFIED

II. SYSTEM PERFORMANCE

A. TRAJECTORY ANALYSIS

1. Orbit Insertion

Gemini Launch Vehicle No. 12 (GLV-12) performed as predicted and inserted the Gemini 12 spacecraft into earth orbit well within the allowable tolerance limits to permit rendezvous with the Agena Target Vehicle.

GT-12 was steered in the lateral plane during Stage II flight to a set of ephemeris data referenced to the time of insertion (or targeting). The values of these targeting parameters are given in Table II-1. The targeted and observed inclination angles were both 28.857 degrees. The targeted wedge angle at liftoff was -0.16 degree. The observed residual wedge angle at insertion was 0.

TABLE II-1

Agena Target Vehicle Ephemeris Data

GMTLO	74,793.308 sec
T_R*	162,245.57 sec
i	28.8569 deg
Ω	-0.18891×10^{-5} rad/sec
V_F	25,728.7 fps

*Relative to Complex 19.

A comparison of the predicted and observed insertion conditions is given in Table II-2. In this table and in all succeeding references to a predicted (nominal) trajectory, the data were obtained from the GLV-12 45-day prelaunch report (Ref. 15), updated to reflect the actual spacecraft weight (8294 pounds), guidance constants, T-1 hour wind and atmospheric data, and the -0.49% pitch programmer bias. The predicted nominal trajectory includes g sensitive TARS roll gyro drift estimated for GLV-12 based on the test data pertinent to the TARS package used for this flight. The value used in the GLV-12 predicted trajectory is 6.335 deg/hr/g (counterclockwise roll) compensated at 2.2 g, i.e., GLV will roll clockwise above 2.2 g axial acceleration.

The predicted trajectory also reflects Stage I engine thrust misalignment of 0.1091 degree nose left yaw. The observed trajectory parameters are those derived by the Martin Company from the final GE MOD III-A 2-pps data. These data have been smoothed and corrected for both refraction errors and systematic biases by the General Electric Corporation before submittal to the Martin Company.

TABLE II-2

Comparison of Insertion Conditions at SECO + 20 Seconds

	Predicted Nominal	GE Mod III-A	Observed Minus Planned	Preliminary Tolerance
Altitude (naut mi)	86.75	86.96	0.21	± 0.583
Inertial velocity (fps)	25,728.1	25,722	-6.1	± 39.32
Inertial flight path angle (deg)	0.0079	-0.08	-0.0879	± 0.2583

2. Derivation of Trajectory Uncertainties

The expected maximum vehicle dispersions and RGS dispersions at BECO and at SECO + 20 seconds were obtained from Refs. 16 and 17, respectively. A root sum square (RSS) of these dispersions is termed the preliminary tolerance. After determination of the preliminary tolerance, the total tolerance may be computed by the arithmetic addition of the preliminary tolerance to the 3-sigma data error of the instrumentation source being considered. Thus,

$$\text{Preliminary tolerance} = \sqrt{(\text{vehicle dispersions})^2 + (\text{RGS dispersions})^2}$$

Total tolerance = preliminary tolerance + 3-sigma data error.

The resulting preliminary tolerance is shown in Table II-3. Because the actual insertion conditions were within the preliminary tolerance and the data error estimates are uncertain at this time, they have been excluded from this report.

3. Flight Plan

The primary objective for GLV-12 was to place the Gemini 12 spacecraft into an elliptical earth orbit with an 87-nautical mile perigee* and 151-nautical mile apogee.* Having achieved orbital insertion at 25,728 fps,** the spacecraft then separates from Stage II (adding 20 fps to spacecraft velocity in the process) and coasts to the desired apogee. The following flight plan was employed to attain the desired conditions.

*Relative to Complex 19.
**Does not include the separation velocity imparted by the spacecraft.

TABLE II-3

Predicted Dispersions at BECO and SECO + 20 Seconds

Performance Parameter	Predicted Nominal Value* (Ref. 15)	Predicted Dispersions		
		Vehicle Dispersion (Ref. 16)	RGS Dispersion (Ref. 17)	RSS of RGS and Vehicle Dispersions
BECO				
Time from liftoff (sec)	153.361	±4.31	N/A	±4.31
Geocentric radius (ft)	21,111,607	±12,199	↑	±12,199
Inertial velocity (fps)	9,813.3	±182		±182
Crossrange (ft)	626.14	±14,671		±14,671
Crossrange velocity (fps)	25.836	±374		±374
Ground range (naut mi)	49.384	±3.16	↓	±3.16
Inertial flight path angle (deg)	18.747	±2.45	N/A	±2.45
SECO + 20 seconds				
Time from liftoff (sec)	360.814	±7.438	±0.077	±7.4384
Geocentric radius (ft)	21,438,755	±1,935	±3,141	±3,689.18
Inertial velocity (fps)	25,728.1	±17.3	±35.31	±39.32
Crossrange (ft)	96,504	±67,208	±518.5	±67,210
Crossrange velocity (fps)	1,179.3	±35.00	±9.91	±36.37
Ground range (naut mi)	544.90	±15.18	±0.142	±15.181
Inertial flight path angle (deg)	0.0079	±0.0721	±0.2480	±0.2583

N/A: Not applicable.

*Updated to include items stated in Section II-1.

A vertical rise is planned for the first 23.04 seconds following lift-off, during which time a programmed roll rate of 1.25 deg/sec is initiated to roll the vehicle from a pad orientation of 84.933 degrees to the flight azimuth of 100.6 degrees.

At this time, an open-loop pitch program, which terminates at 162.56 seconds, is begun (via a three-step rate command). The nominal commanded pitch rates and their times of application are shown in Table II-4.

Guidance commands from the radio guidance system (RGS) are initiated at LO + 168.35 seconds and continue until two seconds prior to SECO; however, velocity cutoff computations continue to SECO. Between SECO and SECO + 20 seconds, the engine shutdown impulse continues to add velocity to the vehicle (approximately 82 fps), and the spacecraft is separated from the sustainer after SECO + 20 seconds.

TABLE II-4

Planned GLV Pitch Program

Program	Rate (deg/sec)	Time from Liftoff (sec)
Step 1	-0.709	23.04 to 88.32
Step 2	-0.516	88.32 to 119.04
Step 3	-0.235	119.04 to 162.56

A comparison of the planned and actual sequences of events is contained in Table II-5, and a profile of the GT-12 flight superimposed on the range planning map appears in Fig. II-1.

4. Trajectory Results

Analysis of the range data and Mod III-A radar data indicates that the performance of GLV-12 was normal and the vehicle flew close to the prescribed ascent trajectory throughout Stages I and II.

Insertion velocity adjust routine (IVAR) imparted a total ΔV of 28 fps to the spacecraft.

Table II-6 shows a reconstruction of the BECO condition by considering the actual engine data, weather conditions, propellant loading, engine misalignments, wind and guidance errors. This table is comprised of those items which can be measured and those which can only be estimated due to lack of suitable instrumentation. The primary factors contributing to the pitch and yaw plane trajectory dispersions at BECO are listed and the effect of each is summarized.

TABLE II-5

GT-12 Flight Events Summary

Measurement	Event	GMT (hr-min-sec)	Time from Liftoff (sec)	
			Actual	Planned
0800/0801	Power transfer	2045:04.15	-89.27	-89
FC B-10	MOCS T-0	2046:30.136	-3.283	-3.36
2104	$87FS_1$ (T-0)	:30.190	-3.229	-3.30
2339	Stage I S/A-1 MDTCPS make	:31.105	-2.314	-2.20
2340	Stage I S/A-2 MDTCPS make	:31.105	-2.314	-2.20
0169	Launch nuts	:33.217	-0.202	-0.20
4421	First motion	:33.308	-0.111	-0.10
4422	Shutdown lockout (backup)	:33.327	-0.092	-0.10
4423	Liftoff	2046:33.419	0	0
0734	Start roll program	:41.41	7.99	8.00
0734	End roll program	:53.89	20.47	20.48
0732	Start pitch program No. 1	:56.47	23.05	23.04
0732	Stop pitch program No. 1	2048:01.68	88.26	88.32
0732	Start pitch program No. 2	:01.68	88.26	88.32
0728	FCS gain change No. 1	:23.10	109.68	110.00
0732	Stop pitch program No. 2	:32.38	118.96	119.04
0732	Start pitch program No. 3	:32.38	118.96	119.04
0735	Staging enable (TARS discrete)	:57.96	144.54	144.64
0741	IPS staging arm timer	:58.40	144.98	145.00
0356	Stage I S/A-1 MDTCPS break	2049:08.113	154.694	153.30
0357	Stage I S/A-2 MDTCPS break	:08.134	154.715	153.30
0032	$87FS_2/91FS_1$ (BECO)	:08.168	154.749	153.36
0502	Start P_{c_3} rise	:08.833	155.414	154.01
0368/369	Stage separation	:08.87	155.45	154.09
0855	Stage II MDFJPS make	:08.899	155.480	154.29
0732	Stop pitch program No. 3	:15.83	162.41	162.56
0740	RGS enable	:15.82	162.40	162.56
0755/0756	First guidance command	:21.43	168.01	168.35
0739	Stage II shutdown enable	2051:50.52	317.10	317.44
0777	Guidance SECO	2052:16.938	343.519	340.88
0519	$91FS_2$	:16.958	343.539	340.90
0522	Shutdown valve relay	:16.95	343.53	340.92
0521	Shutdown squib	:17.01	343.59	340.92
0799	ASCO	:17.01	343.59	340.93
0855	Stage II MDFJPS break	:17.099	343.680	341.20
0699	Spacecraft separation	:40.143	366.724	360.90

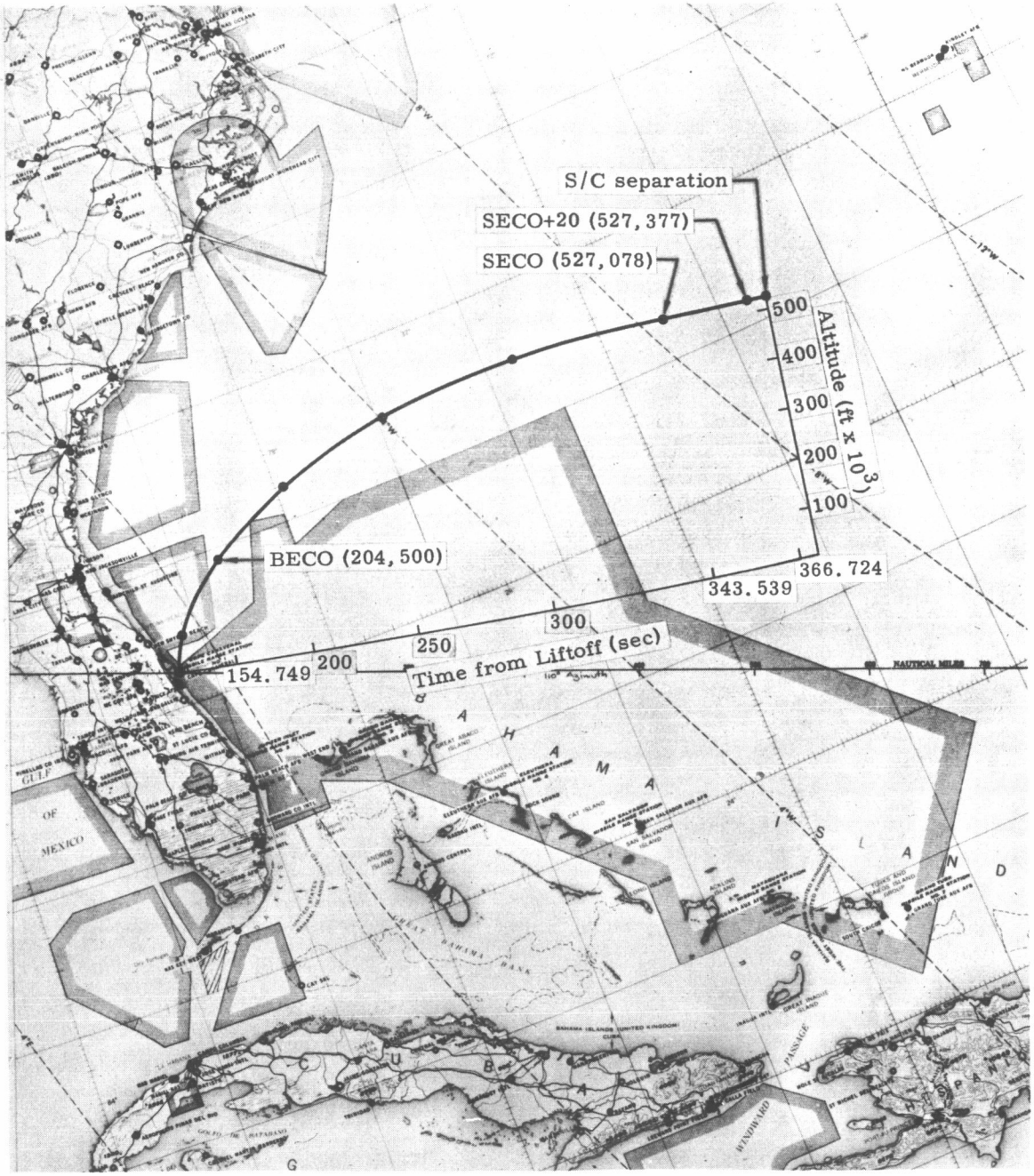

Fig. II-1. GT-12 Boost Flight Path Profile

TABLE II-6
GTA-12 BECO Conditions

		Δ Time (sec)	Δ Altitude (ft)	Δ Velocity (fps)	$\Delta\gamma$ (deg)	ΔY_F (ft)	$\Delta\dot{Y}_F$ (fps)
Measured Parameters							
Thrust Stage I	(-0.47%)	+0.675	-1340	-0.57	-0.229	-72.26	+1.96
Outage (mean 882 lb)	(133 lb)	+0.239	+765	+40.6	-0.023	-2.51	-0.12
T-1 hr wind and weather		--	-1083	+23	-0.09	-240 (RT)	+4.89 (left)
Propellant loading	(+346 lb)	+0.205	-108	+9.1	-0.057	--	--
Trend Indications							
TARS pitch programmer	(-0.12%)	--	+297	-2.8	-0.06	+0.40	+0.02
TARS roll programmer	(+0.544%)	--	--	--	--	-70.3	-1.9
TARS pitch gyro drift	(+4.25 deg/hr)	--	+558	-5.66	+0.122	+6.7	+0.142
TARS yaw gyro drift	(0 deg/hr)	--	--	--	--	--	--
TARS roll gyro drift	(+7.15 deg/hr/g)	--	-2	-0.4	--	+773	+23.1
Engine misalignment in pitch	(-0.10 deg)	--	+1358	-14.27	+0.35	+40.49	+0.73
Engine misalignment in yaw	(-0.149 deg)	--	+24	+0.80	+0.002	-2751	-81.2
Engine misalignment in roll	(0.01 deg)	--	+1	+0.10	--	-251.7	-6.68
Specific impulse	(0.38 sec)	+0.208	+315	+16.06	-0.042	+314.8	-0.08
Σ Apparent increments		+1.327	+787	+65.96	-0.027	-2252.38	-59.1
Measured increments		+1.388	+1830	+99.7	-0.170	-1644 (RT)	-42.66 (RT)

The differences shown in the apparent and measured increments of Table II-6 are well within the allowable tolerance limits presented in Table II-3.

Table II-7 presents the trajectory parameters computed from the smoothed GE Mod III-A, MISTRAM I and II and BET data and the MISTRAM I quick-look data. At BECO and SECO + 20 seconds all of the flight data yielded comparable results.

The predicted trajectory used a launch azimuth of 100.6 degrees, whereas the actual flight azimuth was 100.5 degrees. The difference was due to the fact that the angle roundoff to the nearest tenth of a degree was assumed (for predicted trajectory) on the requested target value of 100.55 degrees. On the flight, the roundoff was not applied until the commanded roll was computed on the basis of the pad alignment. This resulted in a 0.1-degree excess counterclockwise roll and, hence, a 100.6-degree launch azimuth for the predicted trajectory.

The effect on the predicted trajectory due to the 0.1-degree higher launch azimuth is a yaw displacement of 2600 feet to the right in the AFMTC coordinate system at insertion.

All radar measurements were reduced at an AFMTC coordinate system with the + X axis oriented to a 100.6-degree azimuth.

The actual, as well as the predicted, nominal trajectory is presented in graphical form in Figs. II-2 through II-24. On these graphs, the nominal trajectory is that documented in Ref. 15 updated to reflect the items stated in Section II-1. The observed flight data were obtained from the Mod III-A 2-pps data, smoothed and corrected for refraction errors and systematic biases.

A list of the primary tracking sources with the trajectory time interval covered by each is contained in Table II-8.

5. Geodetic and Weather Parameters

Significant geodetic and surface weather parameters for GT-12 flight are shown in Table II-9. T-1 hour atmospheric temperature and pressure variation with altitude is depicted in Fig. II-25. Wind speed and direction variation with altitude is depicted in Fig. II-26. Wind speed was relatively light from liftoff to 20,000 feet, with the direction generally a tailwind (as seen from the launch vehicle) remaining steady to an altitude of 60,000 feet. Maximum wind speed (53 knots) was reached at 46,000 feet, diminishing with increasing altitude to near zero at 62,000 feet. Wind speeds were generally below 10 knots at all altitudes above 62,000 feet.

TABLE II-7

Comparison of GT-12 Predicted and Observed Performance at BECO and at SECO + 20 Seconds

	** Predicted Nominal Trajectory (Ref. 15*)	Tracking Facility			
		GE Mod III-A (2 PPS)	MISTRAM I	MISTRAM I and II	BET
BECO					
Time from LO (sec)	153.361	154.749	154.749	154.749	154.749
Inertial velocity (fps)	9813.3	9890	9890	9885	9890
Altitude (ft)	201,587	204,500	206,070	204,471	204,477
Inertial flight path angle (deg)	18.747	18.67	18.60	18.67	18.67
Ground range (naut mi)	49.384	49.238	51.10	50.53	50.53
Geocentric radius (ft)	21,111,607	21,114,500	21,115,865	21,114,501	21,114,505
Downrange position, X_F (ft)	303,155	310,247	313,751	310,241	310,240
Crossrange position, Y_F (ft)	626.14	-777.66	-804.3	-782	-789.8
Vertical position, Z_F (ft)	199,381	202,164	203,474	202,162	202,169
Downrange velocity, $\dot{X}_F$ (fps)	8002.3	8070.1	8078	8076	8068.4
Crossrange velocity, $\dot{Y}_F$ (fps)	25.836	-21.71	-22.1	-21.9	-21.77
Vertical velocity, $\dot{Z}_F$ (fps)	3035.3	3038.95	3029	3041	3038.6
SECO + 20 seconds					
Time from LO (sec)	360.814	363.539	363.539	363.539	363.539
Inertial velocity (fps)	25,728.1	25,722	25,718	25,710	25,710
Altitude (ft)	527,102	528,377	527,014	526,703	526,704
Inertial flight path angle (deg)	0.00793	-0.08	-0.05	0.025	0.025
Ground range (naut mi)	544.9	550.4	550.0	550.48	550.49
Geocentric radius (ft)	21,438,755	21,440,063	21,438,701	21,438,389	21,438,404
Downrange position, X_F (ft)	3,380,315	3,414,595	3,414,740	3,414,712	3,414,712
Crossrange position, Y_F (ft)	96,504	92,411	92,428	92,516	92,515
Vertical position, Z_F (ft)	259,006	254,819	253,416	253,106	253,105
Downrange velocity, $\dot{X}_F$ (fps)	24,026	24,011	24,011	24,004	24,004
Crossrange velocity, $\dot{Y}_F$ (fps)	1179.3	1172.3	1176.0	1173	1173
Vertical velocity, $\dot{Z}_F$ (fps)	-3847.4	-3941.2	-3972	-3876	-3876
Yaw steering velocity, V_Y (fps)	4.732	8.35	5.181	6.68	6.69
Biased yaw steering velocity, V_Y (fps)	-5.268	--	--	--	--

*Updated to include items stated in Section II-1
**Launch azimuth 100.6 deg used in predicted trajectory.

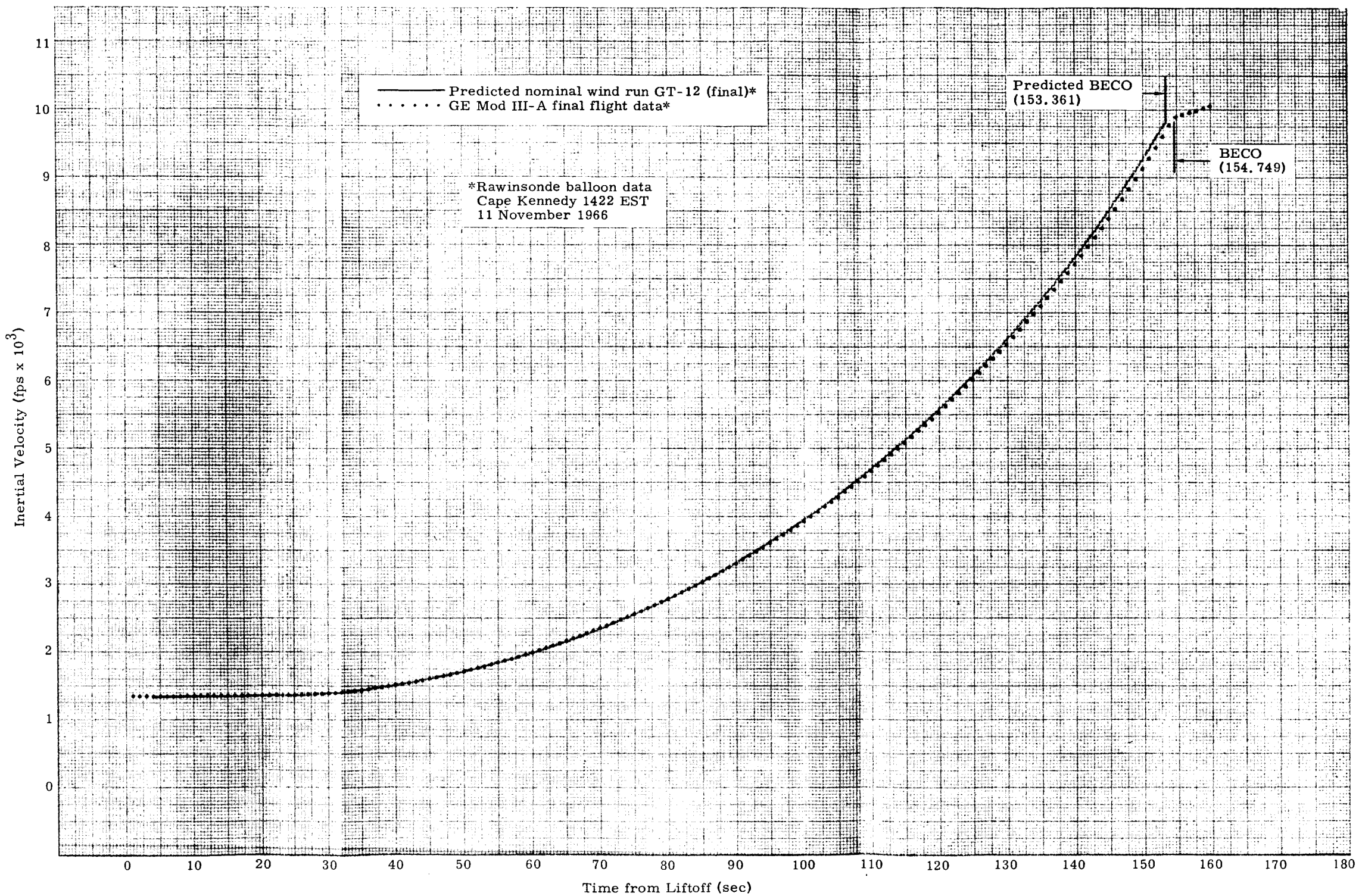

Fig. II-2. Inertial Velocity Versus Time: Stage I Flight

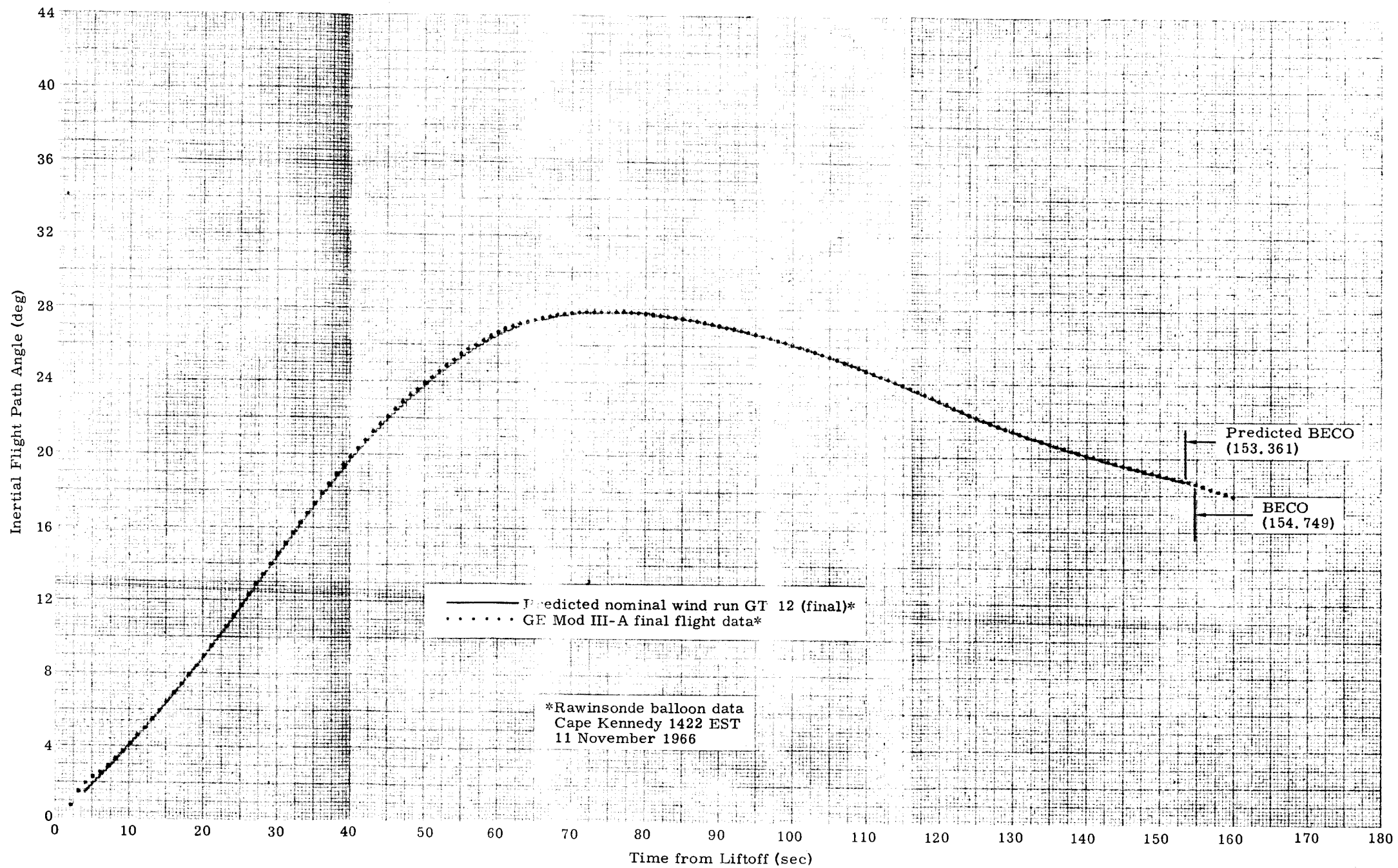

Fig. II-3. Inertial Flight Path Angle Versus Time: Stage I Flight

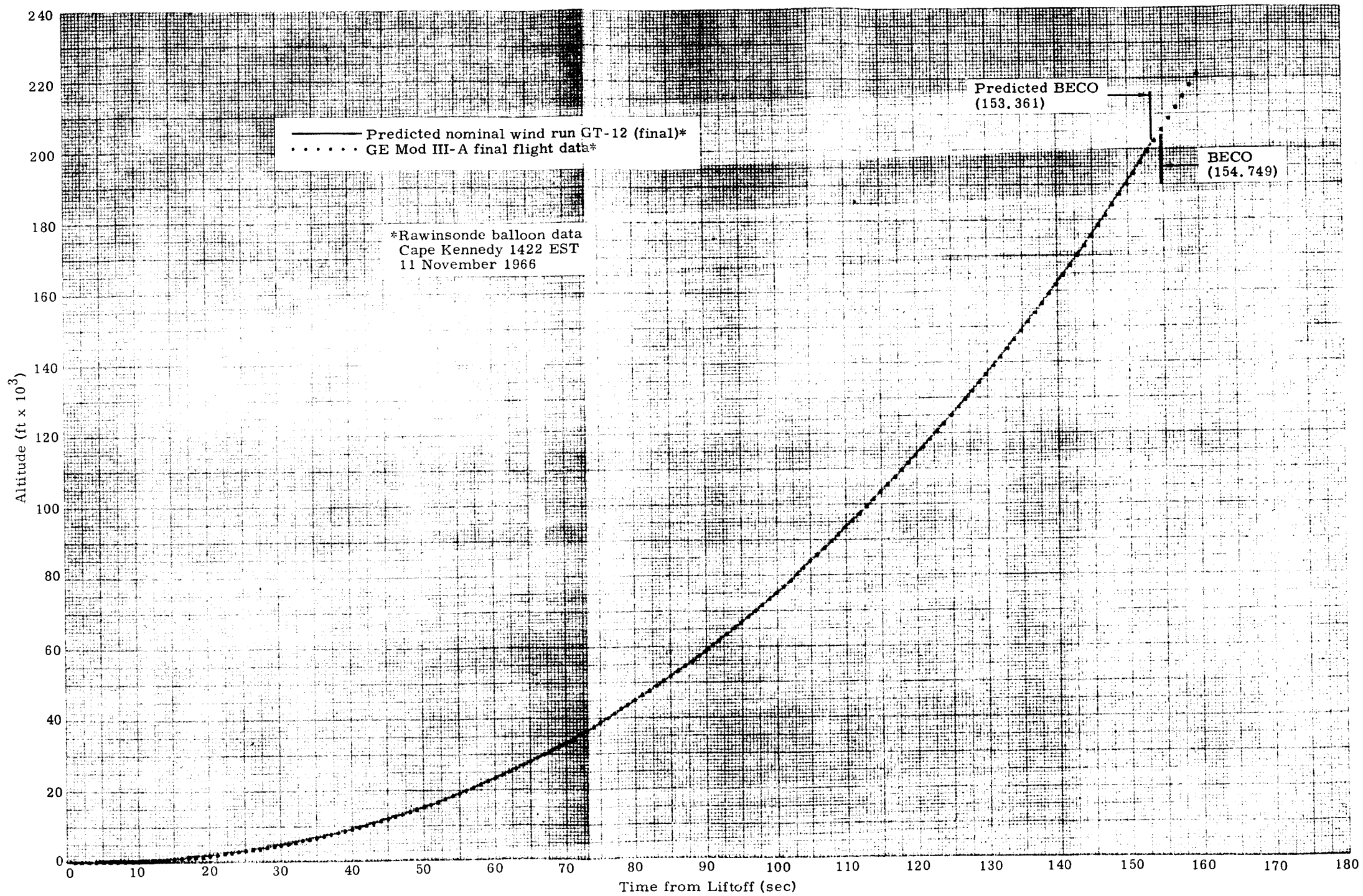

Fig. II-4. Altitude (h) Versus Time: Stage I Flight

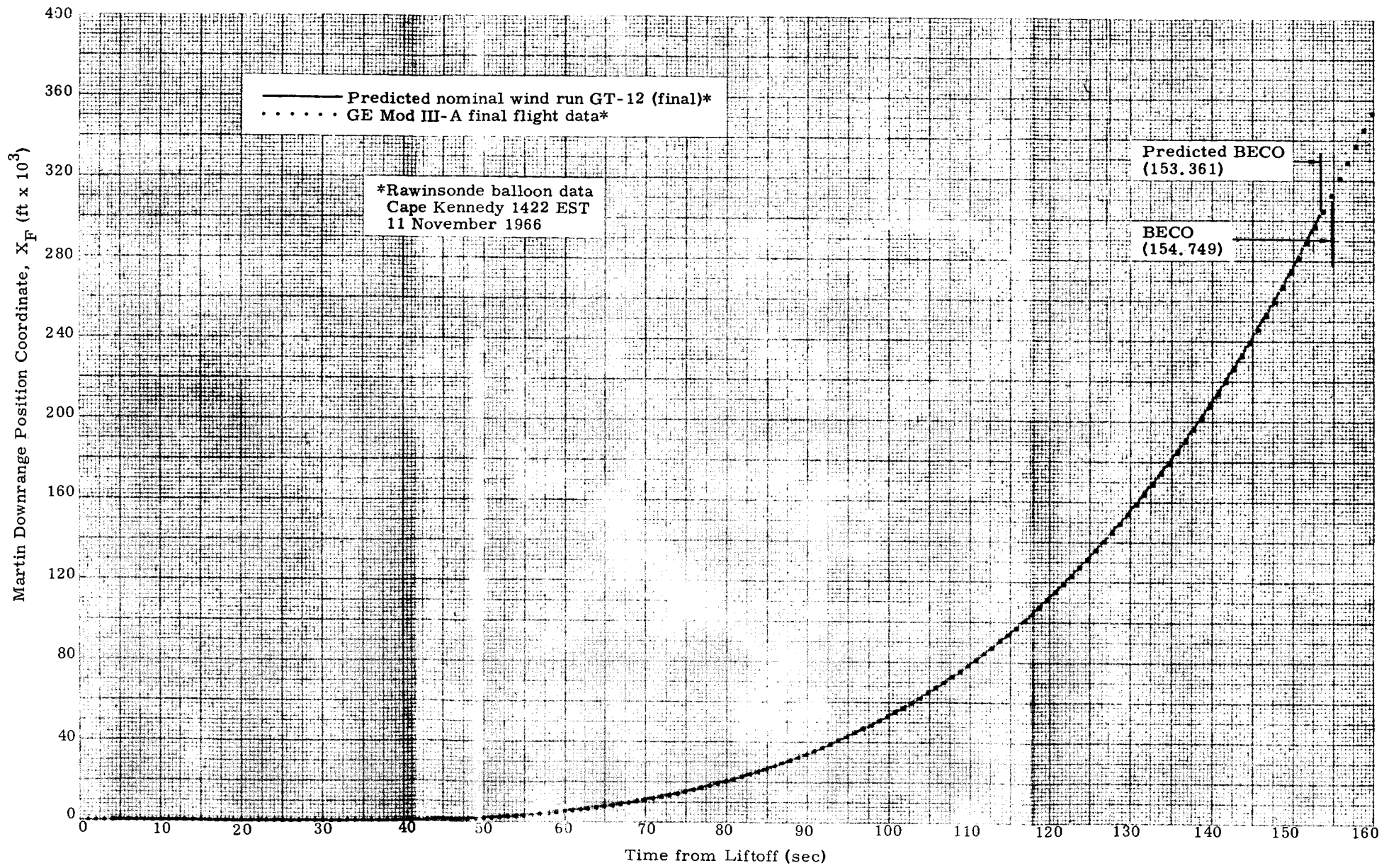

Fig. II-5. Downrange Position Coordinate (X_F) Versus Time: Stage I Flight

[redacted]

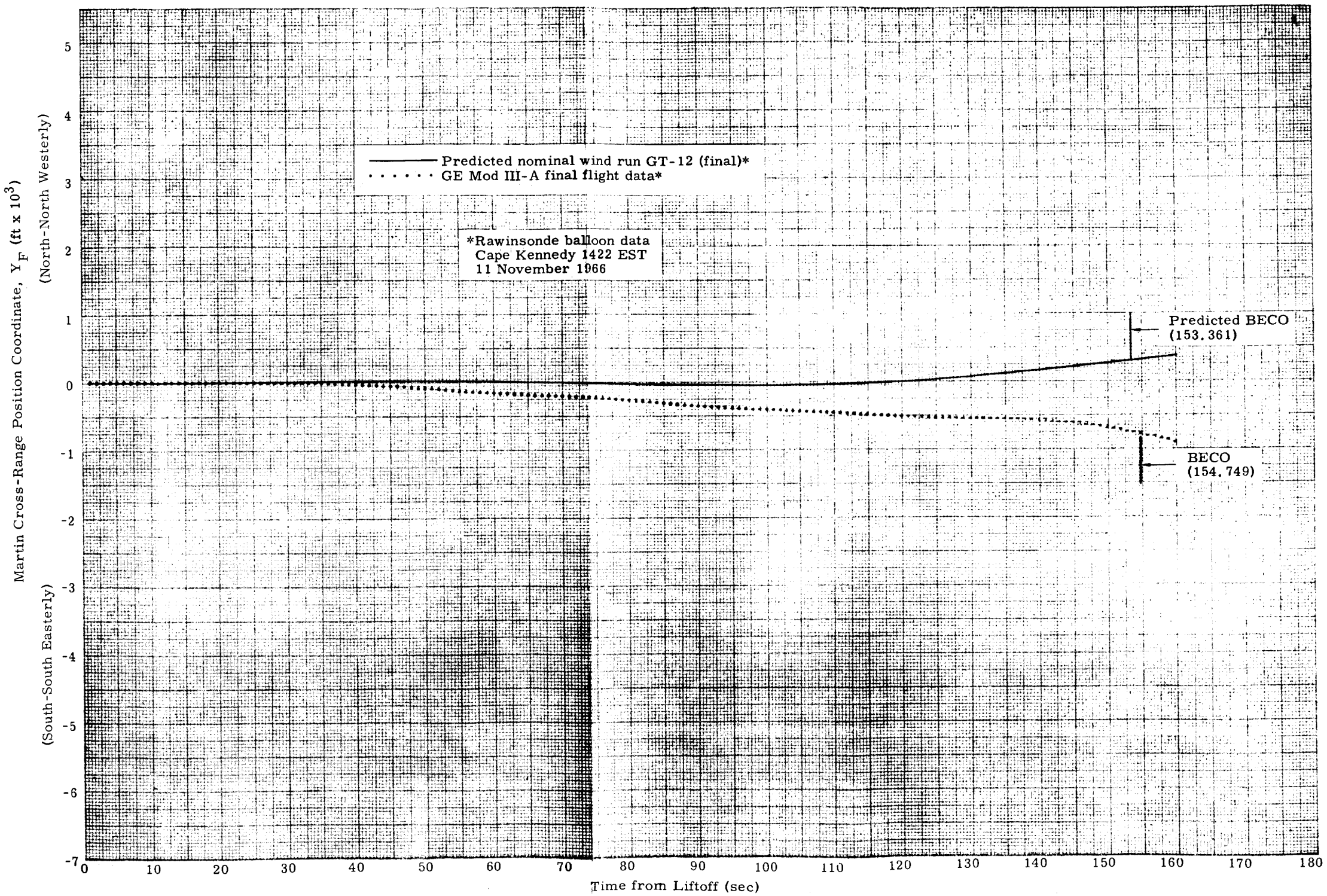

Fig. II-6. Cross-Range Position Coordinate (Y_F) Versus Time: Stage I Flight

[redacted]

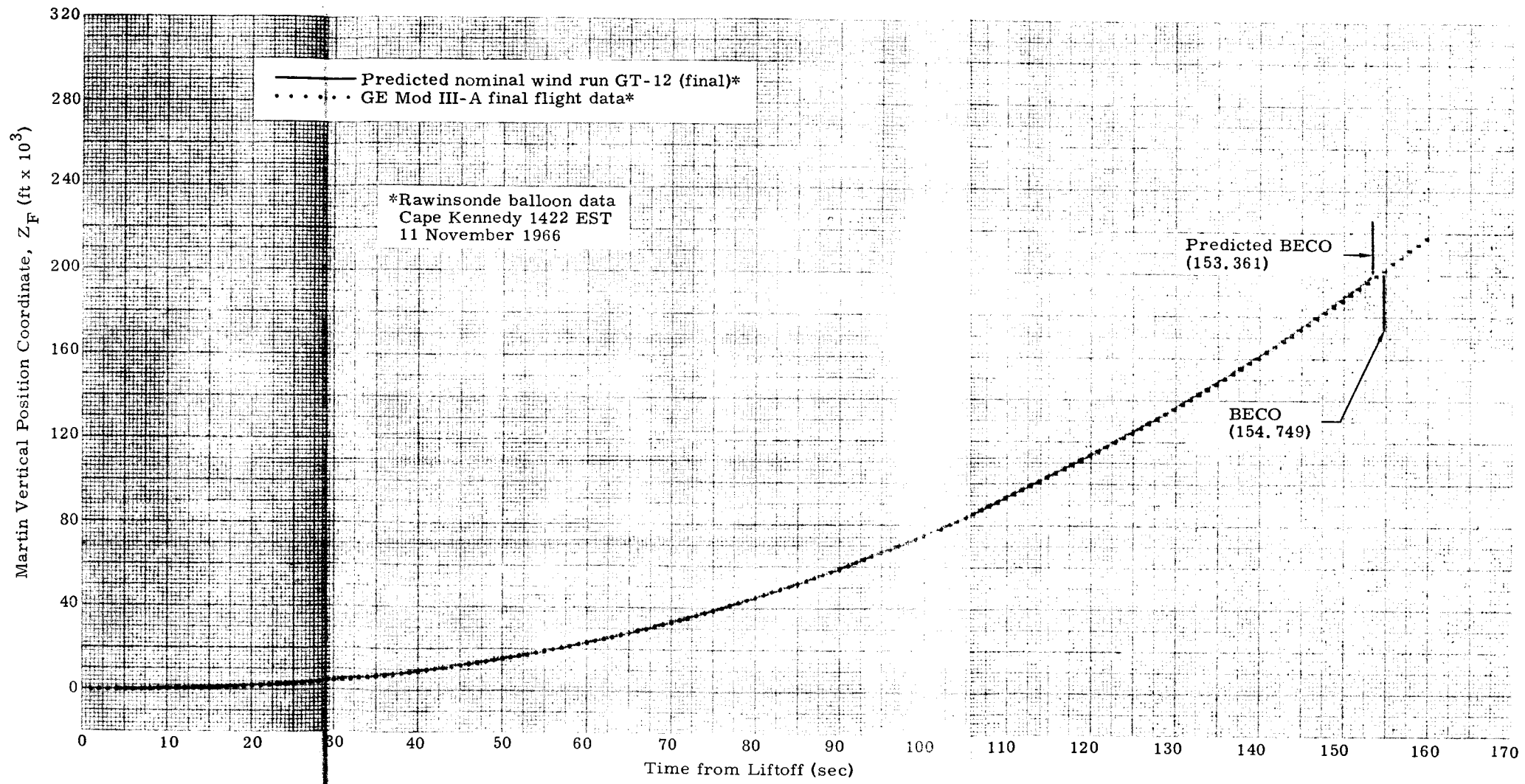

Fig. II-7. Vertical Position Coordinate (Z_F) Versus Time: Stage I Flight

~~CONFIDENTIAL~~

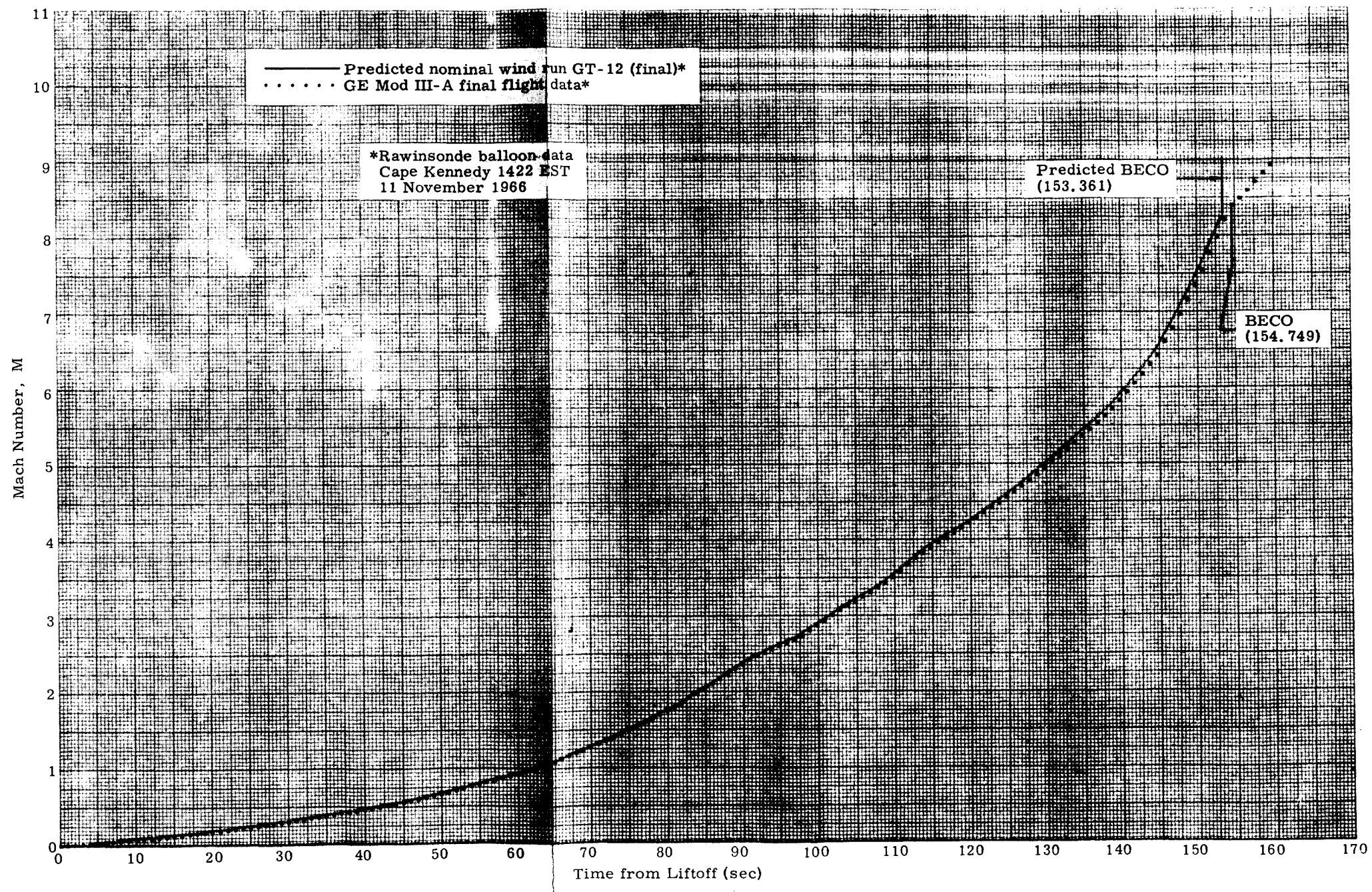

Fig. II-8. Mach Number (M) Versus Time: Stage I Flight

~~CONFIDENTIAL~~

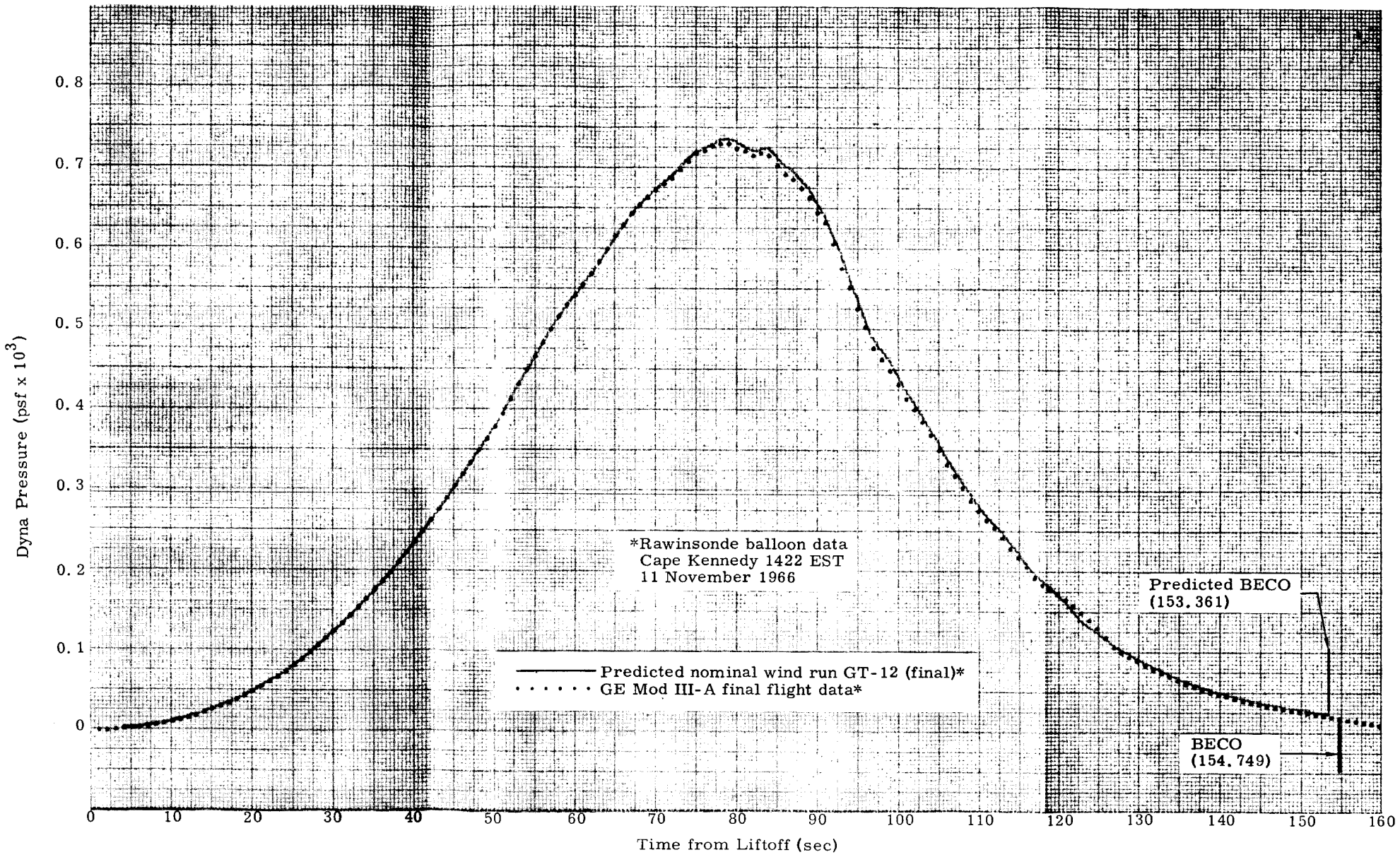

Fig. II-9. Dynamic Pressure (q) Versus Time: Stage I Flight

~~CONFIDENTIAL~~

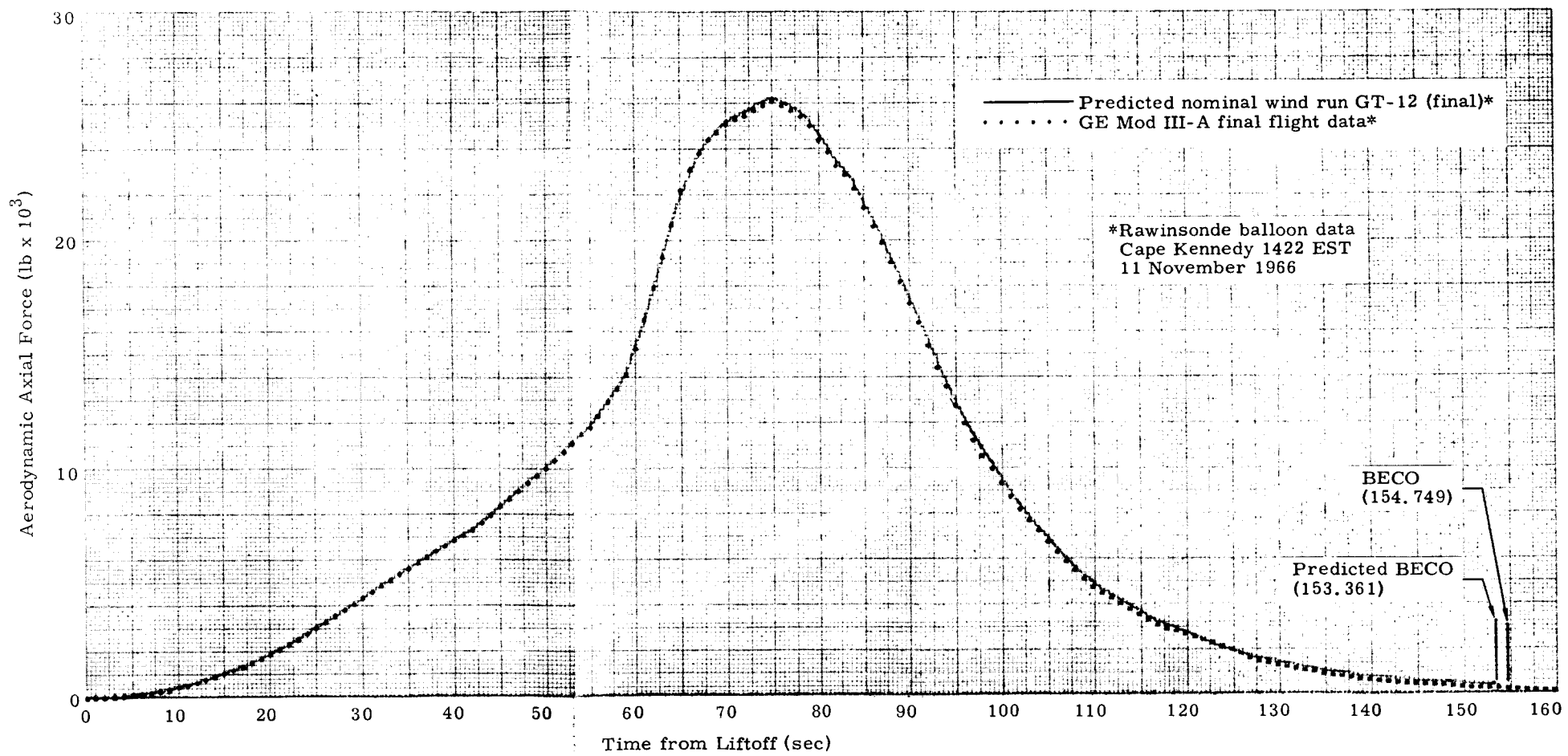

Fig. II-10. Axial Force Versus Time: Stage I Flight

~~CONFIDENTIAL~~

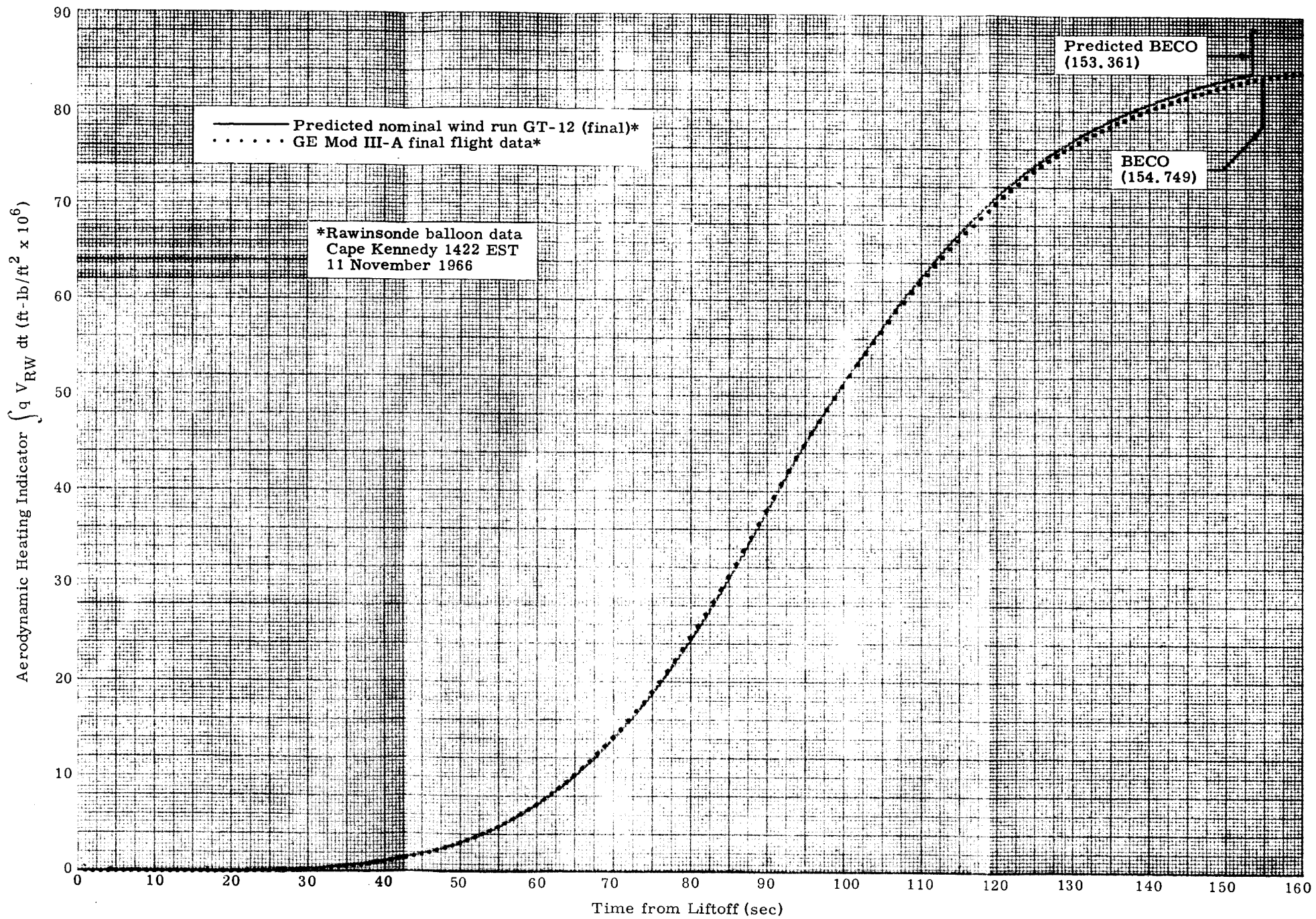

Fig. II-11. Aerodynamic Heating Indicator Versus Time: Stage I Flight

~~CONFIDENTIAL~~

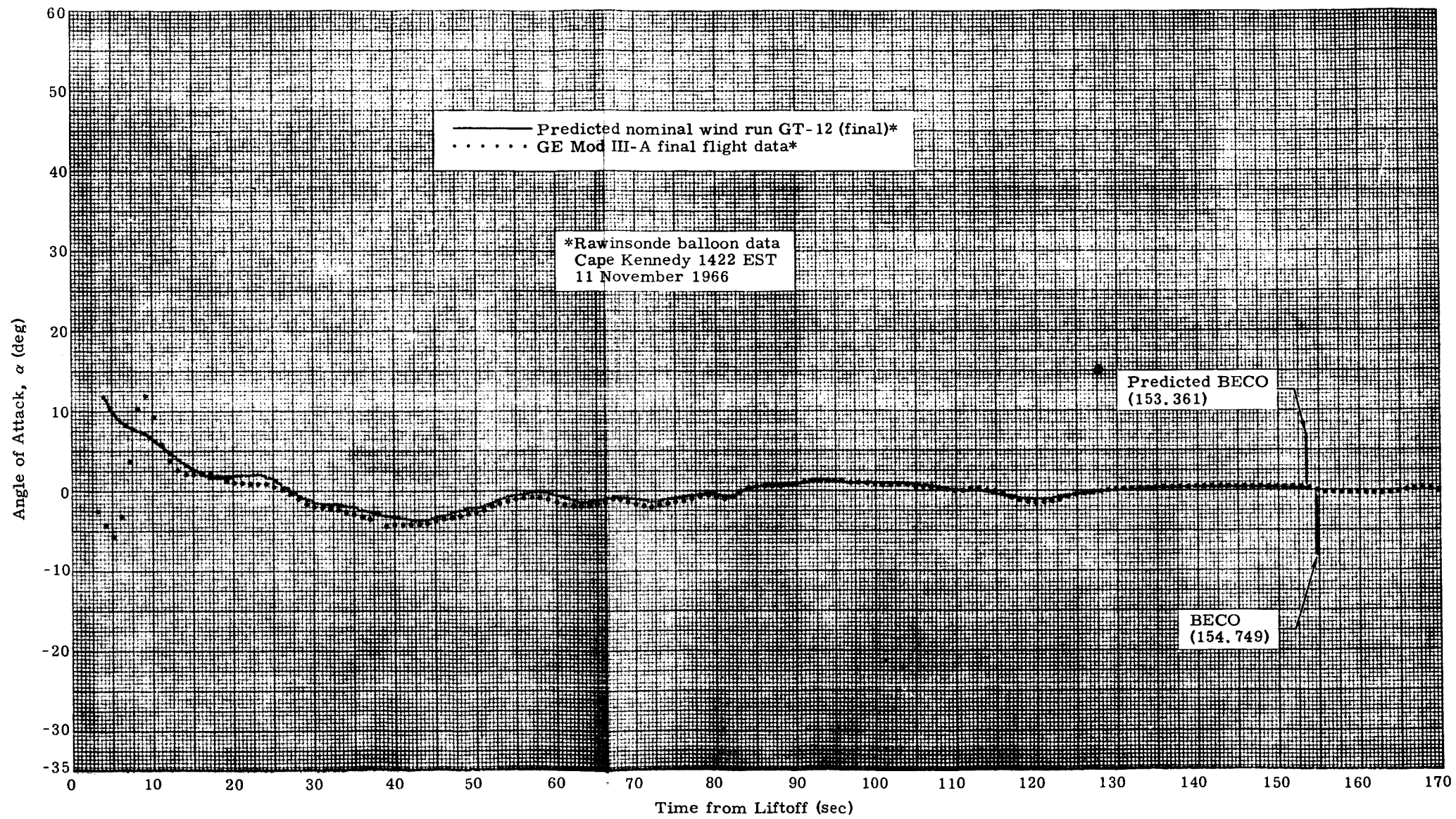

Fig. II-12. Stage I Angle of Attack History

~~CONFIDENTIAL~~

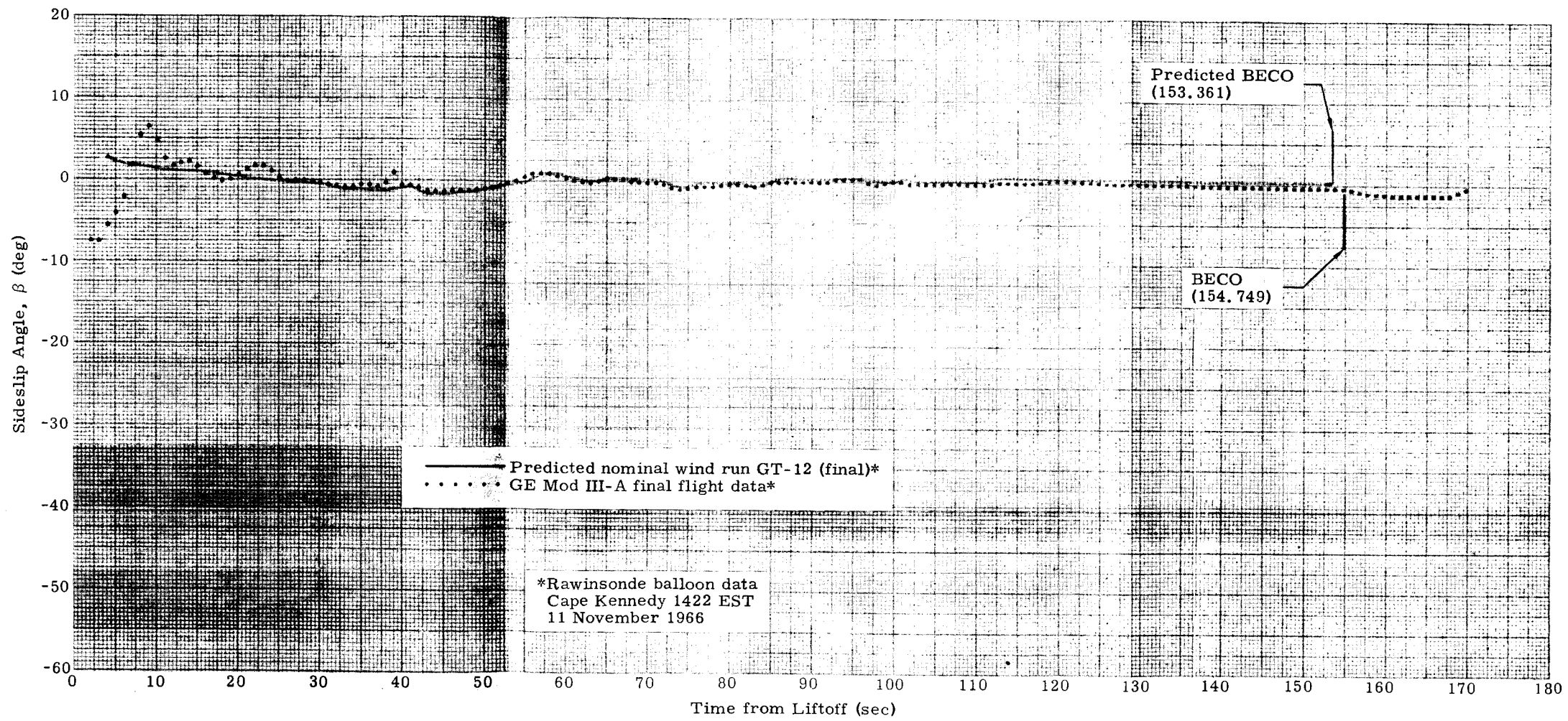

Fig. II-13. Stage I Angle of Sideslip History

~~CONFIDENTIAL~~

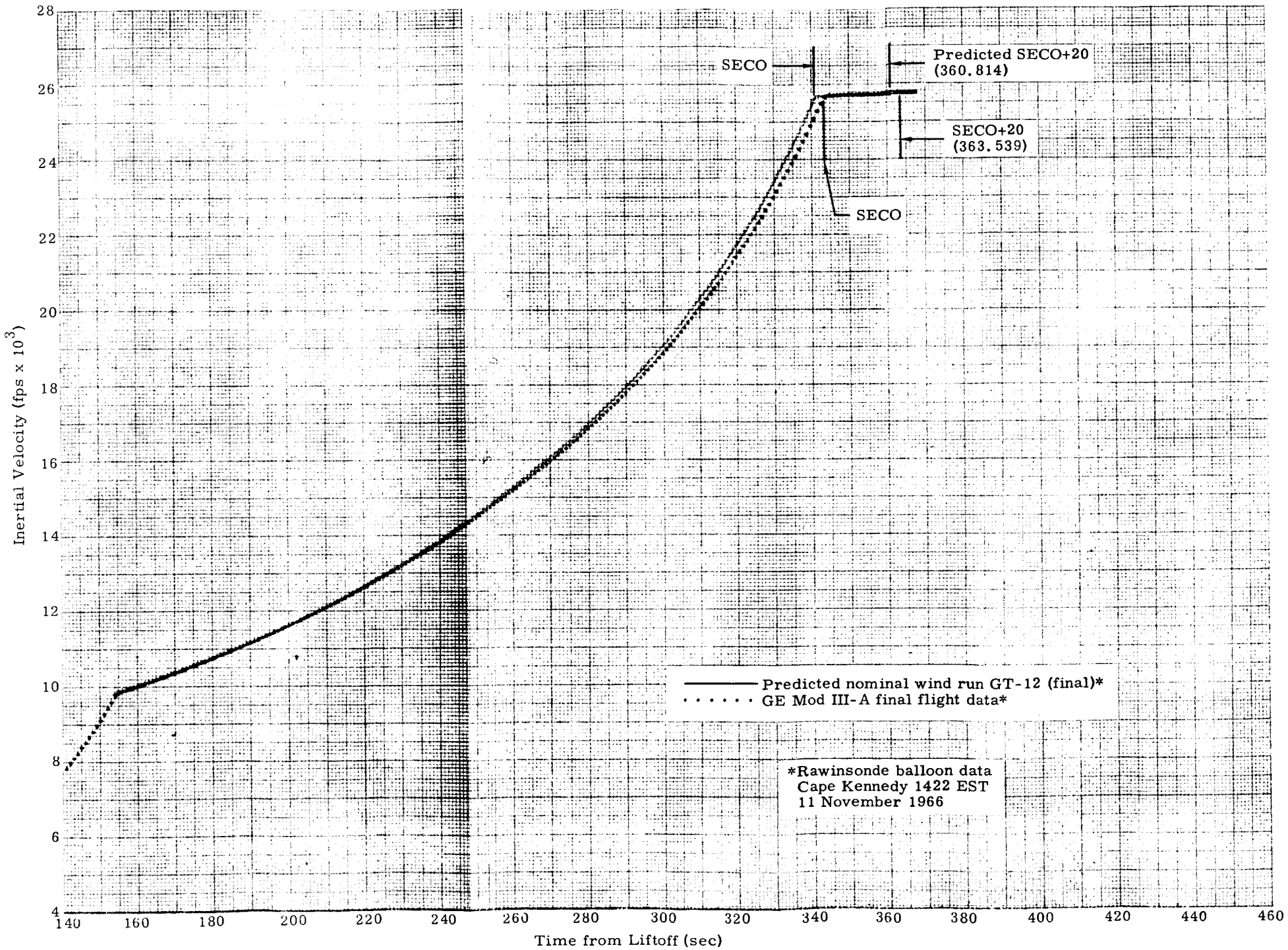

Fig. II-14. Resultant Inertial Velocity (V_I) Versus Time: Stage II Flight

~~CONFIDENTIAL~~

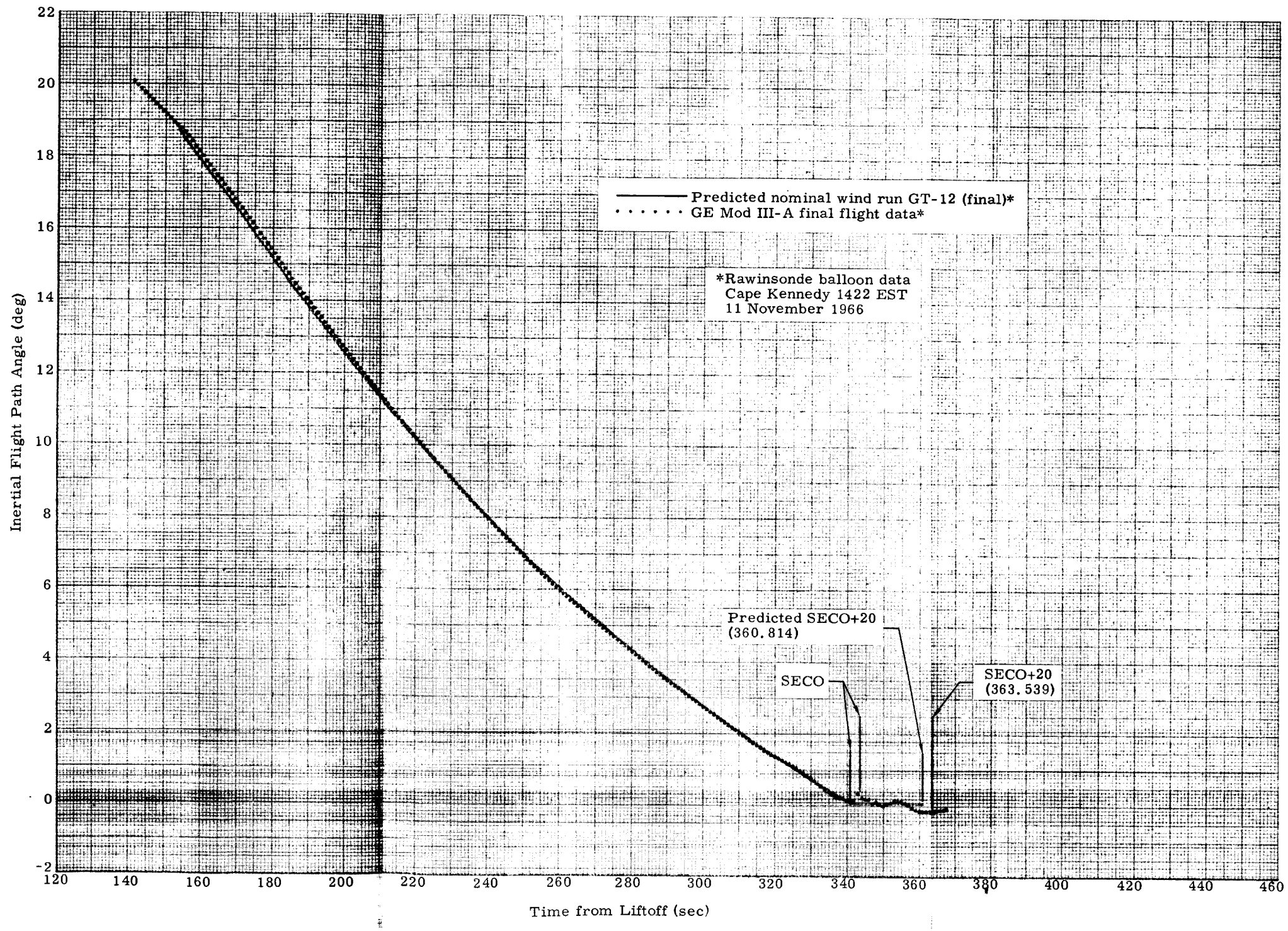

Fig. II-15. Inertial Flight Path Angle (γ_I) Versus Time: Stage II Flight

~~CONFIDENTIAL~~

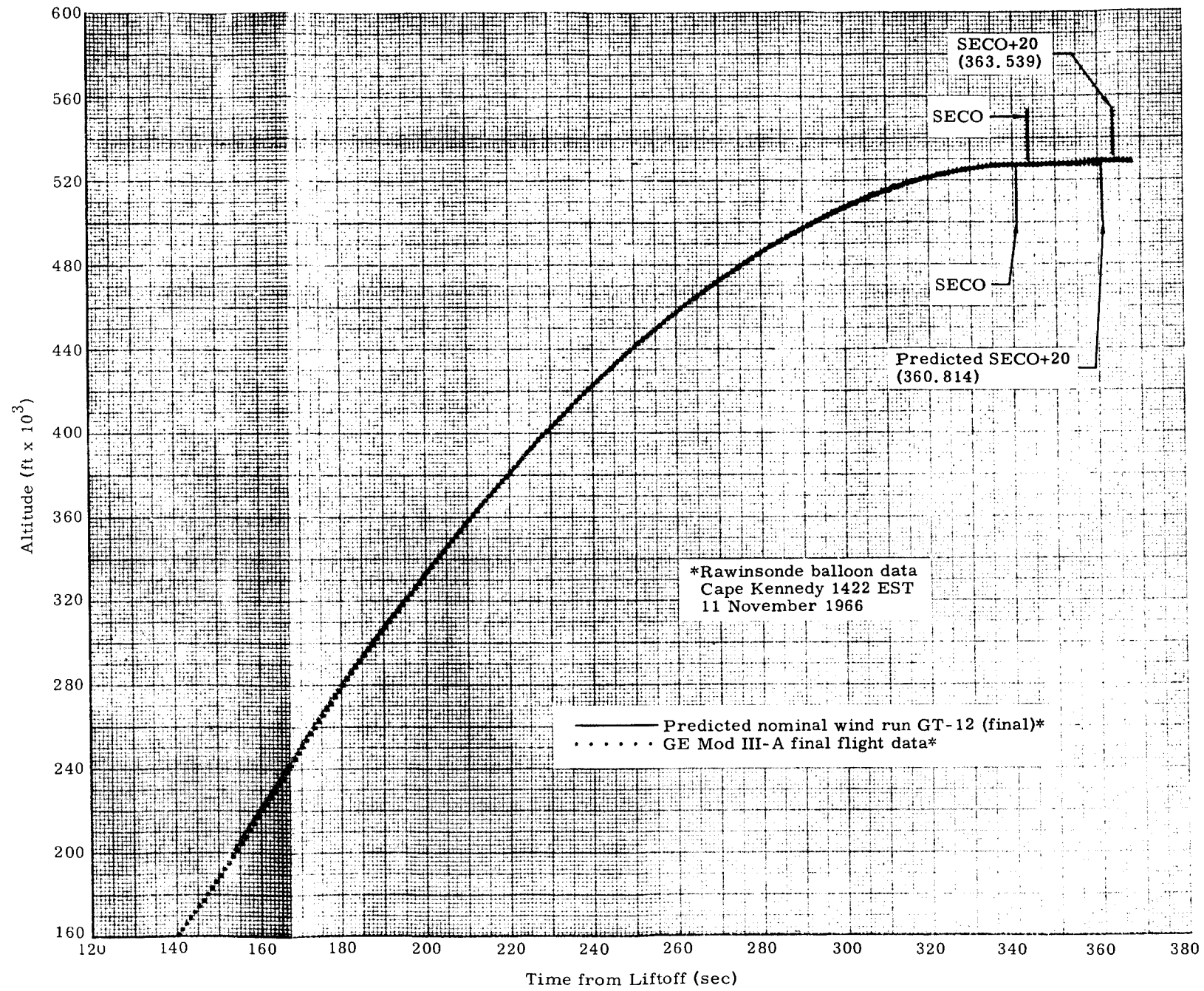

Fig. II-16. Altitude Versus Time: Stage II Flight

~~CONFIDENTIAL~~

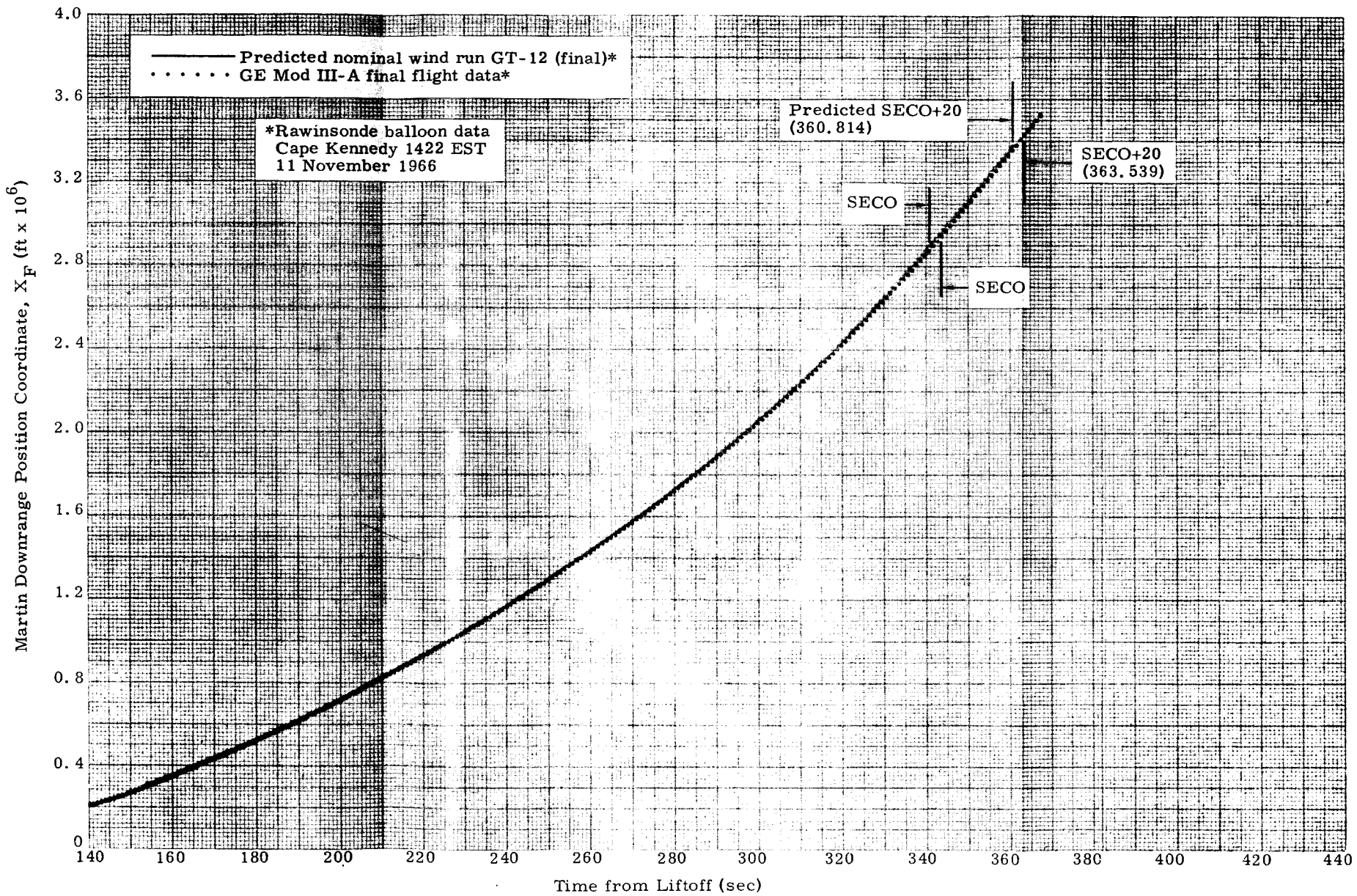

Fig. II-17. Downrange Position Coordinate (X_P) Versus Time: Stage II Flight

CONFIDENTIAL

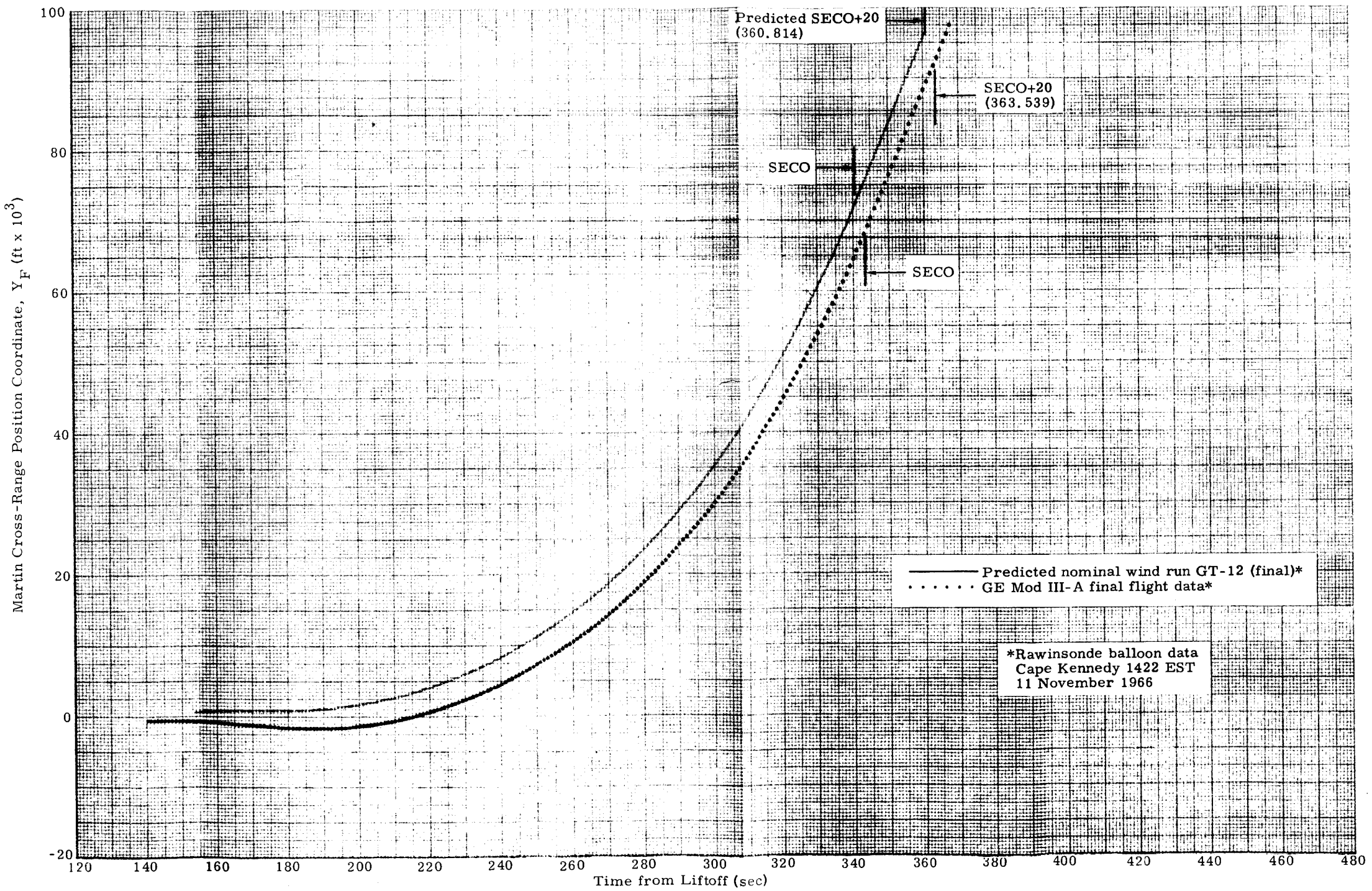

Fig. II-18. Cross-Range Position Coordinate (Y_F) Versus Time: Stage II Flight

CONFIDENTIAL

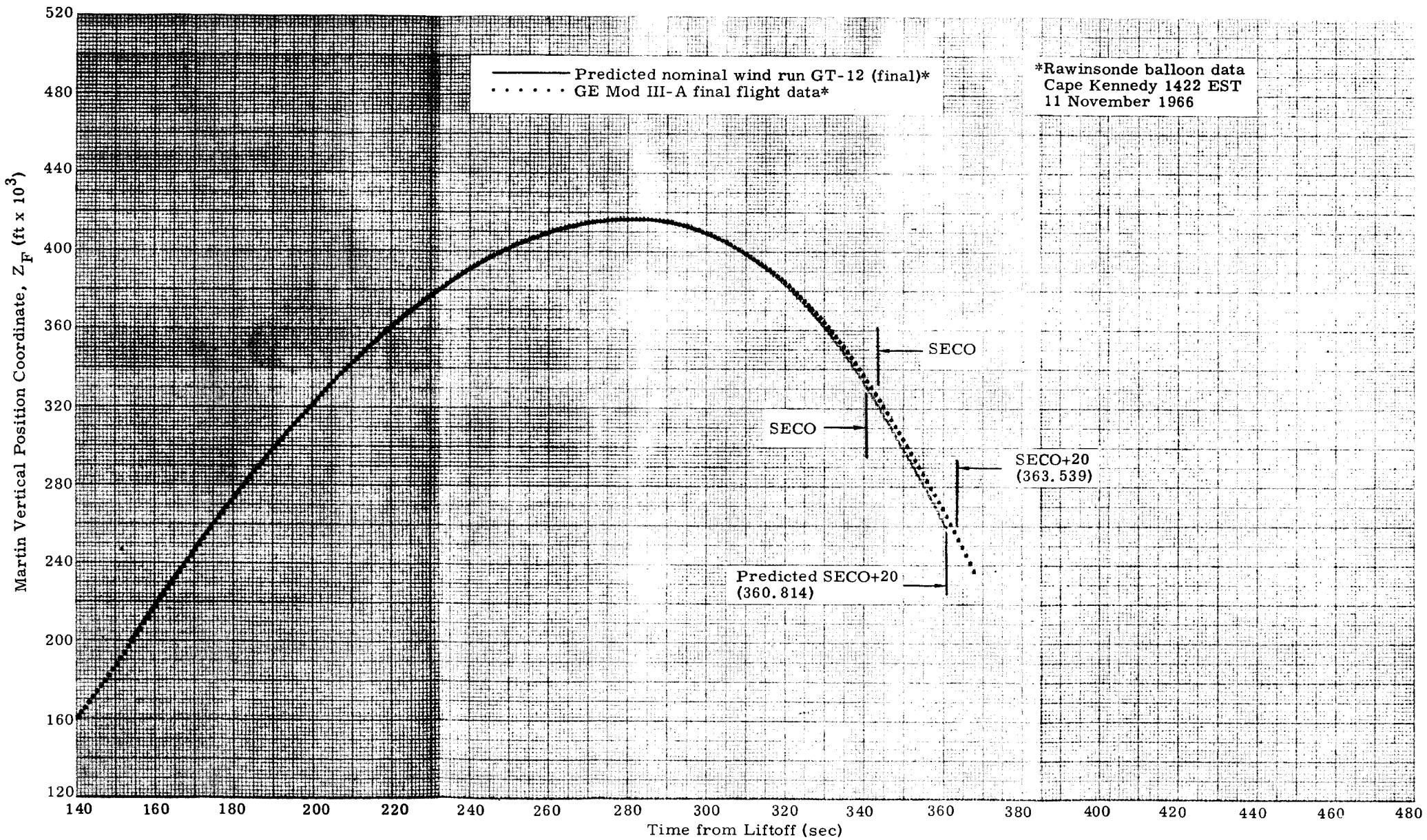

Fig. II-19. Vertical Position Coordinate (Z_F) Versus Time: Stage II Flight

~~CONFIDENTIAL~~

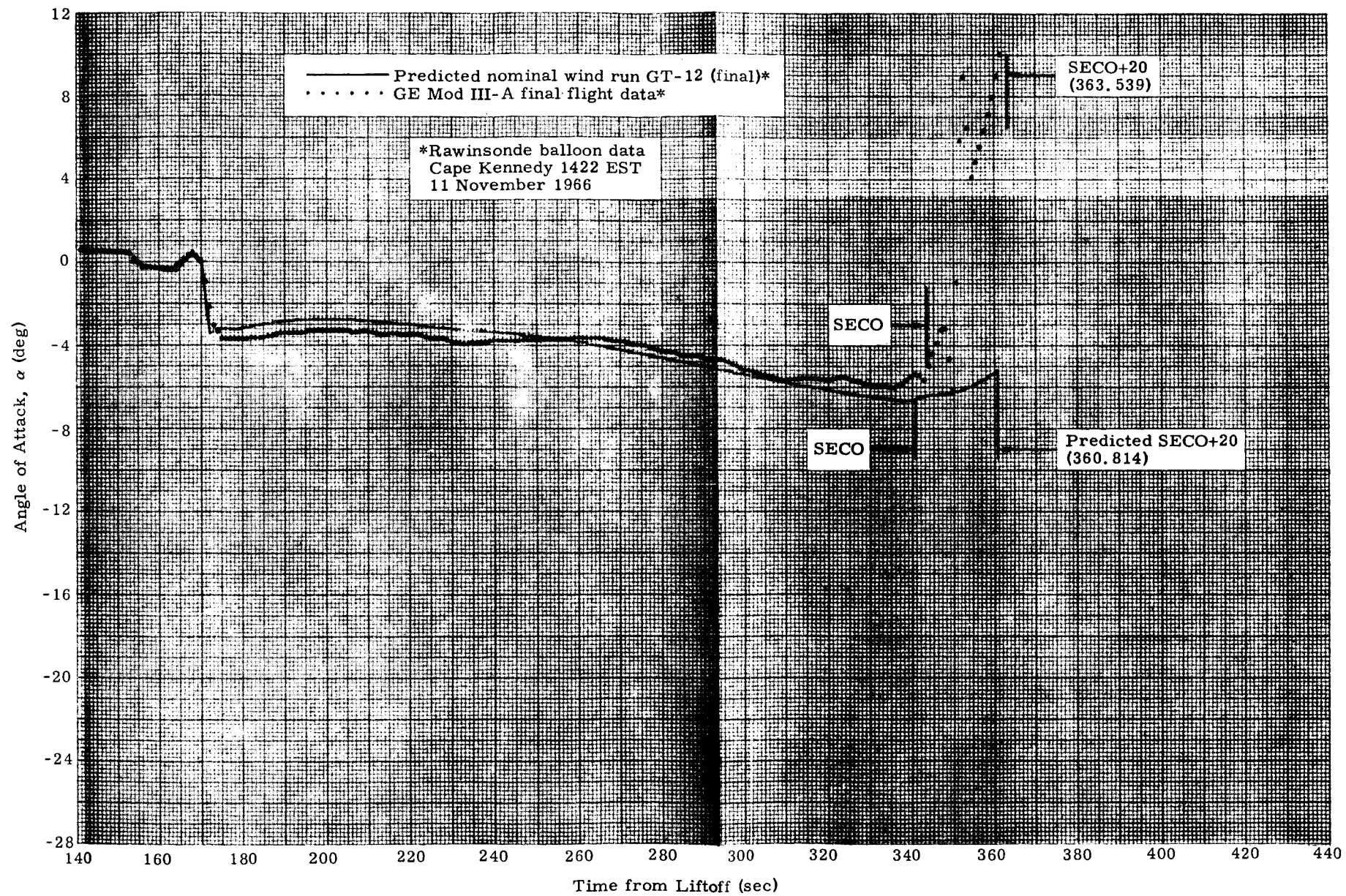

Fig. II-20. Stage II Angle of Attack History

~~CONFIDENTIAL~~

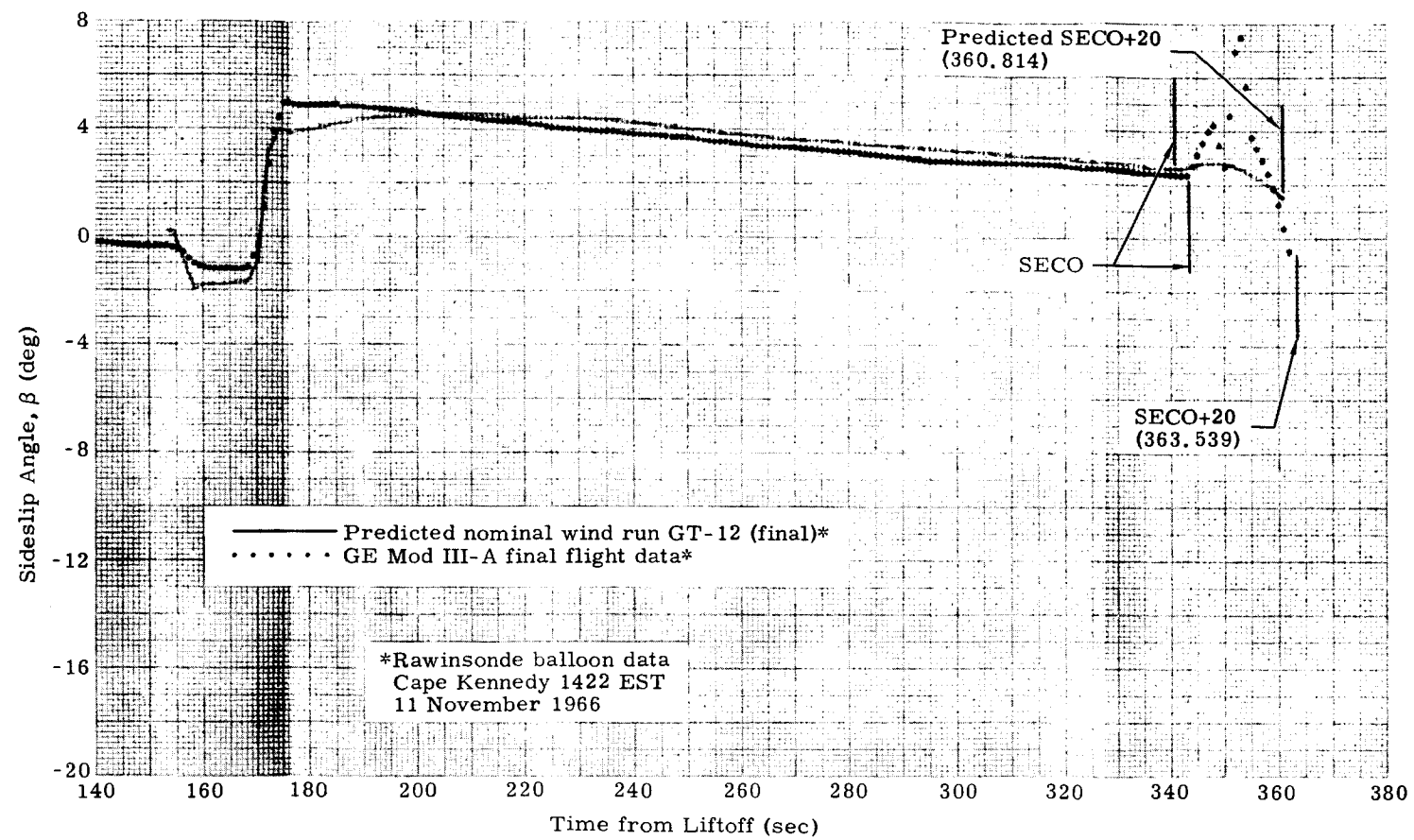

Fig. II-21. Angle of Sideslip Versus Time: Stage II Flight

~~CONFIDENTIAL~~

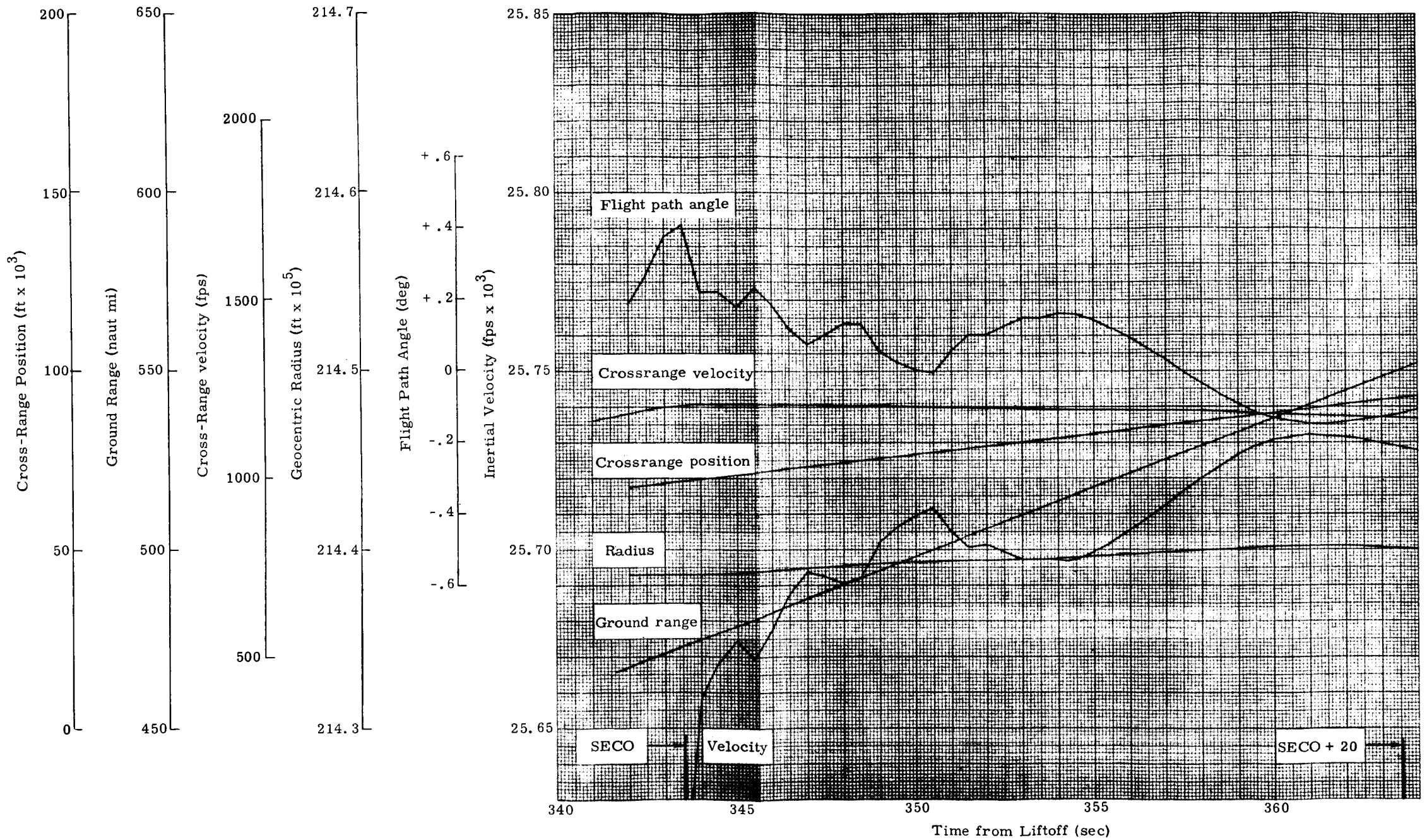

Fig. II-22. GE Mod III-A Flight Data from SECO to SECO + 20 Seconds

~~CONFIDENTIAL~~

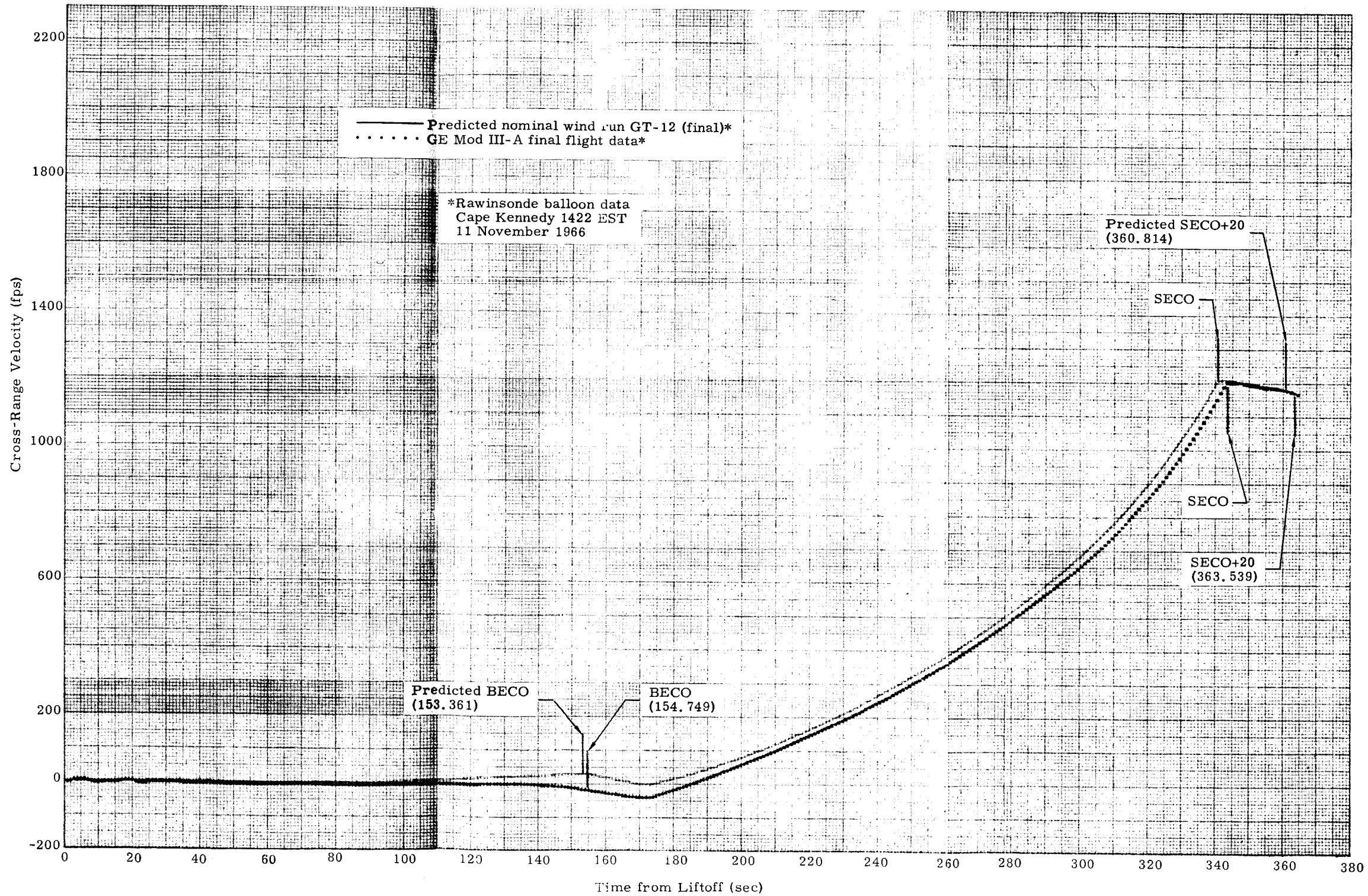

Fig. II-23. Cross-Range Velocity ($\dot{Y}_F$) Versus Time

~~CONFIDENTIAL~~

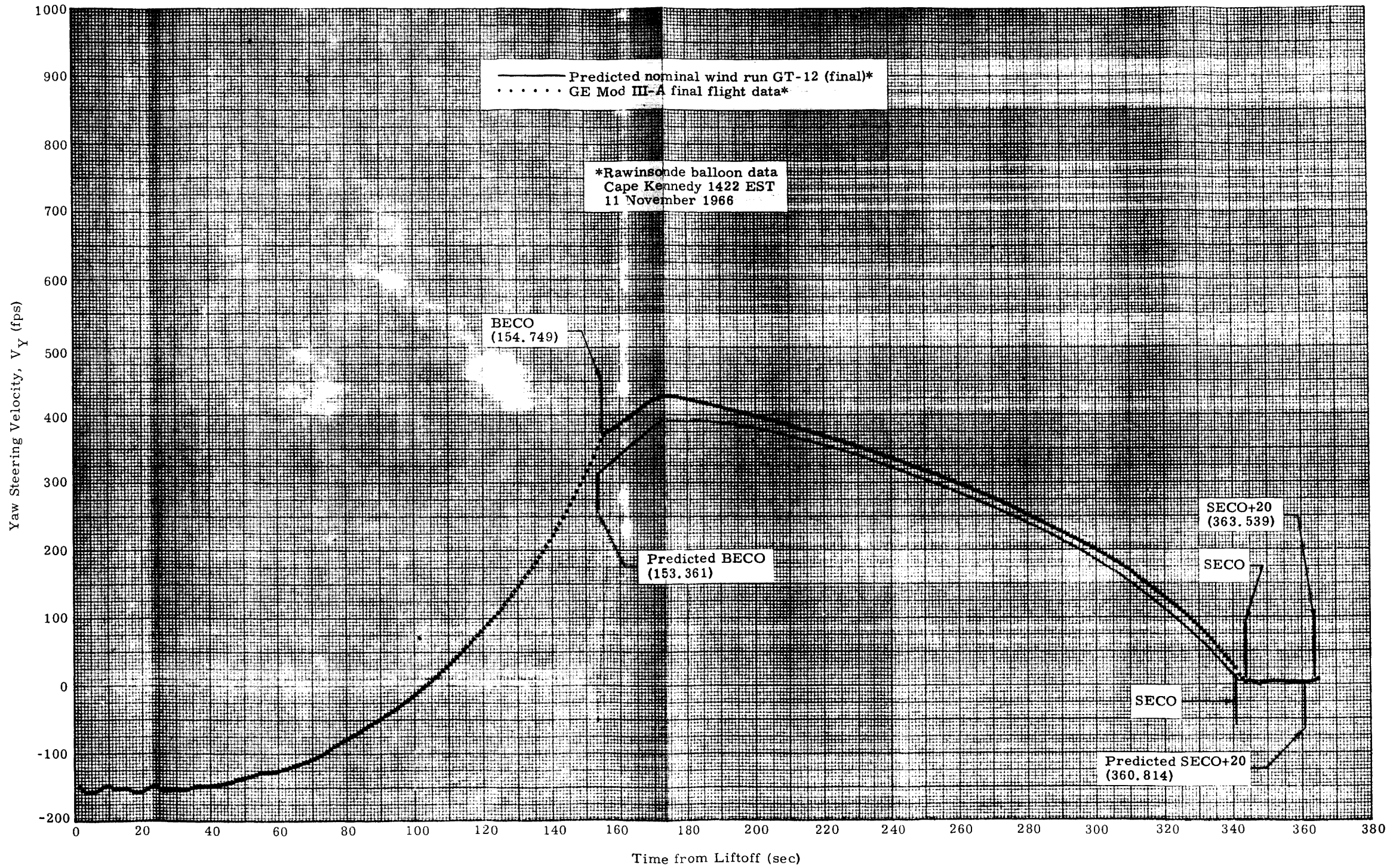

Fig. II-24. Yaw Steering Velocity (V_Y) Versus Time

~~CONFIDENTIAL~~

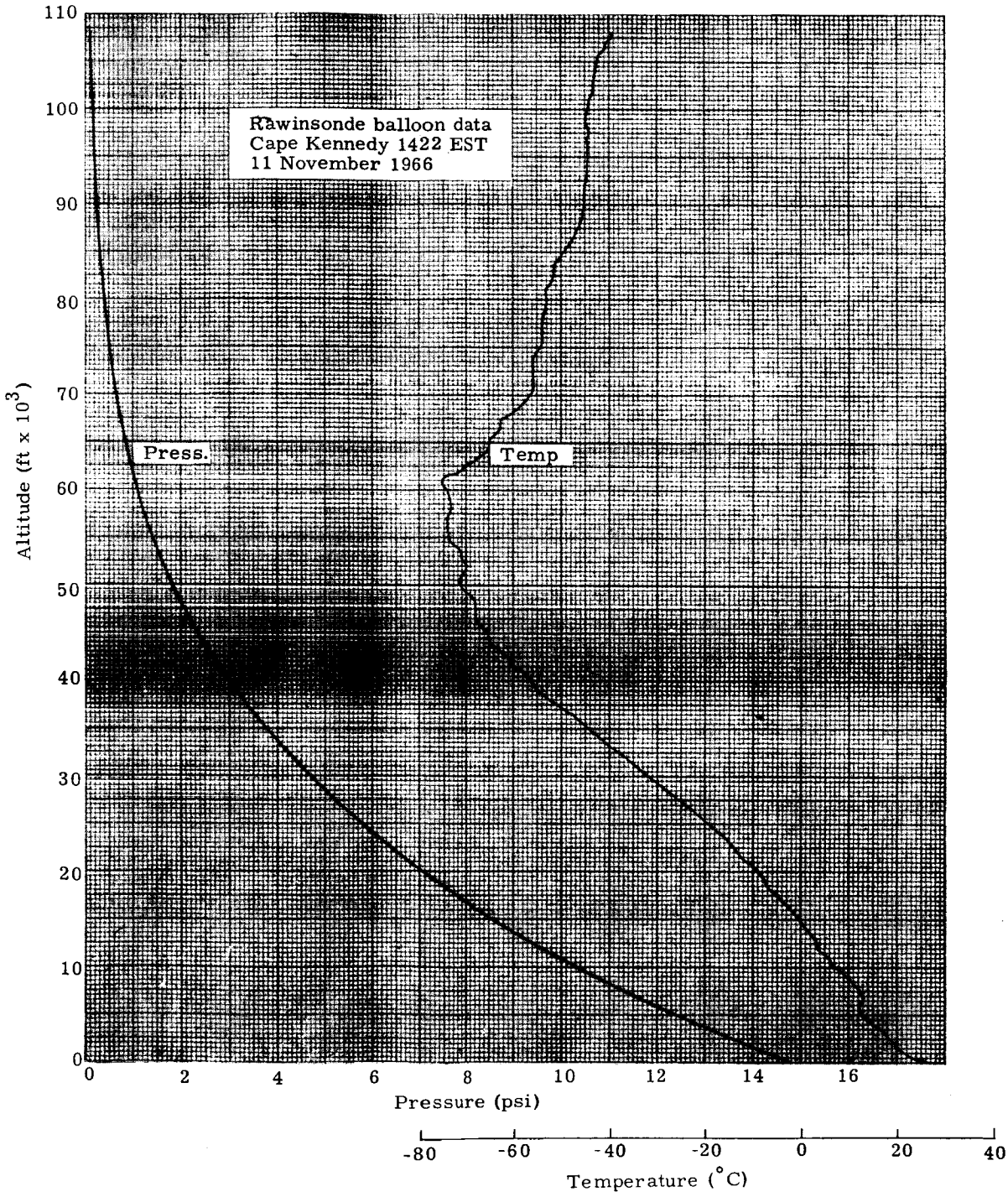

Fig. II-25. Ambient Temperature and Pressure Versus Altitude

~~CONFIDENTIAL~~

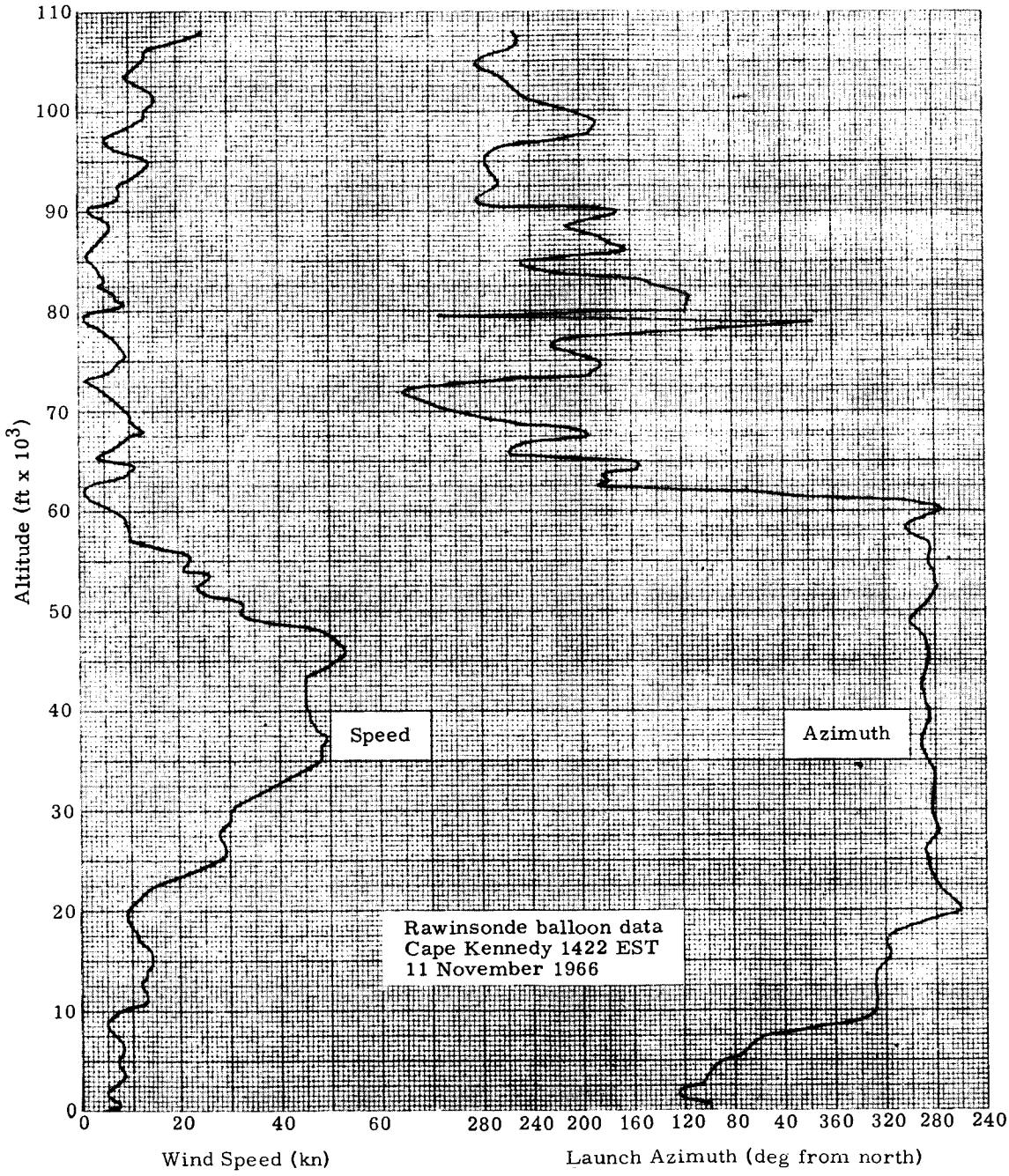

Fig. II-26. Wind Speed and Azimuth Versus Altitude

~~CONFIDENTIAL~~

6. Look Angles

The maximum look angle in pitch (LAP) occurred at LO + 336 seconds, when it attained a value of 20.3 degrees. This maximum value was within the boundary existing at that time, as shown in Fig. II-27. The corresponding look angle in yaw (LAY) was also within the established limitation, as shown in Fig. II-28. The maximum value of LAY was -4.60 degrees, which occurred 343 seconds after liftoff.

TABLE II-8

Data Available for Trajectory Analysis

Source	Type	Station	Flight Coverage (sec from range-0)
GE	Mod III-A radar position, velocity	Cape Kennedy	LO to +369
NASA-MSC	Spacecraft IGS ascent parameters	--	LO to +380
AFETR	MISTRAM position, velocity and acceleration	Valkaria I Eleuthera II	50 to 370 158 to 384

TABLE II-9

Geographic and Weather Conditions at Launch

Location	
Site	Complex 19
Site coordinates:	
Latitude (deg)	28.507 N
Longitude (deg)	80.554 W
Pad orientation (deg)	84.912 true azimuth
Weather	
Ambient pressure (psi)	14.77
Ambient temperature (°F)	76
Dew point (°F)	68

~~CONFIDENTIAL~~

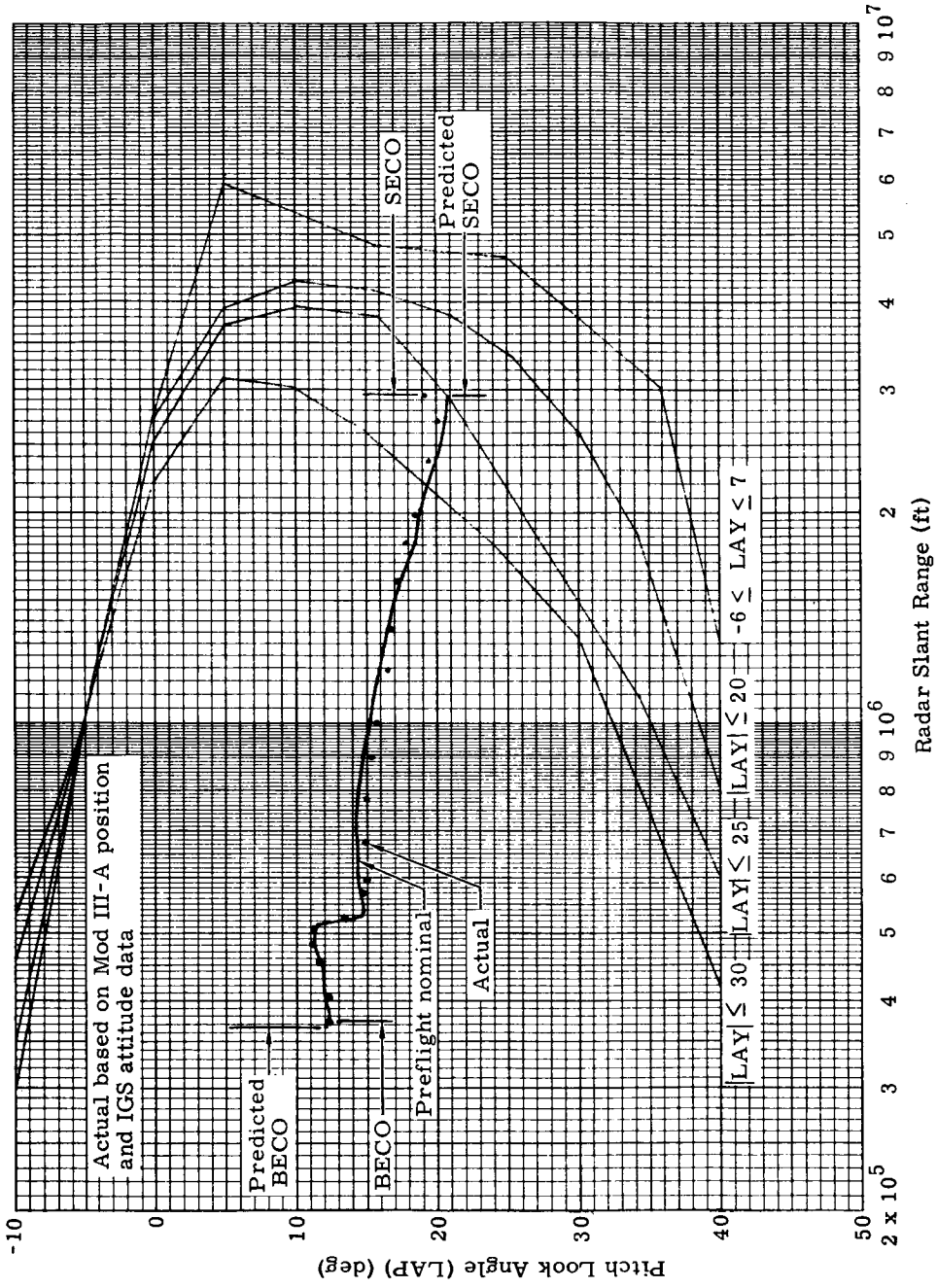

Fig. II-27. Permissible Pitch Look-Angle Envelope

~~CONFIDENTIAL~~

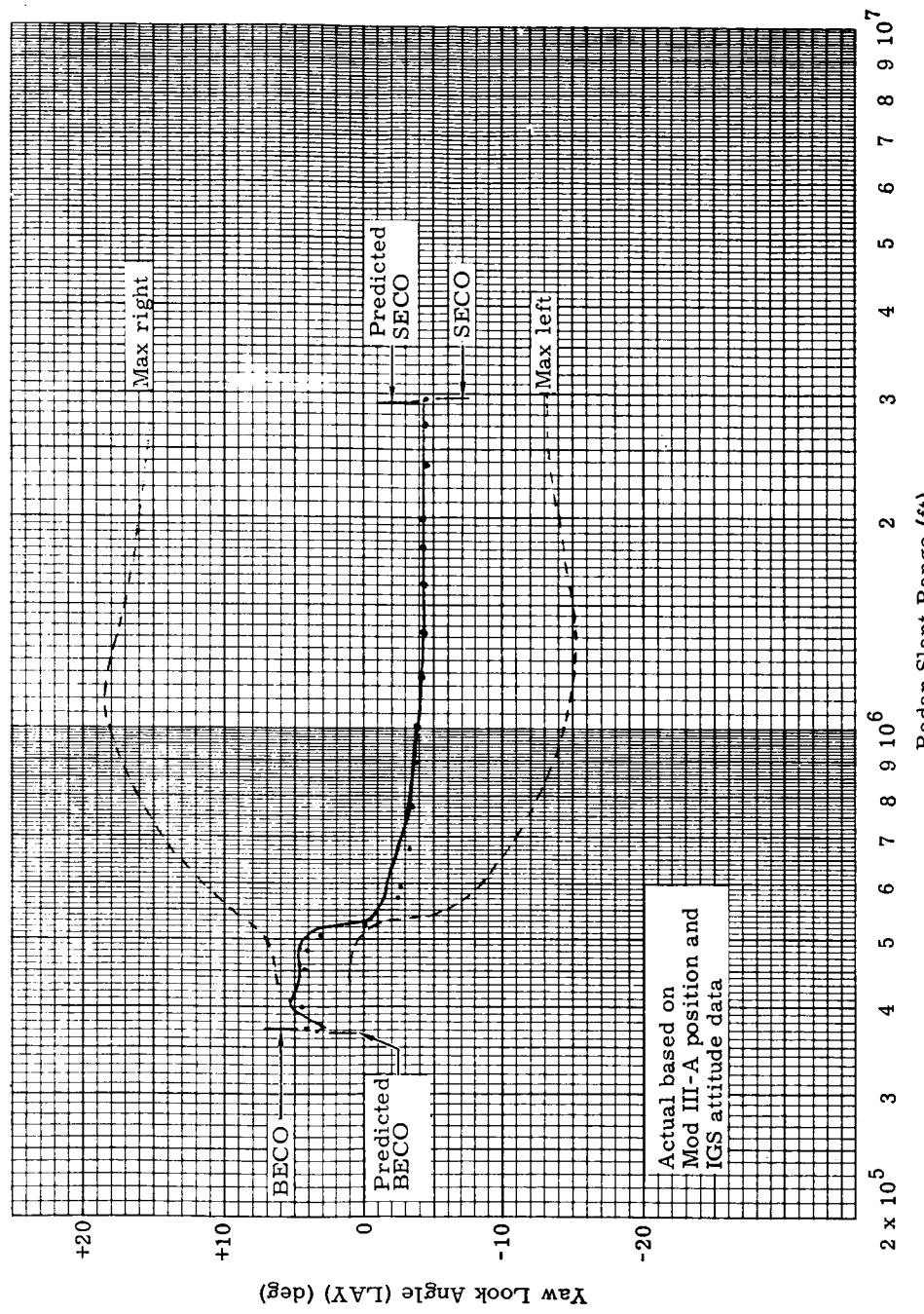

Fig. II-28. Permissible Yaw Look-Angle Envelope

TABLE II-9 (continued)

Relative humidity (%)	71
Surface wind:	
Speed (fps)	8.4
Direction (deg)	080
Winds aloft (max):	
Altitude (ft)	46,000
Speed (fps)	89.3
Direction (deg)	285 true azimuth
Cloud cover	Clear
Reference Coordinate System	
Type	Martin reference coordinate system
Origin	Center of launch ring, Complex 19
Positive X-axis	Downrange along flight azimuth tangent to ellipsoid
Positive Y-axis	To left of flight azimuth tangent to ellipsoid and ⊥ X-axis
Positive Z-axis	Forms a right-handed orthogonal system
Reference ellipsoid	Fischer
Launch	
Initial flight azimuth (deg)	106.51 true azimuth
Roll program (deg)	15.6 ccw

7. Maximum Dynamic Pressure

The maximum dynamic pressure for the GT-12 trajectory was less than design limits. Table II-10 compares the predicted and observed conditions associated with the maximum dynamic pressure. The no wind nominal predicted value of maximum dynamic pressure was 749 psf occurring at 78.8 seconds after liftoff.

TABLE II-10

Trajectory Parameters at Maximum Dynamic Pressure

	Predicted* (nominal)	Observed**
Dynamic pressure (psf)	737.2	730.2
Time from liftoff (sec)	78.6	78.34
Mach number	1.68	1.67
Altitude (ft)	43,000	42,780
Relative flight path angle (deg)	49.89	49.97
Relative wind velocity (fps)	1608	1595
Wind velocity (fps)	74.1	75.8
Wind azimuth (deg from north)	290	290
Angle of attack (deg)	-0.465	-0.573
Angle of sideslip (deg)	-0.256	-0.571

*Ref. 15, updated (see Section II-1).
**Mod III-A 2-pps radar data.

8. Angles of Attack and Sideslip

Predicted and observed histories of angles of attack and sideslip during the ascent are shown in Figs. II-12, II-13, II-20 and II-21. The predicted values were obtained from a digital run utilizing wind and atmospheric information obtained from the 1422 EST Rawinsonde sounding. Observed angles of attack and sideslip were derived using the Mod III-A position and velocity information, IGS attitude data and the aforementioned weather data.

B. PAYLOAD CAPABILITY

Propellants remaining onboard at Stage II low level sensor uncover indicated that a burning time margin (BTM) of 2.62 seconds existed for a command shutdown. The total usable propellant weight was 850 pounds, and the corresponding GLV payload capability was 9218 pounds. These values and the predicted nominal and minimum values appear in Fig. II-29. The predicted capability curves were obtained from the real-time propellant temperature monitoring digital program adjusted to reflect the pre-liftoff temperature changes and the actual Agena ephemeris data used in the guidance equations at launch. The predicted propellant weight and burning time margins are based on the difference between these curves and the 8294-pound spacecraft weight.

[redacted]

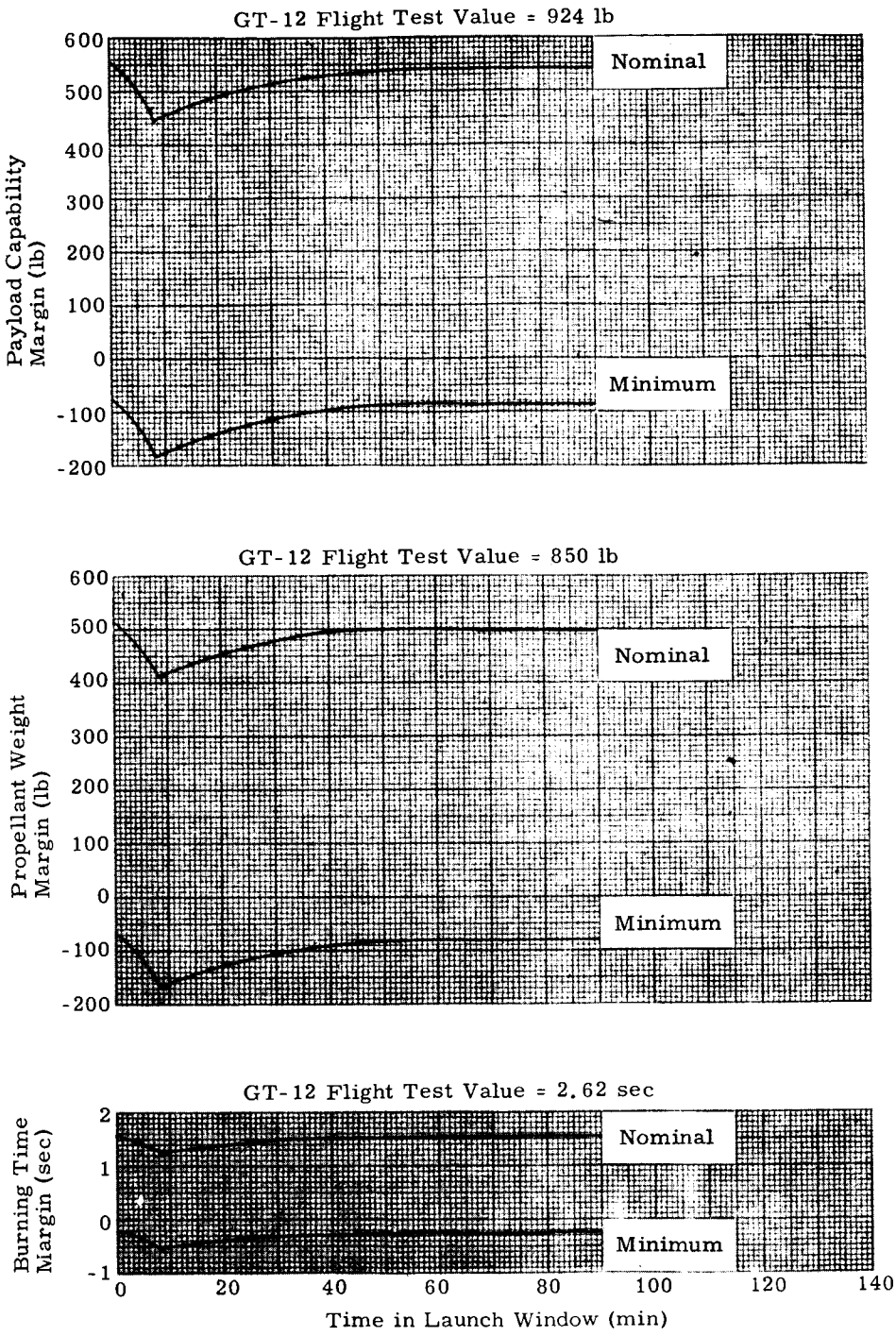

Fig. II-29. Payload Capability

[redacted]

The last payload prediction indicated that the minimum payload capability was 76 pounds less than the spacecraft weight, and the nominal payload capability was 557 pounds greater than the spacecraft weight at the predicted launch time. The actual (postflight reconstructed) GLV capability was 924 pounds greater than the spacecraft weight.

C. STAGING

The staging sequence was normal and physical stage separation occurred as planned. The time interval from staging signal ($87FS_2/91FS_1$) to start of Stage II engine chamber pressure (P_{c_3}) rise was 0.665 second. This compares favorably with the nominal expected time of 0.70 ± 0.08 second. Stage separation occurred 0.037 second following start of P_{c_3} rise.

D. WEIGHT STATEMENT

Table II-11 shows the GT-12 weight history from launch to orbital insertion.

The postflight weight report (Ref. 18) provides the background data for this summary. The report includes a list of dry weight empty changes at ETR and shows a derivation of weight empty from the actual vehicle weighing. Other items covered include the derivation of burnout, BECO, SECO and shutdown weights; weight comparisons with the BLH data; and the center of gravity travel envelope as a function of burn time for the horizontal, vertical and lateral planes.

[redacted]

TABLE II-11

GT-12 Weight Summary

	Weight (lb)			
	Step I	Step II	Step III	Stage Total
Loaded weight	271,496	65,920	8,294(1)	345,710
Start and gain losses	3,618(2)			3,618
Trajectory LO weight	267,878	65,920	8,294	342,092
Propellant consumed to BECO	256,695	11		256,706
Weight at BECO	11,183	65,909	8,294	85,386
Shutdown propellant	298			298
Weight Stage I burnout	10,885(3)	65,909(3)	8,294	85,088
Stage II engine start	10,885	192		11,077
Stage II LO		65,717	8,294	74,011
Propellant consumed to SECO		59,470		59,470
Ablative, covers and water		42		42
Stage II at SECO		6,205	8,294	14,499(4)
Shutdown propellant		127		127
Weight at SECO + 20 seconds		6,078	8,294	14,372(4)

(1) McDonnell/Cape Kennedy.

(2) Event: launch bolts blown.

(3) Includes outage: 133 lb Stage I; 99 lb Stage II.

(4) Includes 850-lb burning margin.

[redacted]

III. PROPULSION SYSTEM

A. ENGINE SUBSYSTEM

The Stages I and II engines operated satisfactorily throughout the flight, and all launch objectives were met. Stage I burning time was 157.978 seconds, and shutdown was initiated by fuel exhaustion. Stage II operation was terminated by guidance command at $91FS_1$ + 188.790 seconds.

Two anomalies occurred during flight, neither of which adversely affected engine performance. These were:

(1) The engine mixture ratio of both stages, corrected to standard inlet conditions, experienced a negative shift from the acceptance test value. Although the shifts did not exceed the 3-sigma run-to-run repeatability; they followed the negative shift trend of both stages on GLV-9, GLV-10 and GLV-11.

(2) A double ignition spike was indicated during the Stage II start transient. This phenomenon has been observed previously in flight and ground tests with no adverse effect on performance.

1. Stage I Engine (LR87-AJ-7, S/N 1012)

a. Configuration and special procedures

GLV-12 configuration and checkout procedures were the same as those used for GLV-11. The following special procedures and inspections were accomplished to ensure vehicle integrity.

(1) The oxidizer and fuel discharge lines were X-rayed both at Martin-Baltimore and at ETR to verify that there were no disjointed spider ball joints. S/A 1 oxidizer discharge line ball joint was found to be out of tolerance when X-rayed at ETR. The line was replaced and X-rays were satisfactory. The remaining lines were all proven satisfactory by X-ray.

(2) As a result of finding metal chips in the engine inlet lines on GLV-11, the GLV-12 engine inlet lines and upper surfaces of the pump impellers were inspected for contaminants. S/A 1 oxidizer inlet line was found to be slightly rusted. The line was cleaned and reinstalled. No contaminants were found in the other lines.

(3) As on GLV-11, the GLV-12 fuel and oxidizer bootstrap lines, hot gas cooler outlet line and lubricant oil cooler outlet line were removed and inspected for damaged teflon liners. The

CONFIDENTIAL

Stage I fuel bootstrap line was rejected and replaced. The remaining lines were satisfactory.

b. Start transient

The S/A 1 and S/A 2 thrust chamber pressure start transients were normal and are presented in Figs. III-1 and III-2. The ignition spikes indicated 86% (678 psia) and 89% (696 psia) of rated thrust for S/A 1 and S/A 2, respectively. The spike values were above the engine model specification allowable (75%); however, CEC transducers were used to measure P_c on this flight. CEC transducers, characteristically, have shown underdamped oscillations which obscure true transient performance and prevent accurate determination of the ignition spike and step level.

Significant start events are tabulated in Table III-1.

TABLE III-1

Stage I Engine Start Parameters

Parameter	S/A 1	S/A 2
FS_1 to initial P_c rise (sec)	0.755	0.760
P_c ignition spike (psia)	678	696
P_c step--approximate (psia)	460	460
P_c overshoot (psia)	None	None

c. Steady-state performance

Stage I engine performance was satisfactory throughout the flight. Flight integrated average performance parameters were close to the preflight predicted values.

Engine performance was calculated from measured flight data with the Martin-Baltimore PRESTO computer program using the Stage I thrust coefficient relationship as modified by Martin-Baltimore. The modification increased thrust and specific impulse approximately 3400 pounds and 2.0 seconds, respectively, above the values calculated using the Aerojet thrust coefficient relationship. The Martin-Baltimore modified thrust coefficient also was used in the preflight predictions.

The Stage I engine average flight performance, integrated from lift-off to $87FS_2$, is compared with the preflight prediction in Table III-2.

CONFIDENTIAL

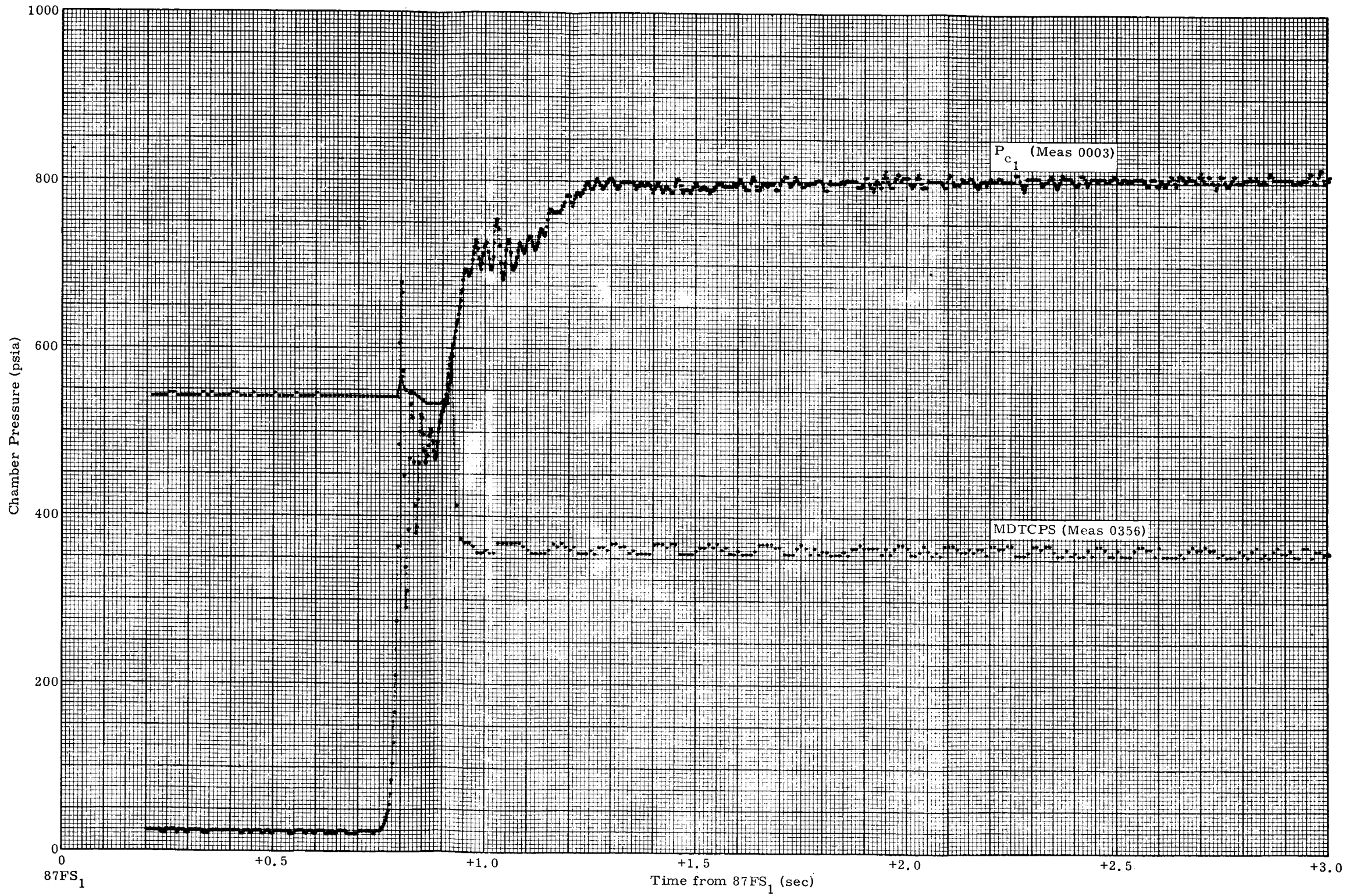

Fig. III-1. S/A 1 Start Transient

~~CONFIDENTIAL~~

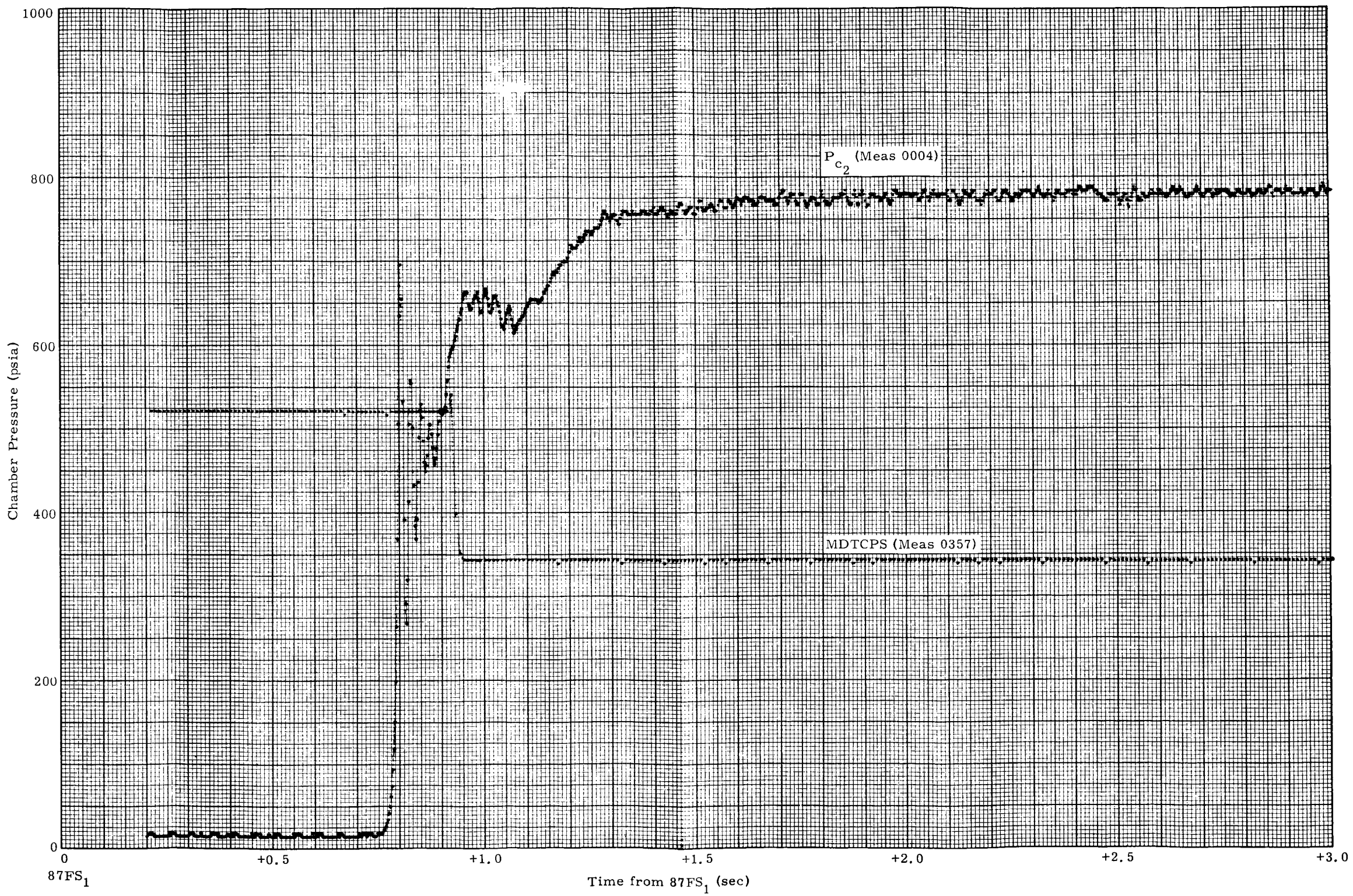

Fig. III-2. S/A 2 Start Transient

~~CONFIDENTIAL~~

TABLE III-2

Stage I Engine Predicted and Flight Performance Comparison

Parameter	Preflight Predicted Average	Flight Average	Difference (%)
Thrust, engine (lb)	461,046	458,899	-0.47
Specific impulse, engine (sec)	276.64	277.02	+0.14
Mixture ratio, engine	1.9166	1.9057	-0.57
Oxidizer flow rate, overboard (lb/sec)	1094.83	1086.09	-0.80
Fuel flow rate, overboard (lb/sec)	571.78	570.46	-0.23

The engine performance calculated throughout Stage I flight is presented in Fig. III-3. The preflight prediction is shown for comparison.

A comparison of measured and reconstructed thrust chamber pressures showed that the drift caused by the thermal environment was approximately -0.3% on this flight compared with ranges to approximately -2% on previous flights.

Stage I engine flight performance calculated at the $87FS_1$ + 55 second time slice and corrected to standard inlet conditions is shown in Table III-3. This is compared with the acceptance test and the predicted flight performance at standard inlet conditions and with the nominal time as used in the preflight prediction. The predicted flight performance at standard conditions was obtained by modifying the nominal acceptance test data for a 4850-pound acceptance-to-flight thrust growth obtained from analysis of Titan II and GLV flights. The engine mixture ratio was biased -0.5% (-0.0097), and specific impulse was biased +0.46 second based on GLV experience. The 55-second time slice performance, corrected to standard inlet conditions, is not representative of the total acceptance or flight performance; however, it is the nominal time used for quoting rated performance. Therefore, because of variations in the time-dependent biases and engine inlet conditions throughout flight, the data are indicative of the corrected performance at 55 seconds only.

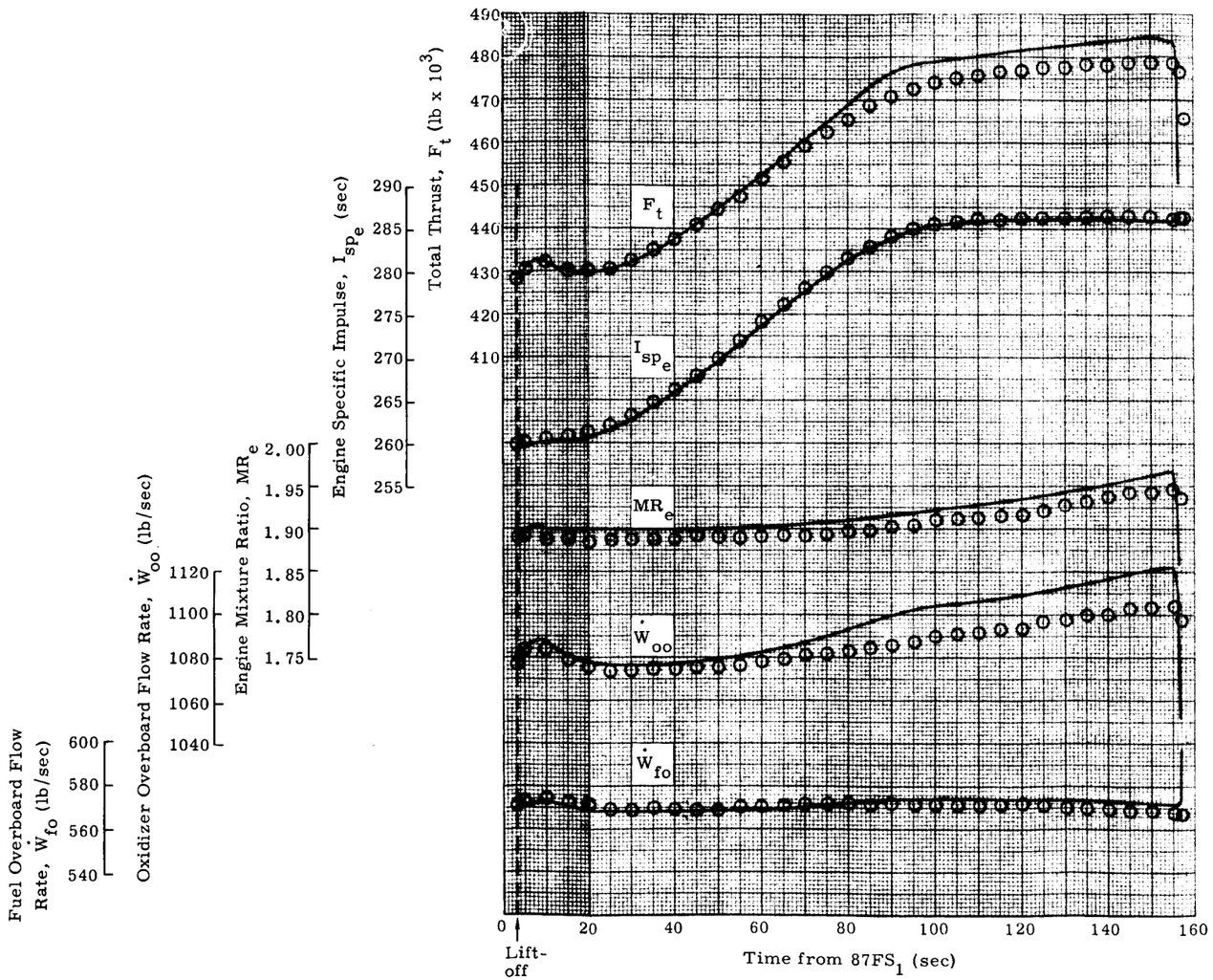

Average Engine Performance Integrated from Liftoff to $87FS_2$

Symbol	Preflight Prediction	Flight Average
F_t(lb)	461,046	458,899
I_{sp_e}(sec)	276.64	277.02
MR_e	1.9166	1.9057
$\dot{W}_{oo}$(lb/sec)	1094.83	1086.09
$\dot{W}_{fo}$(lb/sec)	571.78	570.46

——— Preflight prediction

⊙ Flight performance

Fig. III-3. Stage I Engine Flight Performance

TABLE III-3

Stage I Engine Performance Corrected to Standard Inlet Conditions at FS_1 + 55 seconds

	Acceptance Test*	Predicted Flight (including thrust growth, mixture ratio and I_{sp} biases)	Flight Performance*	Difference from Predicted (%)
Thrust, engine (lb)	428,688	433,538	433,973	+0.10
Specific impulse, engine (sec)	259.44	259.90	260.29	+0.15
Mixture ratio, engine	1.9344	1.9247	1.9196	-0.26
Oxidizer flow rate, overboard (lb/sec)	1088.91	1097.40	1095.88	-0.14
Fuel flow rate, overboard (lb/sec)	563.46	570.71	571.40	+0.12

*Martin-Baltimore modified thrust coefficient relationship used.

All flight data at FS_1 + 55 seconds corrected to standard inlet conditions were close to predicted conditions. The flight engine mixture ratio at standard conditions was -0.77% from the acceptance test value and -0.26% from predicted. A negative acceptance-to-flight mixture ratio shift at standard conditions was experienced on both stages of the flights of GLV-9 through GLV-12.

d. Shutdown transient

Stage I engine shutdown was initiated by fuel exhaustion. Figures III-4 and III-5 show S/A 1 and S/A 2 chamber pressure decays. All engine parameters were normal during the shutdown transient. The engine thrust at staging was approximately 26,000 pounds. Significant events during shutdown are presented in Table III-4.

TABLE III-4

Stage I Engine Shutdown Parameters

Parameter	S/A 1	S/A 2
Time from initial P_c decay to $87FS_2$ (sec)	0.20	0.20
P_c at $87FS_2$ (psia)	410	395
Time from $87FS_2$ to data dropout (sec)	0.71	0.71
P_c at data dropout (psia)	44	47

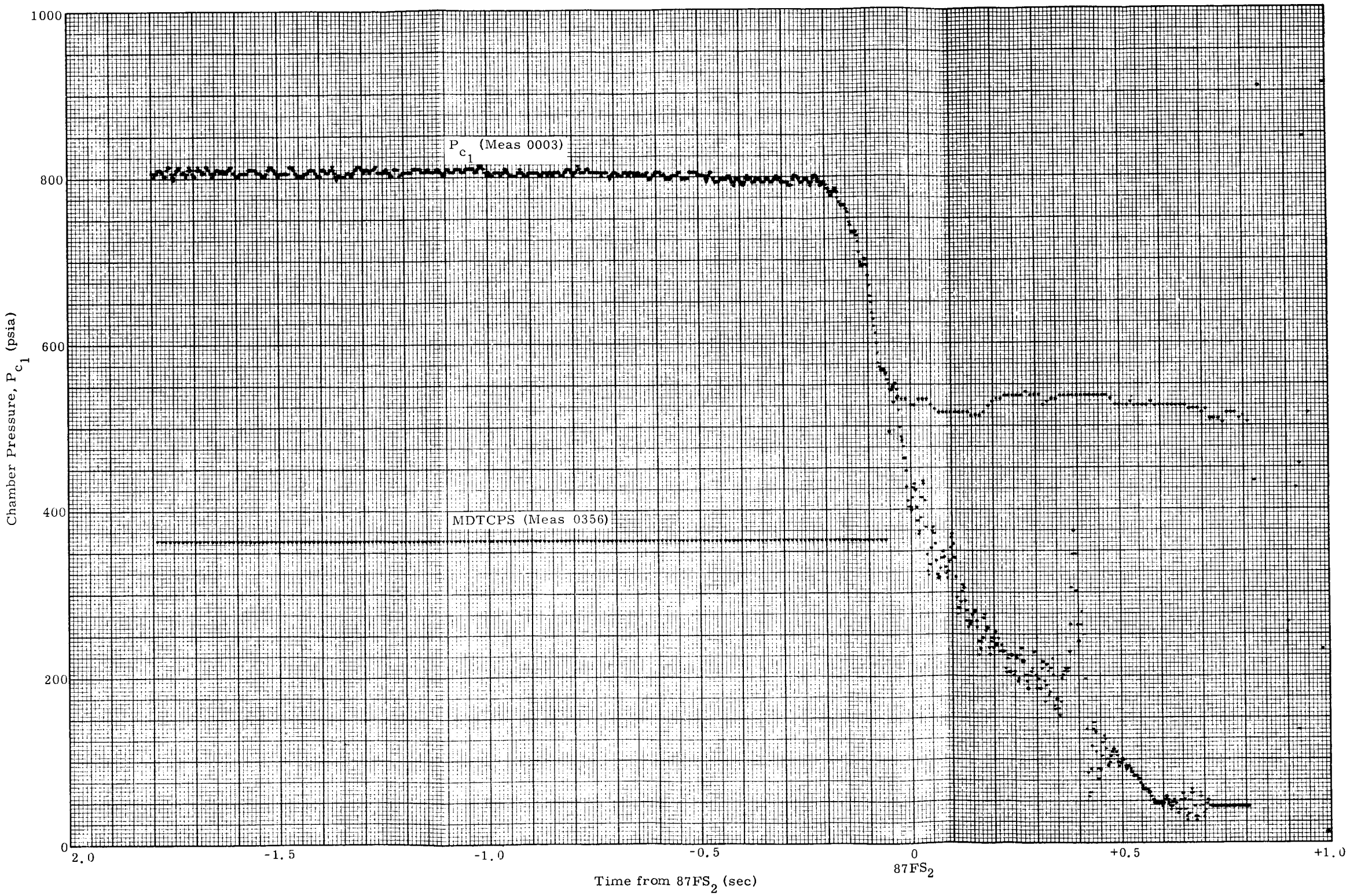

Fig. III-4. S/A 1 Shutdown Transient

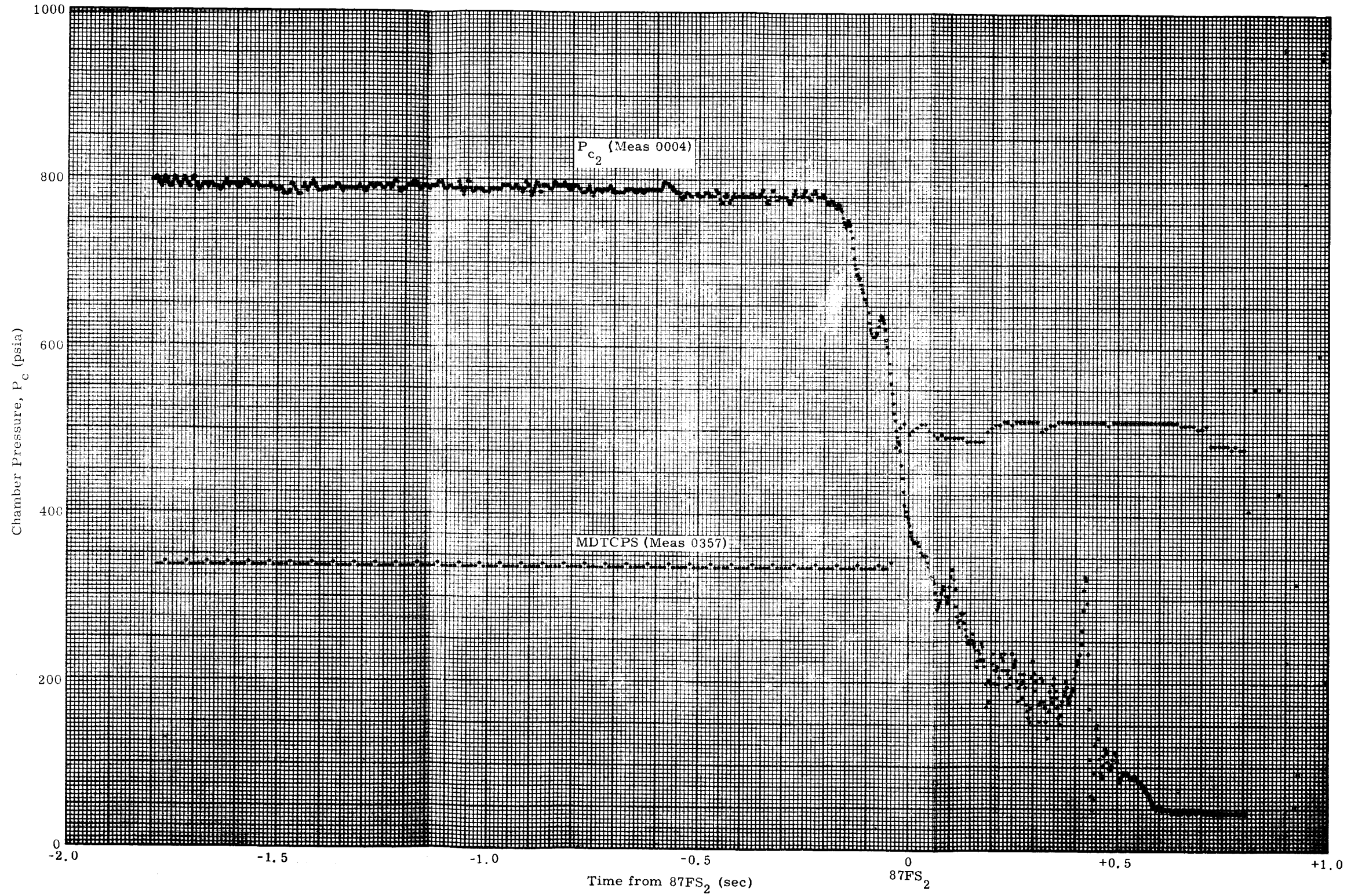

Fig. III-5. S/A 2 Shutdown Transient

e. Engine malfunction detection system (MDS)

The Stage I engine MDS operated within specified limits during the start and shutdown transients and operated satisfactorily throughout flight. Figures III-1 and III-2 illustrate the response times and actuation pressure levels of the malfunction detection thrust chamber pressure switches (MDTCPS) during engine start for S/A 1 and S/A 2, respectively. Figures III-4 and III-5 show the deactuation times and levels during shutdown for S/A 1 and S/A 2, respectively. A summary of the operating characteristics of the switches is tabulated in Table III-5.

f. Engine prelaunch malfunction detection system (PMDS)

The oxidizer pressurant pressure switch (OPPS) and the fuel pressurant differential pressure switch (FPDPS) actuated within specified actuation times and pressures as shown in Table III-5. A plot of PopOi and OPPS is shown in Fig. III-6.

TABLE III-5

Stage I MDS and PMDS Operation

Switch	MDTCPS 1	MDTCPS 2	OPPS	FPDPS
Actuation time				
Time from $87FS_1$ (sec)	0.925	0.925	1.582	0.913
Time from T-0 (sec)	0.981	0.981	1.636	0.967
Required time (sec)*	T+2.2	T+2.2	T+2.2	T+2.2
Actuation pressure				
Measured (psia)	600	595	418	**
Required (psia)	540 to 600	540 to 600	360 to 445	46 to 82 psid
Deactuation time (sec)	FS_2 - 0.055	FS_2 - 0.034	N/A	N/A
Deactuation pressure				
Measured (psia)	555	545	N/A	N/A
Required (psia)	585 to 515	585 to 515	N/A	N/A

* Shutdown timers start from T-0.
** Not instrumented.
N/A = Not applicable.

2. Stage II Engine (LR91-AJ-7, S/N 2006)

a. Configuration and special procedures

GLV-12 configuration and checkout procedures were the same as those used for GLV-11. The following special procedures were performed on GLV-12.

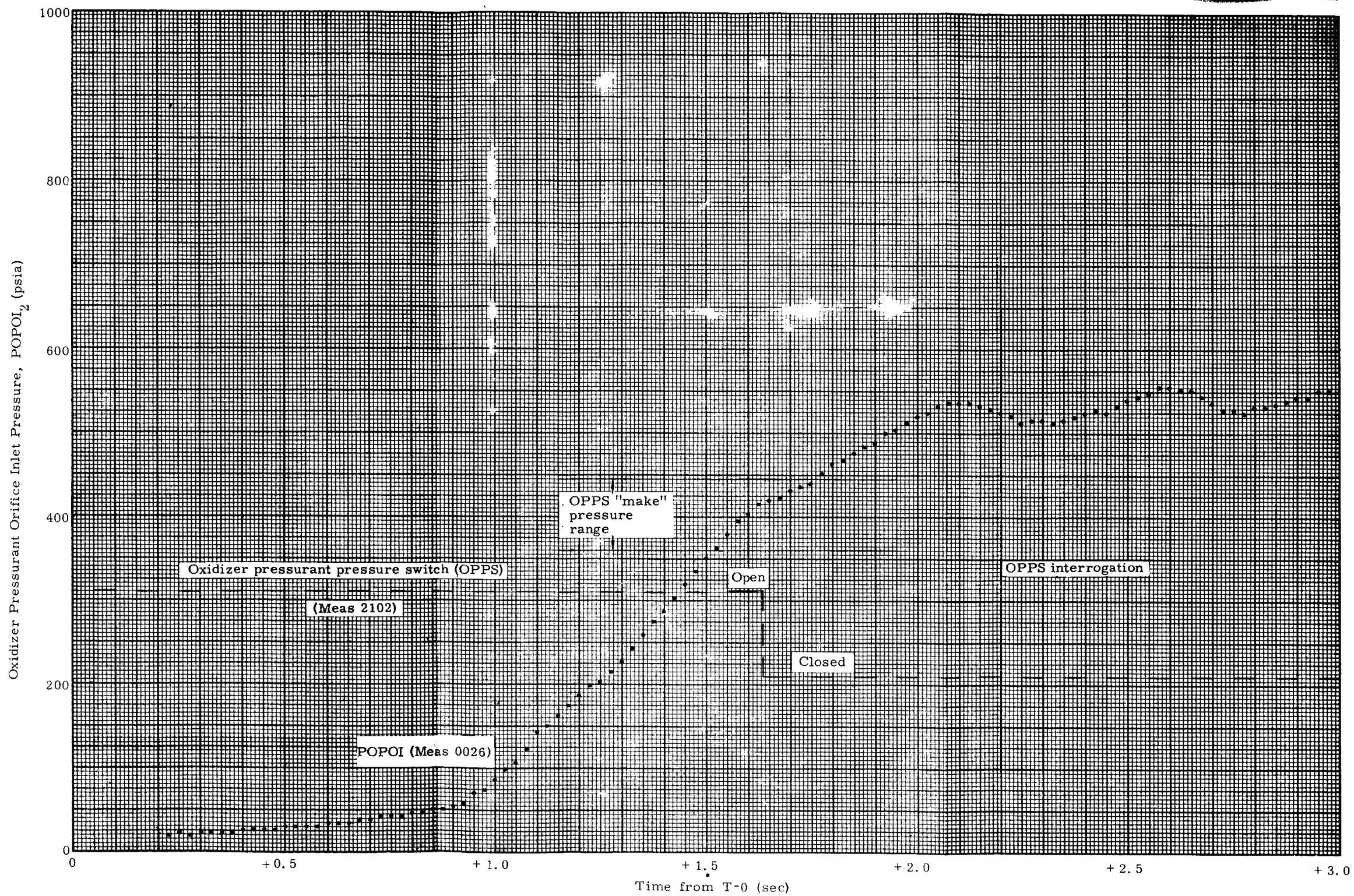

Fig. III-6. S/A 2 Start Transient

~~CONFIDENTIAL~~

(1) Teflon liner inspection was performed on the oxidizer bootstrap line and the hot gas cooler outlet line. Both lines were without defect.

(2) The oxidizer and fuel discharge lines were X-rayed for disjointed spider ball joints both at Martin-Baltimore and at ETR. All joints were proven satisfactory.

b. Stage II engine start transient

The engine start transient, as illustrated by the thrust chamber pressure in Fig. III-7, showed a normal chamber ignition; however, a double ignition spike was indicated. This phenomenon has been observed previously in flight (GLV-4) and has been noted in ground tests with no adverse effect on performance. A possible cause of the double ignition spike indication is a localized detonation near the sensing port, and the measured chamber pressure therefore was not representative of the thrust during the start transient. The CEC transducer was used to measure P_c and exhibited the characteristic underdamped oscillations which obscure true transient performance.

Significant start events are tabulated in Table III-6.

TABLE III-6

Stage II Engine Start Parameters

Parameter	
FS_1 to initial P_{c_3} rise (sec)	0.658
P_{c_3} ignition--first spike (psia)	408
P_{c_3} ignition--second spike (psia)	670
P_{c_3} step (psia)	510
P_{c_3} overshoot (psia)	Not available*

*Staging blackout period.

c. Steady-state performance

Stage II engine steady-state flight performance was satisfactory throughout flight. The average Stage II engine performance integrated over steady-state operation (from $91FS_1$ + 1.2 seconds to $91FS_2$) agreed

~~CONFIDENTIAL~~

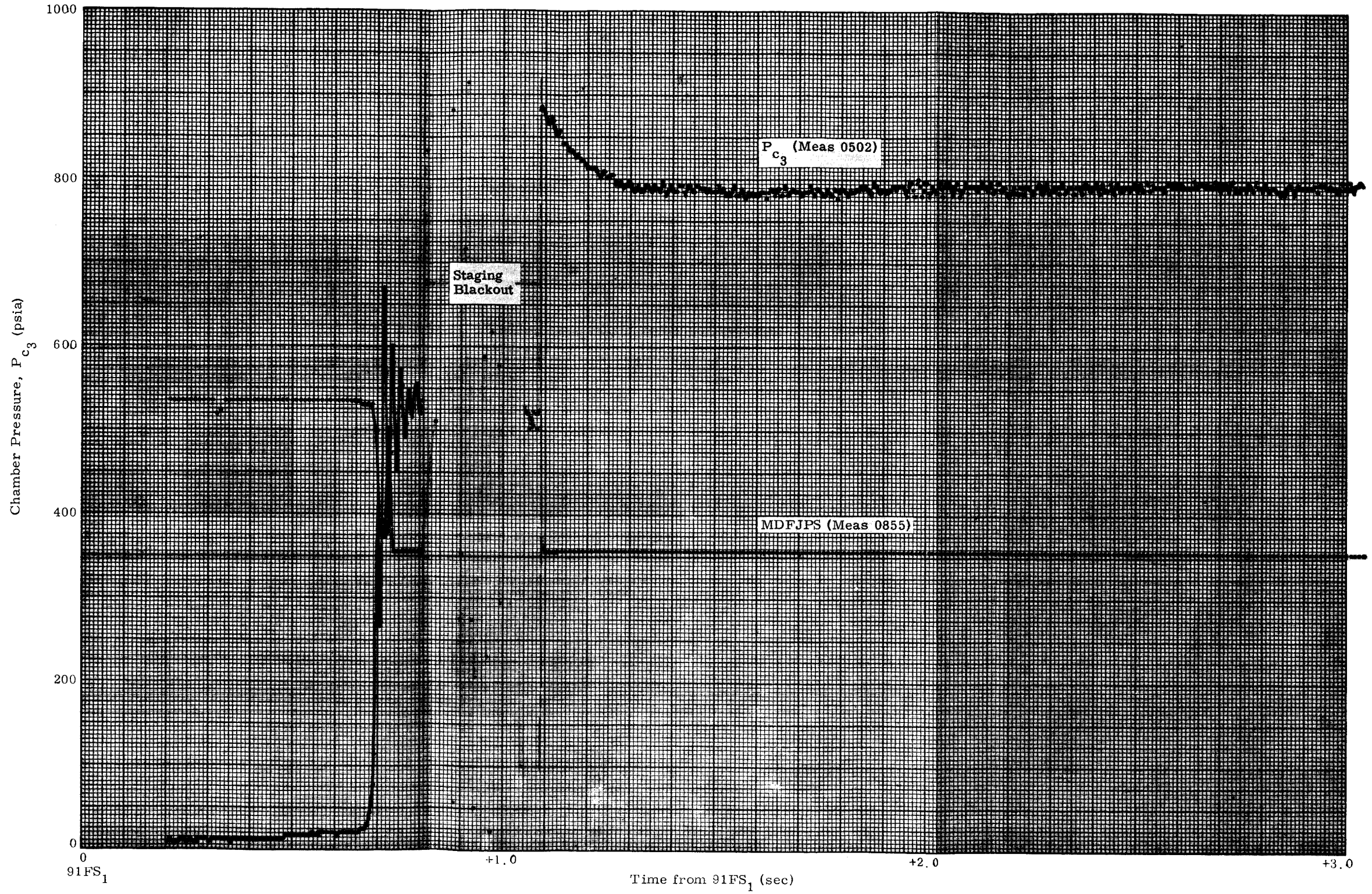

Fig. III-7. S/A 3 Start Transient

closely with preflight predictions. Average flight performance is compared in Table III-7.

TABLE III-7

Stage II Engine Predicted and Flight Performance Comparison

	Preflight Predicted Average	Flight Average	Difference (%)
Thrust, chamber (lb)	100,490	99,296	-1.19
Specific impulse, engine (sec)	312.93	313.22	+0.09
Mixture ratio, engine	1.7685	1.7526	-0.90
Oxidizer flow rate, overboard (lb/sec)	205.29	202.00	-1.60
Fuel flow rate, overboard (lb/sec)	115.83	115.01	-0.71

The engine flight performance calculated with the Martin-Baltimore PRESTO computer program is shown in Fig. III-8 as a function of time from $91FS_1$. The preflight prediction is presented for comparison.

Stage II engine flight performance prediction was run using the Martin-Baltimore derived performance influence curves as a function of oxidizer suction total pressure. It was found that, apparently, more cavitation exists at low oxidizer pump suction pressure than previously predicted. Also, a hysteresis effect was evident as oxidizer suction pressure decreased during the first part of flight and then increased during the latter portion of flight. These changes to the analytical model not only resulted in changes in the Stage II flight average mixture ratio (-0.4%) and specific impulse (+0.16%) from previous predictions but also improved the shape of the predicted curves as a function of time from $91FS_1$.

Engine flight performance at the $91FS_1$ + 55 second time slice corrected to standard inlet conditions is shown in Table III-8. Flight performance was corrected to standard conditions with two analytical models: (1) the model used to correct previous flights to standard conditions to serve as a reference condition, and (2) the model incorporating the Martin-Baltimore derived performance influence curves as a function of oxidizer suction total pressure. These are compared with the acceptance test, the predicted flight performance at standard inlet conditions and the nominal time as used in the preflight prediction. The

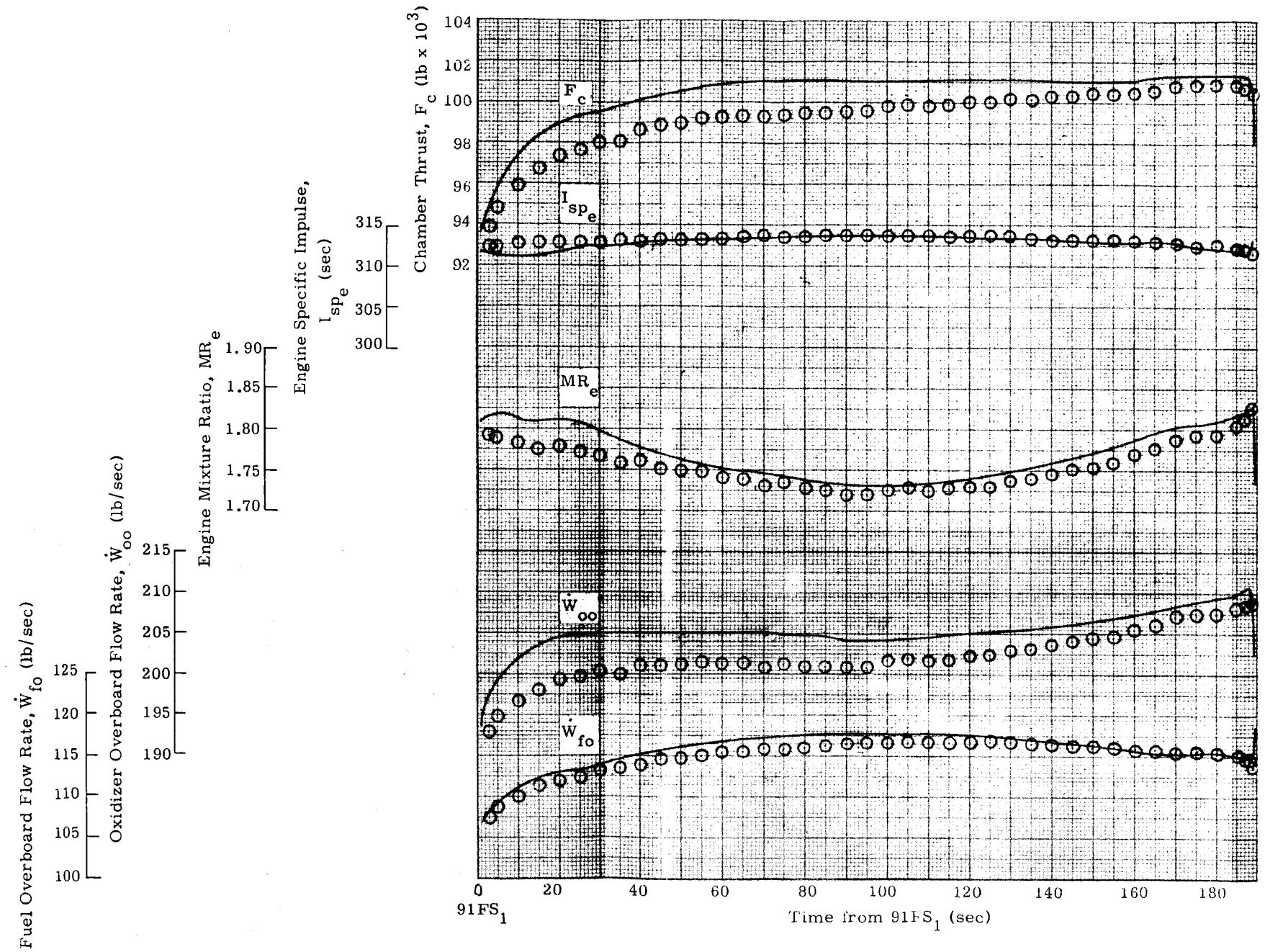

Average Engine Performance Integrated from First Steady-State to $91FS_2$

Symbol	Preflight Prediction	Flight Average
F_c(lb)	100,490	99,296
I_{sp_e}(sec)	312.93	313.22
MR_e	1.7685	1.7526
$\dot{W}_{oo}$(lb/sec)	205.29	202.00
$\dot{W}_{fo}$(lb/sec)	115.83	115.01

—— Preflight prediction
○ Flight performance

Fig. III-8. Stage II Engine Flight Performance

~~CONFIDENTIAL~~

TABLE III-8

Stage II Flight Performance Corrected to Standard Inlet Conditions at $91FS_1$ + 55 Seconds

Parameter	Acceptance Test	Predicted Flight (including thrust growth)	Flight Performance			
			Previous Model		Model Including Martin-Baltimore Post Influence Curves	
			Performance	Difference from Predicted (%)	Performance	Difference from Predicted (%)
Thrust, chamber (lb)	99,789	100,689	99,369	-1.31	99,189	-1.49
Specific impulse engine (sec)	312.04	312.04	312.58	+0.17	312.33	+0.09
Mixture ratio, engine	1.8106	1.8106	1.7810	-1.63	1.7952	-0.85
Oxidizer flow rate, overboard (lb/sec)	206.17	208.03	203.74	-2.06	204.13	-1.87
Fuel flow rate, overboard (lb/sec)	113.62	114.64	114.16	-0.42	113.45	-1.04

predicted flight performance at standard inlet conditions was obtained by adjusting the nominal acceptance test data for a 900-pound acceptance-to-flight thrust growth obtained from analysis of previous Titan II and GLV flights. The 55-second time slice performance corrected to standard inlet conditions is not representative of the total acceptance or flight performance. This is the nominal time used for quoting rated performance, and the data indicate a comparison of corrected performance at 55 seconds only because of variations in time-dependent biases and engine inlet conditions throughout flight.

The most evident features of the performance at standard inlet conditions are the lower-than-expected oxidizer and fuel flow rates. A negative mixture ratio shift resulted from a greater percentage negative shift in oxidizer flow than fuel flow.

The negative shift of mixture ratio from acceptance test conditions continues a trend observed in both stages of GLV-9, GLV-10 and GLV-11.

d. Shutdown transient

Stage II engine shutdown was initiated by guidance command, with $91FS_2$ occurring at $91FS_1$ + 188.790 seconds. The calculated shutdown impulse from $91FS_2$ to $91FS_2$ + 20 seconds was 33,971 lb-sec, and the predicted impulse was 36,100 ± 7000 lb-sec.

~~CONFIDENTIAL~~

The impulse obtained from the ±10 g accelerometer data was 23,069 lb-sec using an average spacecraft/Stage II weight of 14,456 pounds over the time interval from $91FS_2$ to $91FS_2$ + 0.593 second. The initial portion of the shutdown transient is illustrated by the P_{c_3} decay in Fig. III-9. Impulse from $91FS_2$ + 0.593 second to $91FS_2$ + 20 seconds was 10,902 lb-sec, obtained from the ±0.5 g accelerometer data and an average weight of 14,392 pounds. Zero thrust occurred at approximately $91FS_2$ + 14.9 seconds.

Thrust tailoff, calculated from the ±0.5 g axial accelerometer data (Meas 0699), is illustrated in Fig. III-10, which shows that the accelerometer recorded one small post-SECO disturbance. The disturbance was noted at approximately $91FS_2$ + 4.1 seconds, was less than 0.02 g peak-to-peak, and was seen only in the ±0.5 g accelerometer data.

e. Engine malfunction detection system (MDS)

The Stage II engine MDS operated satisfactorily throughout flight. Figures III-7 and III-9 illustrate the response times and chamber pressure correlation of the malfunction detection fuel injector pressure switches (MDFJPS) during the start and shutdown transients, respectively. The fuel injector pressure is not shown since this parameter is not measured. A summary of the significant switch parameters is presented in Table III-9.

TABLE III-9

Stage II MDS Operation

Actuation time (sec)	$91FS_1$ + 0.731
P_c at actuation (psia)	280
Deactuation time (sec)	$91FS_2$ + 0.141
P_c at deactuation (psia)	463

B. PROPELLANT SUBSYSTEM

1. Propellant Loading

a. Loading operations

Two propellant loadings, consisting of tanking tests and the launch loading, were performed on GLV-12. During the tanking test each tank was loaded individually up to high-light with the quantity flowed measured

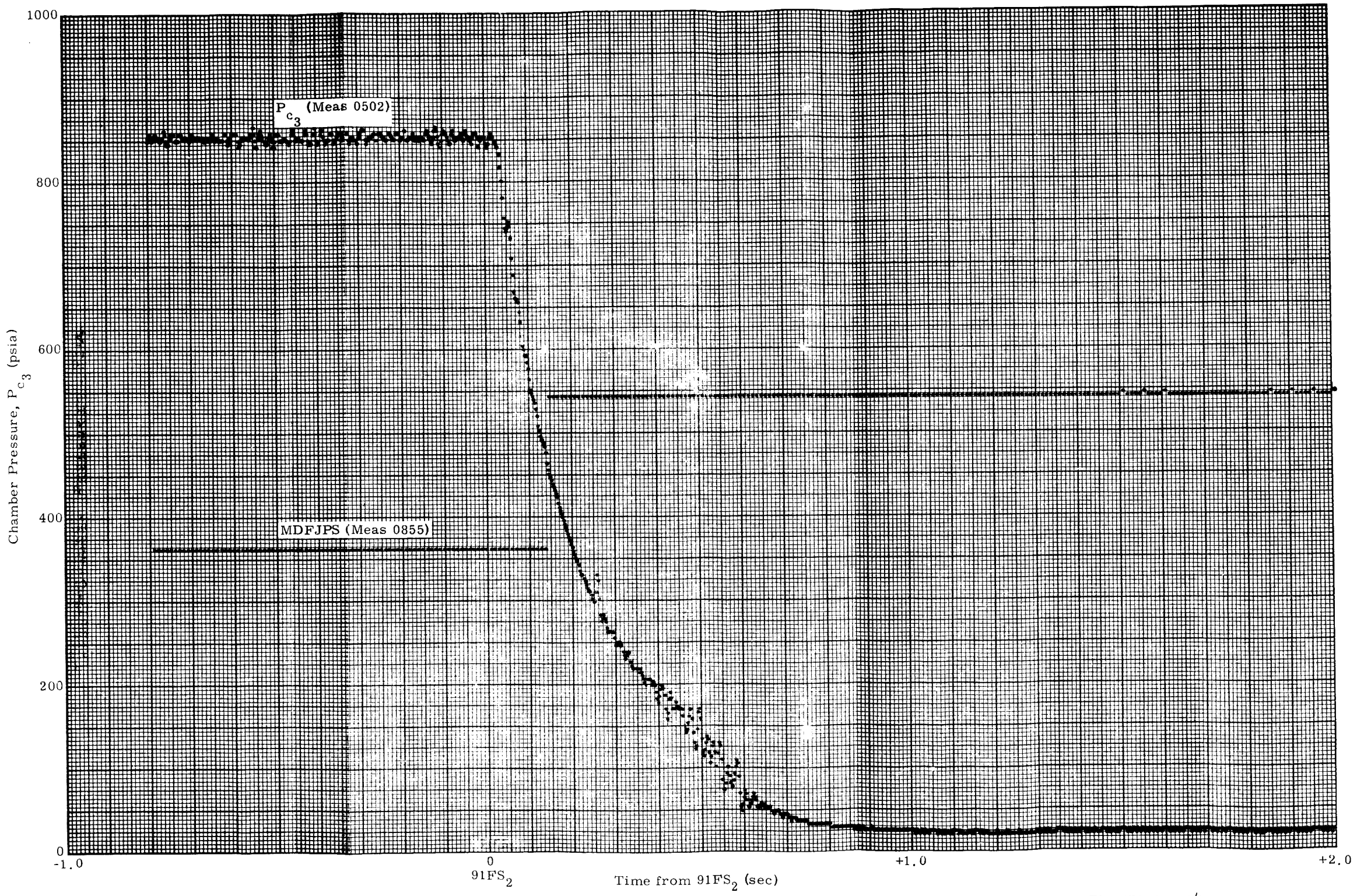

Fig. III-9. S/A 3 Shutdown Transient

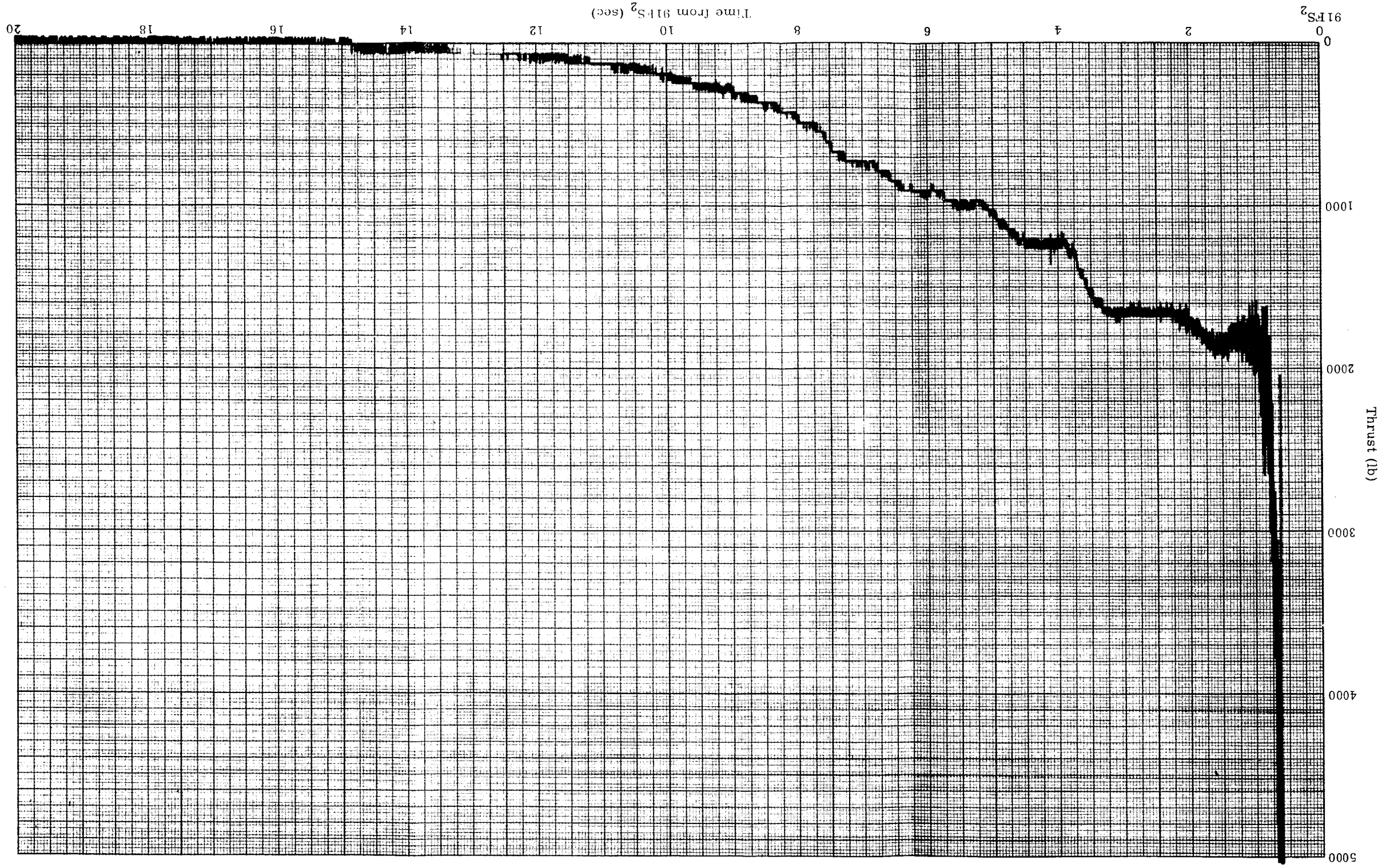

Fig. III-10. Stage II Engine Thrust Tail-Off

~~CONFIDENTIAL~~

by all four meters. The tanks were dual-loaded to mission load for the launch. The primary RSVs were used to service oxidizer and fuel for the tanking test and launch.

The results of the tanking test and launch are presented in Table III-10. The data show good agreement between the flowmeter indicated volume and the calibrated tank volume at high-light for all tanks.

TABLE III-10

Flowmeter Deviation (%) at High-Light Verification

Event	Oxidizer			
	Stage I	Meter	Stage II	Meter
	199168	206360	204277	199167
Tanking test	-0.046	+0.132	+0.289	+0.072
Launch	-0.024	+0.180	+0.249	+0.076
	Fuel			
	199169	202146	206361	199171
Tanking test	+0.142	+0.142	+0.178	+0.220
Launch	+0.147	+0.148	+0.102	+0.163

During Stage I oxidizer tank loading, the tank bottom probe temperature indicated 29.5° F at high-light. Other loading data indicated that the tank bottom temperature should be 1° F higher, and the Stage I oxidizer tank was loaded accordingly. A subsequent check of the temperature probe proved the reading to be correct. The 1° F temperature error resulted in a 12-gallon overload in the Stage I oxidizer tank.

A summary of the loading schedule for the launch operation is presented in Table III-11. Results of the tank loading demonstrate the repeatability of the PTPS system. All propellant loading operations proceeded without malfunction of the PTPS components.

Propellant loads as determined by flight verification are shown in Table III-12. The flight loads were calculated from a propellant inventory, using actual level sensor uncover times and tank calibration data to determine flow rates.

The total integrated in-flight overboard propellant consumption was determined by using the engine analytical model matched to the flow rate between the level sensors.

~~CONFIDENTIAL~~

TABLE III-11

Propellant Loading Schedule

Launch	Event	Time (EST)			
		Stage I Oxidizer	Stage II Oxidizer	Stage I Fuel	Stage II Fuel
11-11-66	Start prechill	0237	0237	0452	0452
	Start load	0253	0253	0511	0511
	High-light	0416	0329	0605	0542
	Load complete	0432	0347	0614	0548

TABLE III-12

Propellant Loading

Tank	Requested Load (lb)	Postflight Recon-structed (%)	Launch Corrected Flowmeter Load (lb)	Difference Requested and Recon-structed (%)	Difference Launch and Recon-structed (%)
Stage I					
Fuel	90,140	90,092	90,157	-0.053	-0.072
Oxidizer	171,199	171,665	171,308	+0.272	+0.208
Stage II					
Fuel	22,126	22,061	22,124	-0.293	-0.284
Oxidizer	38,882	38,781	38,857	-0.259	-0.195

The percentage differences noted in Table III-12 are the best estimates of how the flight data compare with the preflight loading information.

b. Total propellant loads

Total mission loads as determined from flowmeters are shown in Table III-12. The flowmeter readings were corrected for the propellant remaining in the fill lines, the propellant vaporized, the propellant temperature rise from average flowmeter temperature to high-light temperature and actual flow rate.

CONFIDENTIAL

The temperature rise from the average flowmeter temperature to the high-light temperature for the tanking test, launch attempts and launch operation is presented in Table III-13. The loading error analysis assumes the maximum deviation between the average flowmeter temperature and the high-light temperature to be ±1.5° F for Stage I fuel and oxidizer and ±1.3° F for Stage II fuel and oxidizer.

The data shown in Table III-13 were taken from the information in Figs. III-11 and III-12.

TABLE III-13

Average Temperature Rise from Flowmeter to High-Light

Tank	Temperature Rise (° F)		
	Tanking Test	Launch	Predicted
Stage I			
Fuel	1.1	1.0	0.65
Oxidizer	1.8	1.0	1.10
Stage II			
Fuel	2.7	1.3	1.65
Oxidizer	2.3	1.2	1.40

c. Propellant assay

The prelaunch data from the propellant assay laboratory report (sampled on F-14 day) for the oxidizer and fuel are presented in Table III-14. Specification values are also listed. Good agreement between the analysis and specification requirements was obtained. The density was determined by a pycnometer.

2. Propellant Temperature

a. Weather

Table III-15 presents the F-45 day prediction, the F-1 day 1800 hour prediction and the actual 11 November launch weather for GLV-12. The F-45 day prediction was based on a 90% hot April through November day.

CONFIDENTIAL

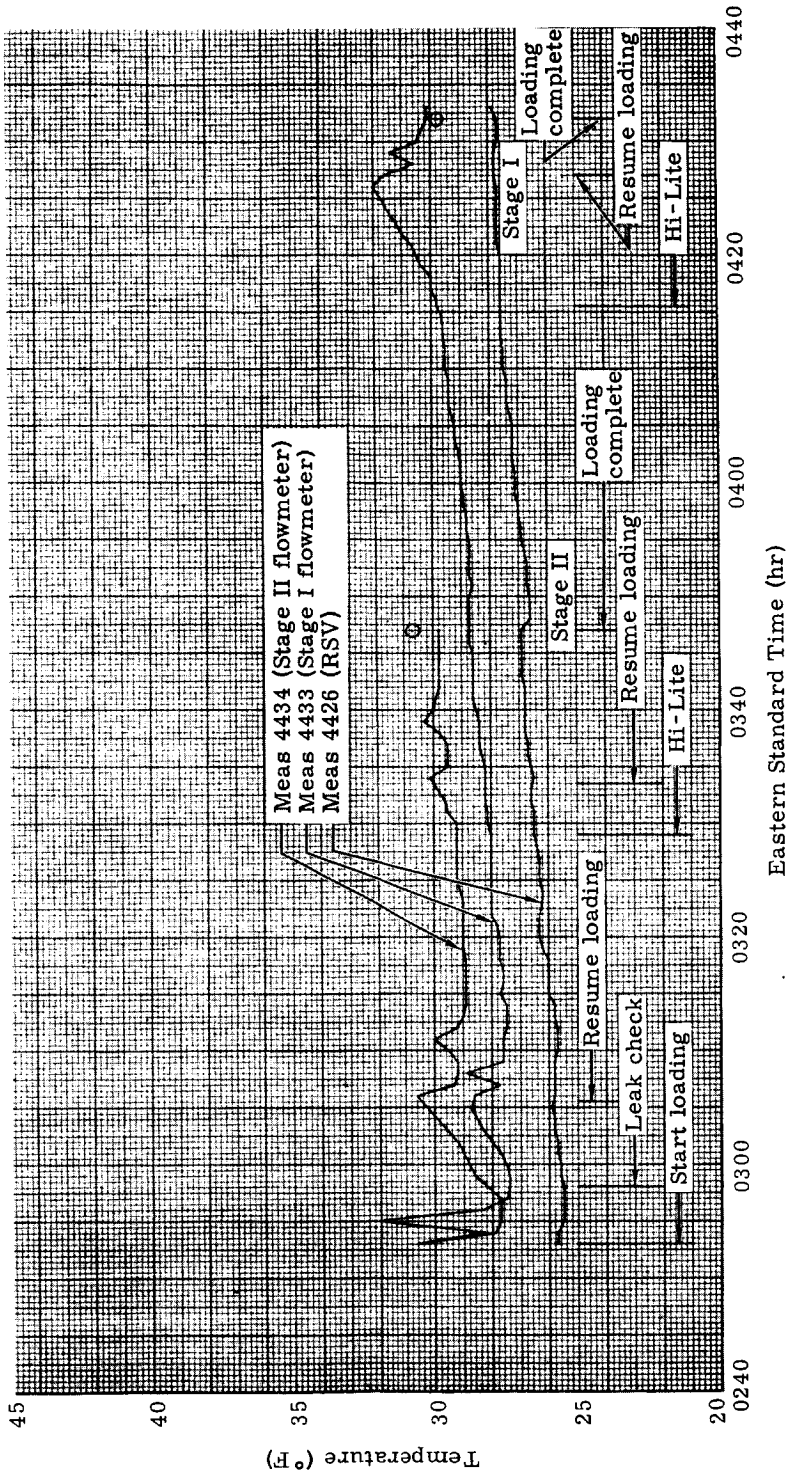

Fig. III-11. Oxidizer Temperatures During Loading

[redacted]

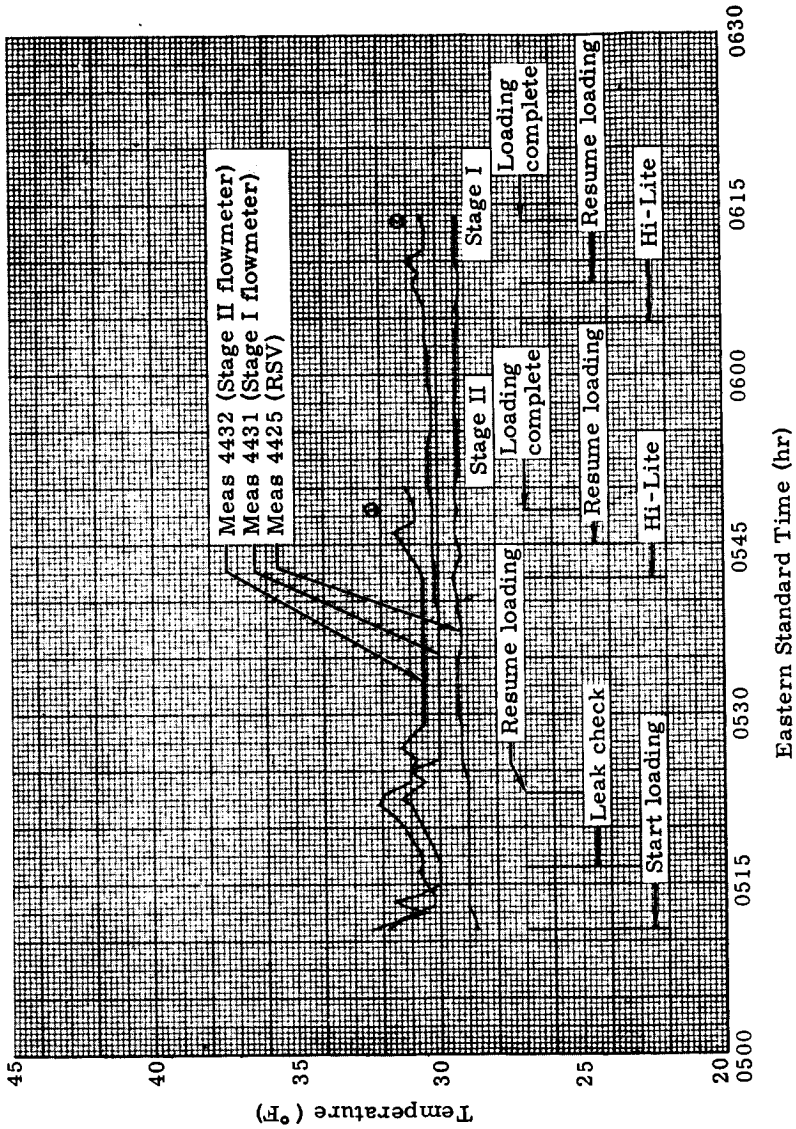

Fig. III-12. Fuel Temperatures During Loading

[redacted]

TABLE III-14

Propellant Assay Summary

	Primary	Secondary	Requirement
Fuel MIL-P-27402 (USAF)			
Hydrazine (%)	51.1	50.9	51 ± 0.8
UDMH plus amines (%)	47.6	47.6	47.0 min
H_2O (%)	1.3	1.5	1.8 max
Total N_2H_4 plus UDMH (%)	98.7	98.5	98.2 min
Solids (mg/liter)	None	0.42	10
Particles on 50 mesh screen	0	0	0
Density (gm/cm^3) at 77° F	0.8989	0.9007	0.894/0.903
Oxidizer MIL-P-26539 (USAF)			
Nitrogen tetroxide (N_2O_4) (%)	99.5	99.6	99.5 min
Chloride as NOCl (%)	0.01	0.01	0.08 max
H_2O equivalent (%)	0.10	0.10	0.1 max
Solids (mg/liter)	None	0.3	10
Nonvolatile ash	*	*	*
Particles on 50 mesh screen	0	0	0

* No data available.

b. Propellant loading temperatures

Table III-16 compares the required propellant temperatures in the RSV outlet (at start of loading) and the tank bottom probe (at high-light) with measured values.

Both oxidizer and fuel differences are within the required tolerances.

c. Liftoff temperatures

A comparison of predicted, actual and reconstructed propellant bulk temperatures appears in Table III-17.

TABLE III-15

Predicted and Actual Weather Conditions for GLV-12

Time (EST)	Dry Bulb Temperature (°F)			Dew Point Temperature (°F)			Wind Speed (kn)			Cloud Cover		
	F-45	F-1 (1800)	Actual	F-45	F-1 (1800)	Actual	F-45	F-1 (1800)	Actual (kn)/ Direction (deg)	F-45	F-1 (1800)	Actual
0300	74.7	65	69	64.0	59	64	6.5	3	6/260	0.5	0.3	0.3
0400	74.6		67	63.8		63	6.5		4/258	0.5		0.3
0500	74.4		68	63.7		63	6.5		5/276	0.5		0.3
0600	74.3	66	68	63.6	59	63	6.5	5	5/295	0.5	0.2	0.3
0700	75.3		68	64.9		64	6.5		5/295	0.5		0.2
0800	77.2		69	66.1		65	8.0		3/311	0.5		0.0
0900	78.8	70	74	67.2	61	67	10.0	5	1/279	0.5	0.3	0.0
1000	80.0		75	68.2		65	11.0		4/042	0.5		0.1
1100	81.3		76	68.8		66	11.5		5/065	0.5		0.2
1200	82.2	75	76	69.2	63	65	12.0	8	6/090	0.5	0.2	0.1
1300	82.4		76	69.4		64	12.5		7/104	0.5		0.1
1400	82.4		75	69.4		64	13.0		5/092	0.5		0.2
1500	81.6	78	75	69.2	64	65	12.5	10	5/101	0.5	0.0	0.2
1600	80.9		75	68.8		65	12.0		7/091	0.5		0.2

TABLE III-16

Propellant Loading Temperatures

System	RSV (° F)			Tank Bottom Probe (° F)		
	Requested	Actual	Δ	Requested	Actual	Δ
Stage I oxidizer	25.0	25.7	+0.7	28.2	29.5	+0.3
Stage II oxidizer	25.0	25.7	+0.7	30.7	30.2	-0.5
Stage I fuel	29.0	28.7	-0.3	32.0	31.3	-0.7
Stage II fuel	29.0	28.7	-0.3	33.3	32.0	-1.3

TABLE III-17

Propellant Bulk Temperature Comparison

System	F-45 Day Prediction	F-0 Day Prediction	Actual	Reconstructed
Stage I oxidizer	45.9	44.7	44.5	44.0
Stage I fuel	48.3	43.6	44.9	44.0
Stage II oxidizer	47.8	45.8	45.8	44.1
Stage II fuel	44.9	43.7	43.9	42.9

Actual bulk temperatures were obtained by averaging the flight temperature profiles and adjusting for the differences listed in Table III-18.

TABLE III-18

Propellant Temperature Comparison Tank Bottom Probe and Pump Inlet

System	Time (sec)	Suction Probe Temperature (° F)	Tank Bottom Probe Temperature (° F)	ΔTemperature (° F)
Stage I fuel	$FS_1 + 5$	44.0	43.6	+0.4
Stage II fuel	$FS_1 + 25$	41.8	41.9	-0.1
Stage I oxidizer	$FS_1 + 6$	41.7	41.0	+0.7
Stage II oxidizer	$FS_1 + 22$	54.8	44.6	+10.2

Correlation of the F-0 day predicted and the actual bulk temperatures was good, as shown on the mixture ratio band plots of Figs. III-13 and III-14. The agreement between the reconstructed and actual stage temperatures is low but within known program capabilities.

~~CONFIDENTIAL~~

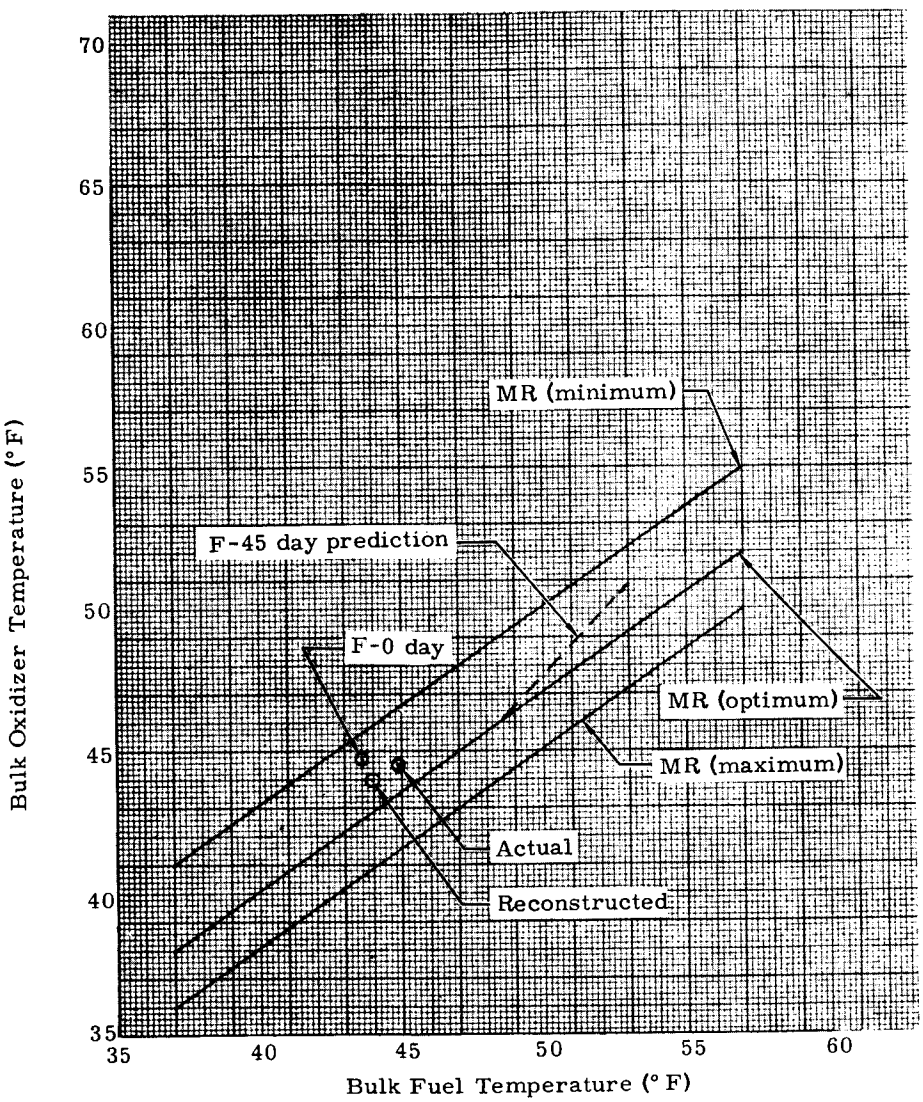

Fig. III-13. Propellant Bulk Temperatures at Liftoff, Stage I

~~CONFIDENTIAL~~

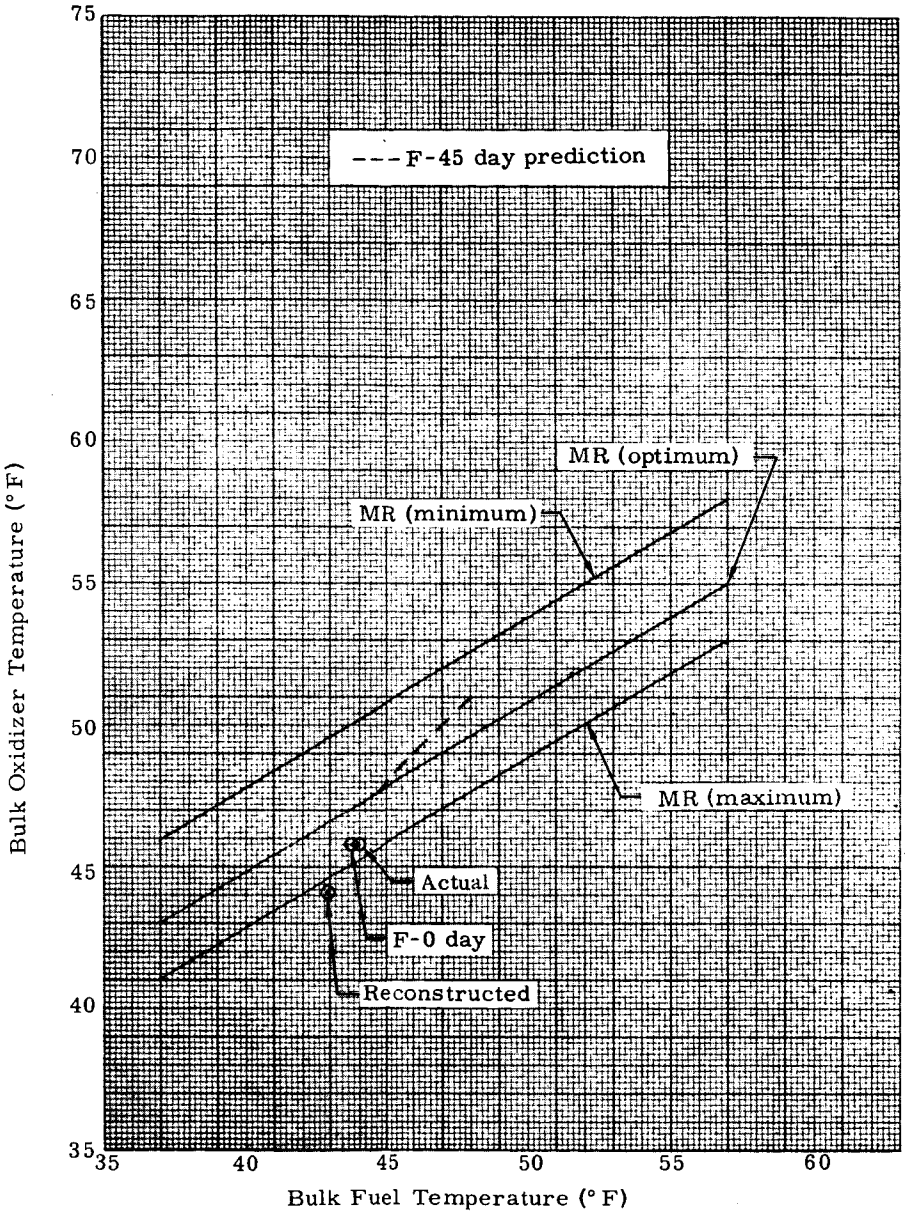

Fig. III-14. Propellant Bulk Temperatures at Liftoff, Stage II

Real-time monitoring was used to give the F-0 day predictions of bulk temperatures. This use of updated predictions (using actual probe readings) prevented any large errors in bulk temperature prediction.

The correlation of F-1 day predicted, actual and reconstructed tank bottom probe readings is shown in Figs. III-15 through III-18. Changes in initial temperatures and weather conditions account for the differences between the F-1 day and reconstructed curves. The differences between the actual and reconstructed points on the Stage II oxidizer tank are attributed to the previously mentioned low program correlation. Updating (using actual probe readings) during the temperature monitoring portion of the countdown eliminated any problem because of these differences.

d. Suction temperatures

The general condition of the pump inlet temperatures was in good agreement with the predicted temperature profiles. These data are shown in Figs. III-19 through III-22. Except for the Stage II oxidizer, the small differences in absolute level may be attributed to differences in predicted and actual weather and predicted and actual thermal stratification. The suction probe for the Stage II oxidizer has a 10.2° F bias in the reading caused by a faulty suction temperature probe.

In Table III-18, a comparison is made between the suction and tank bottom probes at various times after FS_1.

Due to the greater accuracy of the tank bottom probes, the best estimate propellant temperatures are those that would be obtained if the suction probe profile were shifted to agree with the tank bottom probe. In the postflight propellant temperature analyses, this shift has been applied to all four tanks.

3. Propellant Feed System

a. Feedline transients

The maximum transient pressures recorded at the pump inlet instrumentation bosses are listed in Table III-19.

Ignition transient pressures were, in general, similar to GLV-10 and GLV-11 flight data. Telemetry blackout normally experienced during Stage II ignition prevents obtaining data on sustainer engine ignition transients.

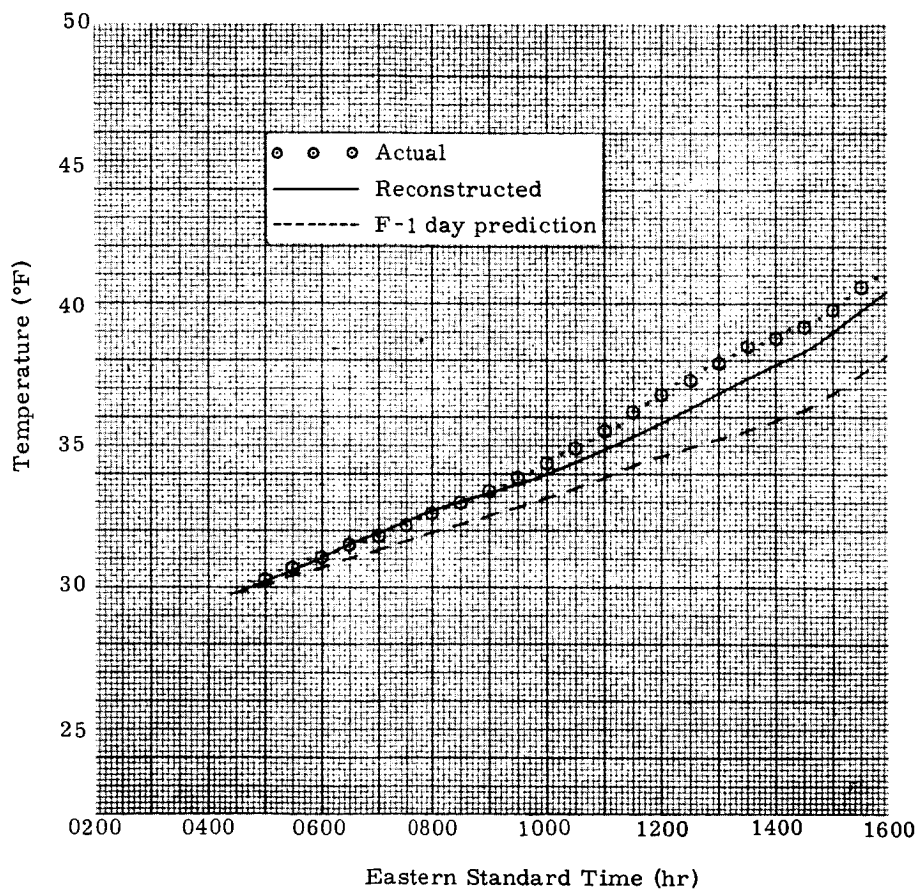

Fig. III-15. Stage I Oxidizer Tank Bottom Probe Temperature (Meas 4128)

~~CONFIDENTIAL~~

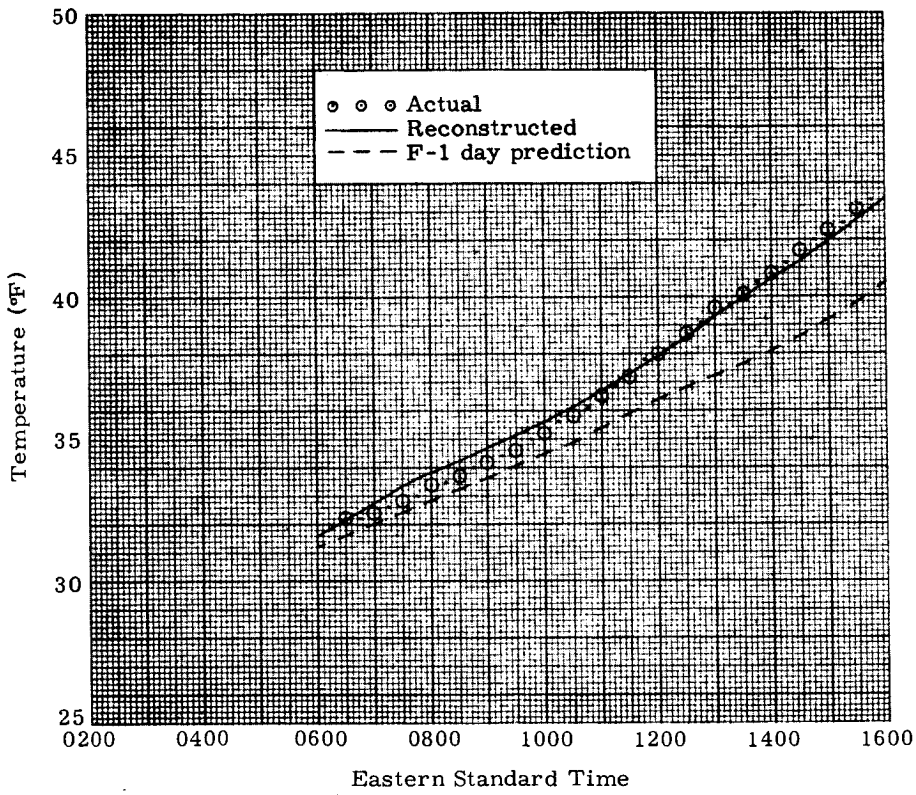

Fig. III-16. Stage I Fuel Tank Bottom Probe Temperature (Meas 4124)

~~CONFIDENTIAL~~

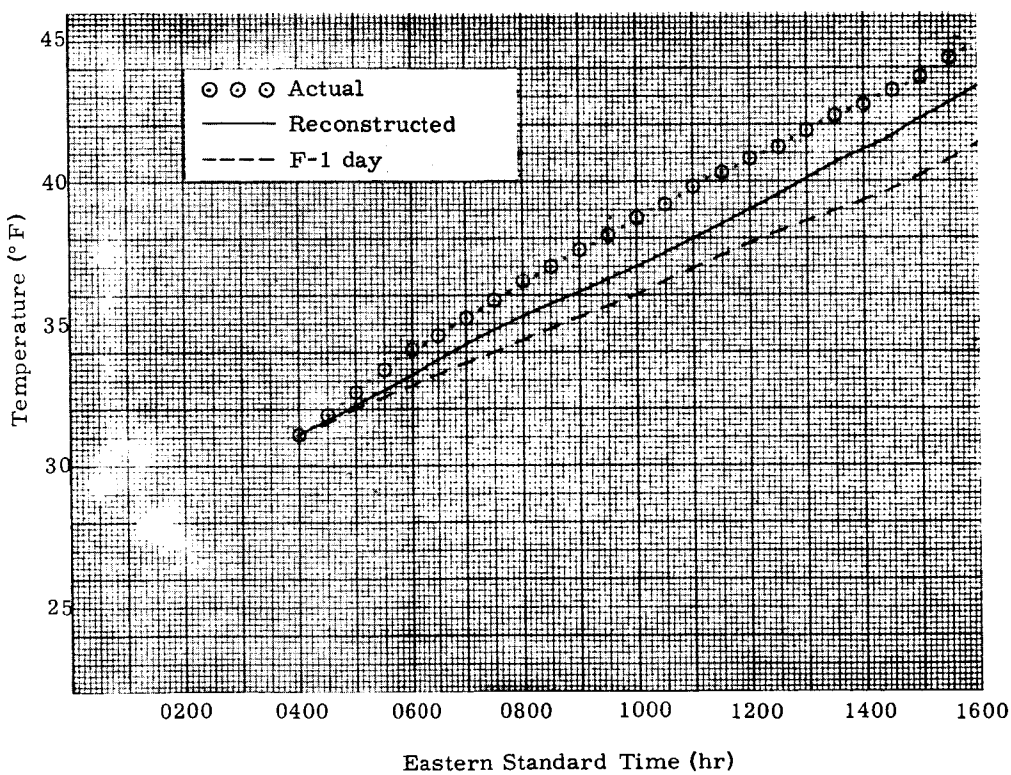

Fig. III-17. Stage II Oxidizer Tank Bottom Probe Temperature (Meas 4604)

[redacted]

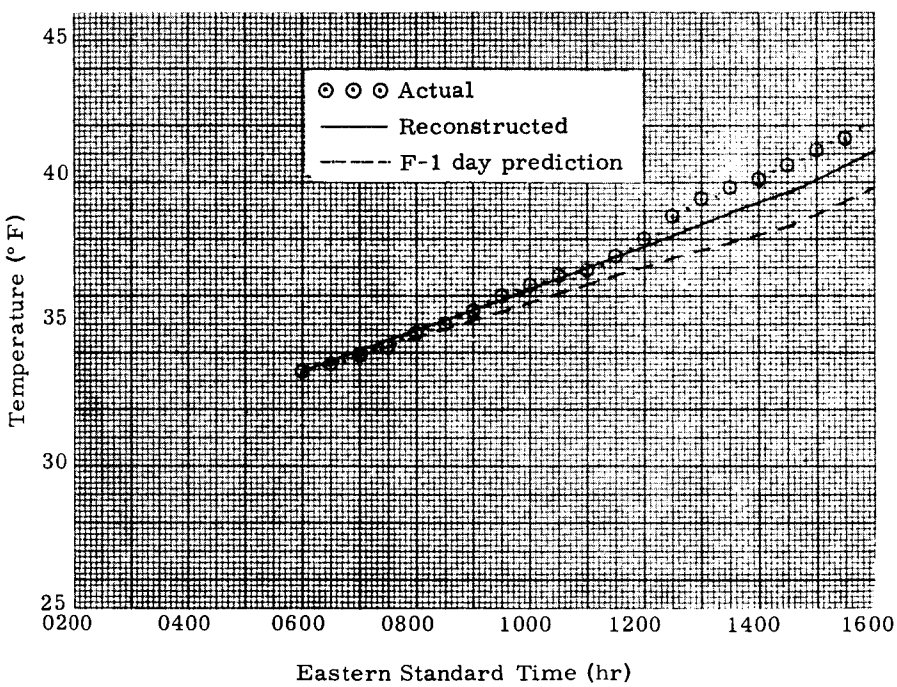

Fig. III-18. Stage II Fuel Tank Bottom Probe Temperature (Meas 4601)

[redacted]

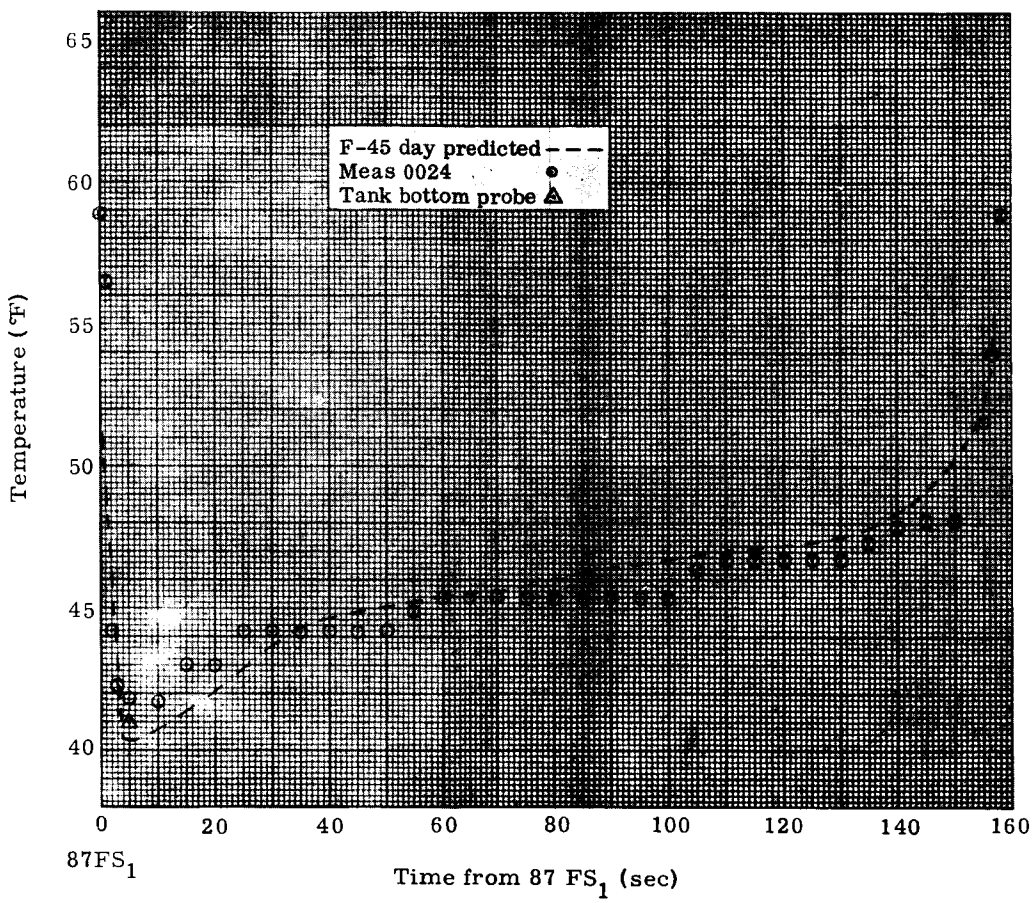

Fig. III-19. Stage I Oxidizer Pump Inlet Temperature

[redacted]

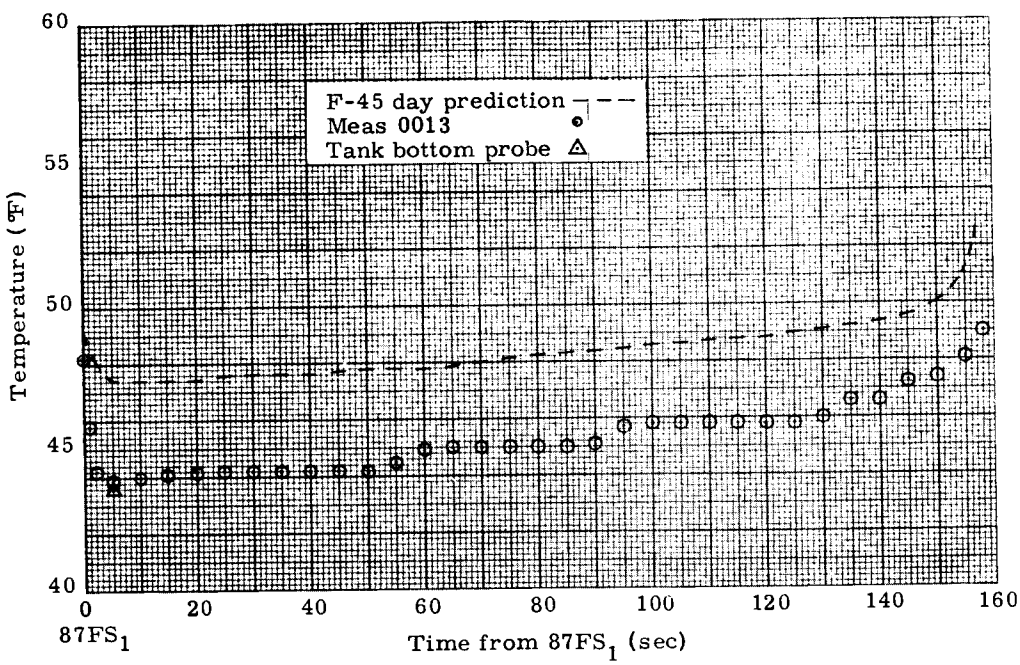

Fig. III-20. Stage I Fuel Pump Inlet Temperature

[redacted]

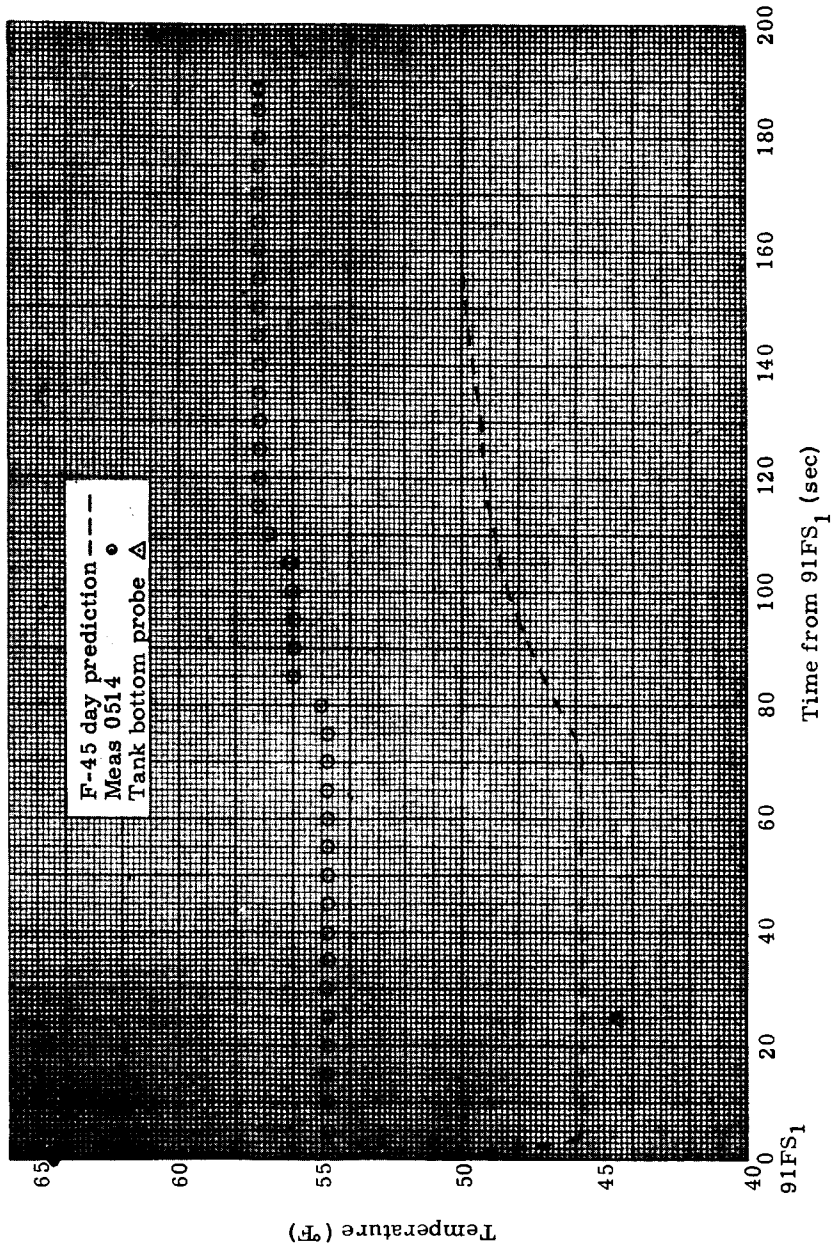

Fig. III-21. Stage II Oxidizer Pump Inlet Temperature

[redacted]

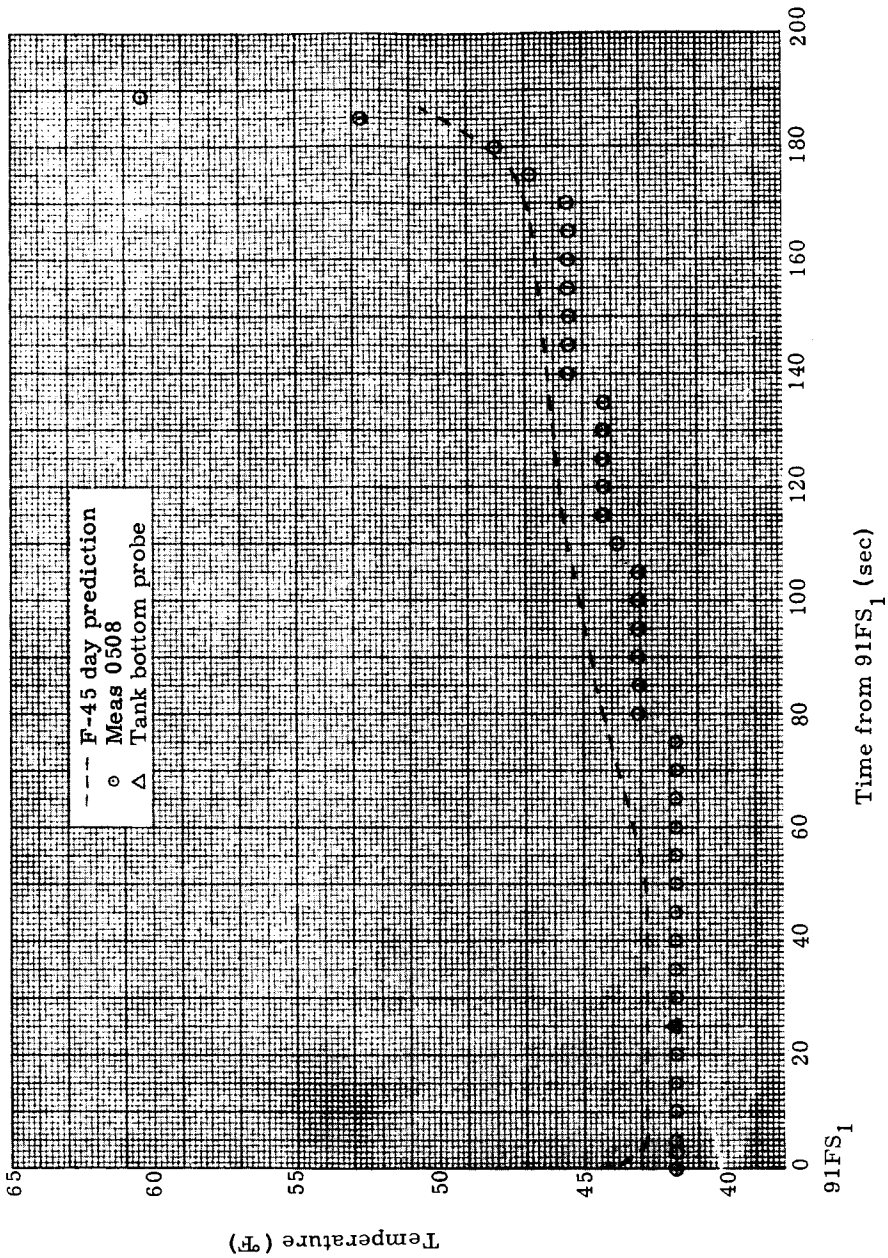

Fig. III-22. Stage II Fuel Pump Inlet Temperature

[redacted]

TABLE III-19

Maximum Transient Pressures at Pump Inlet

Meas	Initial Pressure Wave	At Ignition (psia)	TCV at Closing (psia)	Design Operating Pressure (psia)
Stage I oxidizer (0017)	Negligible	125	Negligible	215
Stage I fuel (0014)	Negligible	Negligible	Negligible	55
Stage II oxidizer (0510)	Negligible	*	52	260
Stage II fuel (0507)	Negligible	*	Negligible	80

*Not available due to telemetry staging blackout.

b. Pump inlet suction pressures

Stages I and II static suction pressures at the suction measurement boss locations are shown in Figs. III-23 through III-26, which present the preflight prediction, the postflight reconstructed and the best estimate of actual flight pressures.

The preflight predicted curves were computed for the GT-12 Preflight Test Report (Ref. 15). The postflight reconstructed curves were based on flight measured values of ullage gas pressure, axial load factors, propellant temperatures and propellant loadings.

The Stage I oxidizer best estimate curve of the static suction pressures at the measurement boss (Meas 0017) consists of an average of the measured pressure and the two oxidizer standpipe pressures (Meas 0033 and 0034) adjusted to the Meas 0017 boss location. The measurements were adjusted for biases during static conditions prior to T-0, when suction pressure was the sum of head pressure and ullage pressure. Biases were -3.4 psi for Meas 0017, 0 psi for Meas 0033, and -1.8 psia for Meas 0034. Stage I fuel suction pressure best estimate at Meas 0014 boss location was an average of measured pressures adjusted for pre-T-0 biases and level of location where applicable.

~~CONFIDENTIAL~~

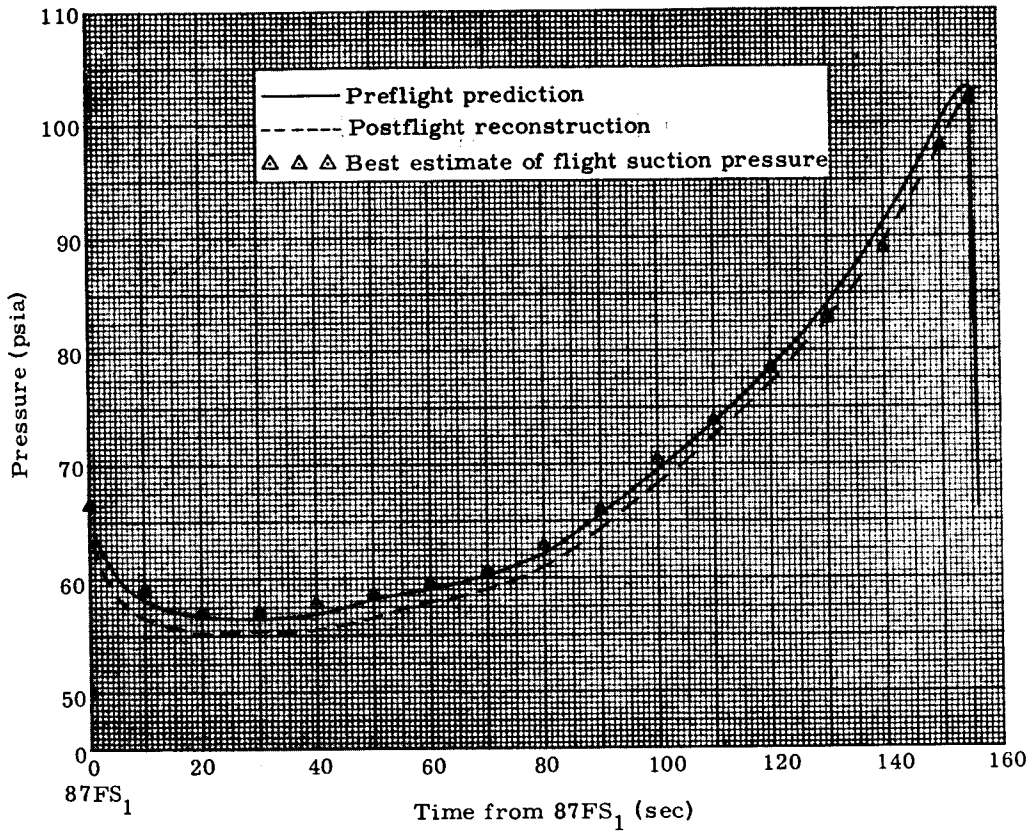

Fig. III-23. Stage I Oxidizer Suction Pressure (Meas 0017)

~~CONFIDENTIAL~~

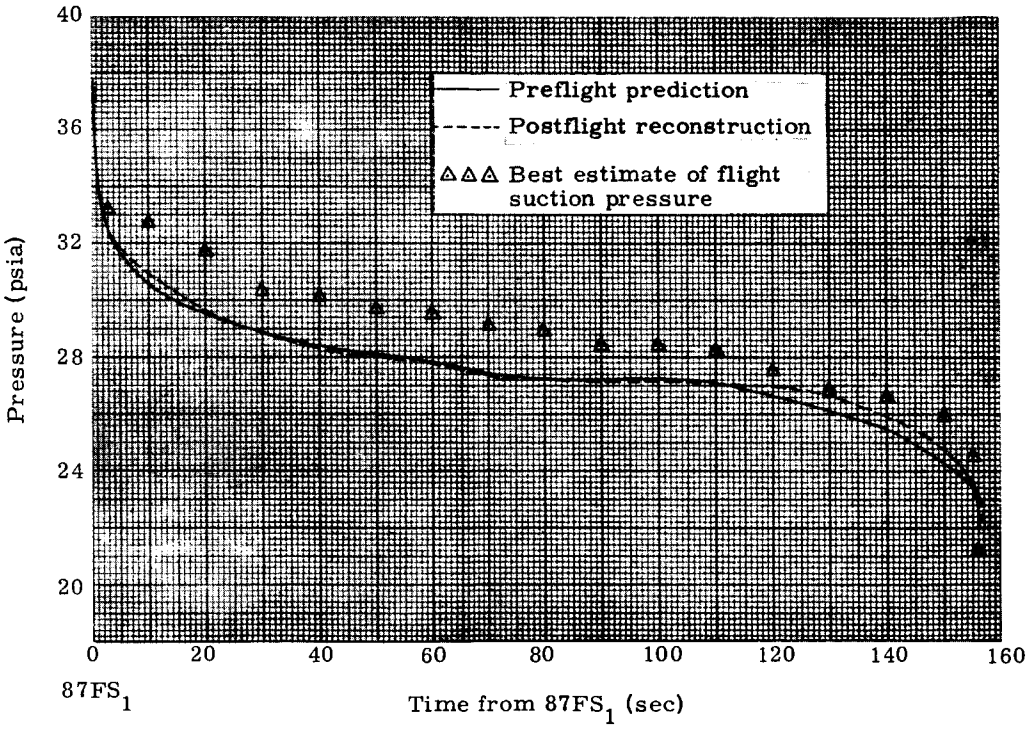

Fig. III-24. Stage I Fuel Suction Pressure (Meas 0014)

~~CONFIDENTIAL~~

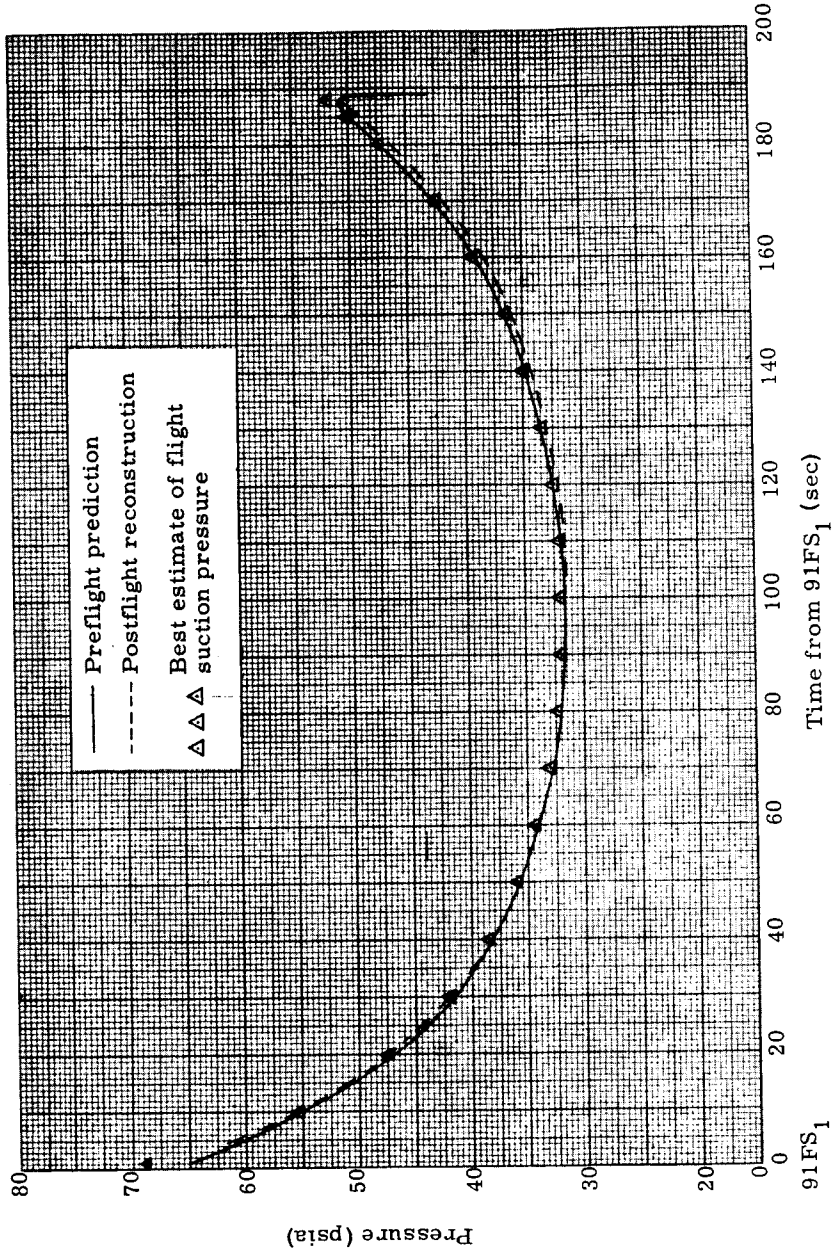

Fig. III-25. Stage II Oxidizer Suction Pressure (Meas 0510)

~~CONFIDENTIAL~~

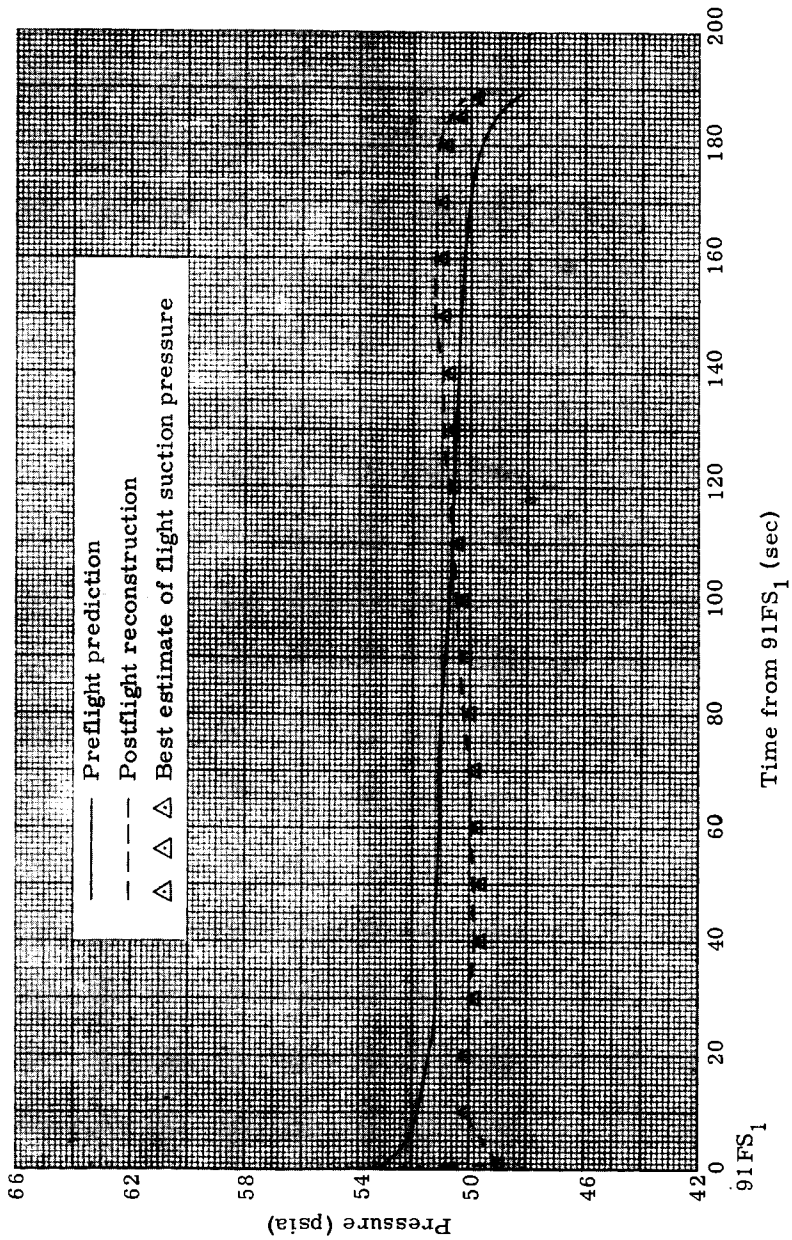

Fig. III-26. Stage II Fuel Suction Pressure (Meas 0507)

[redacted]

Meas 0014 and 0037 were adjusted for pre-T-0 biases of -0.6 psi, and Meas 0014 was also adjusted -0.7 psi to agree with the sum of calculated head and measured ullage pressure at that time. The Stage II fuel suction pressure Meas 0507 was adjusted for a -2.0 psi instrumentation bias, while Stage II oxidizer suction Meas 0510 agreed with reconstructed pre-T-0 conditions.

Flight suction pressure reconstruction was satisfactory, and differences between measured and reconstructed pressures were within specified instrumentation tolerances.

c. NPSH supplied

The NPSH supplied at the engine turbopump inlet during the start phase and during steady-state operation is shown in Table III-20.

TABLE III-20

Minimum NPSH Supplied

Stage and Tank	Minimum NPSH Supplied During Start Transient (psia)	Starting NPSH Required (1) (psia)	Limited Operation NPSH Required (2)	Minimum Steady-State NPSH Supplied (psia)	Unlimited Operation NPSH Required (1) (psia)
Stage I oxidizer	52.9	(4)	28.2 psia for 135 sec	51.4	46.1
Stage I fuel	33.0	17.1	17.1 psia for 120 sec	24.3	23.1
Stage II oxidizer	(3)	38.4	19.2 psia for 120 sec	26.0	22.4
Stage II fuel	(3)	39.8	39.8 psia for 120 sec	45.3	43.4

(1) Extracted from SCNP S75015, page 1, and SCNP S85008, page 1. Oxidizer values represent NPSH required at FS_1 fuel values at engine start.

(2) Time given represents cumulative operating time from engine acceptance at given NPSH levels. Data were extracted from source (1).

(3) Not available due to telemetry blackout.

(4) 38.4 psia required at FS_1. No specific requirement during start transient.

~~CONFIDENTIAL~~

4. Propellant Utilization

a. Level sensor uncover

Figures III-27 and III-28 show the predicted, actual and reconstructed level sensor uncover times for Stages I and II. Measured level sensor uncovering times are tabulated in Table III-21.

Reconstructed level sensor uncover times show closer agreement to the actuals in most cases. Reconstructed level sensor uncover times are based on feeding actual flight conditions of propulsion system reconstructed propellant loadings, ullage gas pressures and propellant temperatures into the propulsion system performance program.

Slosh, as indicated by on and off signals at the time of level sensor uncovering, was evident during this flight for the Stage II oxidizer and fuel high level sensors, and the oxidizer outage sensor. All other sensor uncoverings were clean.

b. Best estimate level sensor uncover times

Table III-22 contains the best estimate average level sensor uncover times for the GLV-12 flight. Also shown are the integrated average temperatures between level sensor uncoverings and the corresponding densities. The measured average uncover times shown in Table III-22 were decreased by 0.058 second to allow for the built-in level sensor delay of 0.033 second and the PCM digital sampling rate of 0.050 second.

Table III-23 contains the level sensor volumes and delta volumes used in the level sensor flow rate analysis. The Stages I and II oxidizer and fuel calibrated high level sensor volumes were checked at Cape Kennedy using the propellant transfer and pressurization system. Stages I and II outage and shutdown level sensor volumes were checked using the actual counts of flowmeter pulses during the special loading.

c. Flow rates

Table III-24 presents the predicted and the actual volumetric flow rates between level sensors.

d. Mixture ratio

Table III-25 shows the Stages I and II predicted and actual in-flight average engine mixture ratios for GLV-12.

The predicted in-flight average engine mixture ratios were biased from engine acceptance test mixture ratios by -0.47% for Stage I and -0.40% for Stage II. The mixture ratio biases were determined from

[redacted]

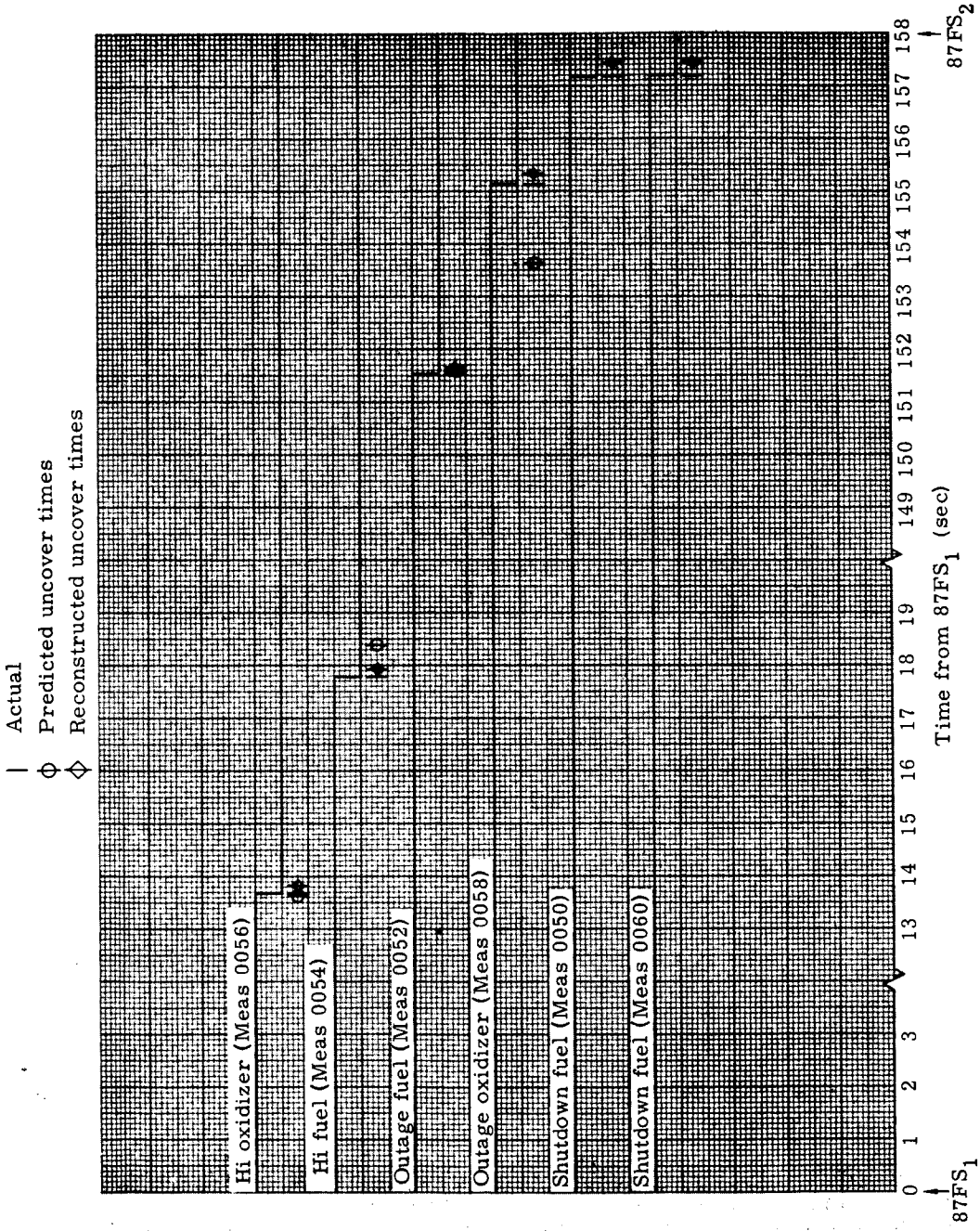

Fig. III-27. Stage I Level Sensor Operation

[redacted]

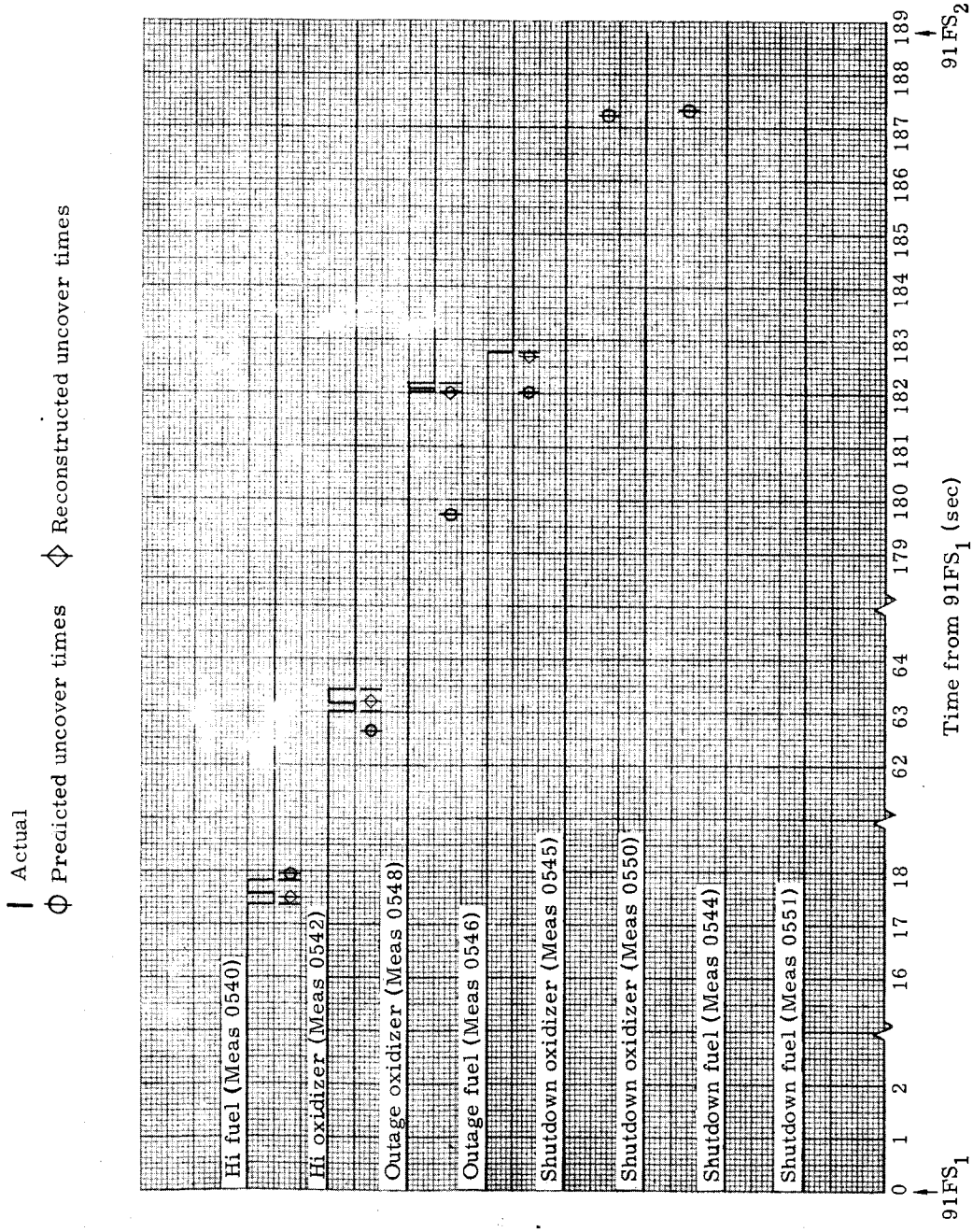

Fig. III-28. Stage II Level Sensor Operation

[redacted]

TABLE III-21

Measured Level Sensor Uncover Times

Meas	Sensor	Uncover Time (GMT)	Average Uncover Time (GMT)	Remarks
	Stage I			
0056	Oxidizer high	2046:43.927	2046:43.927	Clean
0058	Oxidizer outage	2049:05.382	2049:05.382	Clean
0054	Fuel high	2046:48.027	2046:48.027	Clean
0052	Fuel outage	2049:01.772	2049:01.772	Clean
0050	Fuel shutdown	2049:07.422	2049:07.427	Clean
0060	Fuel shutdown	2049:07.432		Clean
	Stage II			
0542	Oxidizer high	2050:11.445	2050:11.445	0.40-sec slosh
0548	Oxidizer outage	2052:10.336	2052:10.336	0.15-sec slosh
0540	Fuel high	2049:25.818	2049:25.818	0.45-sec slosh
0546	Fuel outage	2052:11.001	2052:11.001	Clean
0545	Oxidizer shutdown			Did not uncover
0550	Oxidizer shutdown			Did not uncover
0544	Fuel shutdown			Did not uncover
0551	Fuel shutdown			Did not uncover

[redacted]

TABLE III-22

Best Estimate Average Sensor Uncover Times

Quadrant	Meas	Sensor	Average Uncover Time (GMT)	ΔTime (sec)
		Stage I		
I	0056	Oxidizer high	2046:43.869	141.455
I/IV	0058	Oxidizer outage	2049:05.324	
I	0054	Fuel high	2046:47.969	133.745
III	0052	Fuel outage	2049:01.714	
I	0050	Fuel shutdown	2049:07.369	
III	0060	Fuel shutdown		
		Stage II		
IV	0542	Oxidizer high	2050:11.387	118.891
I/IV	0548	Oxidizer outage	2052:10.278	
I	0540	Fuel high	2049:25.760	165.183
I	0546	Fuel outage	2052:10.943	
II	0545	Oxidizer shutdown	Did not uncover	
IV	0550	Oxidizer shutdown		
II	0544	Fuel shutdown	Did not uncover	
IV	0551	Fuel shutdown		

Tank	Integrated Average Temperature (between uncoverings) (°F)	Corresponding Density (lb/ft^3)
Stage I oxidizer	45.1	91.99
Stage I fuel	44.9	57.13
Stage II oxidizer	46.4	91.89
Stage II fuel	43.7	57.17

~~CONFIDENTIAL~~

TABLE III-23

Averaged Volumes at Level Sensor Locations

Tank	Sensor	Averaged Volumes (stretch included) (ft^3)	Δ Volumes (ft^3)
Stage I oxidizer	High level	1711.26	1673.24
	Outage	38.02	
Stage I fuel	High level	1402.20	1337.28
	Outage	64.92	
Stage II oxidizer	High level	285.17	262.69
	Outage	22.48	
Stage II fuel	High level	352.41	334.62
	Outage	17.79	

TABLE III-24

Propellant Volumetric Flow Rate

Tank	Predicted (ft^3/sec)	Actual (ft^3/sec)
Stage I oxidizer	11.945	11.822
Stage I fuel	10.038	10.000
Stage II oxidizer	2.247	2.211
Stage II fuel	2.042	2.026

TABLE III-25

Engine Mixture Ratio

System	Predicted Mixture Ratio	Mixture Ratio Actual	Deviation (%)
Stage I	1.9166	1.9057	-0.57
Stage II	1.7685	1.7526	-0.90

~~CONFIDENTIAL~~

GLV flight experience with particular emphasis on the negative mixture ratio shifts noted on GLV-9, GLV-10 and GLV-11. The mixture ratios of both stages shifted negatively further than anticipated, as shown in Table III-25. The total in-flight average mixture ratio shifts from engine acceptance test mixture ratios were -1.04% for Stage I and -1.3% for Stage II.

Sensitivity coefficients applied to the delta between the predicted and actual variations in average suction pressure and temperature between sensor uncoverings yield the information shown in Table III-26.

TABLE III-26

Mixture Ratio Pressure and Temperature

System	Pressure (psi)	Mixture Ratio (pressure)	Δ Temperature (°F)	Mixture Ratio (temperature)	Mixture Ratio (total)
Stage I					
Oxidizer	-1.3	-0.00166	-0.5	+0.00116	-0.00050
Fuel	+0.1	-0.00048	-3.2	-0.00521	-0.00569
Total Stage I		-0.00214		-0.00405	-0.00619
Stage II					
Oxidizer	-0.1	-0.00026	+8.1	-0.02118	-0.02144
Fuel	-0.3	+0.00084	-1.4	-0.00233	-0.00149
Total Stage II		+0.00058		-0.02351	-0.02293

By applying the delta mixture ratio (total shown in Table III-26) to the predicted (F-45 day revised) between sensors mixture ratios, the run-to-run variation can be calculated. The mixture ratio deviation along with the allowable run-to-run dispersions is shown in Table III-27.

TABLE III-27

Mixture Ratio Deviation

System	Predicted Mixture Ratio (corrected for pressure and temperature variations)	Mixture Ratio Actual	Deviation (%)	Allowable Run-to-Run Dispersion (%)
Stage I	1.9121	1.9049	-0.38	±1.38
Stage II	1.7446	1.7532	+0.49	±2.28

e. Outage and trapped propellant

Table III-28 shows the mean and maximum (99%) outage predicted for GLV-12. Also shown are the actual outages as calculated using the information contained in the reconstructed propellant inventories (Tables III-32 and III-33).

TABLE III-28

Outage Prediction

System	Predicted (F-45)		Predicted (F-0)		Actual
	Mean	Max (99%)	Mean	Max (99%)	
Stage I	0.343% 882 lb	1.006% 2584 lb	0.322% 827 lb	1.057% 2714 lb	0.052% oxidizer 133 lb
Stage II	0.342% 208 lb	1.020% 621 lb	0.368% 224 lb	1.033% 629 lb	0.163% oxidizer 99 lb

All outages are presented in pounds and as percent of total steady-state propellants as taken from Ref. 15. The values used for total steady-state propellants are 256,780 pounds for Stage I and 60,901 pounds for Stage II.

The trapped propellants for Stages I and II are given in Tables III-32 and III-33.

f. Start and propellant consumption

The predicted and actual propellant consumptions during the Stage I holddown period are shown in Table III-29.

TABLE III-29

Stage I Holddown Propellant Consumption

Stage I	Oxidizer (lb)		Fuel (lb)	
	Predicted	Actual	Predicted	Actual
Holddown consumption (TCPS to liftoff)	2145	2182	1138	1173

The Stages I and II start consumptions shown in Tables III-32 and III-34, respectively, were selected from Ref. 19 and were modified to allow for the difference between propellant out of the tanks (as listed in

Ref. 19) and propellant overboard. The predicted holddown consumption was derived from the engine analytical model and previous flight test data, while the actual value was derived from the posttest rocket engine system total operation (PRESTO) engine performance reconstruction program.

g. Vapor retained

The predicted and actual values of vapor retained in the tanks as a result of pressurization gases and propellant vaporization during flight are shown in Table III-30.

TABLE III-30

Pressurization Gas Inventory

System	Oxidizer (lb)		Fuel (lb)	
	Predicted	Actual	Predicted	Actual
Stage I				
Vapor retained:				
Oxidizer tank	328	328	0	0
Fuel tank	8	9	92	92
Vaporized	7	6	0	0
Stage II				
Pressurization fuel tank	4	4	49	49
Vaporization oxidizer tank	9	9	0	0

h. Shutdown

Stage I shutdown was caused by fuel exhaustion. The predicted and actual values for the propellants consumed during shutdown are shown in Table III-31. The actual values were obtained by integrating a curve (derived from PRESTO) of flight flow rate versus time after $87FS_2$.

Stage II shutdown was initiated by a guidance command; therefore, the propellants were not exhausted as in Stage I. The predicted and actual values for the propellants consumed during shutdown are shown in Table III-31. The actual values were computed using altitude shutdown impulse.

CONFIDENTIAL

TABLE III-31

Propellant Shutdown Consumption

System	Oxidizer (lb)		Fuel (lb)	
	Predicted	Actual	Predicted	Actual
Stage I	446	265	27	33
Stage II	76	71	60	56

i. Propellant inventory

The reconstructed propellant inventories for GT-12 are shown in Tables III-32 and III-33 for Stages I and II, respectively. The inventory consists of both nonusable and usable propellants. The burning time margin for Stage II was 2.631 seconds.

5. Components

a. Prevalves

During the launch countdown, all prevalve functions were performed without incident. Prevalves installed for the flight are identified in Table III-34.

b. Level sensors

GLV-12 incorporated 14 Bendix optical-type propellant level sensors. These are identified in Table III-35. All sensors performed satisfactorily during the propellant loadings and during flight.

c. Fuel accumulators

Accumulator piston response on this flight was similar to that of other flights utilizing the same configuration (GLV-3 through GLV-11). This response is presented in Fig. III-29. Dynamic friction levels for the dry accumulators were measured prior to installation of the accumulator assemblies at Martin-Baltimore and again prior to flight at ETR. A summary of these friction measurements is presented in Table III-36 as peak-to-peak values (twice the equivalent friction force in one direction).

CONFIDENTIAL

TABLE III-32

GLV-12 Stage I Constructed Propellant Loading

Predicted in-flight engine mixture ratio	1.9166	±2.52%	
Average in-flight mixture ratio (engine)	1.9057	±1.71%	
Outage (percent of total usable propellants)		0.052%	
	Oxidizer (lb)	Fuel (lb)	Total (lb)
Nonusable propellants			
A. Fuel bleed	0	23	23
B. Start consumption ($87FS_1$ to TCPS)	209	45	254
C. Holddown (TCPS to LO) (2 sec)	2,182	1,173	3,355
D. Trapped above interface at shutdown	0	20	20
E. Trapped below interface at shutdown	235	309	544
F. Vapor retained at shutdown			
1. For pressurization			
a. Oxidizer tank	328	0	328
b. Fuel tank	9	92	101
2. Vaporized	6	0	6
G. Total nonusable	2,969	1,662	4,631
Usable propellants			
A. Steady-state overboard (LO to $87FS_2$)	168,298	88,397	256,695
B. Shutdown transient (FS_2 to 0% thrust)	265	33	298
C. Outage	133	0	133
D. Total usable	168,696	88,430	257,126
Total propellant loaded	171,665	90,092	261,757
Propellant load at LO	169,274	88,851	258,125
Weight of initial pressurizing gas			
A. Fuel tank (N_2)			8
B. Oxidizer tank (N_2 + NO_2)			18

CONFIDENTIAL

TABLE III-33

GLV-12 Stage II Constructed Propellant Loading

Predicted in-flight engine mixture ratio	1.7685	±2.52%	
Average in-flight mixture ratio (engine)	1.7526	±1.55%	
Outage (percent of total usable propellants)		0.163%	
Burning time margin		2.631 sec	
	Oxidizer (lb)	Fuel (lb)	Total (lb)
Nonusable propellants			
A. Fuel bleed	0	11	11
B. Trapped above interface at FS_2 + 20 sec	0	0	0
C. Trapped below interface at FS_2 + 20 sec	20	14	34
D. Vapor retained after FS_2			
1. Pressurization (fuel tank)	4	49	53
2. Vaporization (oxidizer tank)	9	0	9
E. Total nonusable	33	74	107
Usable propellants			
A. Start consumption (FS_1 to FS_1 + 1.2 sec)	135	54	189
B. Steady-state overboard (FS_1 + 1.2 sec to FS_2)	37,894	21,576	59,470
C. Shutdown consumption (FS_2 to 0% thrust)	71	56	127
D. Steady-state residuals (after FS_2)			
1. Burning time margin	549	301	850
2. Outage	99		99
E. Total usable	38,748	21,987	60,735
Total propellants loaded	38,781	22,061	60,842
Weight of initial pressurizing gas			
A. Fuel tank (N_2)			5
B. Oxidizer tank (N_2 + NO_2)			29

CONFIDENTIAL

TABLE III-38

Comparison of Significant Pressurization System Parameters at FS_1 + 100 Seconds

Parameter	Preflight Predicted	Flight Data	Postflight Reconstructed
Stage I Fuel Tank ①			
Tank pressure (P_{FT}) (psia)	22.5	22.4	22.5
Nozzle inlet temperature (T_{FPOI}) (° F)	218	--	218 ②
Flow ratio (W_{FP}/Q_{FS}) (lb/ft^3)	0.0651	--	0.0654
Stage I Oxidizer Tank ③			
Tank pressure (P_{OT}) (psia)	18.8	18.4	19.4
Orifice inlet, specific enthalpy (H_{OPOI}) (Btu/lb)	334	--	329 ②
Flow ratio (W_{OP}/Q_{OS}) (lb/ft^3)	0.1761	--	0.1788
Stage II Fuel Tank ④			
Tank pressure (P_{FT}) (psia)	47.7	47.6	47.8
Nozzle inlet temperature (T_{FPOI}) (° F)	229	--	229 ②
Flow ratio (W_{FP}/Q_{FS}) (lb/ft^3)	0.1394	--	0.1392
Stage II Oxidizer Tank			
Tank pressure (P_{OT}) (psia)	13.4	13.7	13.8
Propellant flow rate (Q_{OS}) (ft^3/sec)	2.2274	--	2.1944

① Nozzle diameter, FPN Stage I Fuel, 0.480 in.

② Assumed, temperature not instrumented.

③ Flow control venturi coefficient, 0.0513.

④ Nozzle diameter, FPN Stage II Fuel, 0.260 in.

2. Flight Pressurization

Stages I and II ullage gas pressure time histories are shown in Figs. III-31 through III-34, which show flight-measured, preflight predicted, and postflight reconstructed pressures. The flight-measured pressures were obtained by averaging the telemetered output from each pair of pressure transducers in the individual tanks. The preflight predicted pressure curves were taken from Ref. 15. The postflight reconstruction was based on flight measured values of engine performance, propellant temperatures and propellant loadings. A comparison of significant pressurization system parameters, taken at FS_1 + 100 seconds, is given in Table III-38. Figures III-35, III-36 and III-37 present the preflight predicted and the in-flight estimated pressurization gas characteristics at the orifice or nozzle inlet.

3. Component Performance

All tank pressure sensors functioned normally. The maximum pressure differences between pairs of sensors in each of the individual propellant tanks are shown in Table III-39.

TABLE III-39

Pressure Difference Between Tanks Pressure Transducer Pairs

Tank	Maximum Difference (psi)	Maximum Allowable Difference (psi)
Stage I oxidizer	0.27	1.50
Stage I fuel	0.29	1.50
Stage II oxidizer	0.86	2.25
Stage II fuel	0.48	2.25

TABLE III-34

Prevalve Identification

Description	Part No.	Serial No.
Stage I oxidizer S/A 1 (fill and drain)	PS47510007-139	0700017
Stage I oxidizer S/A 2 (drain)	PS47510007-159	0700013
Stage II oxidizer S/A 3 (fill and drain)	PS47510005-199	0600061
Stage I fuel S/A 1 (fill and drain)	PS47510005-159	0600016
Stage I fuel S/A 2 (drain)	PS47510005-169	0600017
Stage II fuel S/A 3 (fill and drain)	PS47510006-059	0400018

TABLE III-35

GLV-12 Propellant Level Sensor Identification

	Stage I					Stage II				
Location	Meas	Quadrant	Volume (ft)*	Confi-guration	Serial No.	Meas	Quadrant	Volume (ft^3)	Confi-guration	Serial No.
Oxidizer tank										
High level	0056	I	1711.26	-039	000558	0542	IV	285.17	-039	000545
Outage	0058	I/IV	38.02	-039	000489	0548	I/IV	22.48	-039	000437
Shutdown	--	0000		--	--	0545	II	5.31	-039	000445
Shutdown	--	--		--	--	0550	IV	5.09	-039	000301
Fuel tank										
High level	0054	I	1402.20	-059	000551	0540	I	352.41	-049	000556
Outage	0052	III	64.92	-049	000303	0546	I	17.79	-049	000554
Shutdown	0050	I	7.34	-049	000300	0544	II	1.87	-049	000202
Shutdown	0060	III	7.45	-049	000302	0551	IV	1.97	-059	000498

*Volume to interface including tank stretch at uncover time.

TABLE III-36

Dynamic Friction Levels for Dry Accumulators

S/A	Serial	*Peak-to-Peak Friction (psi)	
		Bench	Preflight
1	B032	0.60	0.80
2	B034	0.30	1.00

* Maximum acceptable values = 2.0 psi.

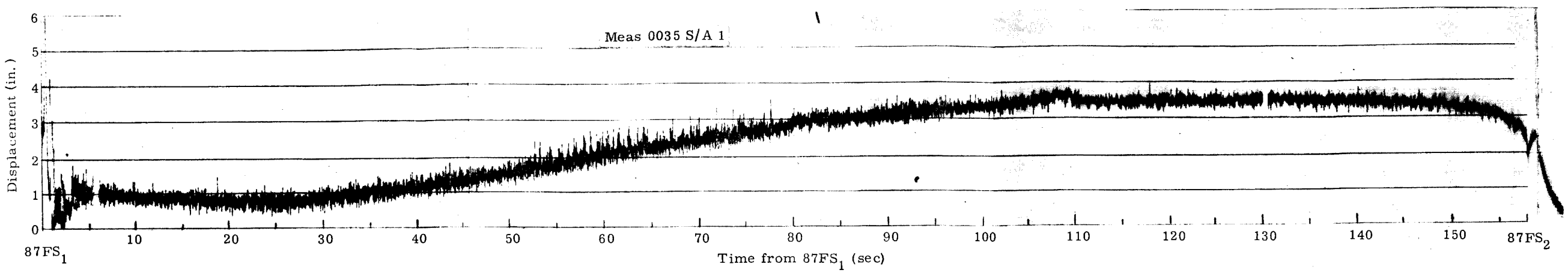

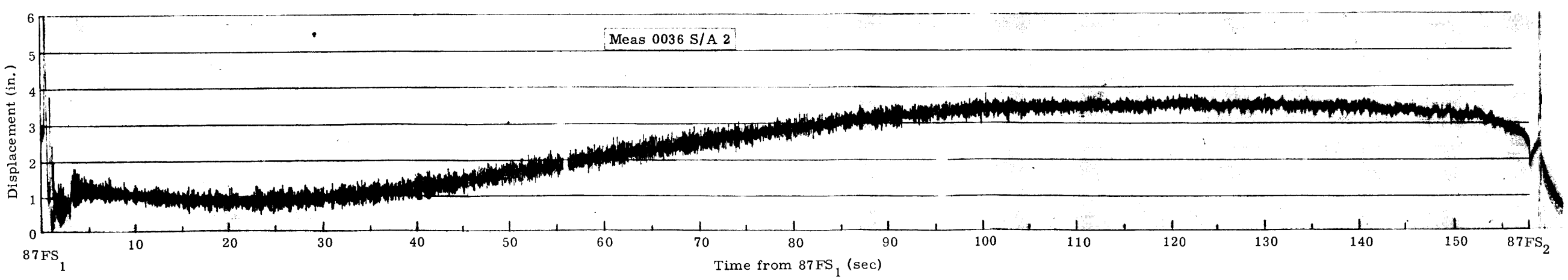

Fig. III-29. Fuel Accumulator Piston Travel

Observed flight data do not indicate significant differences in friction level between accumulators. No significance is attributed to differences between the dry friction value obtained at Martin-Baltimore and at ETR, as long as the maximum value is less than 2 psi.

d. Standpipes

The oxidizer standpipes were charged at T-62 minutes with the remote charge system. No problems were encountered during the charging operation. The data obtained from Meas 0033 (S/A 1) and Meas 0034 (S/A 2) were consistent with suction pressure Meas 0017 throughout Stage I flight.

e. POGO performance

Flight data indicated that this flight exhibited longitudinal oscillation of ±0.14 g, one of the lowest values obtained on any Titan II or GLV flight.

Additional details on POGO will be found in Chapter XII of this report.

C. PRESSURIZATION SUBSYSTEM

1. Prelaunch Pressurization

At approximately T-190 minutes all four propellant tanks were pressurized, through AGE, from blanket pressure levels to flight pressure levels. The resultant time-pressure profiles (Fig. III-30) indicate that the process was normal. The tank ullage lockup pressures obtained from landline measurements at T-0 and the related normal operating pressure ranges are presented in Table III-37.

TABLE III-37

Tank Ullage Lockup Pressures

Meas	Parameter	Normal Range (psia)	Measured (psia)
4125	Stage I fuel tank	27.5 to 31.5	30.7
4129	Stage I oxidizer tank	30.5 to 34.5	33.8
4602	Stage II fuel tank	49.5 to 54.5	51.8
4605	Stage II oxidizer tank	53.5 to 57.5	56.8

CONFIDENTIAL

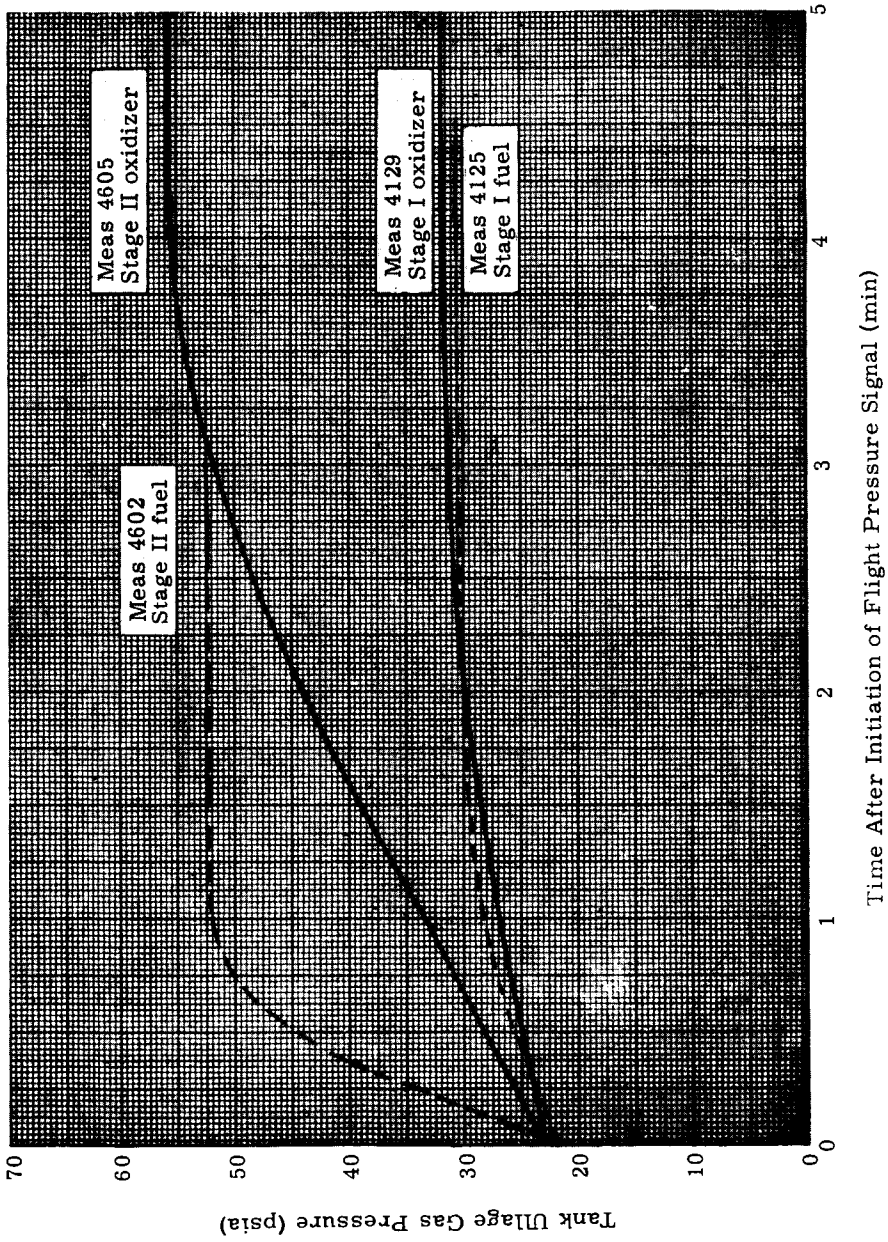

Fig. III-30. Tank Pressurization Cycle (blanket to flight pressure)

CONFIDENTIAL

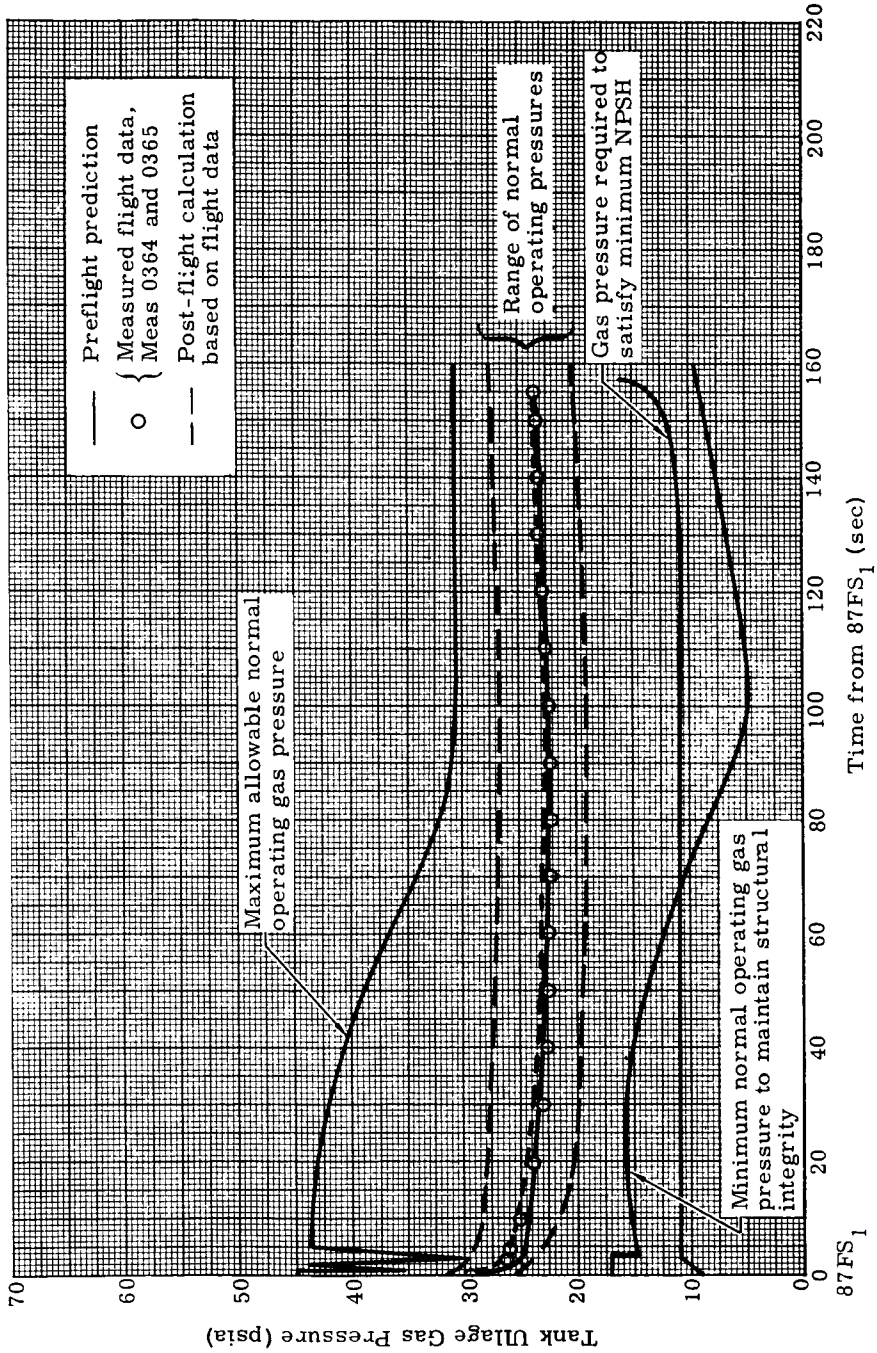

Fig. III-31. Stage I Fuel Tank Ullage Pressure History

CONFIDENTIAL

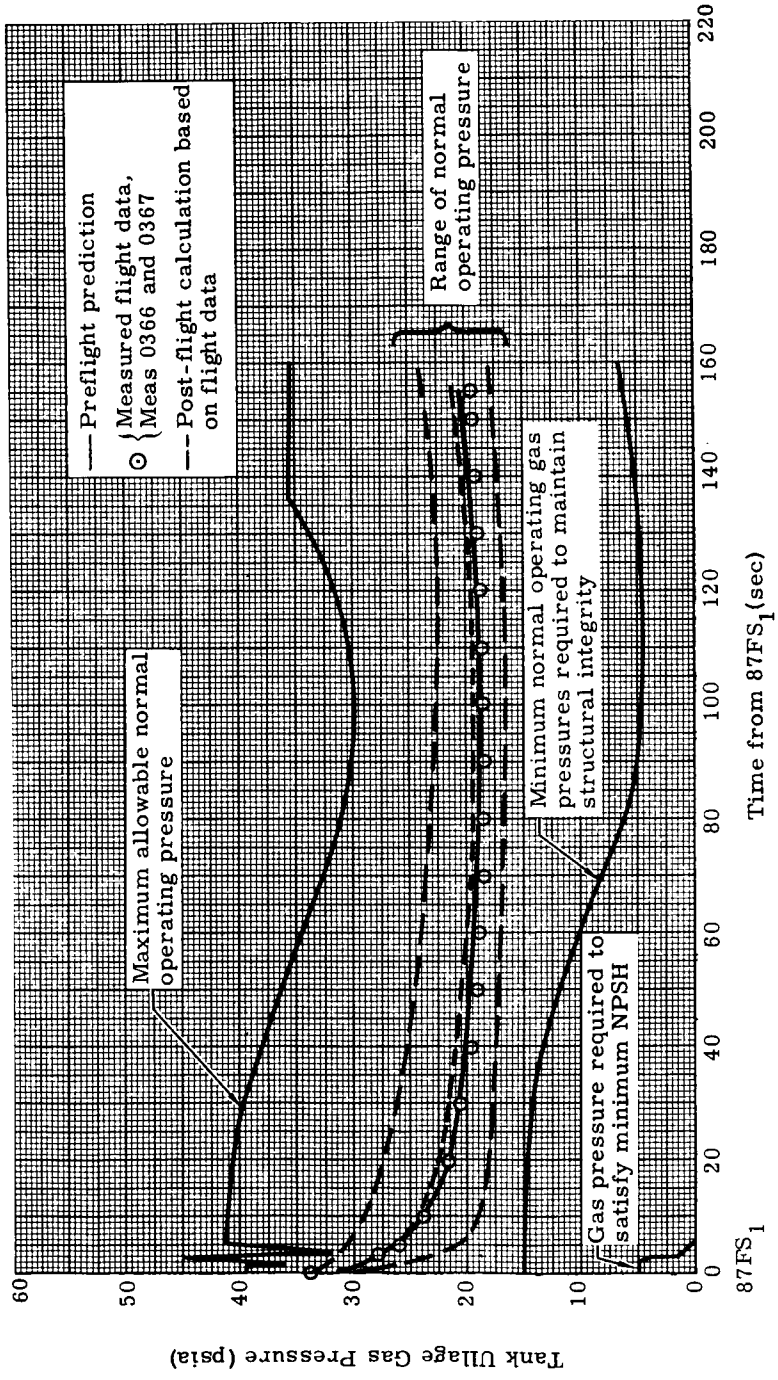

Fig. III-32. Stage I Oxidizer Tank Ullage Pressure History

CONFIDENTIAL

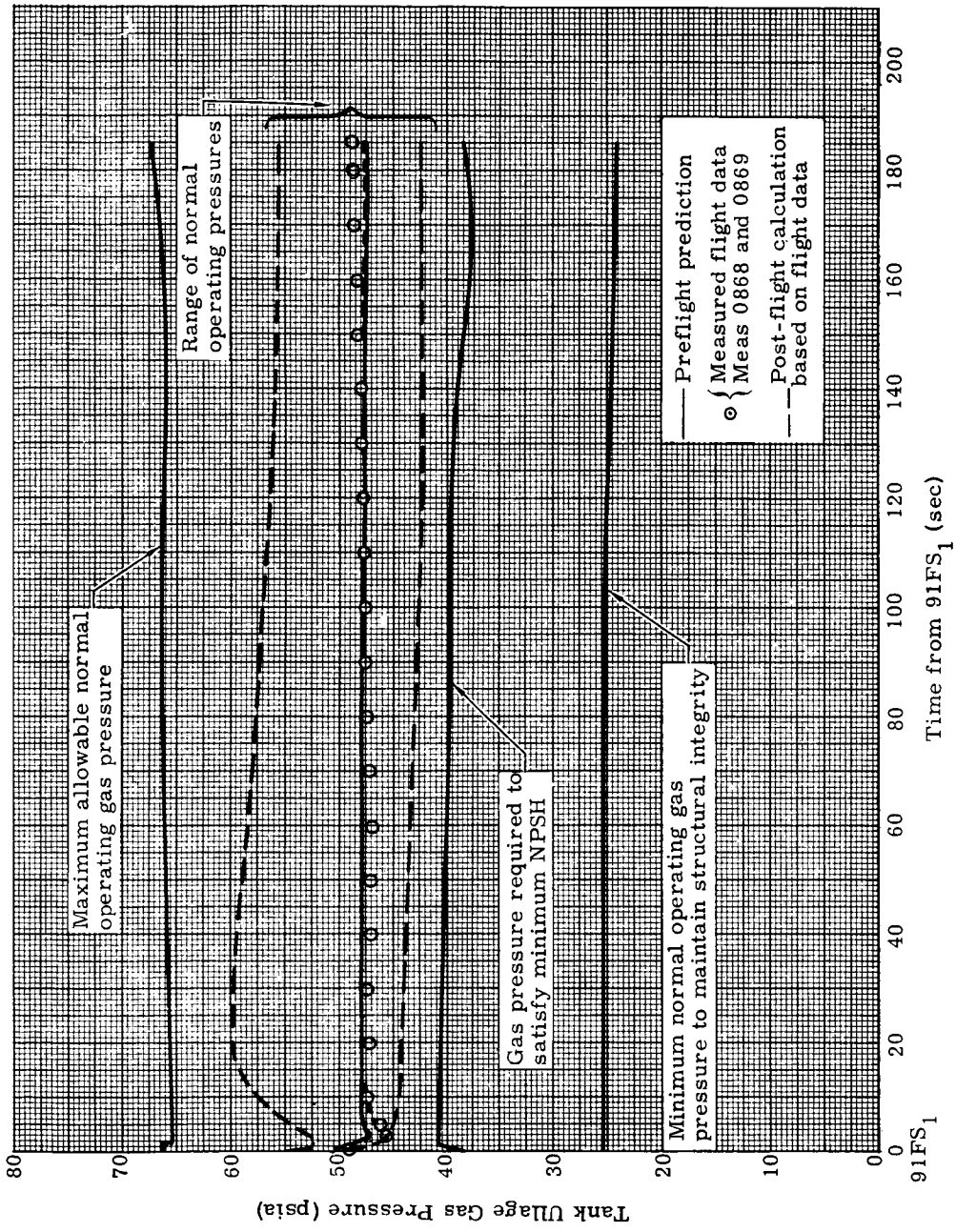

Fig. III-33. Stage II Fuel Tank Ullage Pressure History

[redacted]

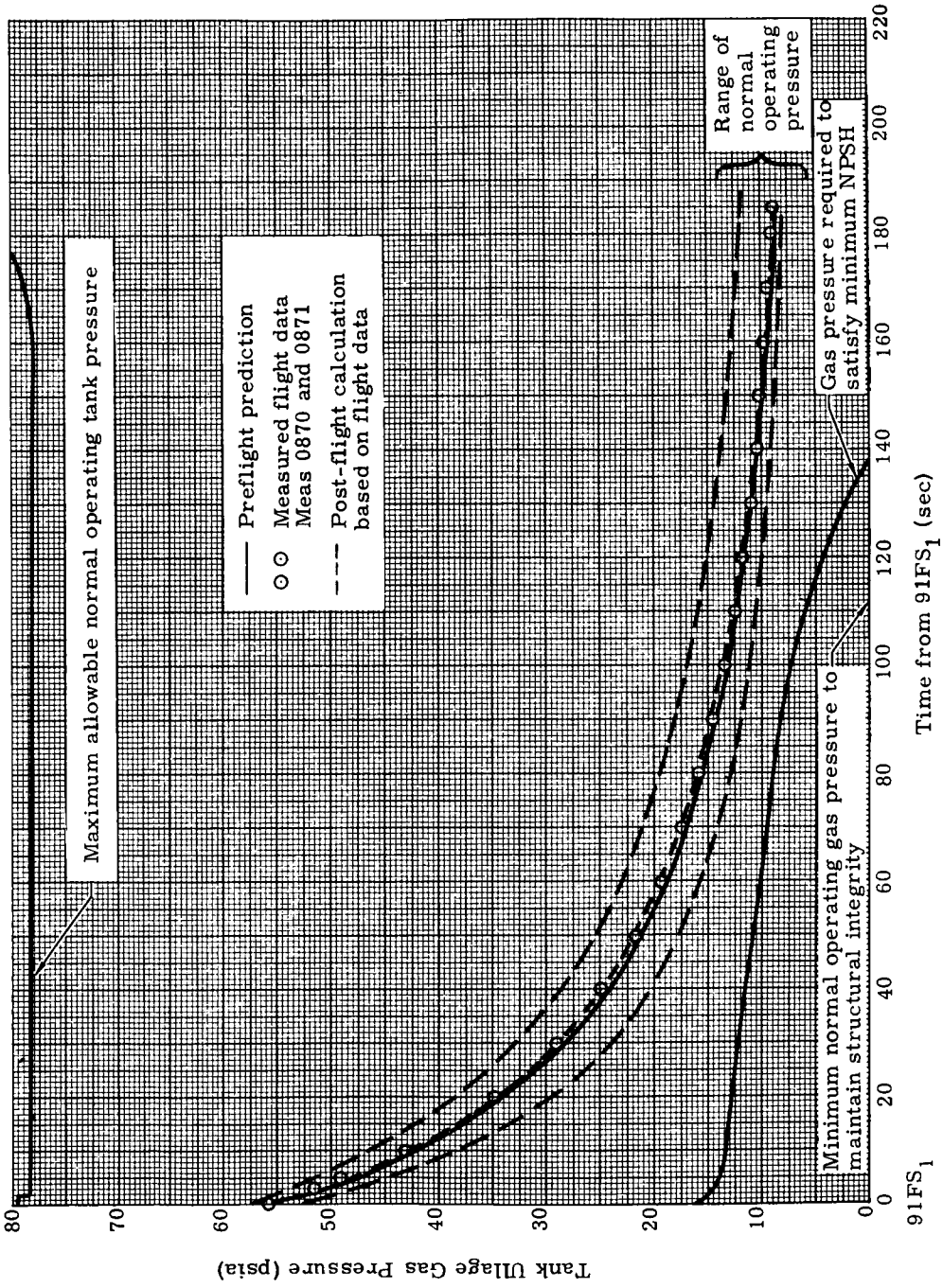

Fig. III-34. Stage II Oxidizer Tank Ullage Pressure History

[redacted]

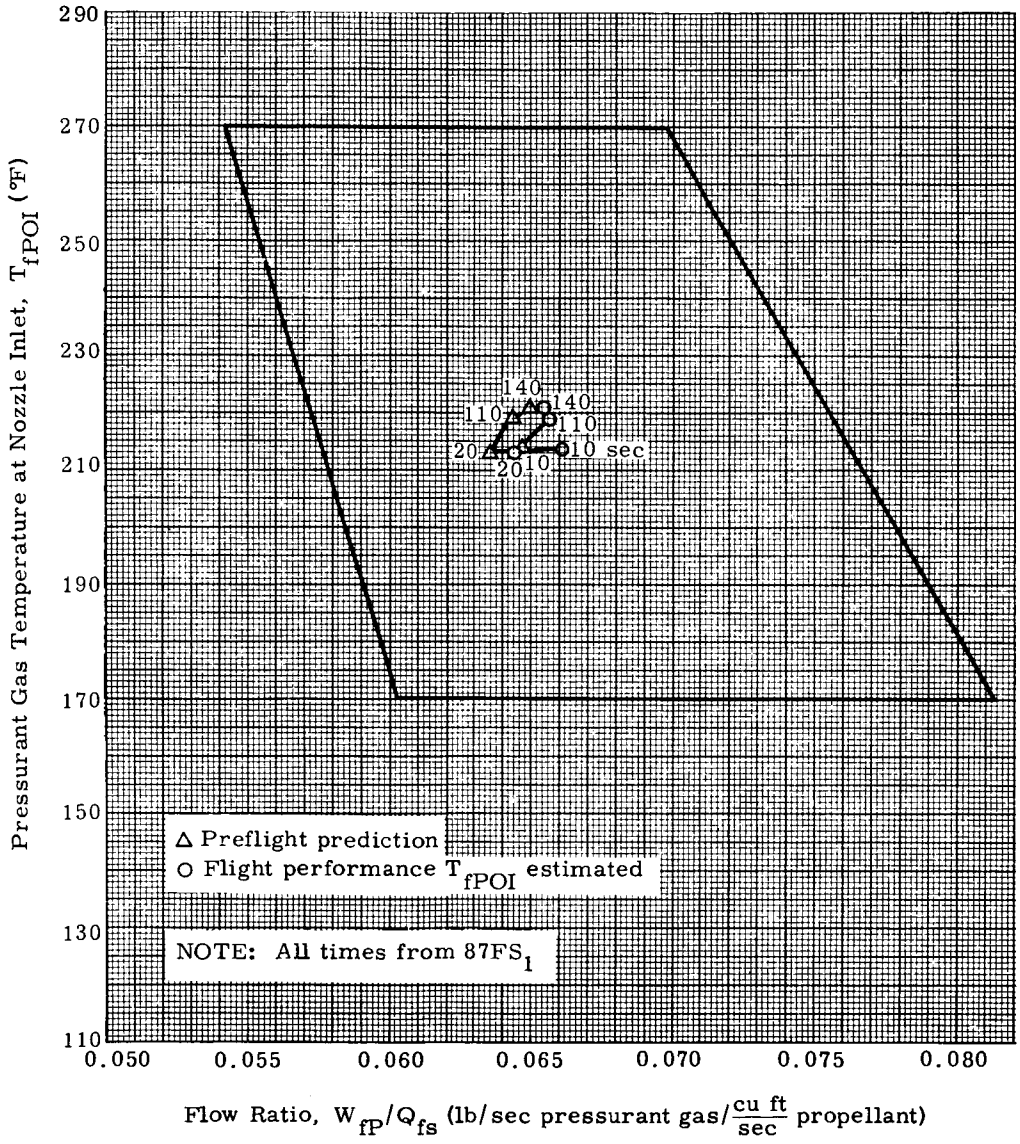

Fig. III-35. Stage I Fuel Tank Pressurant Performance

~~CONFIDENTIAL~~

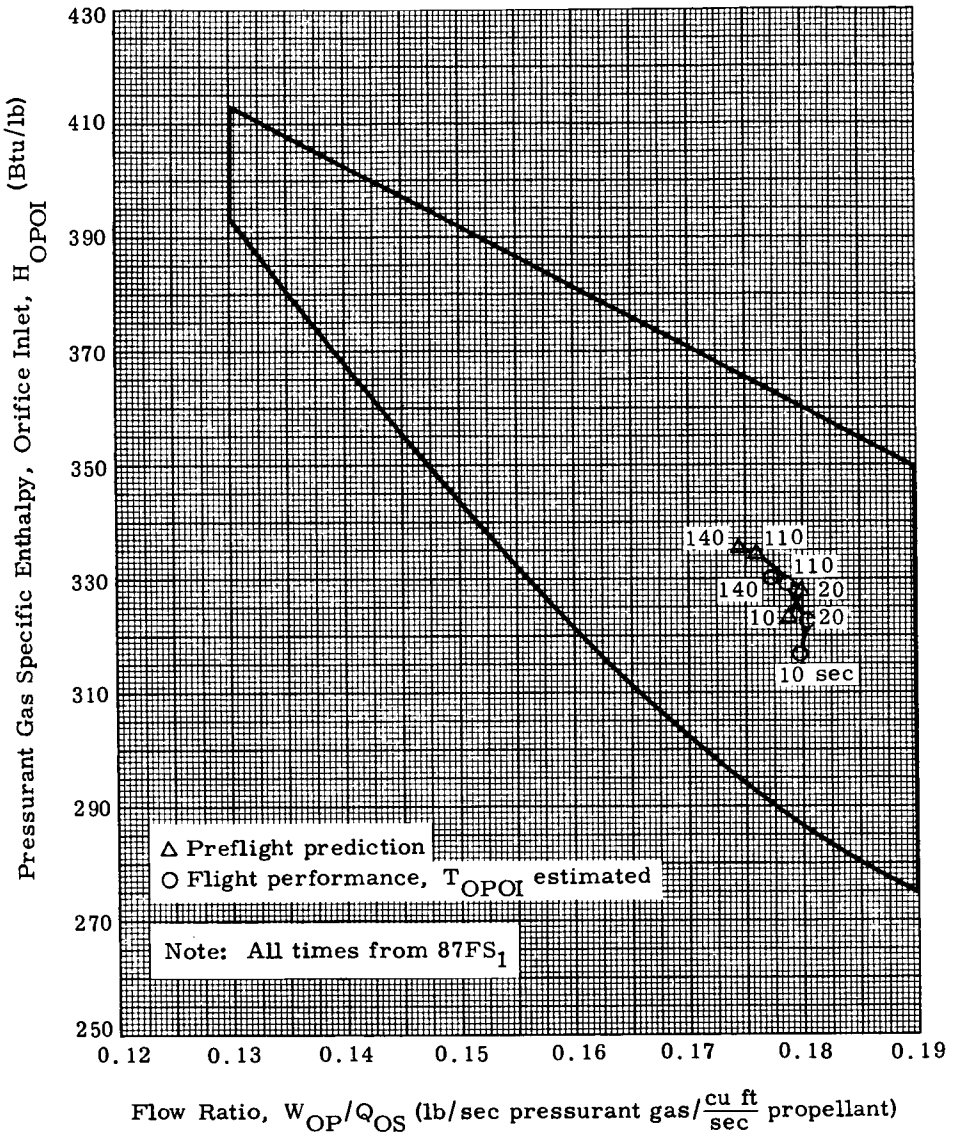

Fig. III-36. Stage I Oxidizer Tank Pressurant Performance

~~CONFIDENTIAL~~

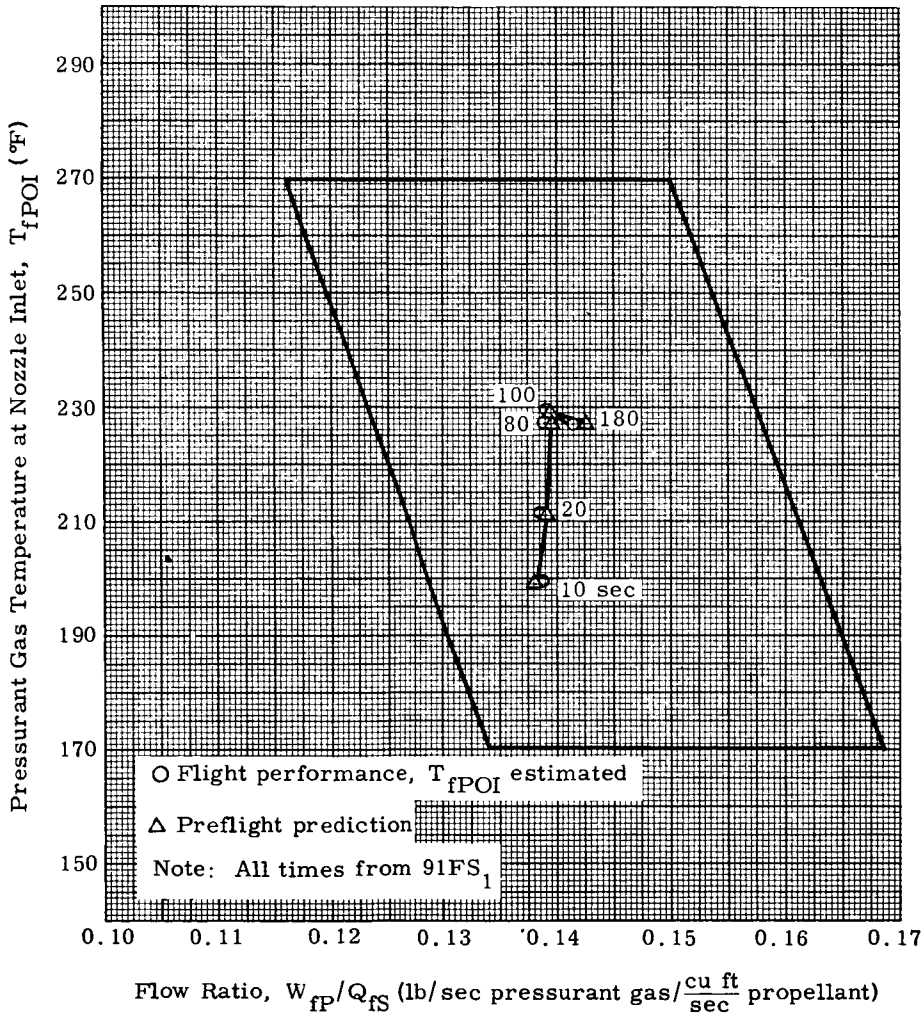

Fig. III-37. Stage II Fuel Tank Pressurant Performance

IV. FLIGHT CONTROL SYSTEM

Analysis of the GT-12 flight control system (FCS) measured parameters indicated proper system operation during both Stages I and II flight. The primary FCS was in command throughout the flight, and no switchover to the secondary system was required.

A. STAGE I FLIGHT

1. Ignition and Liftoff Transients

Normal actuator transient disturbances occurred during engine ignition; the maximum actuator travel recorded during the ignition and holddown period is presented in Table IV-1.

TABLE IV-1

Actuator Travel During Holddown

Actuator Designation	Ignition Transient		Maximum Travel During Hold-down Null Check (in.)
	Maximum Travel (in.)	Time from LO (sec)	
Pitch, 1_1	-0.05	-2.43	0.04
Yaw/Roll, 2_1	+0.07	-2.41	0.03
Yaw/Roll, 3_1	+0.07	-2.42	0.02
Pitch, 4_1	-0.06	-2.43	0.03

The combination of thrust and engine misalignments at full thrust initiated a roll transient at liftoff, with a maximum roll rate of 1.0 deg/sec counterclockwise (CCW). The corrective response of the FCS, shown in Fig. IV-1, introduced a roll attitude error bias of 0.05 degree CCW, correcting for an equivalent engine misalignment of +0.01 degree.

2. Roll and Pitch Programs

The TARS roll and pitch programs performed normally, as shown in Table IV-2.

3. Stage I Flight Performance

The TARS and IGS attitude error signals indicate excellent correlation during Stage I flight for the pitch, yaw and roll axes and are pre-

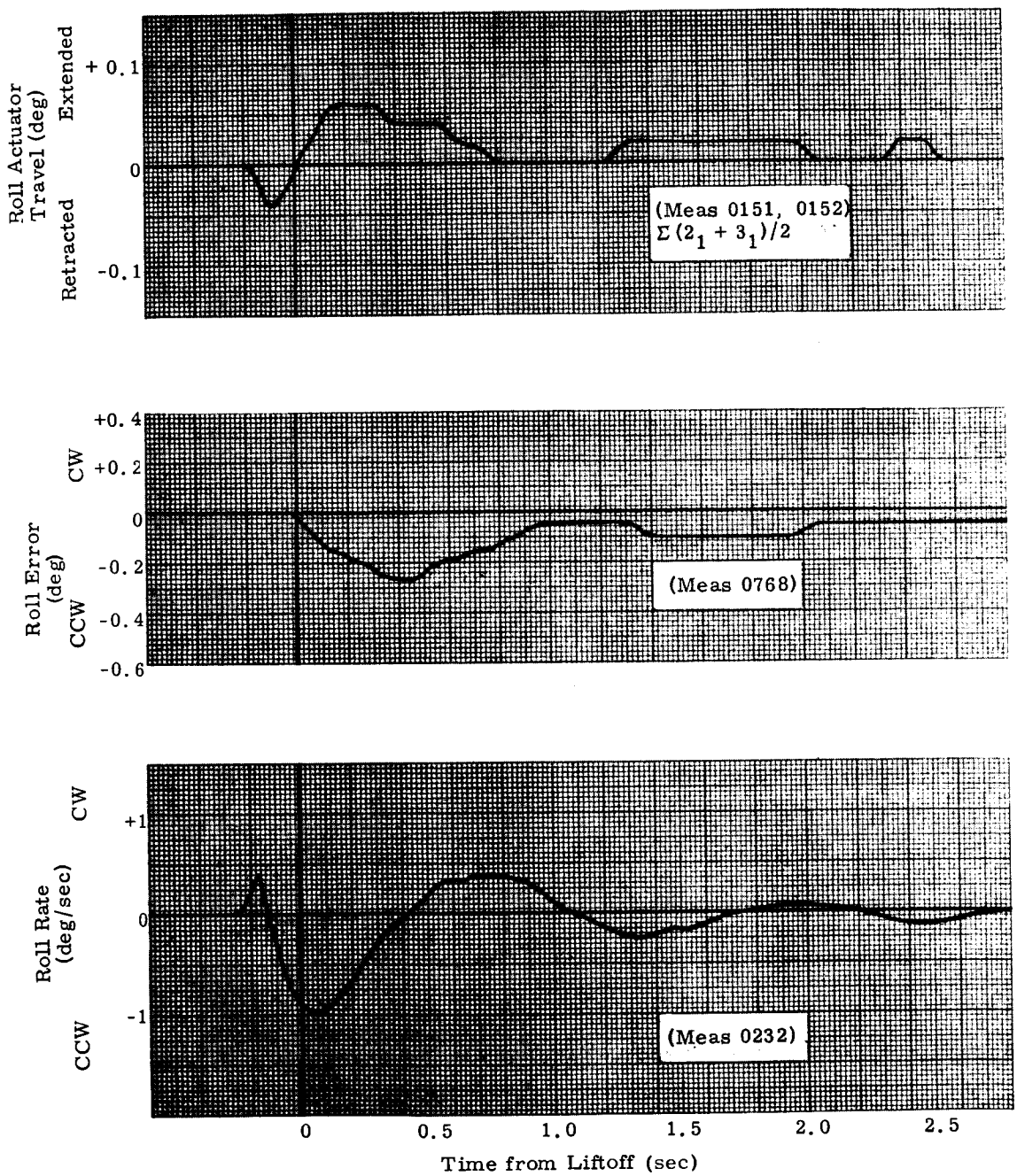

Fig. IV-1. Liftoff Roll Transients

TABLE IV-2

TARS Roll and Pitch Programs

Program	Time from Liftoff (sec)	Nominal Time (sec)	Average Rate Gyro (deg/sec)	Torquer Monitor Indication (deg/sec)	Nominal Rate (deg/sec)
Roll					
Start	7.99	8.00	-1.25	-1.25	-1.25
Stop	20.47	20.48			
Pitch Step 1					
Start	23.05	23.04	-0.71	-0.69	-0.709
Pitch Step 2					
Start	88.26	88.32	-0.52	-0.50	-0.516
Pitch Step 3					
Start	118.96	119.04	-0.22	-0.25	-0.235
Stop	162.41	162.56			

sented in Figs. IV-2, IV-3 and IV-4, respectively. The dispersions (TARS attitude minus IGS attitude) at BECO were -0.36 degree in the pitch axis, +0.02 degree in the yaw axis and +0.70 degree in the roll axis.

Analysis of the FCS attitude error signals indicates satisfactory vehicle response to guidance programs and to vehicle disturbances caused by prevailing winds aloft. The control system response to these disturbances was normal and well controlled.

Stage I gain change occurred at LO +109.68 seconds, during which time adequate vehicle stability was maintained. The attitude error transient at gain change was a pitch-up increase from 0.53 degree to 1.26 degrees. The yaw axis was at null; therefore, no transient resulted.

The maximum vehicle rates and attitude errors recorded during Stage I flight are shown in Tables IV-3 and IV-4, respectively.

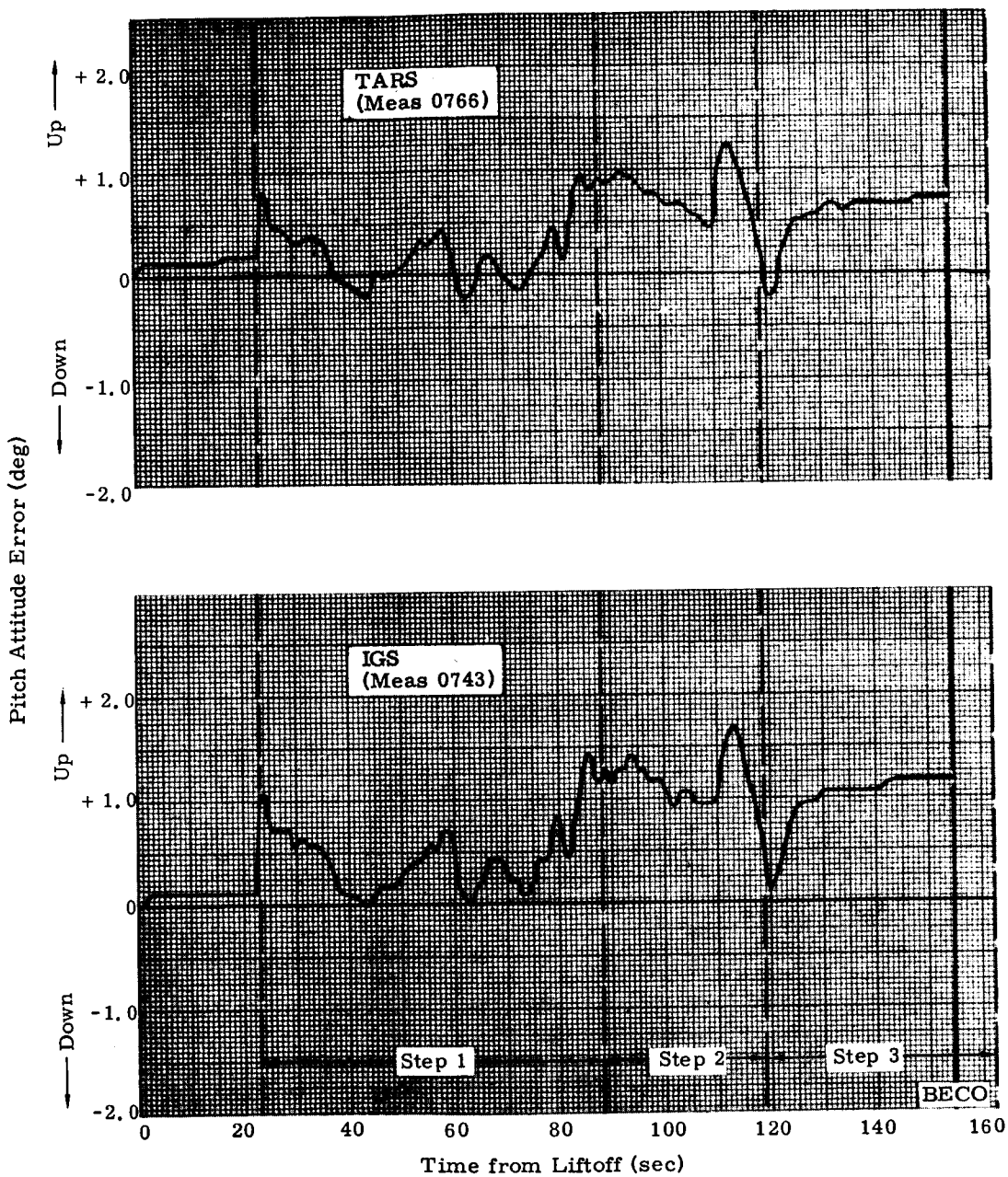

Fig. IV-2. Pitch Attitude Error History During Stage I Flight

UNCLASSIFIED

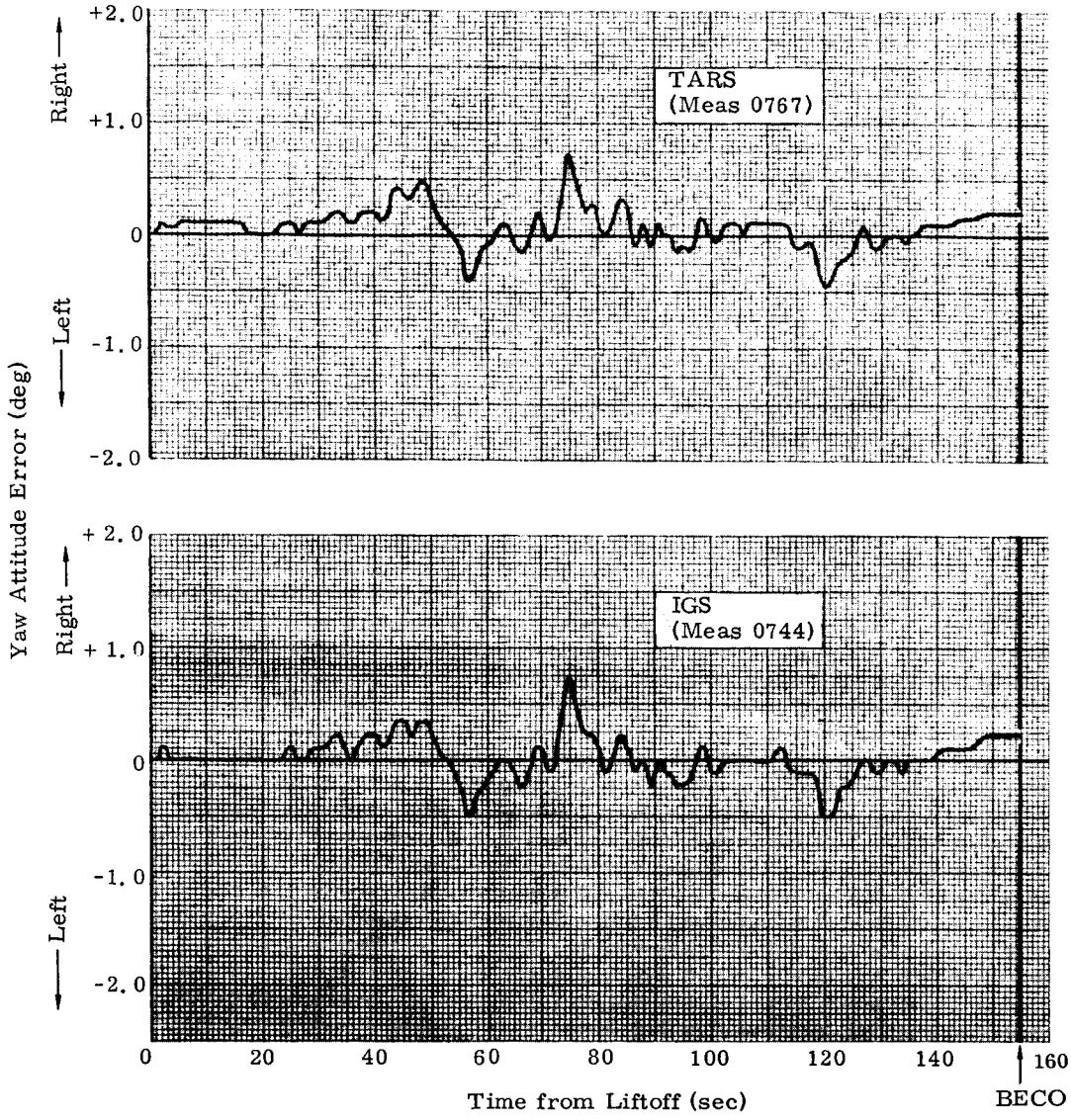

Fig. IV-3. Yaw Attitude Error History During Stage I Flight

UNCLASSIFIED

UNCLASSIFIED

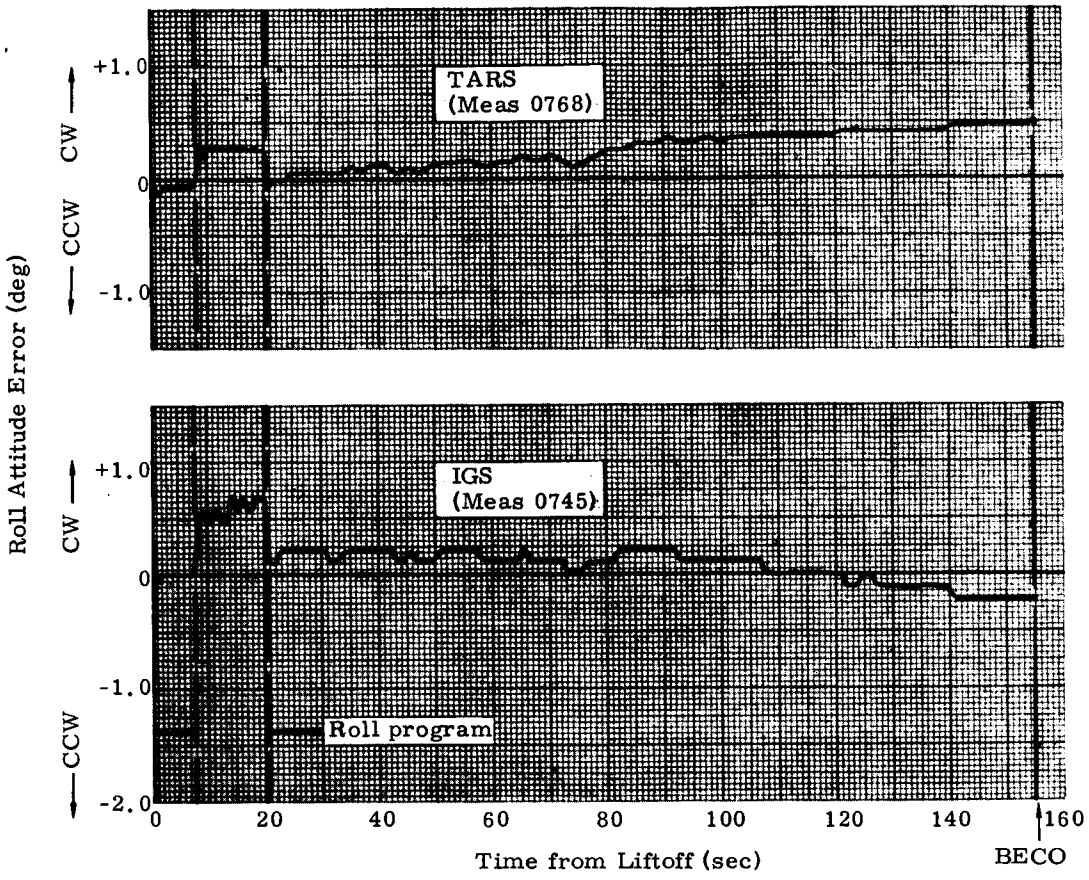

Fig. IV-4. Roll Attitude Error History During Stage I Flight

UNCLASSIFIED

TABLE IV-3

Maximum Rates During Stage I Flight

Axis	Primary		Secondary	
	Maximum Rates* (deg/sec)	Time from LO (sec)	Maximum Rate* (deg/sec)	Time from LO (sec)
Pitch				
Stage I	+0.18	0.5	+0.39	0.0
	-0.99	25.3, 60.2 and 80.9	-0.97	25.2 and 80.3
Stage II	+0.20	0.1	+0.20	0.5
	-0.99	60.4	-0.96	60.4
Yaw				
Stage I	+0.48	73.0	+0.48	72.7
	-0.29		-0.27	
Stage II	+0.49	73.0	+0.49	72.6
	-0.29		-0.29	76.6
Roll				
Stage I	+0.50	154.6	+0.39	154.6
	-1.61	8.6	-1.60	8.7

*Bias removed.

TABLE IV-4

Maximum Attitude Errors During Stage I Flight

Axis	Maximum Attitude Error* (deg)	Time from LO (sec)
Pitch	+1.26 -0.21	113.5 43.3, 62.5 and 120.5
Yaw	+0.74 -0.47	74.3 119.9
Roll	+0.53 -0.26	154.7 0.3

*Bias removed.

B. STAGE II FLIGHT

1. Stage Separation

Stage I engine shutdown was caused by fuel depletion. The thrust tailoff characteristics of fuel depletion shutdown show larger magnitude oscillations than those for an oxidizer or command shutdown. The pressure differential between the two thrust chambers resulted in high frequency structural and rate gyro resonances, as indicated by the FCS gyros. The maximum rates are shown in Table IV-5.

TABLE IV-5

Maximum Rate Gyro Indications During Staging

Axis	From BECO to Separation		From Stage Separation to Telemetry Blackout		From Telemetry Black-out to +1 sec	
	Maximum Rates (deg/sec)	Time from BECO (sec)	Maximum Rates (deg/sec)	Time from BECO (sec)	Maximum Rates (deg/sec)	Time from BECO (sec)
Pitch						
Primary	+2.70	0.47	+0.60	0.76		
	-3.27	0.49	-1.48	0.72	-1.28	1.14
Secondary	+3.92	0.47	+1.50	0.74		
	-4.23	0.49	-2.58	0.73	-1.47	1.14
Yaw						
Primary	+0.77	0.57	+0.87	0.72	+0.97	1.09
	-1.28	0.47	-0.99	0.73		
Secondary	+0.87	0.42	+1.34	0.73	+1.06	1.30
	-1.44	0.47	-0.79	0.74		
Roll						
Primary	+0.98	0.01			+1.86	1.44
	-3.23	0.31	-3.62	0.74		
Secondary	+0.98	0.01			+1.85	1.44
	-3.02	0.31	-3.33	0.74		

The actual vehicle rigid body rates obtained by data smoothing are within the rate limits and are shown with the maximum attitude error change from pre-BECO level in Table IV-6.

TABLE IV-6

Maximum Rigid Body Rates and Attitude Change During Staging

Axis	Rigid Body Rate (deg/sec)	Time from BECO (sec)	Maximum Attitude Change (deg)	Time from BECO (sec)
Pitch	-0.9	1.2	-0.58	1.6
Yaw	+0.8	1.5	+0.95	2.6
Roll	-2.5	0.3	-1.68	1.1

2. Stage II Flight Performance

The pitch and yaw attitude errors during flight are shown in Figs. IV-5 and IV-6.

Normal response to the radio guidance commands was substantiated by the TARS and rate gyro signals.

C. POST-SECO FLIGHT

1. Vehicle Motions

Time histories of the pitch, yaw and roll primary and secondary attitude errors while operating on primary system control are shown in Fig. IV-7. The maximum vehicle rates during the period following SECO are presented in Table IV-7.

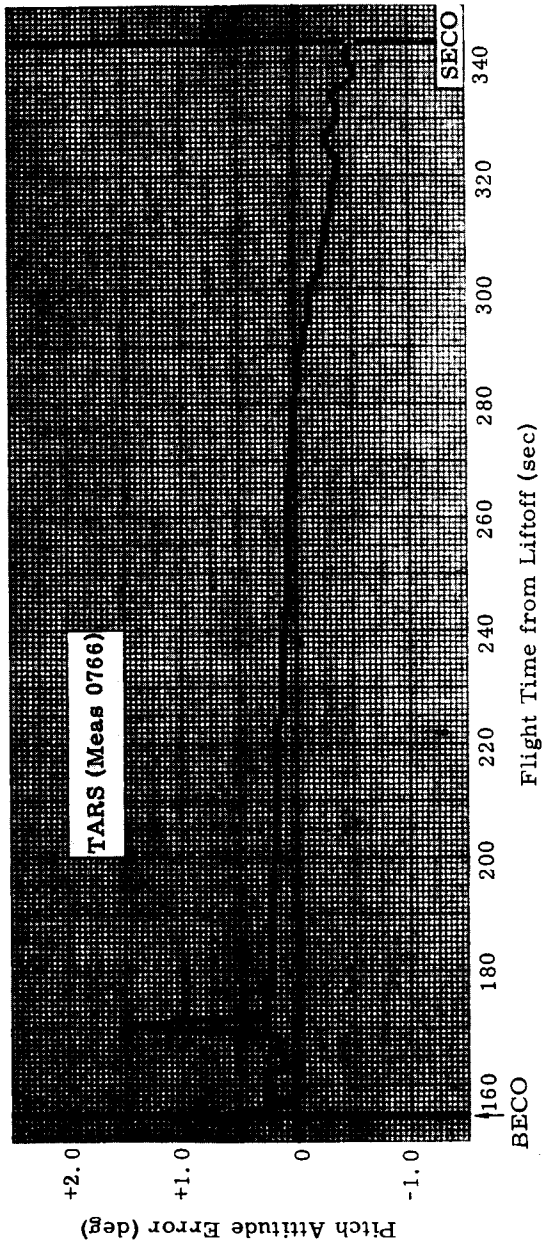

Fig. IV-5. Pitch Attitude Error During Stage II Flight

UNCLASSIFIED

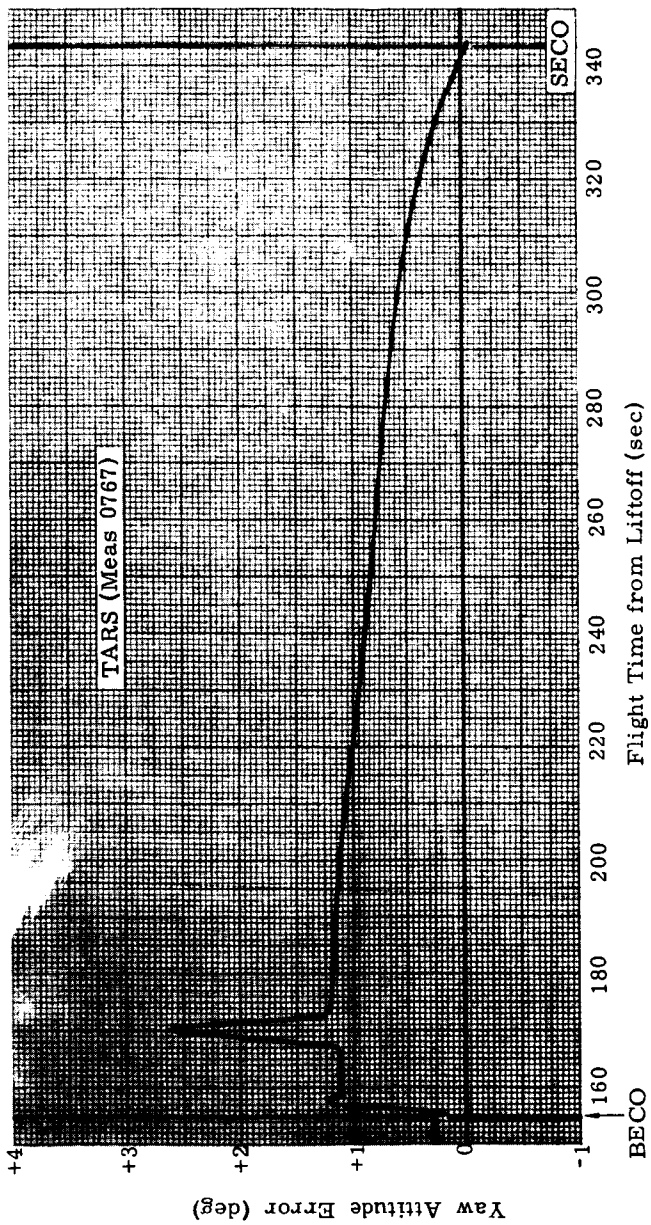

Fig. IV-6. Yaw Attitude Error During Stage II Flight

UNCLASSIFIED

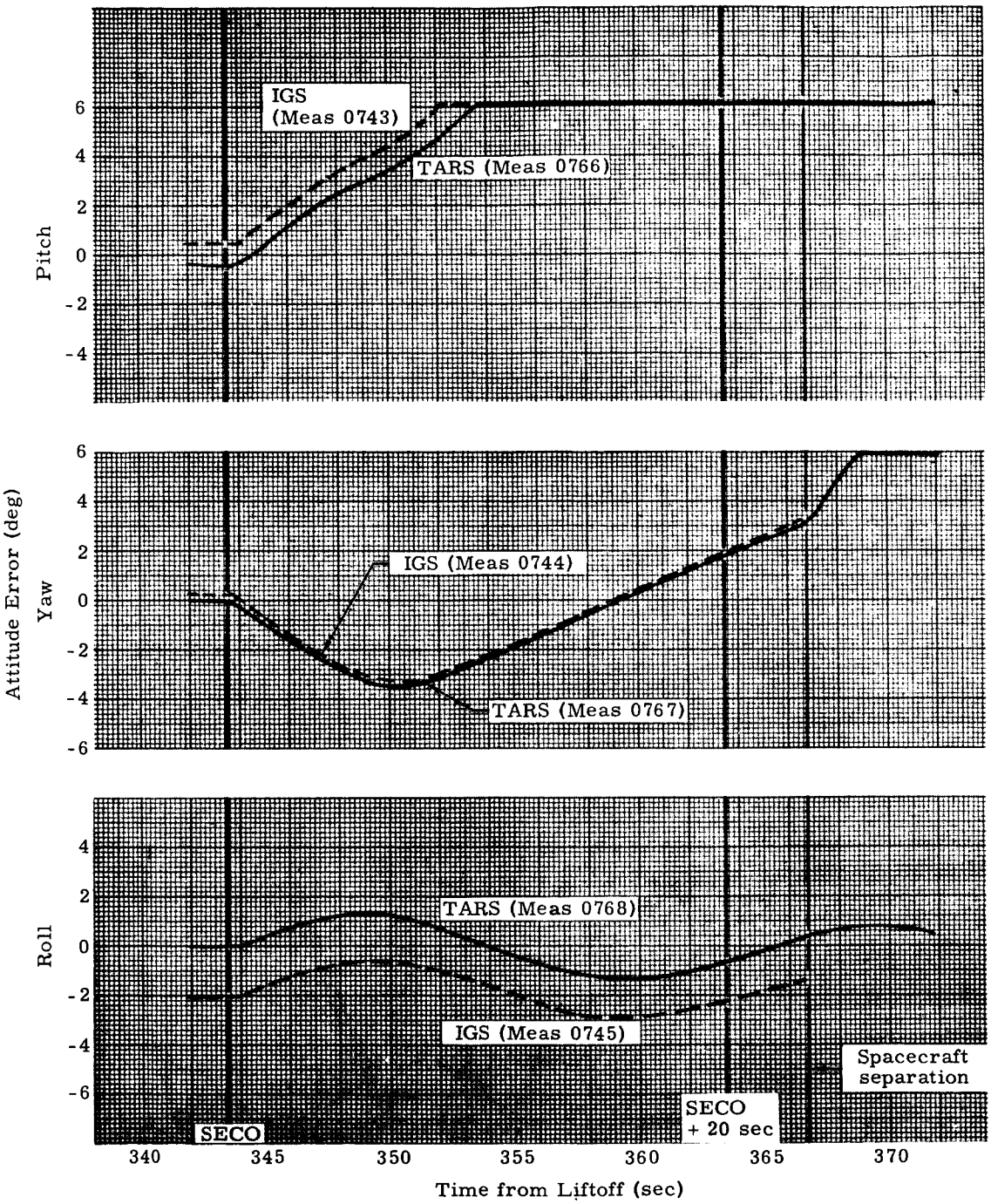

Fig. IV-7. Attitude Errors During Post-SECO Flight

TABLE IV-7

Post-SECO Vehicle Rates

	Pitch		Yaw		Roll	
	Rate (deg/sec)	Time from SECO (sec)	Rate (deg/sec)	Time from SECO (sec)	Rate (deg/sec)	Time from SECO (sec)
Maximum Positive						
Primary	+0.80	2.03 and 7.23	+0.47	10.33	+0.40	0.53
Secondary	+0.80	1.53 and 7.68	+0.49	10.28	+0.41	0.48
Maximum Negative						
Primary	-0.09	0.03	-0.69	1.63	-0.38	8.18
Secondary	-0.19	0.08	-0.69	1.68	-0.39	9.73
Insertion						
Primary	+0.50	20.0	+0.47	20.0	+0.19	20.0
Secondary	+0.40		+0.49		+0.20	
Spacecraft Separation						
Primary	+0.50	23.20	+0.47	23.20	+0.29	23.20
Secondary	+0.50		+0.49		+0.31	

V. HYDRAULIC SYSTEM

Analysis of telemetered data revealed that the GT-12 hydraulic system performed satisfactorily during Stages I and II flight.

Prior to SFT, the engine-driven hydraulic pumps were replaced with newly cleaned units, thereby minimizing the probability of contamination during vehicle system tests requiring hydraulic power. The newly installed pumps were checked with a gauss meter to verify free motion of the compensator.

A. STAGE I

1. Primary Subsystem

The final Stage I hydraulic system pressure and level check in the countdown was performed automatically by the sequencer. At T-180 seconds, function control A-7 initiated the motor-driven pump run, which pressurized the secondary system. Approximately 70 seconds later, AGE, using the motor pump, automatically selected and pressurized the primary system. Electric motor pump pressure was a normal 3165 psia at T-0. Engine start transients starting at $87FS_1$ + 0.78 second produced flow demands which dropped primary pressure to 2705 psia at $87FS_1$ + 0.89 second. Pressure recovery occurred immediately, indicating proper pump compensator response. The pressure overshoot on recovery peaked at 3150 psia at $87FS_1$ + 1.15 seconds. A steady-state pressure of 3008 psia was reached at $87FS_1$ + 1.65 seconds. There were no significant pressure perturbations either at liftoff or during flight. Pressure decayed normally during flight to 2721 psia at staging.

Prior to T-110 seconds, the static reservoir level was 55.2% full, and it decreased to a normal 33.0% full at T-0. The level increased during flight to 46.8% full at staging. This 13.8% increase is a result of normal fluid expansion with increasing fluid temperature.

The steady-state reservoir levels and the level changes during system pressurization were normal.

Primary and secondary system pressures and pressure switch actuation points are shown in Fig. V-1.* A comparison of primary system pressure for GT-12 and GT-11 launches during engine start and hold-down is presented in Fig. V-2.*

*The pressure values quoted were obtained from telemetered data. It has been determined that primary and secondary pressure readings are low by 67 psi and 100 psi, respectively. This bias was due to a change in transducer outputs subsequent to calibration by the vendor. The magnitude of the error was determined by comparing vendor acceptance data on Stage I pumps with telemetered data. The GT-12 curves plotted in Figs. V-1, V-2 and V-3 were corrected to include the respective bias.

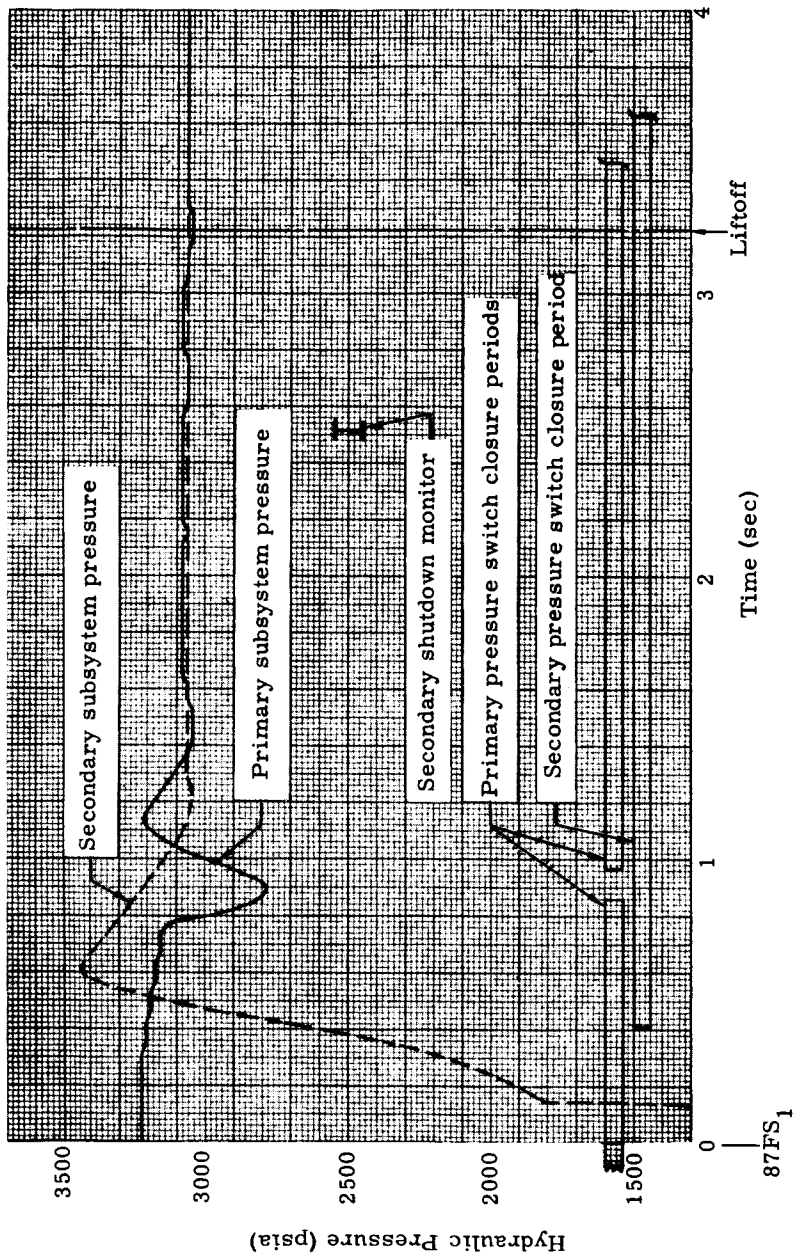

Fig. V-1. Stage I Hydraulic System Pressure Variation During Engine Start and Holddown

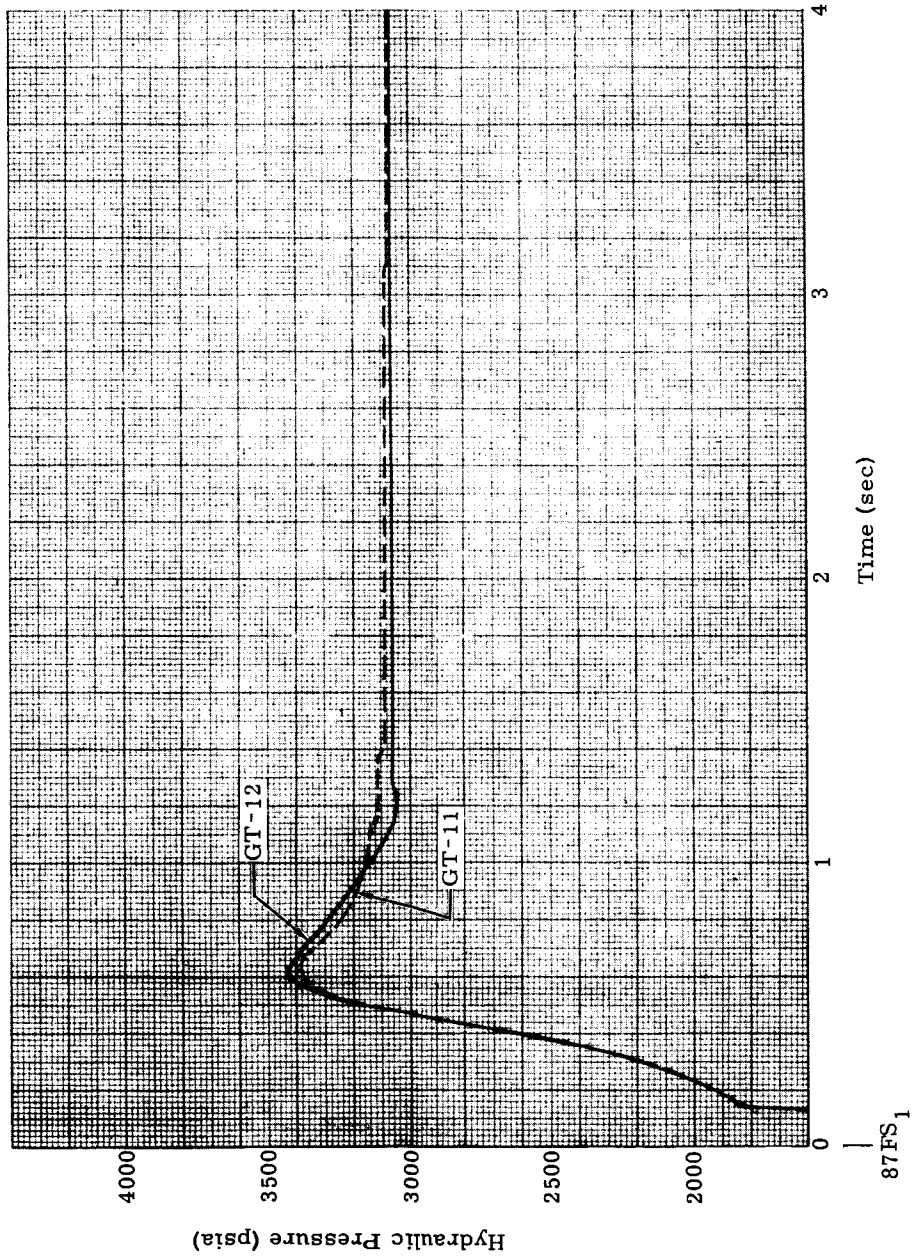

Fig. V-3. Comparison of Secondary System Hydraulic Pressure During Engine Start and Holddown

UNCLASSIFIED

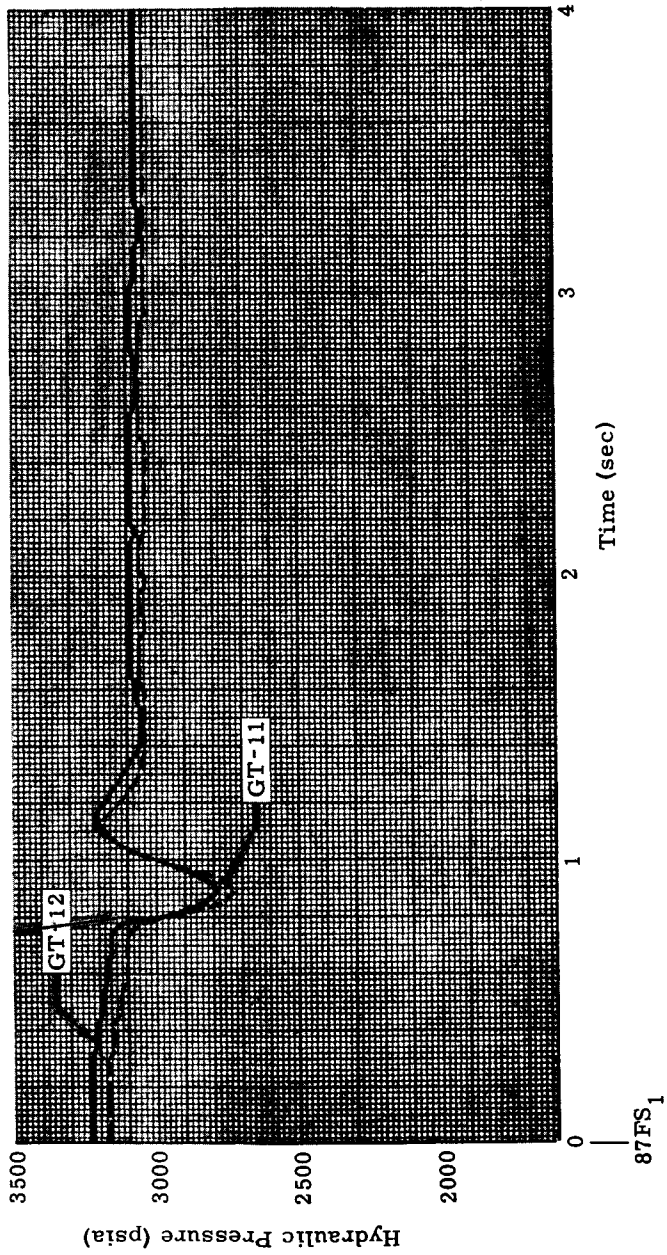

Fig. V-2. Comparison of Primary System Hydraulic Pressure During Engine Start and Holddown

UNCLASSIFIED

2. Secondary System

The final Stage I secondary hydraulic system pressure and reservoir level check was performed during a sequencer-initiated, motor-driven pump run from T-180 seconds to T-110 seconds. The indicated accumulator precharge was 1710 psia. Motor pump pressure was a normal 3100 psia at T-110 seconds.

The static reservoir level, which was normal at 55.0% full prior to pressurization at T-3 minutes, decreased to 30.4% full at T-110 seconds. These levels and the level changes during pressurization and depressurization of the system were normal.

At T-0 the system was unpressurized (soft). Pressure began to develop immediately as start cartridge energy rotated the engine turbine. Pressure overshoot reached a maximum of 3330 psia, indicating excellent pump compensator response. A steady-state pressure of 2965 psia was reached at $87FS_1$ + 1.30 seconds. At the pressure shutdown interrogation point, the pressure remained steady at 2965 psia.

There were no pressure perturbations during flight, since the system remained in a standby condition. Pressure decayed normally during flight to 2694 psia at staging.

The reservoir level stabilized at 33.9% full after engine start, increasing during flight to 44.2% full at staging. This 10.3% increase is a result of normal fluid expansion with increasing fluid temperature.

A comparison of secondary system pressures during engine start and holddown for GT-12 and GT-11 launches is presented in Fig. V-3.*

B. STAGE II

The final Stage II hydraulic system pressure and level check was performed during a sequencer-initiated, motor-driven pump run from T-240 to T-180 seconds. The indicated accumulator precharge was 1800 psia. Electric motor pump pressure stabilized at a normal 3190 psia. The static reservoir level was 58.2% full, decreasing to 37.2% full after pressure application and again increasing to 59.4% full upon removal of pressure at T-3 minutes.

During engine start-up at staging, the indicated accumulator precharge was 1740 psia and pressure overshoot was to 3845 psia. Steady-state pressure after engine start was 2895 psia, decreasing to 2749 psia at SECO. No significant pressure perturbations occurred during flight. After SECO the pressure fluctuated with engine rpm, a normal reaction to the low and variable turbine speeds occurring during this period.

*See footnote page V-1.

The reservoir level was a normal 59.4% full prior to staging. After staging, the level stabilized at 39.2% full, gradually increasing to 41.9% full at SECO. This 2.7% increase is a result of normal fluid expansion with increasing fluid temperature.

The reservoir levels and changes in level during pressurization and depressurization of the system were normal.

VI. GUIDANCE SYSTEMS

A. RADIO GUIDANCE SYSTEM PERFORMANCE

1. Rate Beacon

Rate beacon performance was satisfactory. Good lock was maintained from approximately LO + 29.6 seconds to SECO + 26.6 seconds. Final loss of lock occurred at approximately SECO + 31.2 seconds. The loss of lock at Stage I engine ignition is normal; relock occurs as the primary antenna is brought into favorable ground station view.

Values of the rate beacon telemetered functions during flight are listed in Table VI-1.

TABLE VI-1

RGS Telemetered Functions

Function	Meas	Maximum Value	Minimum Value
Rate Beacon			
Received signal No. 1	0750	4.22 vdc*	4.14 vdc*
Phase detector	0751	3.10 vdc*	2.66 vdc*
Power out	0752	4.32 vdc*	4.28 vdc*
30-volt supply	0746	2.90 vdc	2.88 vdc
Pulse Beacon			
Magnetron current	0753	3.88 vdc**	3.80 vdc**
AGC	0754	-9.5 dbm**	-45.4 dbm**
15-volt supply	0747	4.24 vdc	4.18 vdc
Decoder			
10-volt supply	0748	4.48 vdc	4.46 vdc

* Does not include normal periods of unlock.
**Does not include antenna crossover period.

2. Pulse Beacon

Pulse beacon performance also was satisfactory. Good lock* was maintained through Stage I engine ignition and up to approximately SECO + 33.8 seconds. Complete loss of lock occurred at approximately SECO + 42.0 seconds.

Normal oscillations during the antenna crossover period were observed in AGC from approximately LO + 26.5 seconds to LO + 76.6 seconds. During this time the minimum signal level received by the beacon was -62.5 dbm. A small percentage of messages was not received by the pulse beacon during the period of peak AGC oscillations (antenna crossover period). This occurred on six of the twelve Gemini flights and is considered normal. The normal ground station signal level increase occurred at LO + 91.4 seconds and was observed on telemetry to be approximately 21.7 dbm.

Values of the pulse beacon telemetered functions during flight are listed in Table VI-1.

3. Decoder

Decoder performance was normal. Comparisons of the decoder telemetry data with the Burroughs computer-generated output data indicate that pitch and yaw steering signals and the SECO discrete were received and executed properly.

Values of the decoder telemetered functions are listed in Table VI-1.

4. Guidance Commands

a. Pitch steering

The decoder pitch steering output for the entire Stage II flight period is shown in Fig. VI-1.

The initial decoder output command began at approximately LO + 167.986 seconds and built up to approximately 7.0% pitch down. This command was maintained for 0.5 second. Subsequently the pitch command increased to the maximum 100% pitch-down (-2.0 deg/sec) value, which was maintained for approximately 1.0 second.

---

*"Good lock" is defined as the condition in which no messages are missed by the pulse beacon. The ground station does not lose lock, however, unless a number of consecutive messages are missed.

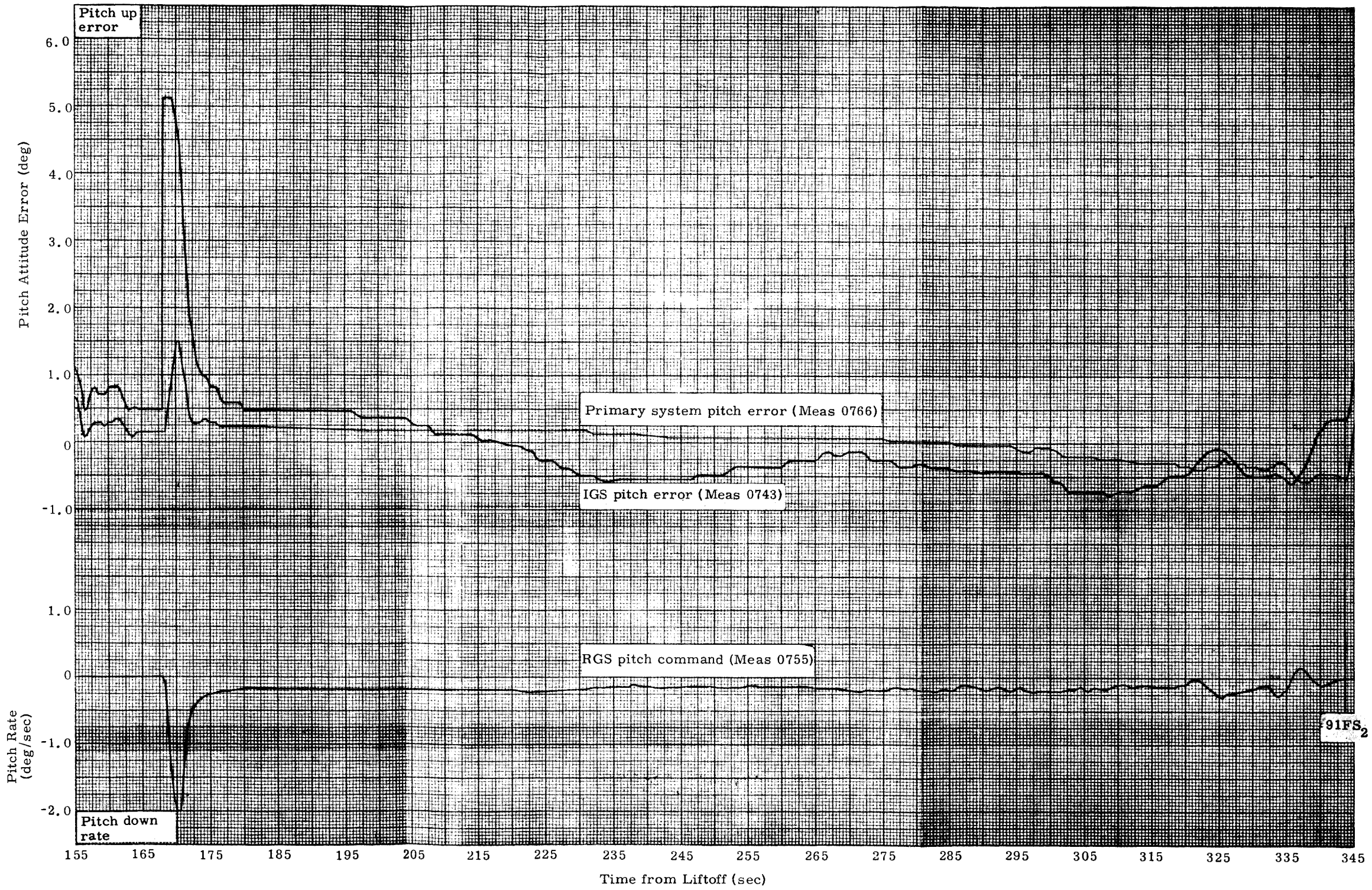

Fig. VI-1. Stage II RGS/IGS Pitch Flight History

Thereafter, the pitch steering command decreased to 0.25 deg/sec pitch down within 5 seconds and remained between zero and 0.25 deg/sec pitch down for the remainder of Stage II flight with the exception of the last 20 seconds prior to SECO.

For the last 70 to 80 seconds of Stage II flight, oscillations were apparent on both the Burroughs and the airborne pitch steering command outputs. These oscillations were similar to those observed on previous Gemini flights, and the maximum peak-to-peak excursion was approximately 0.45 deg/sec.

b. Yaw steering

Decoder yaw steering commands began at approximately LO + 168.437 seconds and built up to the maximum 2.0 deg/sec yaw left. This command was maintained for approximately 1.0 second. Thereafter, the yaw command decreased to 0.05 deg/sec yaw left within 6 seconds. Subsequently, yaw commands remained within ± 0.05 deg/sec for the remainder of Stage II flight. The decoder yaw steering output for the entire Stage II flight is shown in Fig. VI-2.

c. Discrete commands

The times for the computer-generated SECO/ASCO commands and the vehicle responses are shown in Table VI-2.

TABLE VI-2

SECO/ASCO Events

Signal	Meas	Time from Liftoff (sec)
Ground station SECO	--	343.486 ± 0.003
Ground station ASCO	--	343.491 ± 0.003
Decoder discrete output	0777	343.519 ± 0.005
$91FS_2$	0519	343.539 ± 0.005
ASCO	0799	343.592 ± 0.025

The data shown in Table VI-2 indicate that the SECO time delay from ground station issuance to $91FS_2$ was 53 ± 8 milliseconds. The time delay between $91FS_2$ and ASCO reception was 53 ± 30 milliseconds.

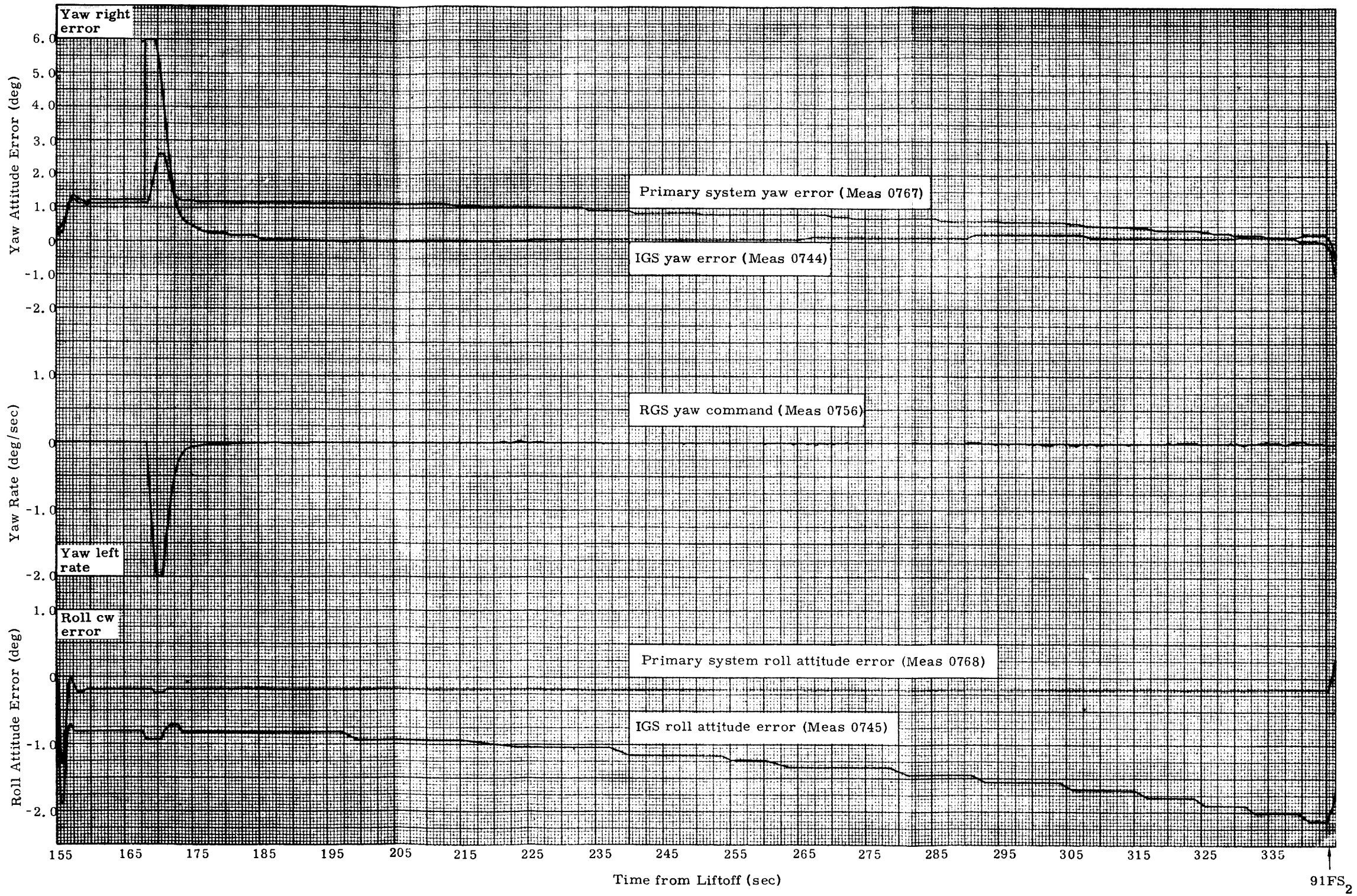

Fig. VI-2. Stage II RGS/IGS Yaw/Roll Flight History

UNCLASSIFIED

B. SPACECRAFT INERTIAL GUIDANCE SYSTEM ASCENT PERFORMANCE

1. Prelaunch Nulls

The prelaunch IGS attitude error null signals were as follows:

Pitch	-0.087 degree
Yaw	+0.140 degree
Roll	+0.025 degree

These signals were well within the specification values of ± 0.42 degree in pitch and yaw and ± 1.30 degrees in roll.

2. Stage I Performance

IGS performance during Stage I flight correlated well with the primary system. This is shown by a comparison of IGS and corresponding primary system attitude errors in Figs. IV-2 through IV-4, which show the dispersions between IGS and primary system attitude errors at BECO. These dispersions are primarily due to TARS and IGS in tolerance drifts and programmer errors.

The IGS Stage I gain change discrete was issued at LO + 110.161 seconds ± 0.025 second, which was well within the specification time of 110.00 seconds ± 1%.

3. Stage II Performance

IGS attitude errors indicated that IGS performance during Stage II flight was normal.

a. Stage II pitch

IGS Stage II pitch attitude error is shown in Fig. VI-1. Primary system pitch attitude error and RGS pitch steering commands are shown for comparison.

IGS closed-loop pitch guidance began at LO + 168.087 seconds. IGS pitch attitude error built up to +5.11 degrees shortly thereafter and remained at this value for approximately 1.3 seconds. Figure VI-1 shows that, due to the RGS pitch rate command, the TARS pitch attitude error built up during this same time period to about +1.5 degrees. IGS pitch behavior during this period was normal and compares well with primary system behavior in correcting the vehicle trajectory errors.

UNCLASSIFIED

As the RGS pitched the vehicle down, IGS pitch attitude error decreased to +0.5 degree within 11 seconds. For the remainder of Stage II flight, IGS pitch output remained within limits of +0.5 to -0.8 degree. The pitch-up attitude error (pitch-down command), which built up just prior to SECO, was due to the influence on the vehicle of the RGS pitch steering oscillations. This effect, due to erroneous noise induced RGS pitch commands, has been noted on previous flights.

b. Stage II yaw

IGS Stage II yaw attitude error is shown in Fig. VI-2. Primary system yaw attitude error and RGS yaw steering commands are shown for comparison. Yaw steering began at the same time as pitch. The IGS yaw attitude error saturated at +5.97 degrees shortly thereafter and remained on saturation for approximately 1.5 seconds. Figure VI-2 shows that the TARS yaw attitude error built up during this same period to approximately +2.6 degrees due to the RGS yaw left rate command. Therefore, IGS yaw behavior during this period appears to be normal and compares well with the primary system behavior in correcting the vehicle trajectory.

Thereafter, the IGS yaw attitude error decreased to +0.05 degree within 17 seconds as the RGS command yawed the vehicle left. For the remainder of Stage II flight, the IGS yaw attitude error remained within limits of +0.05 to +0.30 degree.

c. Stage II roll

IGS roll attitude error for Stage II is shown in Fig. VI-2, with TARS roll attitude error shown for comparison. As shown by the increase in IGS roll output during the latter portion of Stage II flight, there was an apparent drift rate between TARS and IGS roll. The drift rate was CCW, IGS with respect to TARS. The dispersion is predominantly due to TARS roll gyro g-sensitive drift; this type of drift was noted on all flights. The disturbance indicated in roll between approximately LO +168 and LO +174 seconds is due to vehicle motions resulting from the pitch and yaw guidance commands coupling into roll. This coupling is normal and was experienced to some degree on all flights.

VII. ELECTRICAL SYSTEM ANALYSIS

A. CONFIGURATION

The launch vehicle airborne electrical system components installed for the GT-12 flight were identical to those used on GLV-11.

B. COUNTDOWN AND FLIGHT PERFORMANCE

The airborne electrical system functioned as designed during the launch and flight, with all parameters within specifications. Power transfer was comparatively smooth and liftoff occurred without incident.

During staging, the IPS current trace indicated that a squib shorted to structure, maintaining a current increase of approximately 22 amperes until stage separation. This compares with other staging shorts encountered on the GT-2, GT-6 and GT-11 flights.

Currents to the Stage II redundant shutdown squibs at SECO were not detected on either the APS or IPS trace; however, squib operation was confirmed by Meas 0521.

At spacecraft separation, the launch vehicle/spacecraft electrical interface was cut by a guillotine in the adapter. This caused a 7.7-ampere spike on IPS and a 29.0-ampere spike on APS for approximately 100 milliseconds. These guillotine shorts are expected and have occurred on all spacecraft separations except GT-8.

A summary of electrical system parameters measured at power transfer and during flight is presented in Table VII-1.

UNCLASSIFIED

TABLE VII-1

GLV-12 Launch Measurements

Meas	Parameter	At Power Transfer			At Liftoff	At Staging			At SECO			At Spacecraft Separation		
		Before	During	After		Before	During	After	Before	During	After	Before	During	After
0800	IPS (volts)	30.1	29.0	30.1	29.9	29.6	28.3	29.7	29.7	29.7	29.7	29.9	29.6	29.9
0804	IPS (amp)	28.5	28.5	28.5	26.1	27.9	50.3	24.4	23.2	24.4	23.8	23.8	31.5	23.8
0801	APS (volts)	30.3	30.1	30.4	29.7	29.8	29.5	30.0	29.7	29.7	29.7	30.0	28.7	30.0
0805*	APS (amp)	24.4	24.4	24.4	34.6	23.8	30.3	20.3	19.7	28.5	22.0	22.0	51.0	21.4
0802	400 cycle Phase A (volts)	114.4	114.4	114.4	114.5	114.4	114.4	114.4	114.4	114.4	114.4	114.4	114.4	114.4
0803	400 cycle Phase A (cps)	399.1	399.1	399.1	399.1	399.1	399.1	399.1	399.1	399.1	399.1	399.1	399.1	399.1
0726	25-vdc power supply (volts)	25.3	25.3	25.3	25.3	25.3	25.3	25.3	25.3	25.3	25.3	25.3	25.4	25.3

*Including TARS heater cycling current.

UNCLASSIFIED

VIII. INSTRUMENTATION SYSTEM

A. AIRBORNE INSTRUMENTATION

1. Prelaunch and Countdown Status

The airborne instrumentation system operated within specified limits during GT-12 prelaunch testing and countdown. No components in the system were replaced after simulated flight test.

Ambient checks during the launch countdown verified that all measurements were operating satisfactorily prior to T-0.

2. Data Acquisition

The measurement program for this launch consisted of 150 PCM analog signals and 38 PCM bilevel signals. All channels except Channel 17 (Meas 0514) functioned properly throughout the flight.

The oxidizer pump inlet temperature (Meas 0514) took an apparent 10.2° F offset at the time of propellant loading and retained the offset throughout the flight. By using the last data from landline Meas 4604 (Stage II oxidizer tank bulk temperature), the data from Meas 0514 were corrected, and satisfactory data were obtained during the flight.

3. Instrumentation System Parameters

Instrumentation system parameters, as measured in flight, are compared with specified limits (Table VIII-1). All data were within the required limits.

4. Telemetry Signal Strength (244.3 mc)

Telemetry signal strength records indicated satisfactory signal levels for data acquisition from the launch vehicle from liftoff to approximately SECO + 220 seconds. The anticipated staging blackout lasted approximately 280 milliseconds.

The Cape Kennedy Tel II and Tel III ground stations monitored the entire flight of the launch vehicle. The Grand Bahama Island station acquired data from approximately LO + 44 seconds to the end of the flight. The Grand Turk station acquired data during Stage II flight.

UNCLASSIFIED

TABLE VIII-1

Instrumentation System Parameters

Meas	Description	Required PCM Count / Required Engineering Units	PCM Count / Engineering Units: At Liftoff	At 87FS$_2$/ 91FS$_1$	At 91FS$_2$	At SECO + 20
0810	5-volt power supply	203 ± 1	204	204	203	204
		5.000 V ± 0.035	5.028	5.028	5.003	5.028
0811	40-volt power supply	229 ± 3	228	228	228	228
		40.00 V + 0.64 - 0.44	39.90	39.90	39.73	39.73
0813	PCM mercury cell	73 ± 1	73	73	73	73
		1.335 to 1.375 V	1.355	1.355	1.355	1.355
0814	PCM mercury cell	73 ± 1	73	73	73	73
		1.335 to 1.375 V	1.355	1.355	1.355	1.355
0815	PCM mercury cell	73 ± 1	73	73	73	73
		1.335 to 1.375 V	1.355	1.355	1.355	1.355
0816	+30-volt power supply	193 ± 3	193	193	193	193
		29.92 to 30.06 V	30.01	30.01	30.01	30.01
0817	-30-volt power supply	209 ± 3	210	210	210	210
		-29.92 to -30.08	-29.98	-29.98	-29.98	-29.98

UNCLASSIFIED

B. LANDLINE INSTRUMENTATION

1. Countdown Status

The landline instrumentation system operated satisfactorily from the start of propellant conditioning through the launch countdown up to liftoff. All instrumentation holdfire functions monitored in the blockhouse remained within specification throughout the countdown.

2. Data Acquisition

During propellant loading and launch countdown for GT-12, a total of 153 measurements, consisting of 33 on stripchart recorders for loading, 54 landline on stripcharts, 13 on oscillograph, and 24 on magnetic tape for launch, were monitored and recorded.

Data acquisition for all landline monitored data was 100%.

IX. RANGE SAFETY AND ORDNANCE

A. COMMAND CONTROL RECEIVERS

1. Countdown Performance

The command receiver shutdown, destruct and ASCO tests were successfully completed. Telemetry records indicated a stable signal strength of approximately 175 microvolts from the start of range telemetry records until liftoff. The signal strength levels for this prelaunch period were consistent with previous open-loop tests on GLV-12.

2. Flight Performance

Command receivers S/N 68 (APS) and S/N 74 (IPS) were flown on GLV-12. The RF carrier signal level at the command receiver reached a maximum of 2800 microvolts at LO + 76.28 seconds. The carrier signal was transferred as follows: Cape Kennedy low power to Cape Kennedy high power at LO + 66.68 seconds, Cape Kennedy high power (Station 1) to Grand Bahama Island (GBI) (Station 3) at LO + 119.53 seconds, and GBI to Grand Turk Island (GTI) (Station 7) at LO + 258.58 seconds. The command receivers issued the ASCO signal at LO + 343.596 seconds, with the signal coming from the GTI transmitter. The signal level at the time of ASCO was about 200 microvolts.

B. MISTRAM

1. Countdown Performance

The MISTRAM open-loop checks with the MACK Station were successfully completed. The MACK station input signals were stable from T-5 minutes until T-0, when the MACK station shut down. The transponder telemetry signals were consistent with other open-loop testing on GLV-12.

2. Flight Performance

a. Airborne transponder

Transponder S/N 152 was flown on GLV-12. Telemetry data and ground station reports indicated that the MISTRAM system had a highly successful flight operation. The transponder locked on to the ground Station 1 (Valkaria) at LO + 9.43 seconds. From the time of initial lock-up until handover from System I to System II, there were no system unlocks. There was the normal 1.3-second loss of signal due to the staging plume.

b. MISTRAM Station 1 (Valkaria)

Station 1 operated in active track from LO + 21 seconds until LO + 389.2 seconds, at which time handover to Station 2 (Eleuthera) occurred. There was a normal 1.3-second interruption in this active track because of the staging ionization plume. The primary use of MISTRAM data for impact prediction is from T + 60 seconds until spacecraft separation. With the time of spacecraft separation at LO + 366.724 seconds, MISTRAM was used for a period of 306.724 seconds (99.57% of the time) as the source of IP data. Utilization of the primary and secondary IP plots is shown in Table IX-1.

TABLE IX-1

Range Safety Plotboards Impact Prediction

Primary Plotboard		Secondary Plotboard	
System	Usage Time (sec)	System	Usage Time (sec)
MISTRAM	339.7	Mod III	280.6
Patrick AFB TPQ-18	1.3	Merritt Island TPQ-18	20.5
Cape Kennedy FPS-16	48.3	Patrick AFB TPQ-18	17.7
Bermuda FPS-16	8.1	Grand Bahama Island TPQ-18	72.8
Grand Turk Island	10.1	Cape Kennedy FPS-16	15.9
	407.5		407.5

c. MISTRAM Station 2 (Eleuthera)

Station 2 operated in passive track from LO + 120 seconds until LO + 390 seconds. With the handover from Station 1 at approximately LO + 390 seconds, Station 2 continued in intermittent active track through LO + 450 seconds. Station 2 data were not used as source data for the impact predictor.

C. ORDNANCE

Stages I and II prevalves, Stage I engine start cartridges and drop-weights ordnance operated satisfactorily.

Launch release ordnance nuts operated properly, with all nuts detonating as evidenced by the finding of the four studs and lower nuts.

Stage separation explosive nuts and Stage II engine start cartridge ordnance operated as required. The TARS timer arm signal occurred at LO + 144.518 seconds, and the IPS staging arm timer was actuated at LO + 144.979 seconds. Both times were compatible with GLV-12 trend data on these timers.

X. MALFUNCTION DETECTION SYSTEM

A. CONFIGURATION

The malfunction detection system (MDS) hardware installed on GLV-12 for the launch countdown and flight is presented in Table X-1.

TABLE X-1

MDS Components

Nomenclature	Part Number	Manufacturer	Serial Number
Rate switch package	PS830600015-027	Giannini	4020
Malfunction detection package	424-7569205-189	Martin	B035
Tank pressure transducers, Stage I	PS746000002-023	Servonics	Fuel A 1125 Fuel B 1139 Oxidizer A 1116 Oxidizer B 1113
Tank pressure, transducers, Stage II	PS746000002-025	Servonics	Fuel A 2114 Fuel B 2119 Oxidizer A 2129 Oxidizer B 2121
Stage separation connectors	CCI8119A1-9 CCI8119A1-6	Cannon	00067 00034
MDS engine switches Stage I	284321	Aerojet	S/A 1 primary 0001245 S/A 1 redundant 0001258 S/A 2 primary 0001246 S/A 2 redundant 0000805
MDS engine switches Stage II	711049-1	Aerojet	S/A 3 primary 0000786 S/A 3 redundant 0001257

Data analysis indicated proper performance of all the MDS hardware.

B. SYSTEM PERFORMANCE

Performance of the MDS during the launch countdown and flight was satisfactory.

1. Engine Pressure Switches

Operation of the Stage I engine malfunction detection thrust chamber pressure switches (MDTCPS) and the Stage II engine malfunction detection fuel injector pressure switches (MDFJPS) for the flight is summarized in Table X-2. These switches are required to "make" in a pressure range of 540 to 600 psia and "break" in a pressure range of 585 to 515 psia. During launch the Stage I engine start transient was of sufficient amplitude and time duration to cause the S/A 1 MDTCPS switches to respond momentarily to the thrust chamber pressure. All MDS engine pressure switches operated properly and within specification requirements.

TABLE X-2

Flight Operation of MDS Engine Pressure Switches

	S/A 1 (Meas 0356)	S/A 2 (Meas 0357)	S/A 3 (Meas 0855)
Make (540 to 600 psia)	2046:31.115 at 590 psia	2046:31:115 at 590 psia	2049:08.899 *
Break (585 to 515 psia)	2049:08.113 at 567 psia	2049:08.134 at 550 psia	2052:17.099 *

*S/A 3 fuel injector pressure is not instrumented on the Gemini Launch Vehicle; hence, make and break pressures were not available.

2. Switchover

The MDS switchover circuitry functioned properly throughout the flight. There were no switchover commands, and no switchover was executed, indicating proper performance of the circuitry.

3. Vehicle Rate Detection

The spin motor rotation detectors (SMRDs) contained in the malfunction detection package functioned properly. The SMRDs monitor rate switch package (RSP) gyro rotation speed and thereby its rate sensing capability.

The rate switch package operated properly throughout the countdown and flight. There were no MDS rate switch operations during any portion of the flight from liftoff through SECO. Table X-3 compares the maximum launch vehicle rates, measured during the period from liftoff through SECO, with the RSP switch settings.

TABLE X-3

Maximum Vehicle Rate Compared with Rate Switch Settings

		Stage I Flight	Flight Event	Stage II Flight	Flight Event
Rate Switch Settings (deg/sec)	Pitch	+2.5: -3.0	N/A	±10	N/A
	Yaw	±2.5	N/A	±10	N/A
	Roll	±20.0	N/A	±20	N/A
Maximum Vehicle Rates (deg/sec)	Pitch	-0.99	Wind shear	-1.87	RGS steering
	Yaw	+0.49	Wind shear	-2.24	RGS steering
	Roll	-1.61	Roll program	-2.34	Staging

Following SECO +24 seconds (after spacecraft separation), there were six operations of the rate switches. The rate gyro outputs verified that rate switch performance was in agreement with the RSP specification limits. Table X-4 summarizes the rate switch operation.

TABLE X-4

Rate Switch Operation

Specification Switch Operation Limits (deg/sec)	RSP Calibration Data	Time of Rate Switch Operation	Rate Gyro Output	
			Primary (deg/sec)	Secondary (deg/sec)
Yaw A close (2.08 to 2.92)	2.39 to 2.47	SECO + 24.7 sec	2.25	2.44
Yaw B close (2.08 to 2.92)	2.60 to 2.71	SECO + 25.7 sec	2.4	2.5
Yaw B open (2.71 to 1.93)	2.17 to 2.23	SECO + 27.3 sec	2.05	2.2
Yaw A open (2.47 to 1.79)	2.19 to 2.29	SECO + 27.6 sec	2.0	2.1
Pitch A close (2.08 to 2.92)	2.44 to 2.57	SECO + 40.2 sec	2.55	2.48
Pitch B close (2.08 to 2.92)	2.29 to 2.44	SECO + 41.2 sec	2.70	2.5

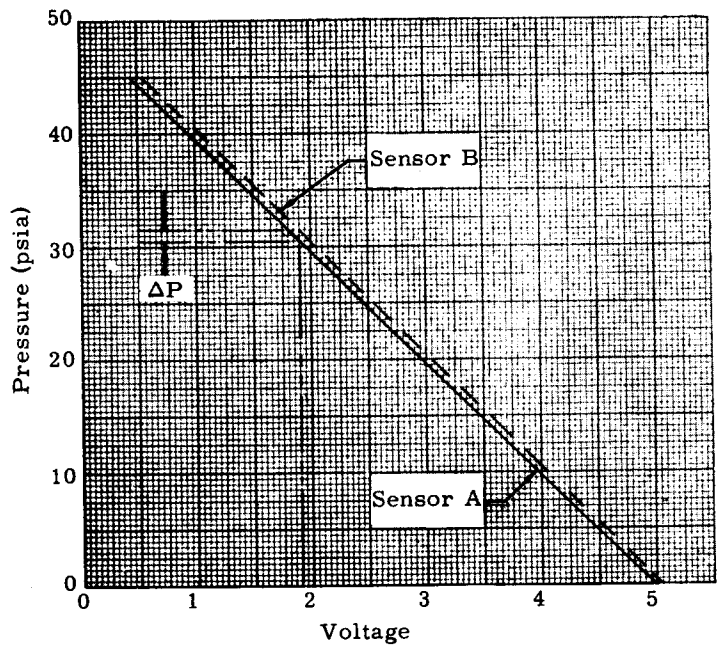

Fig. X-1. Calibration Curves for Stage I Fuel Tank Pressure Transducers

4. Tank Pressure Sensors

All MDS tank pressure transducers operated properly throughout the countdowns and flight. The maximum difference between the transducer pairs on each tank is presented in Table X-5.

TABLE X-5

Maximum Voltage and Pressure Differences Between Tank Pressure Transducer Pairs

	ΔVolts (telemetry)	Percent of Transducer Full Range	Δpsi	Percent of Transducer Full Range
Stage I fuel	0.027	0.54	0.15	0.30
Stage I oxidizer	0.027	0.54	0	0
Stage II fuel	0.077	1.54	0.8	1.07
Stage II oxidizer	0.086	1.72	1.0	1.33

Figure X-1 presents the calibration curves for the Stage I fuel tank pressure transducer pairs (A and B) to clarify the percentage variations between voltages and psi, shown in Table X-5. The maximum difference of 1.72% of transducer full-range output voltage is well within the transducer and telemetry system errors.

XI. CREW SAFETY

A. PRELAUNCH WINDS OPERATIONS

One week prior to the GT-12 launch (3 November 1966), the upper air winds at Cape Kennedy exceeded the Gemini design specification winds from 28,000 to 44,000 feet. An analog loads simulation was performed using these winds to determine if the Gemini go no-go criteria (limit load) had been exceeded. The load at Station 935 reached a maximum level of 95.5% of limit load. If this large wind shear had occurred on launch day, the recommendation would have been to go.

The prelaunch winds operations planned for GT-12 were identical to all flights since GT-9A, except that analog load simulations were made on every wind forecast received. All equipment performed satisfactorily, and all runs were completed on schedule.

Wind data released by the Air Weather Service for GT-12 are presented in Figs. XI-1 through XI-3. The T-0 sounding in Fig. XI-3 is not part of the scheduled prelaunch wind operations and is shown for reference only. The prelaunch winds operations performed on each of the wind data releases are summarized in Table XI-1.

TABLE XI-1

Summary of Prelaunch Winds Operations

Run No.	Time of Data Release to Martin-Baltimore	Operation
1	F-2 day 1100 EST 11-7-66	Wind comparison to specification. Wind in specification; load ratio 0.87; status go.
2	F-1 day 1100 EST 11-8-66	Wind comparison to specification. Trajectory, vehicle loads, vehicle response, and switchover structural and temperature constraints determined by computer programs. Wind in specification; load ratio 0.77; status go.
3	F-1 day 1100 EST 11-9-66	Same as F-1 day (11-8-66) except load ratio 0.75.
4	F-1 day 1100 EST 11-10-66	Same as F-1 day (11-8-66) except load ratio 0.73.

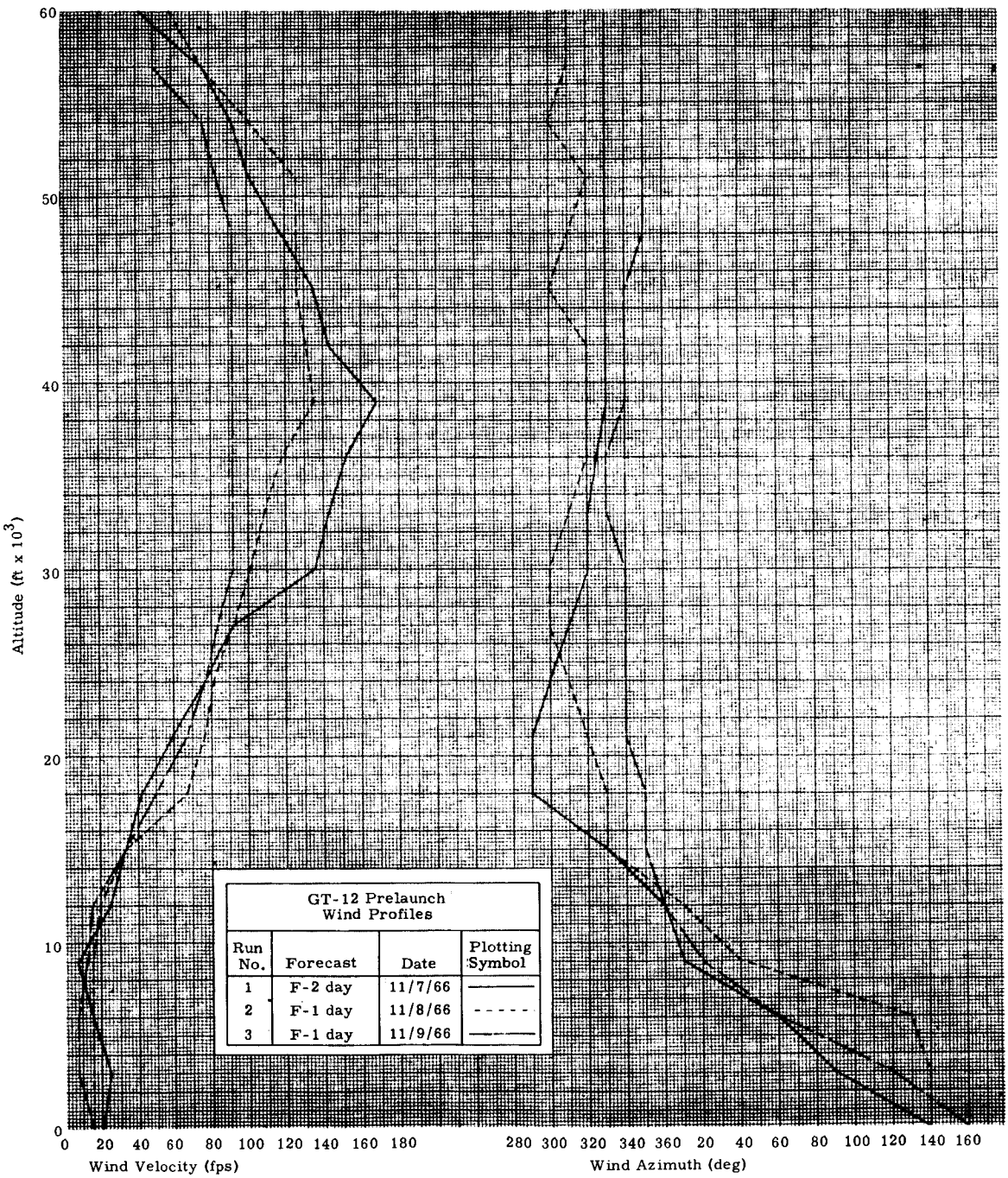

Fig. XI-1. F-2 and F-1 Day Wind Profiles

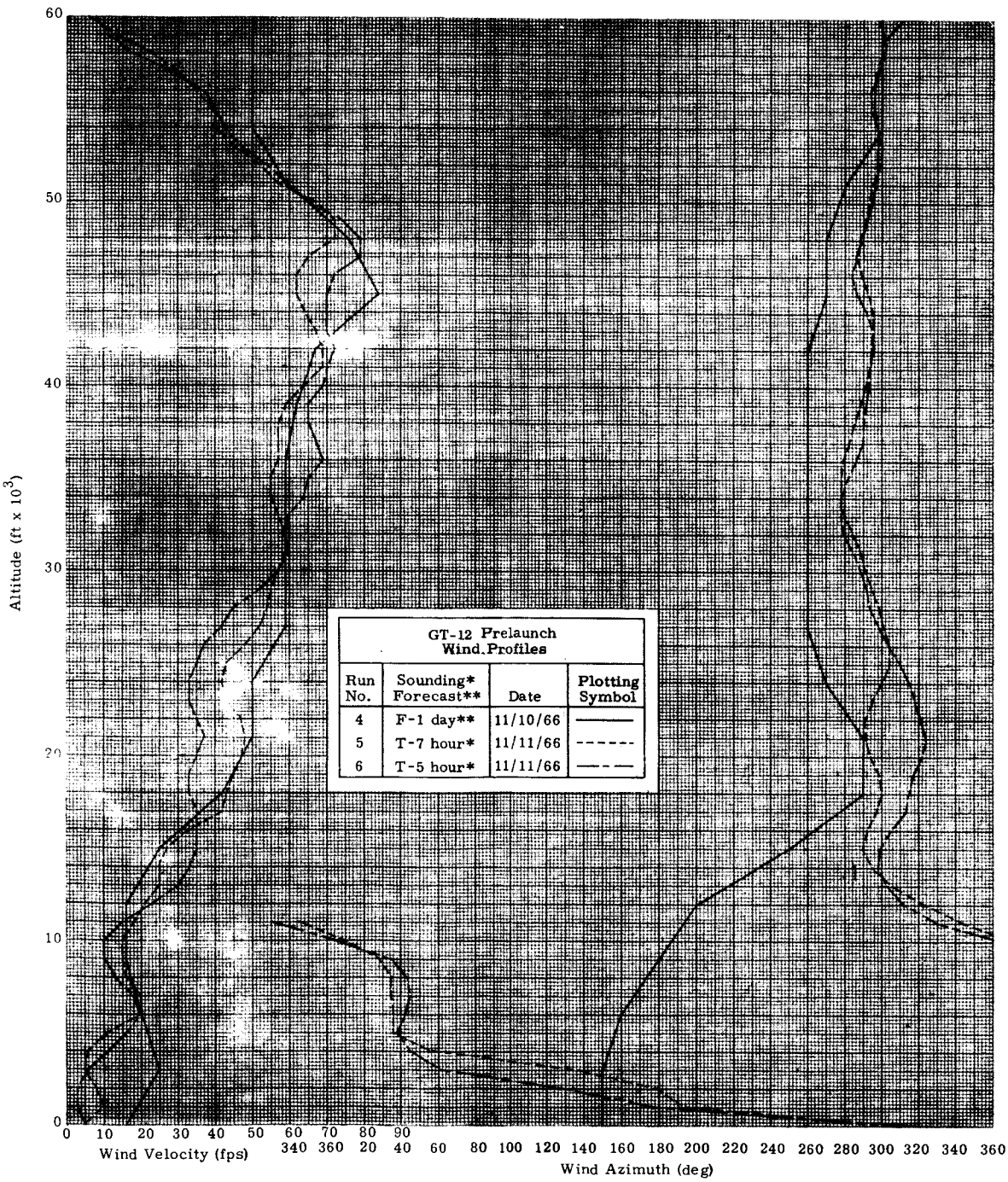

Fig. XI-2. F-1 Day, T-7 and T-5 Hour Wind Profiles

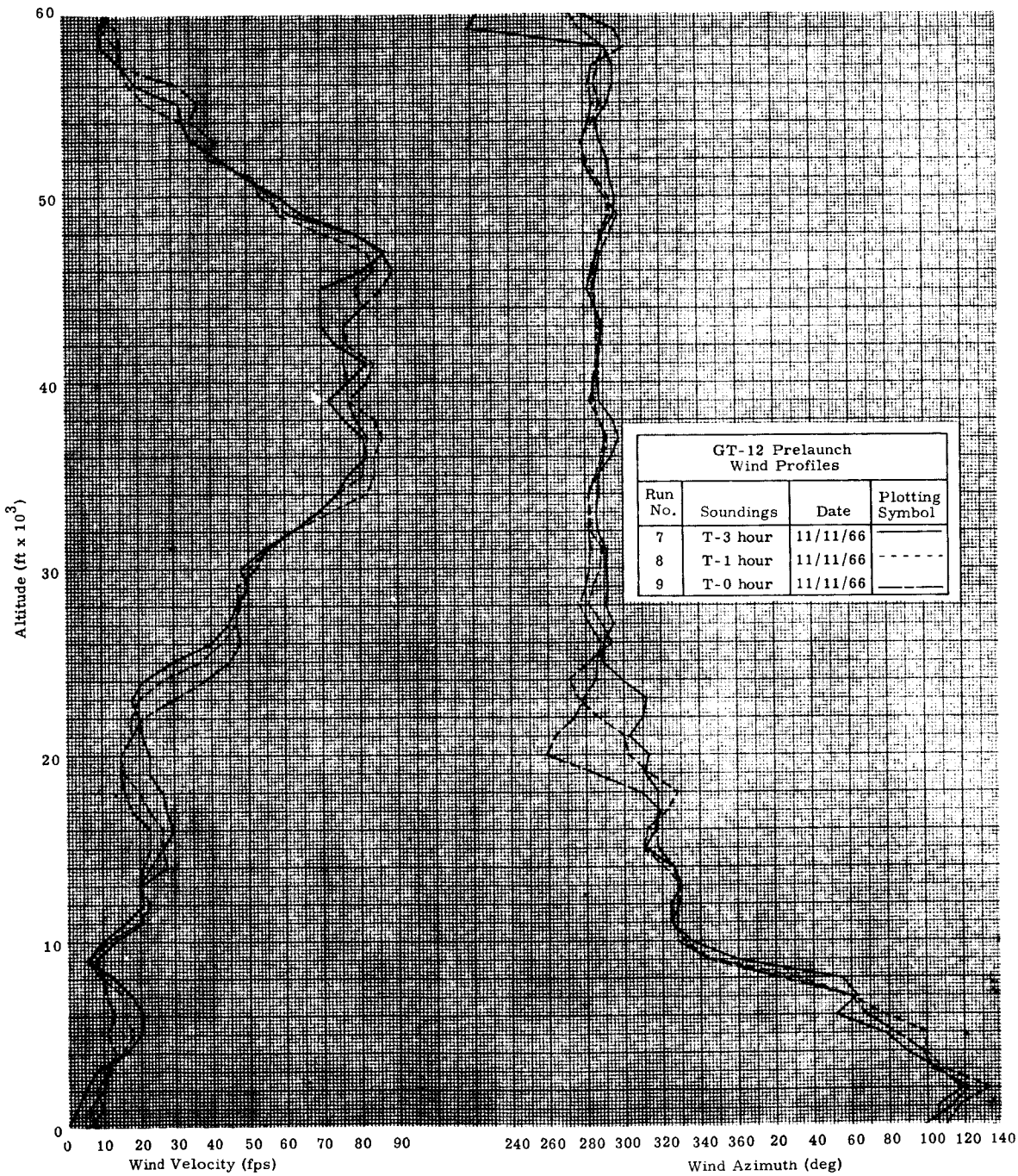

Fig. XI-3. T-3, T-1 and T-0 Hour Wind Profiles

TABLE XI-1 (continued)

Run No.	Time of Data Release to Martin-Baltimore	Operation
5	T-7 hours 0845 EST 11-11-66	Back-up trajectory computation completed by computer programs. Load ratio 0.73.
6	T-5 hours 1045 EST 11-11-66	Wind comparison to specification. Trajectory, vehicle loads, vehicle response, tank underpressure constraints, and switchover structural and temperature constraints determined by computer programs. Wind in specification; load ratio 0.74; status go.
7	T-3 hours 1245 EST 11-11-66	Same as T-5 hour run except load ratio 0.75.
8	T-1 hour 1445 EST 11-11-66	Wind comparison to specification. Wind in specification; load ratio 0.77; status go. Status phoned to Cape Kennedy and MCC-Houston prior to launch.

B. SLOW MALFUNCTION MONITORING

1. Prelaunch Phase

Prelaunch activities at MCC-Houston began on 4 November 1966 with a test of the data links with Baltimore. The data links, datafax and data card, were both satisfactory.

The original F-1 day, 8 November 1966, data were received on time. However, the secondary autopilot problem and subsequent launch delay precluded scribing a back-up slide.

The back-up slide scribing on 10 November 1966 was delayed several hours due to a defective computer tape. The problem was corrected by fabricating a new tape from the symbolic deck to ensure that the problem would not recur on launch day.

The T-5 hour trajectory and structure-temperature data for 11 November 1966 were received on time at MCC-Houston. The data were hand plotted on the staff support room (SSR) 30- x 30-inch plotboard sheets, and the card deck was held in reserve for real-time

computer complex (RTCC) utilization in the event that the T-3 hour data were not available in time to scribe the 10- x 10-foot display in the MOCR. The T-3 hour data were received on time, and all data were scribed in both the MOCR and the SSR by T-26 minutes. The countdown after the AATV launch was normal at MCC-Houston. The T-3 minute update from Burroughs was on time and agreed perfectly with the desired A_L at 100.6 degrees. Liftoff occurred at 2046:33.419 GMT on 11 November 1966.

2. Launch Phase

a. Stage I

Thrust misalignment at liftoff was slight in all three axes as observed on the strip chart recordings in pitch (Fig. XI-4) and in yaw-roll (Fig. XI-5).

The $\tilde{V}_I - \tilde{\gamma}_P$ actual trajectory and the T-3 hour predicted trajectory were in closest agreement observed throughout the program (Fig. XI-6). The $\tilde{V}_Y - T_E$ actual plot was approximately 50 fps less than predicted at BECO (Fig. XI-7).

The TARS and IGS were in close agreement throughout Stage I flight both in attitude errors and in programmed functions.

Staging conditions on the guidance monitor displays were $\tilde{V}_I$ = 10,048 fps, $\tilde{\gamma}_P$ = 18.3 degrees and $\tilde{V}_Y$ = -38 fps. The IGS attitude errors at staging were 0.72 degree nose up in pitch, zero degrees in roll and 0.12 degree nose right in yaw.

b. Stage II

RGS and IGS were in perfect agreement during the guided portion of Stage II flight. The RGS pitch displayed a slightly noisy operation for approximately the last 60 seconds of powered flight. The noisy ω_{pn} signal and subsequent noisy $V_I - \gamma_P$ trace on plotboard VA were much less than observed on past flights and caused no monitor concern.

	Stage II	Stage I	
	1-Sec Marks from Liftoff		1
Nose Down ↓	θ_{e_s} 743 ± 6°	θ_{e_s} 743 ± 6°	1
	SWO 872 - 874		2
Nose Down ↓	θ_{e_p} 766 ± 6°	θ_{e_p} 766 ± 6°	2
	GCP 728		3
Stage II Nose Down ↓ Stage I	δB_p GE/B ± 5°	$\dot{\theta}_c$ 732 MSB	3
	GCS 773		4
Nose Down ↓	ω_{pN} GE/B ±2°/sec	$\delta\theta_1$ 153 ± 5°	4
	Guid Init TARS 740		5
Nose Down ↓	$\dot{\theta}_g$ 755 ±2°/sec	$AP\theta_1$ 770 MSB	5
	δ_6 Guid Start GE/B		6
Nose Down ↓	ω_{ps} GE/B ± .5°/sec	$\delta\theta_2$ 150 ± 5°	6
	δ_7 SSCO GE/B		7
Nose Down ↓	$\delta\theta$ 651 ± 3°	$AP\dot{\theta}_2$ 771 MSB	7
	SWO Command		8
Roll CW ↓	———	$\dot{\phi}_c$ 734 MSB	8

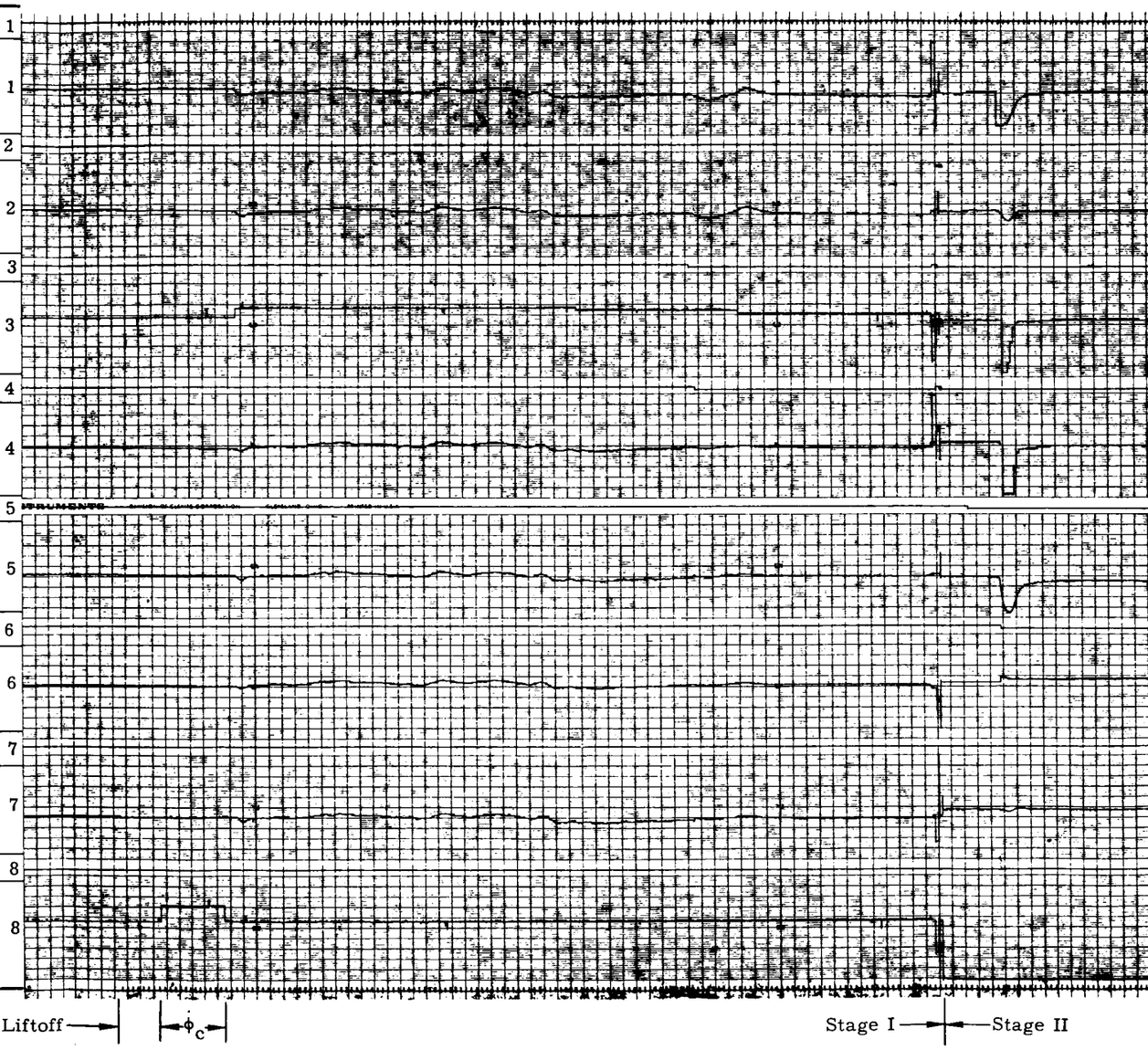

Fig. XI-4. Houston-MCC Recording Pitch Axis

	Stage II	Stage I	
	1-Sec Marks from Liftoff		1
Roll CW ↓	ϕ_{e_s} 745	ϕ_{e_s} 745 ± 6°	1
—	SWO 872 or 874		2
Roll CW ↓	ϕ_{e_p} 768 ± 6°	ϕ_{e_p} 768 ± 6°	2
—	GCP 728		3
Yaw Right ↓	ψ_{e_s} 744	ψ_{e_s} 744 ± 6°	3
—	GCS 773		4
Yaw Roll Axis ↓	ψ_{e_p} 767 ± 6°	ψ_{e_p} 767 ± 6°	4
—	Guid Init TARS 740		5
Yaw Right ↓	± 2°/sec W_{YN} GE/B	$\delta\psi_1$ 152 ± 5°	5
—	δ_6 GE/B		6
Yaw Right ↓	• 2°/sec $\dot{\psi}_g$ 756	$AP\psi_1$ 769 MSB	6
—	δ_7 SSCO GE/B		7
Yaw Right ↓	$\delta\psi$ 650 ± 3°	$\delta\psi_2$ 151 ± 5°	7
—	SWO Command		8
Roll CW ↓	$\delta\phi$ 652 ± 33°	$AP\psi_2$ 772 MSB	8

~~CONFIDENTIAL~~

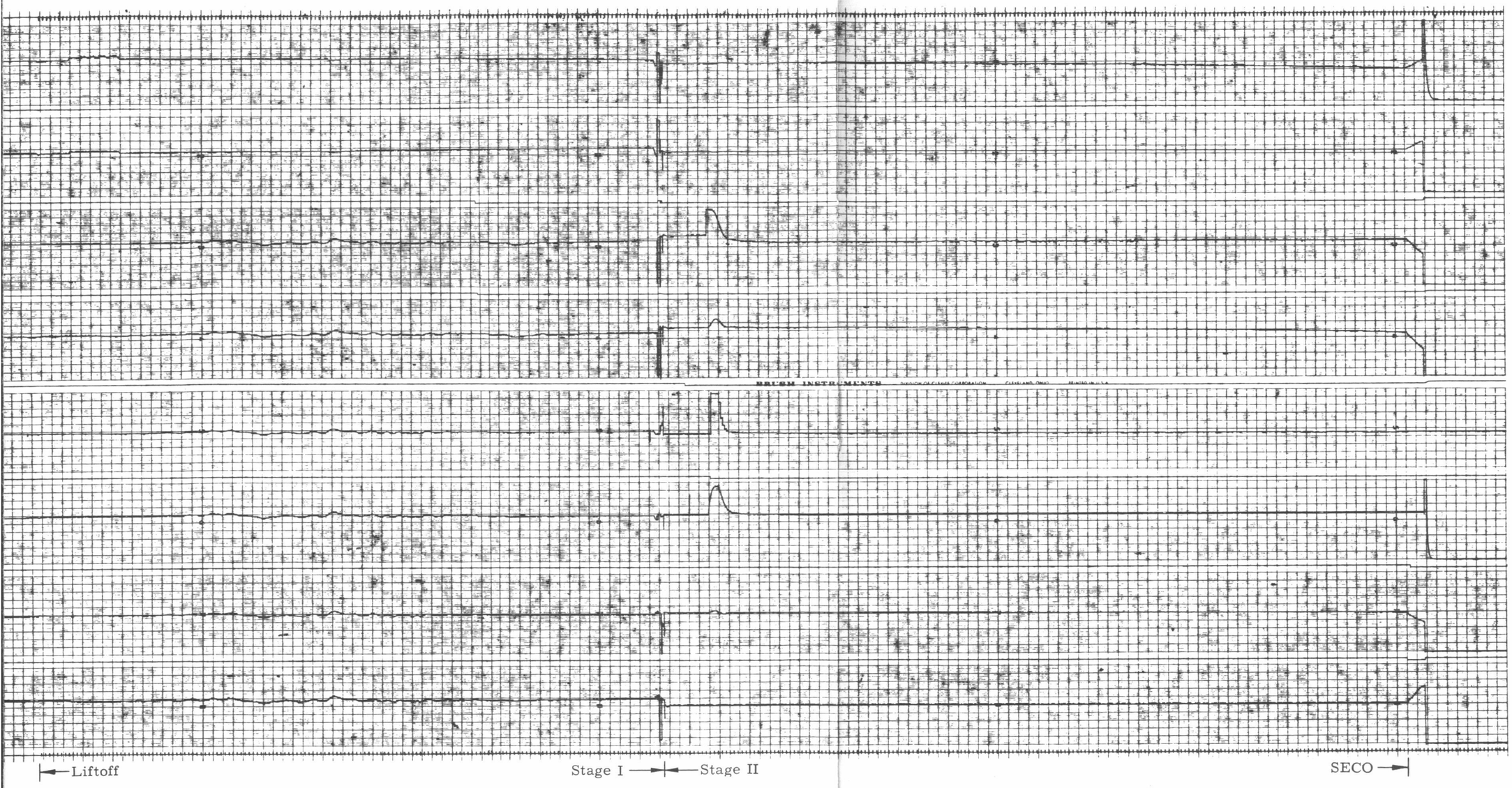

Fig. XI-5. Houston-MCC Recording Yaw-Roll Axes

~~CONFIDENTIAL~~

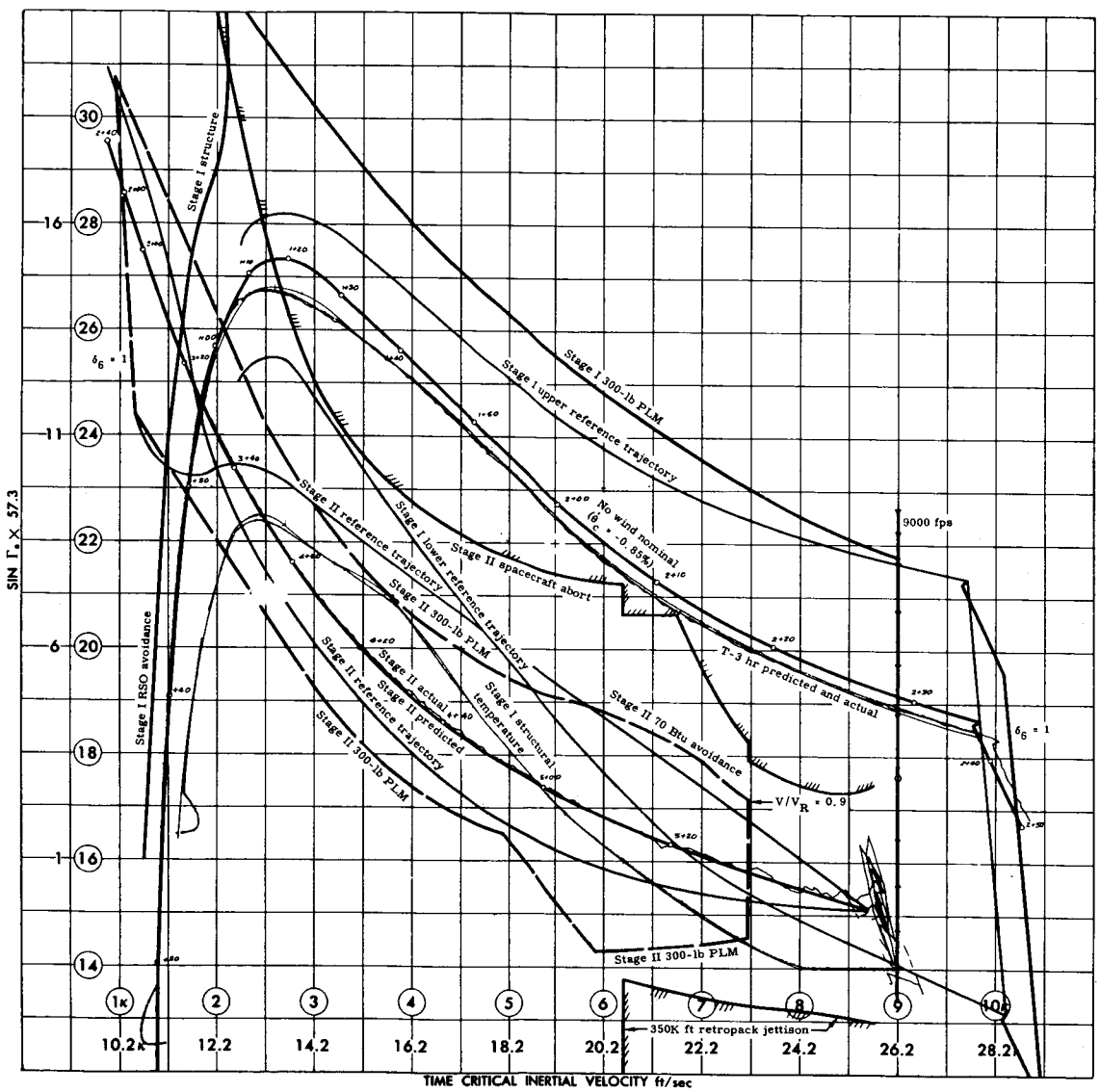

Fig. XI-6. Houston-MCC SSR Plotboard VA

~~CONFIDENTIAL~~

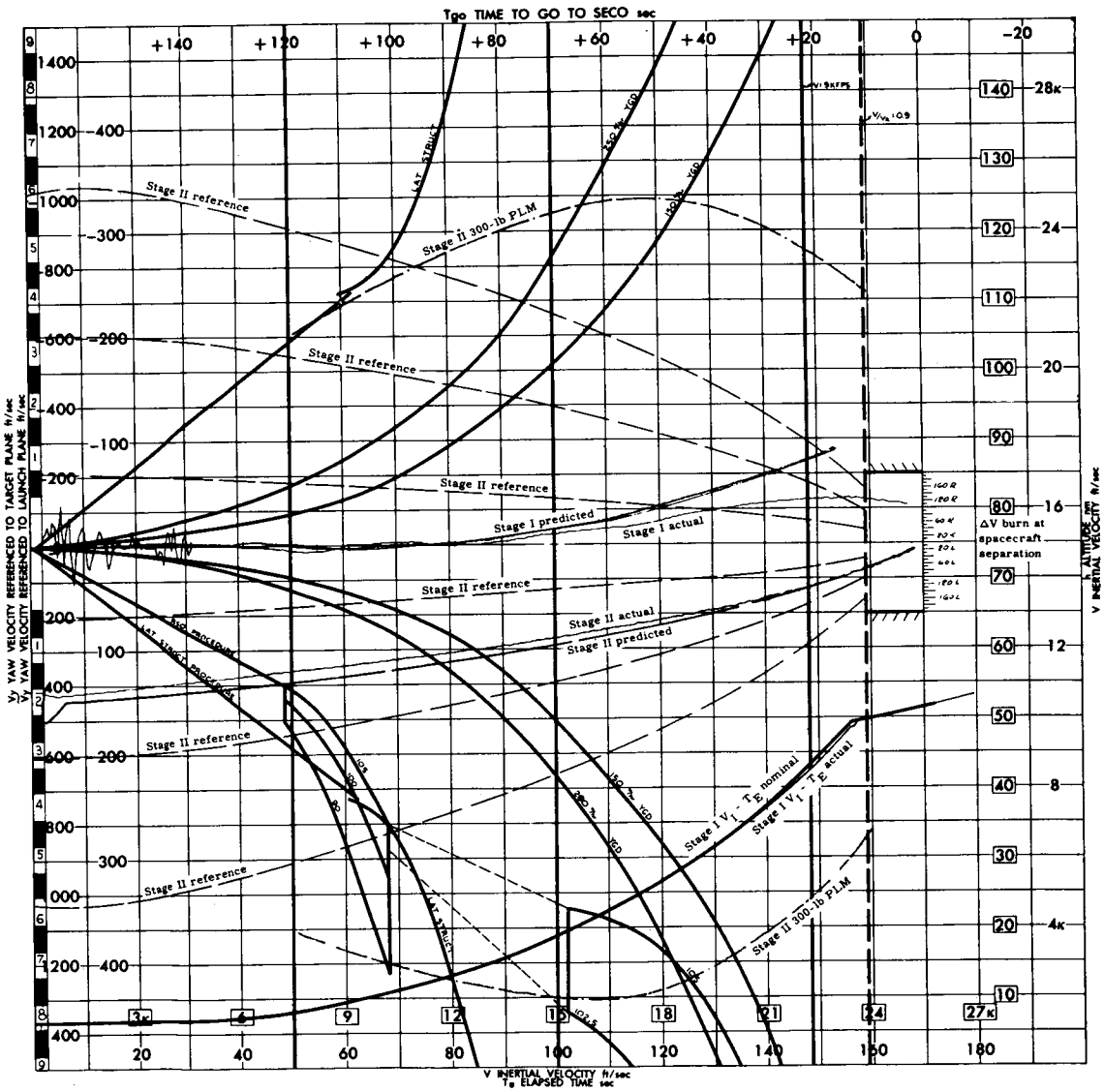

Fig. XI-7. Houston-MCC SSR Plotboard IIIA

~~CONFIDENTIAL~~

C. STAGING ANOMALY

A review of motion picture films from ground tracking stations and a downrange KC-135 aircraft indicates abnormal behavior of Stage I after staging. After a normal Stage II engine ignition and a separation of 30 to 40 feet, the Stage I oxidizer tank was observed to rupture and vent. This was followed by a delayed rupture of the fuel tank.

Figure XI-8 shows a comparison of the times of significant events as indicated by telemetry and visual observations made from three different vantage points. The ALOTS camera view was at right angles to the vehicle flight path while the Melbourne and Cocoa Beach views were at two different angles to the aft end of the vehicle. MDTCPS break and BECO corresponded with the time the Stage I engine light went out. The time at which the bright red oxidizer first blew out the exhaust ports corresponds well with the telemetered time of the rapid Stage II engine chamber pressure rise. Stage I engine firing could not be seen on the ALOTS film because the luminous inner surface of the engine bell was faced away from the camera; however, the other two films show that BECO coincides with the frame in which the Stage I engine light was observed to go out.

Two Stage I engine chamber pressure resurges were observed during thrust tailoff. The first resurge (0.1 second after BECO) was small but may have been the cause of the red flash aft of the Stage I engine. The second resurge (0.4 second after BECO) was large (45% of full thrust), and it appeared on film as though the engine were burning at full thrust for one frame.

All three films showed the yellow gas generator exhaust emerging from the exhaust ports 0.5 second after BECO. The bright red oxidizer flash at Stage II engine start is obvious on all three films. The time of interstage breakup is approximately 0.07 second later than that of Titan II N-25. However, it is still considered to be normal. At 1.3 seconds after BECO, the Stage I oxidizer tank ruptured and released a cloud of red vapor which dissipated in 0.5 second. Stage I was observed to be still virtually intact after the oxidizer gas was released. One frame prior to the rupture, Stage I separation was observed to be approximately 32 feet, and Stage I was pitched down at an apparent angle of 17 degrees.

An interstage or oxidizer tank dome fragment was observed to be traveling down the length of the Stage I fuel tank starting 0.6 second after the Stage I oxidizer tank ruptured. The fragment appeared to hit the aft end of the fuel tank wall and create a small leak. The leak became larger until at 0.9 second after the oxidizer tank rupture, the Stage I fuel tank ruptured. Stage I fuel tank panels then blew out, and the Stage I oxidizer tank and the Stage I engine assembly jackknifed about the area where the fuel tank had been.

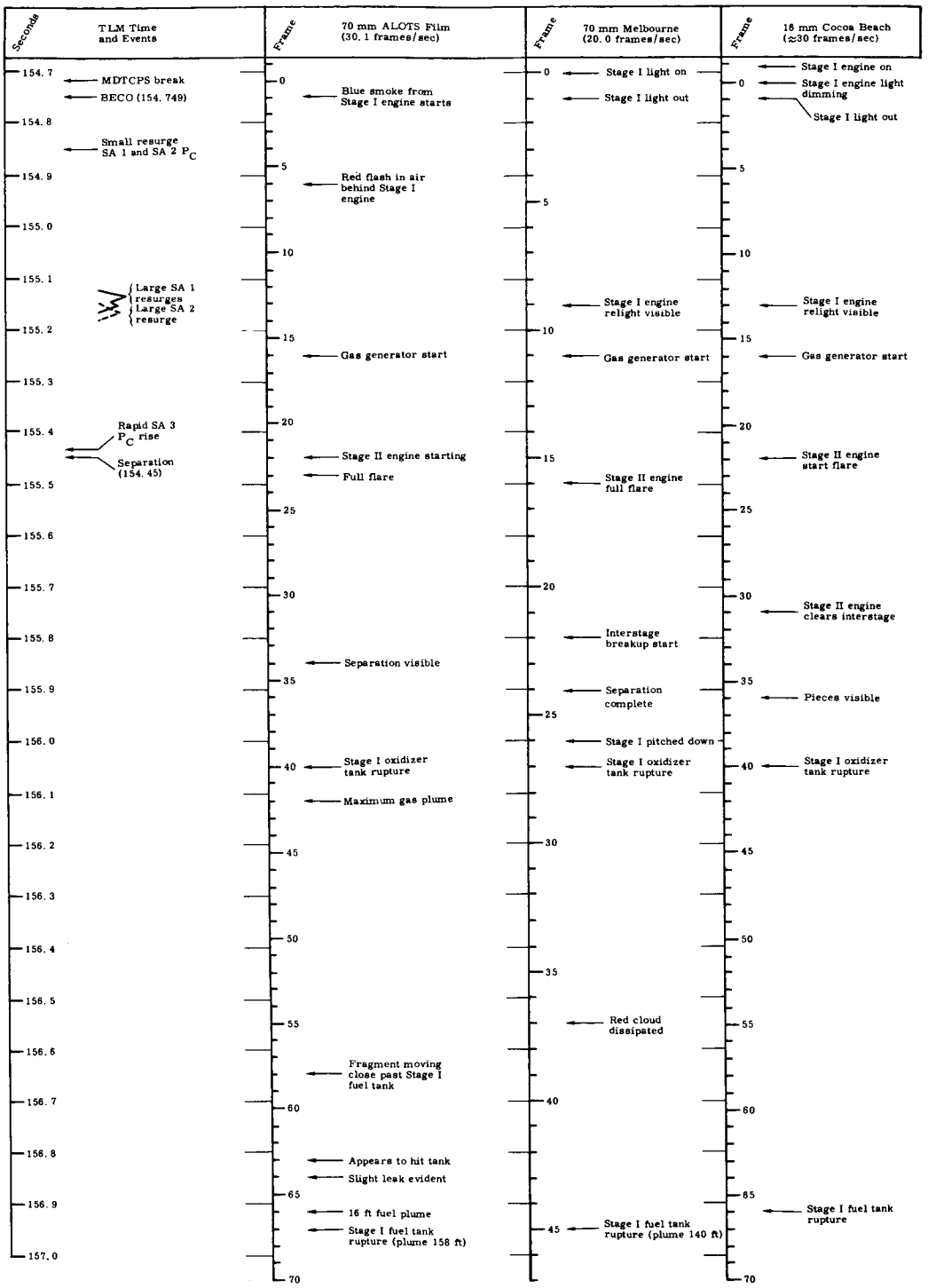

Fig. XI-8. Staging Event Time Correlation

This is the second flight of the GLV series in which a staging anomaly was observed. A similar event occurred during staging of GT-10 and was also observed during the flight of Titan II B-6, B-15, N-8 and N-11. The plume diameter of venting gases versus time from $87FS_2$ is shown in Fig. XI-9 for the flights under study. The Titan II N-18 plume plot is shown but was attributed to inadvertent destruct and, therefore, is not classified in the same family of events. It is also noted that the Stage I flight of N-11 was terminated prematurely by a POGO shutdown and, therefore, exhibits different plume characteristics. The other GLV and Titan events show similar plume characteristics, e.g., time after $87FS_2$, rate of expansion and a two-phase venting which is attributed to sequential rupture of tanks. However, the greatest time delay for any event to date between rupture of tanks was observed on GT-12, where 0.9 second elapsed between rupture of the oxidizer and fuel tanks.

Conclusions as to the cause and consequences of the GT-12 staging anomaly are as follows.

(1) The most probable causes of Stage I tank rupture were the following:

(a) Penetration of the oxidizer dome or sidewall by debris from the interstage breakup. Stage I attitude divergence, observed during and after separation, resulted in asymmetrical interstage breakup and debris acceleration by the Stage II engine toward the diverging Stage I. Observed Stage I engine resurges during staging contributed to attitude divergence. Interstage and/or oxidizer tank debris penetration was the probable cause of fuel tank rupture. After oxidizer tank rupture, Stage I continued to tumble and presented a larger target for accelerated debris. This conclusion is consistent with the observed fragment trajectory and the time delay previously discussed.

(b) Burnthrough of the Stage I oxidizer dome surface after exposure by cracking and/or flaking of the dome ablator. The integrity of the ablator was verified by special prelaunch inspection. However, because of the observed initial venting at the forward end of Stage I, this possible cause cannot be eliminated.

(2) Consequences of the staging anomaly were not detrimental to the GT-12 mission.

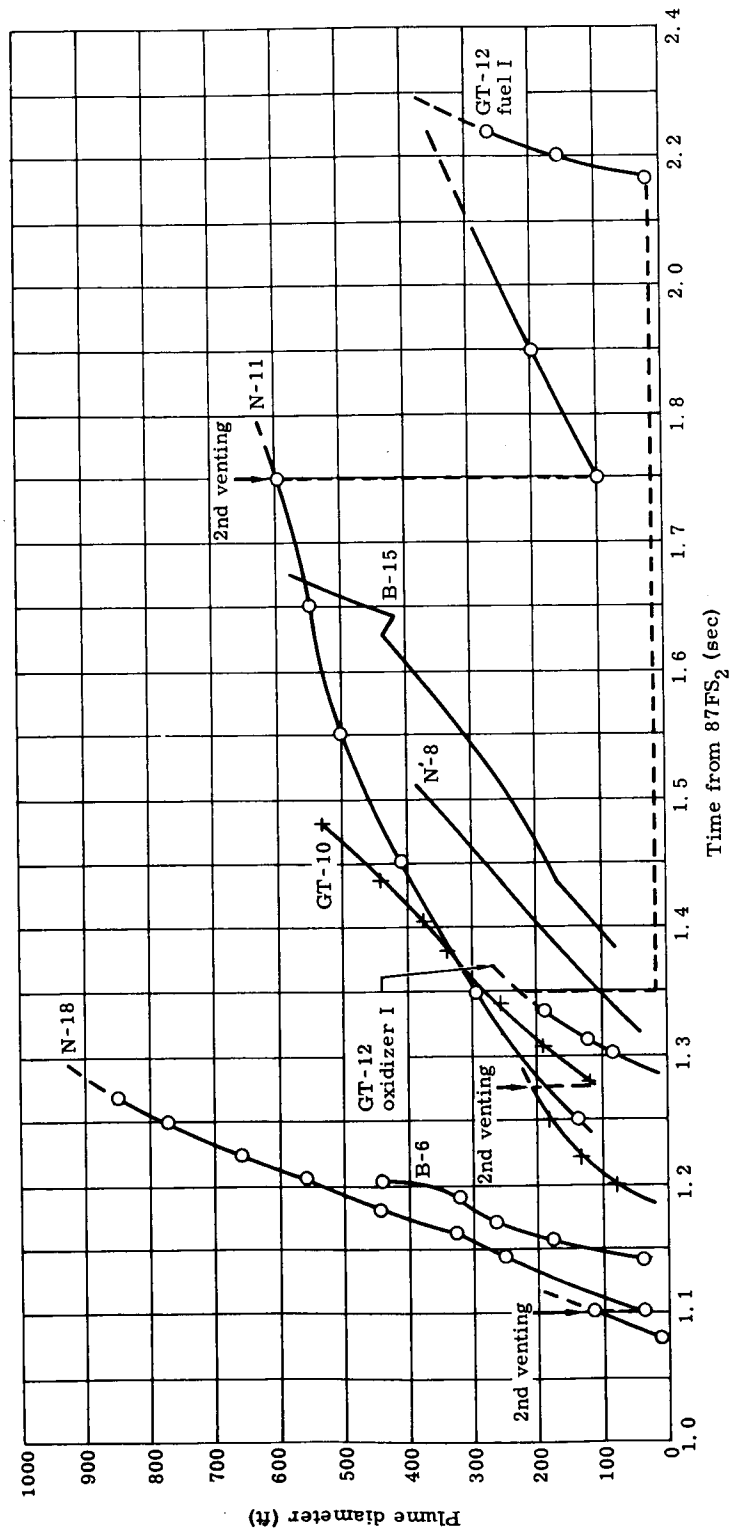

Fig. XI-9. Staging Event Plume Diameter

(a) Rapid growth of the venting oxidizer gases enveloped Stage II for 0.07 second. However, there was no indication of intense heat or overpressure at the aft end of Stage II.

(b) Observed particle velocities along the flight path were on the order of 100 fps with respect to Stage II. This is well below the engine plume penetration limits.

(c) There were no effects on Stage II flight performance indicated by telemetry or visual observation.

XII. AIRFRAME SYSTEM

A. STRUCTURAL LOADS

Analysis of GT-12 flight data indicates that the loads experienced were well within the structural capability of the launch vehicle. Characteristically, the most critical loading occurred at pre-BECO, where the load aft of Station 320 reached 87.3% of design limit load in compression (DLL_c). Instrumentation for dynamic response data consisted of rate gyros for lateral dynamic loads and axially mounted accelerometers for longitudinal dynamic loads. No anomalies affecting the airframe occurred during flight.

1. Preignition

The 1 g deadweight distribution is the only contribution to steady axial loading in the preignition period. Ground winds were approximately 7 mph from a direction of from 080 degrees to 090 degrees, resulting in steady bending loads of 12,000 in.-lb and wind induced oscillatory (WIO) loads of ±41,000 in.-lb (Fig. XII-1) at Station 1224. The WIO response represents approximately 2% of the WIO design limit bending moment; Table XII-1 shows the comparison of GLV WIO loads to date.

TABLE XII-1

Comparison of WIO Loads

Flight	Ground Winds		WIO Load at Station 1224 (% of WIO design limit bending moment)
	Velocity (mph)	Azimuth (deg)	
GT-1	13 to 17	188 to 193	52
GT-2	7 to 10	321 to 326	5
GT-3	14	150	29
GT-4	5	040	3
GT-5	4	053	2
GT-7	14 to 20	320 to 330	40
GT-6A	4 to 7	200 to 225	2
GT-8	16 to 18 (gusts to 22)	333 to 340	46
GT-9A	20	080	26
GT-10	12	000	20
GT-11	3 (gusts to 6)	210 to 237	4
GT-12	7	080 to 090	2

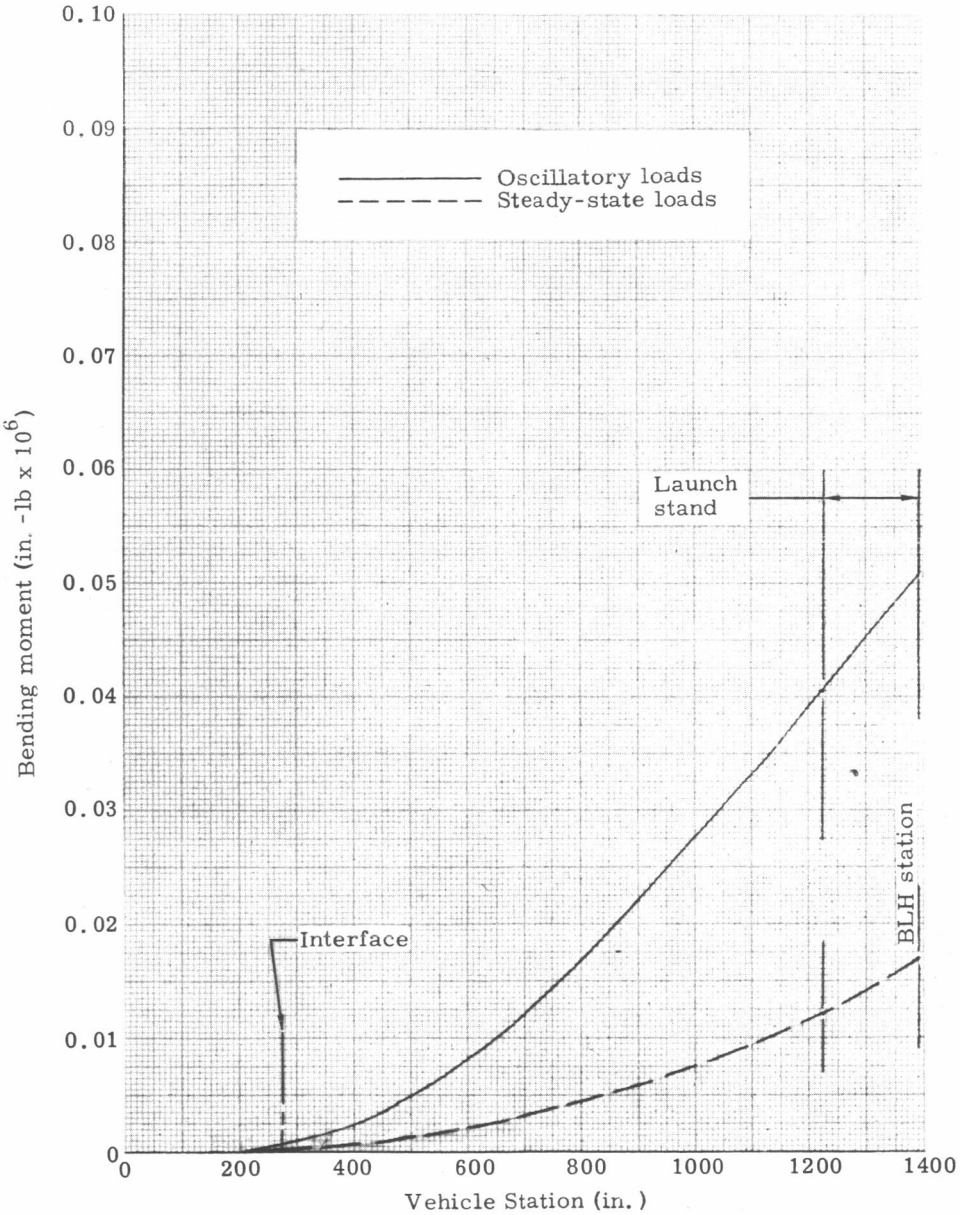

Fig. XII-1. Bending Moments Due to Ground Winds: Preignition

2. Launch Prerelease

Ignition transients were normal, and the attendant dynamic axial loads as measured by the BLH system together with the steady axial load are shown in Fig. XII-2. The prerelease lateral dynamic loading was due to the combined effects of ground winds and engine start transients; this loading is shown in Fig. XII-3.

3. Launch Postrelease

A comparison (Table XII-2) of the GT-12 liftoff load factor with those of previous launches indicates that this flight experienced one of the lowest initial steady accelerations, which was anticipated.

TABLE XII-2

Comparison of Liftoff Load Factors

Flight	Liftoff Load Factor (g)
GT-1	1.27
GT-2	1.27
GT-3	1.27
GT-4	1.27
GT-5	1.28
GT-7	1.26
GT-6A	1.25
GT-8	1.26
GT-9A	1.26
GT-10	1.27
GT-11	1.25
GT-12	1.25

Dynamic deformation modes in evidence at postrelease consisted of the first, second and third structural bending and Stage I engine modes in the lateral plane and the first axial mode in the longitudinal direction. Frequency correlation between calculated and observed modes at significant times during the flight is given in Figs. XII-3 and XII-4; the resulting dynamic bending moment in the postrelease condition is shown in Fig. XII-3.

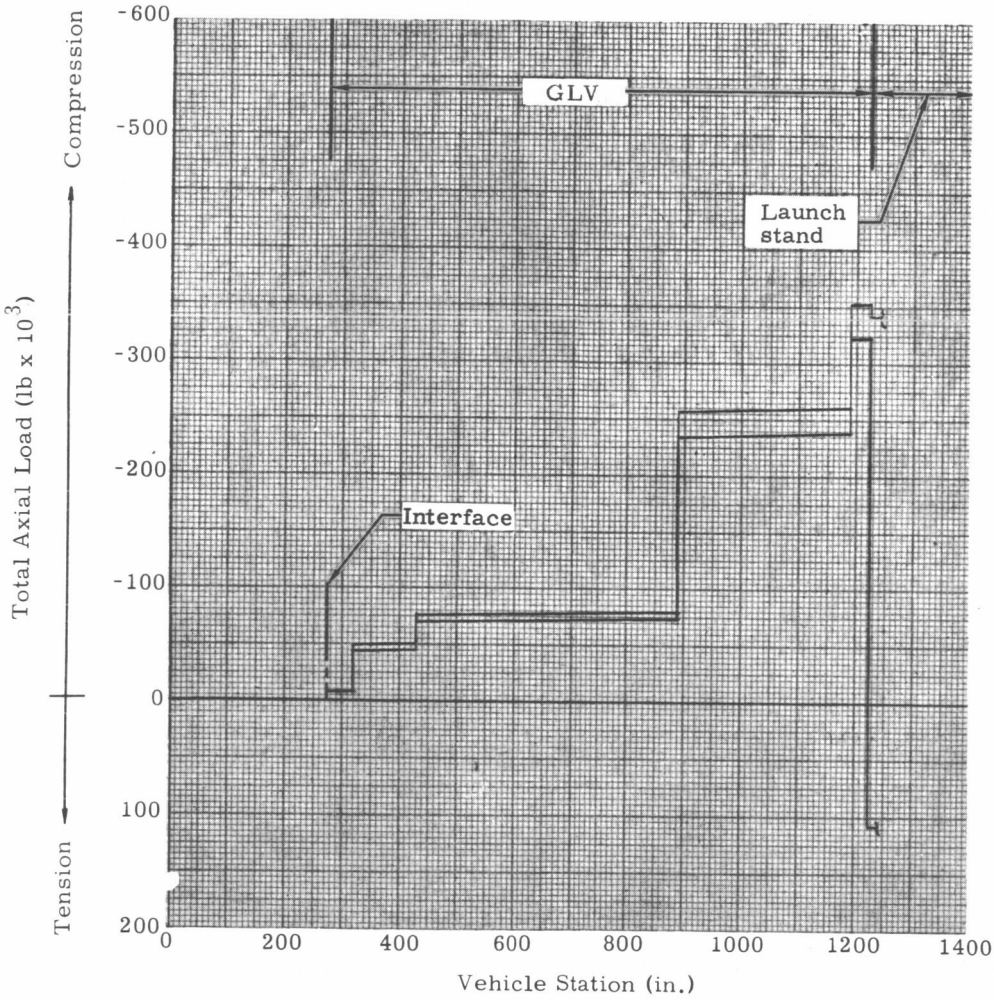

Fig. XII-2. Dynamic Axial Load Envelope: Prelaunch

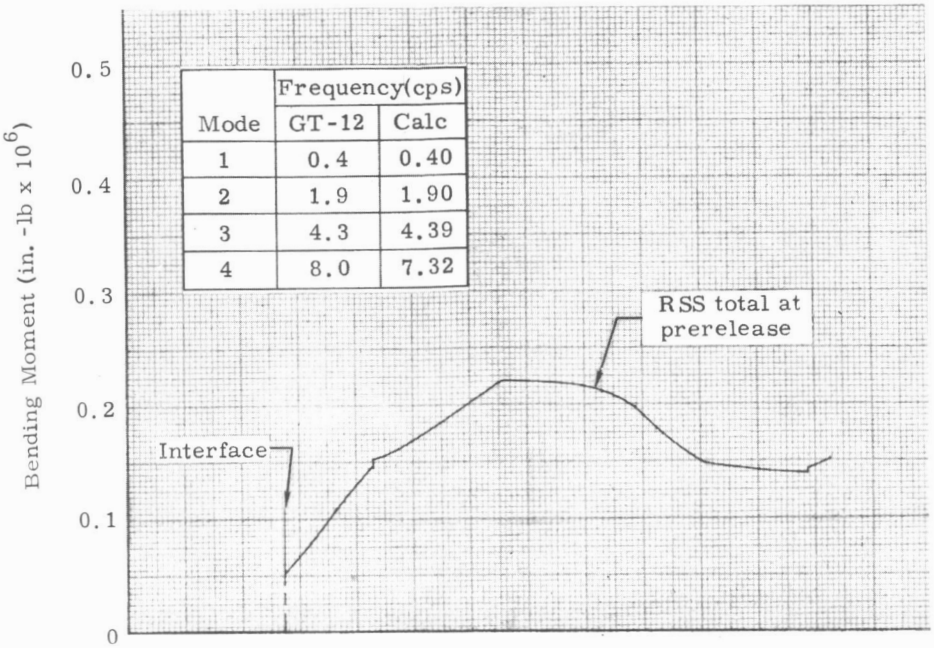

Mode	Frequency(cps) GT-12	Calc
1	0.4	0.40
2	1.9	1.90
3	4.3	4.39
4	8.0	7.32

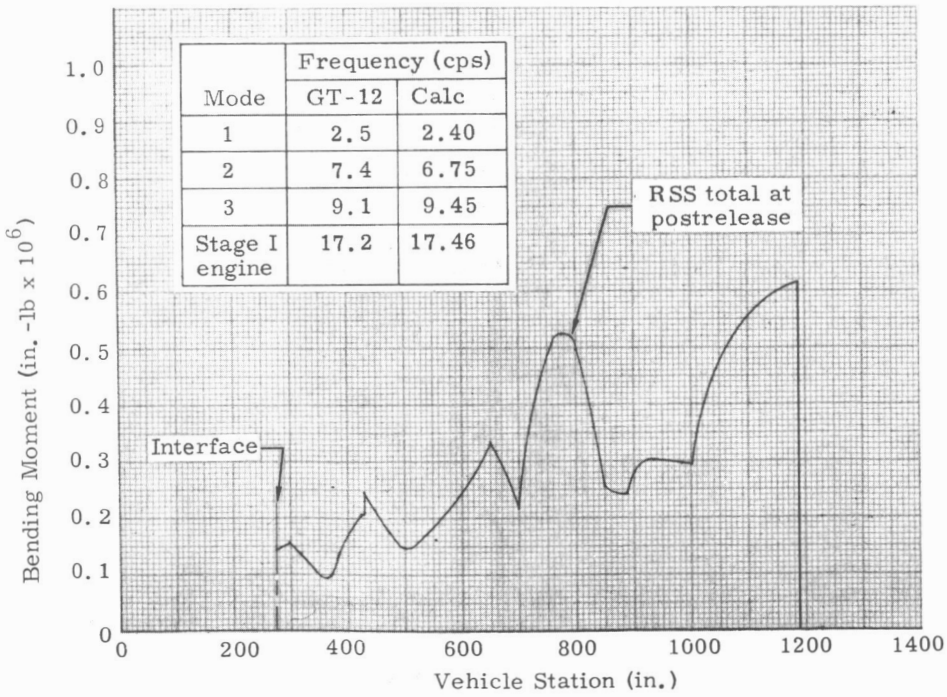

Mode	Frequency (cps) GT-12	Calc
1	2.5	2.40
2	7.4	6.75
3	9.1	9.45
Stage I engine	17.2	17.46

Fig. XII-3. Total Lateral Dynamic Load Envelope: Prerelease and Postrelease

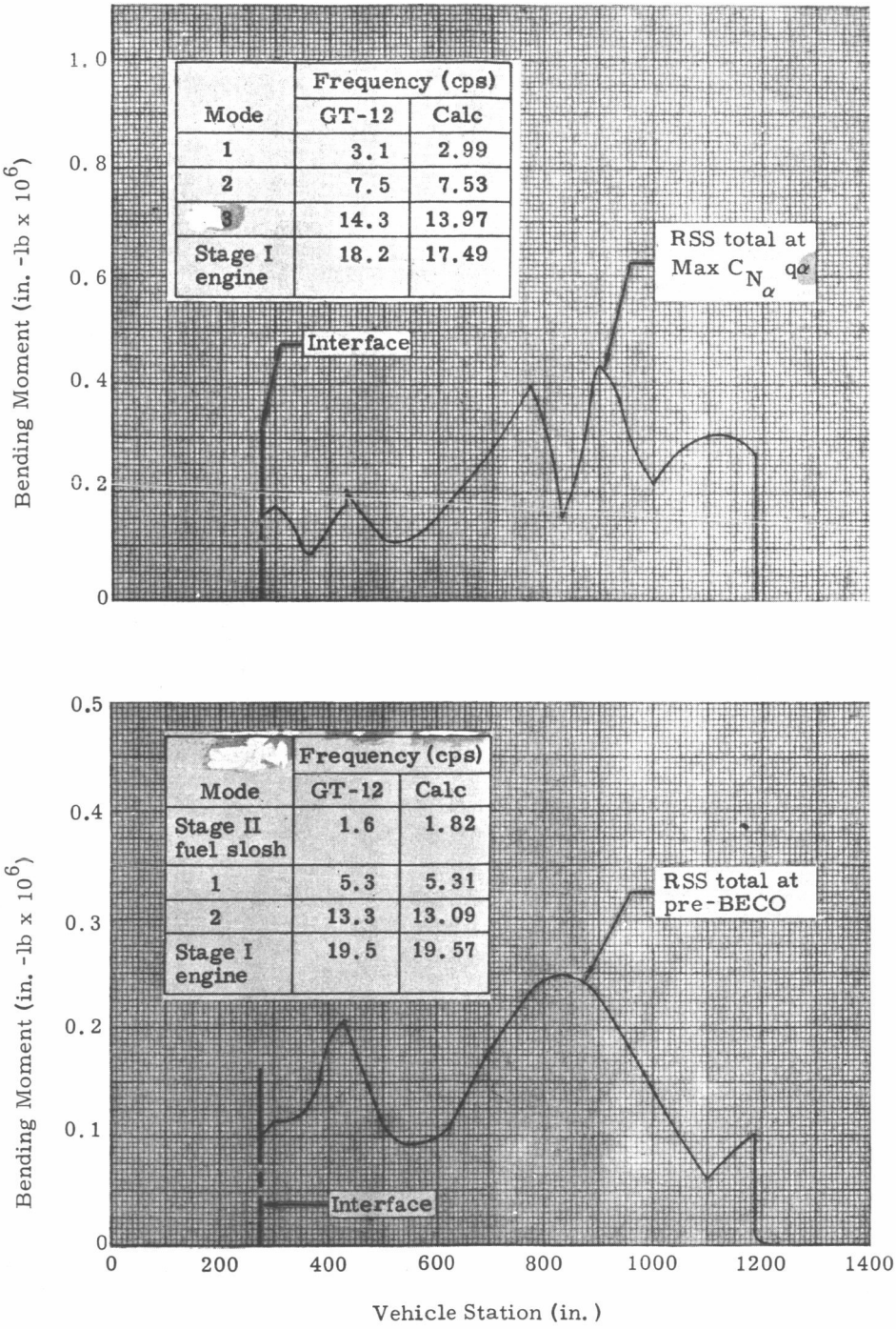

Mode	Frequency (cps) GT-12	Frequency (cps) Calc
1	3.1	2.99
2	7.5	7.53
3	14.3	13.97
Stage I engine	18.2	17.49

Mode	Frequency (cps) GT-12	Frequency (cps) Calc
Stage II fuel slosh	1.6	1.82
1	5.3	5.31
2	13.3	13.09
Stage I engine	19.5	19.57

Fig. XII-4. Total Lateral Dynamic Load Envelope: Max C_{N_α} $q\alpha$ and Pre-BECO

4. Stage I Flight

The most significant periods of Stage I flight for airframe loading occurred at Max C_{N_α} $q\alpha$ and pre-BECO; Max C_{N_α} $q\alpha$ occurred at LO + 74 seconds, and maximum loading (pre-BECO) occurred at LO + 154 seconds.

Winds aloft during the boost phase of flight were moderate. The wind magnitude at LO + 74 seconds was 32% of the design specification level, and the wind azimuth (tail) was similar to that of previous flights. The combined effects of moderate wind magnitude, azimuth and near-nominal trajectory resulted in lower-than-average airframe loading at Max C_{N_α} $q\alpha$. The comparison of in-flight airframe loading for all Gemini launches is shown in Table XII-3.

TABLE XII-3

Structural Loads Comparison

Flight	At Max C_{N_α} $q\alpha$ Station 935 (% of DLL_c)	At Pre-BECO Station 320^+ (% of DLL_c)
GT-1	79.6	86.0
GT-2	77.5	90.1
GT-3	75.9	87.4
GT-4	82.6	91.0
GT-5	69.2	88.7
GT-7	70.4	88.7
GT-6A	72.3	93.3
GT-8	80.2	92.8
GT-9A	71.9	89.1
GT-10	71.8	88.8
GT-11	69.8	90.1
GT-12	67.8	87.3

Dynamic bending moments obtained from the rate gyro responses in the Max C_{N_α} $q\alpha$ and pre-BECO regions of flight are shown in Fig. XII-4. Steady axial acceleration at pre-BECO is given in Table XII-4.

TABLE XII-4

Steady Axial Accelerations at Pre-BECO

Flight	Pre-BECO Axial Acceleration (g)
GT-1	5.61
GT-2	5.69
GT-3	5.63
GT-4	5.63
GT-5	5.55
GT-7	5.56
GT-6A	5.46
GT-8	5.57
GT-9A	5.52
GT-10	5.53
GT-11	5.49
GT-12	5.52

Stage I engine shutdown transients, as recorded by the axial accelerometers, were rougher than usual and are attributed to the fuel exhaustion-type shutdown and to an apparent momentary reignition. Similar fuel exhaustion shutdowns were experienced on GT-4, GT-8, GT-9A, GT-10 and GT-11.

Motion picture tracking films indicate that the Stage I engine reignited momentarily, confirming the accelerometer data. Stage separation was followed by the appearance of a reddish-brown cloud and, then, a white cloud; considerable debris also was evident from the tracking film. This visual evidence indicates that the Stage I oxidizer tank (reddish-brown cloud) and the Stage I fuel tank (white cloud) ruptured after staging. Telemetry data do not show the cause(s) of rupture of the propellant tanks, but these events had no effect on the satisfactory operation of Stage II. A similar occurrence of Stage I oxidizer tank rupture after staging was noted on GLV-10 and was documented in Chapter XII of Ref. (2).

The Gemini 12 astronauts reported during technical debriefings that they saw three flashes of light during the staging sequence. These flashes most likely coincide with Stage II engine ignition and the two vapor clouds which resulted from rupture of the Stage I propellant tanks.

5. Stage II Flight

Propellant slosh oscillations, associated with the calculated Stage II fuel slosh mode, occurred continuously from LO + 235 seconds to LO + 320 seconds; the amplitude of the oscillations was small (±0.19 deg/sec at LO + 299 seconds), as indicated by both pitch (predominant) and yaw rate gyros. In addition, propellant slosh transients reaching an amplitude of ±0.16 deg/sec (similar to that experienced on previous flights) occurred immediately after staging and lasted approximately 14 seconds.

Axial dynamic oscillations occurred throughout Stage II flight with a frequency of approximately 6.5 cps to 25 cps and a maximum amplitude of ±0.10 g at LO + 287 seconds at the spacecraft/launch vehicle interface. Analysis of these data indicates that the oscillations were normal and had no adverse effect on Stage II operation.

The steady axial acceleration at SECO, shown in Table XII-5, was lower than on any GLV flight and was anticipated. This is attributed to a combination of relatively low thrust level at SECO, one of the heaviest GLV spacecrafts ever orbited and trajectory requirements for this mission. Stage II engine shutdown at SECO, as indicated by axial acceleration decay transients, was normal.

TABLE XII-5

Steady Axial Accelerations at SECO

Flight	SECO Axial Acceleration (g)
GT-1	7.35
GT-2	7.70
GT-3	7.50
GT-4	7.42
GT-5	7.56
GT-7	7.23
GT-6A	7.33
GT-8	7.20
GT-9A	7.20
GT-10	7.20
GT-11	7.17
GT-12	7.13

There was one minor indication of post-SECO disturbance on the low range (±0.5 g, Meas 0699) axial accelerometer. The time of occurrence of this disturbance and its associated g level was 0.02 g peak-to-peak at SECO + 4.10 seconds. Spacecraft separation from the sustainer occurred at SECO + 23.19 seconds.

6. Total Airframe Loads

A summary of the total airframe loads (quasi-steady axial, dynamic and equivalent axial loads from quasi-steady and dynamic bending moments) for significant structural loading conditions at critical stations is presented in Table XII-6. Complete vehicle loading at significant flight times is shown in Figs. XII-5 through XII-9. The maximum load at any station and the loading condition for which it occurred are shown in Fig. XII-10.

TABLE XII-6

Summary of Total Airframe Loads

Flight Condition	Total Airframe Load (% of DLL_c at critical station)	Critical Station
Prerelease	66.8	1188*
Postrelease	78.7	1188*
Max C_{N_α} $q\alpha$ (LO + 74 sec)	67.8, 87.2	935, 1188*
Pre-BECO (LO + 154 sec)	87.3	320*
Pre-SECO (LO + 343 sec)	70.5	276.8*

*Just aft of station

B. POGO

Analysis of GT-12 telemetry data showed that the POGO suppression devices (fuel accumulators and oxidizer standpipes) operated satisfactorily. No pressure oscillations associated with airframe structural resonances were detected in either the oxidizer or the fuel feedline.

Bandpass filtering of the analog reconstruction of PCM/FM telemetry (Meas 0670) indicates that the maximum intermittent longitudinal

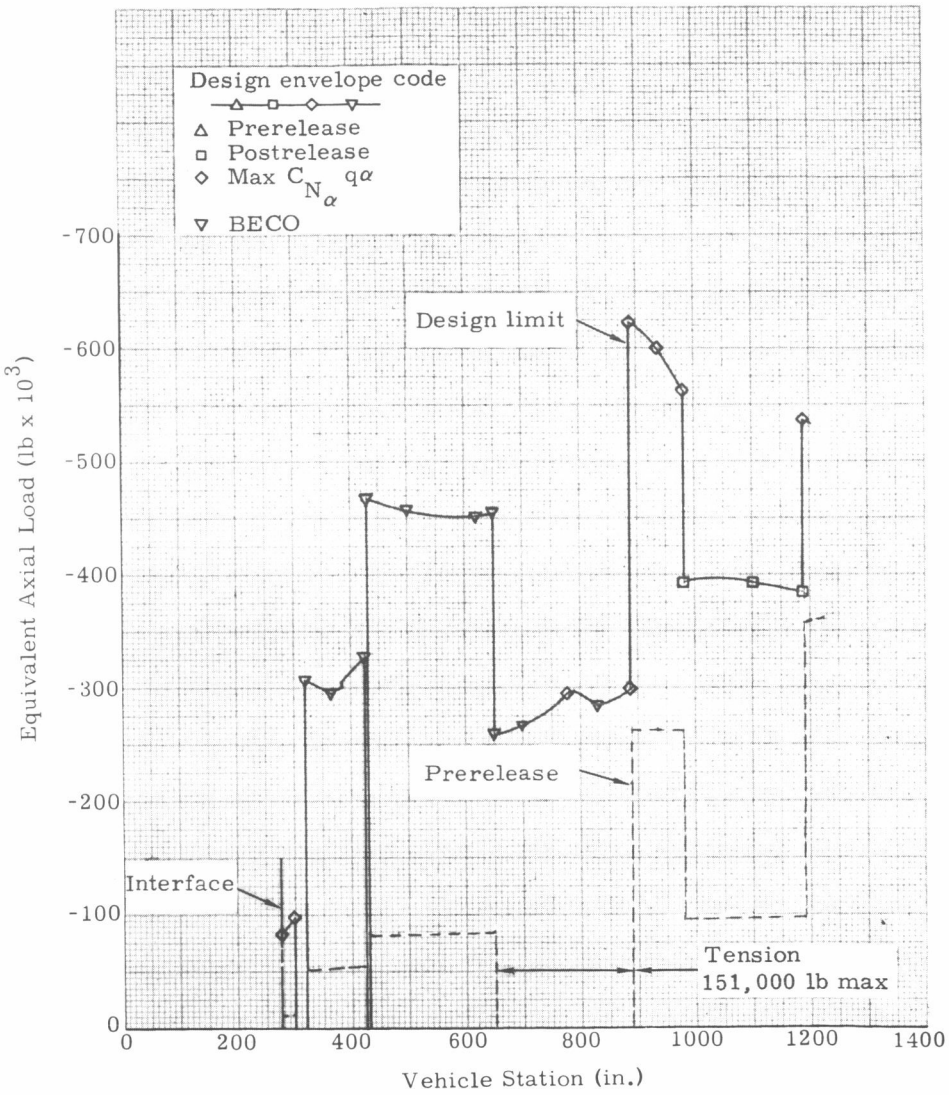

Fig. XII-5. Equivalent Axial Load: Prerelease

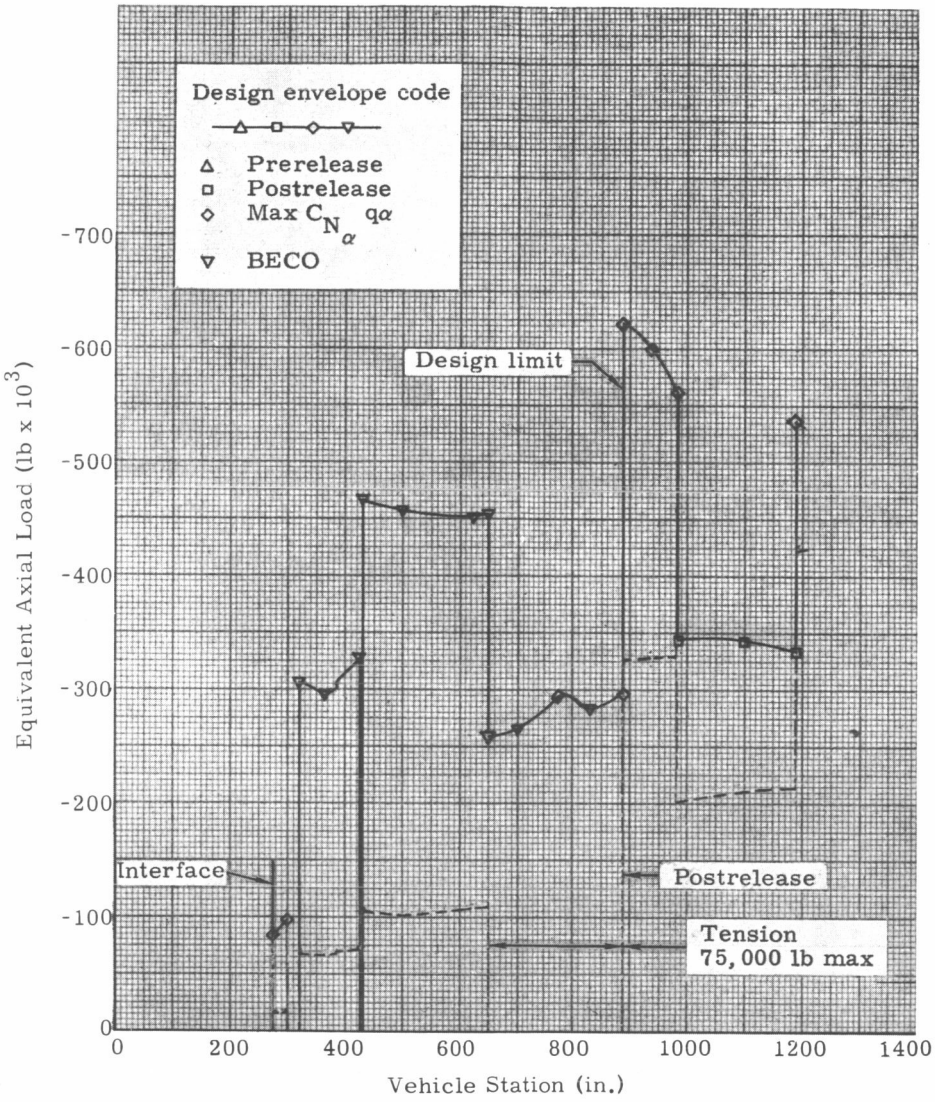

Fig. XII-6. Equivalent Axial Load: Postrelease

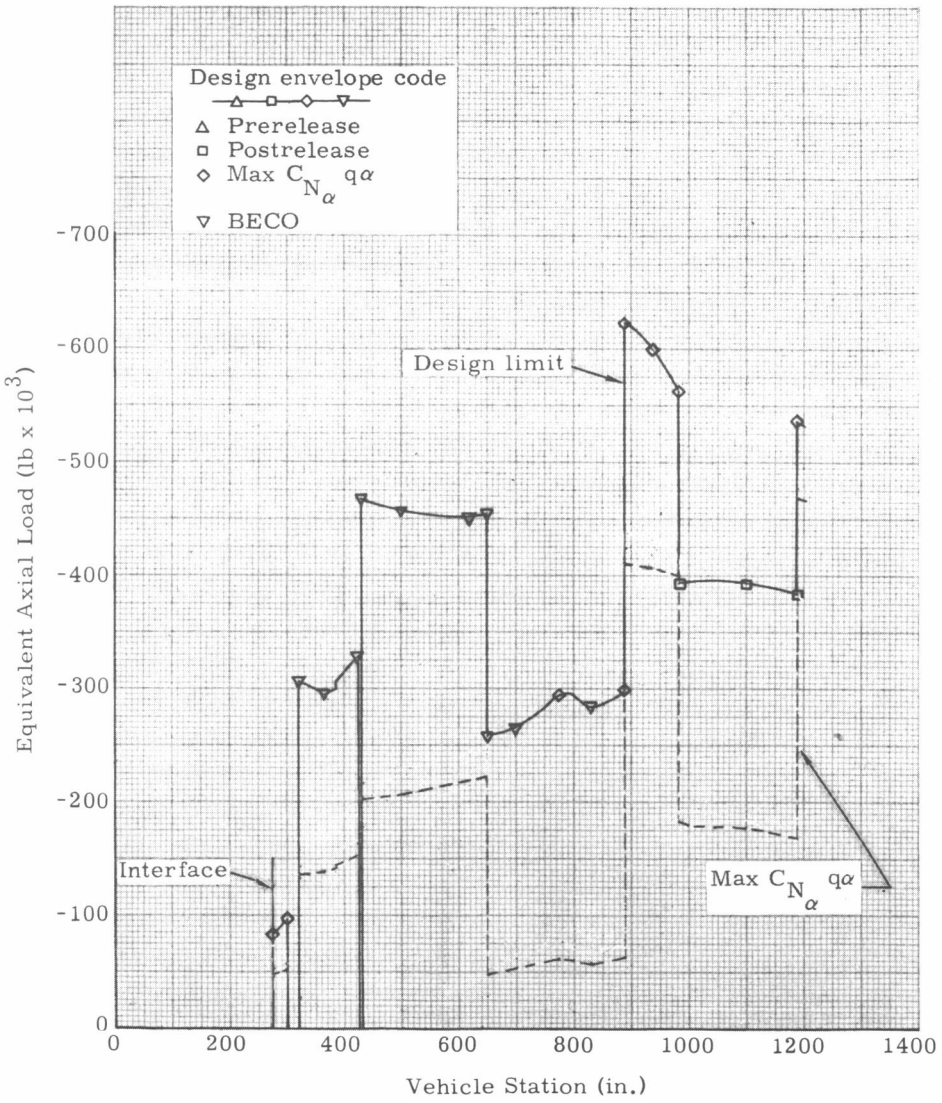

Fig. XII-7. Equivalent Axial Load: Max C_{N_α} $q\alpha$

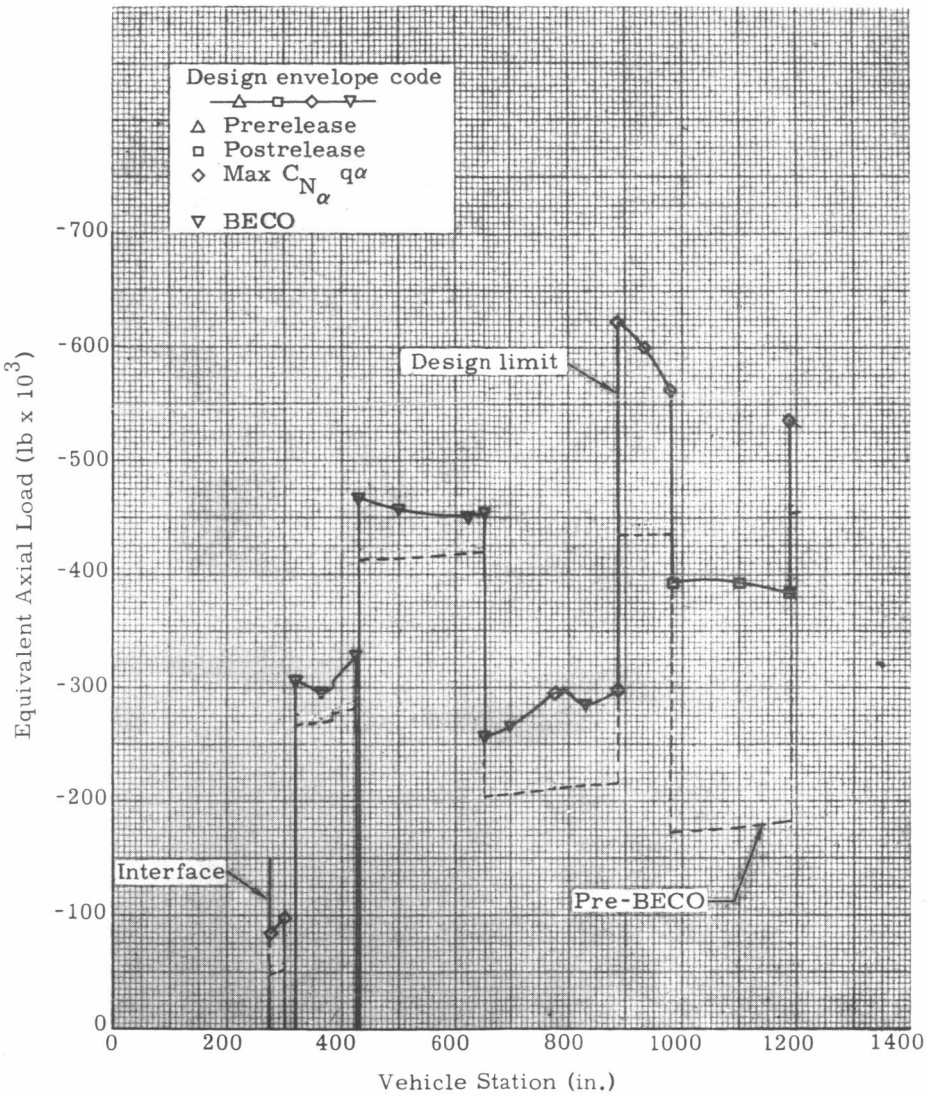

Fig. XII-8. Equivalent Axial Load: Pre-BECO

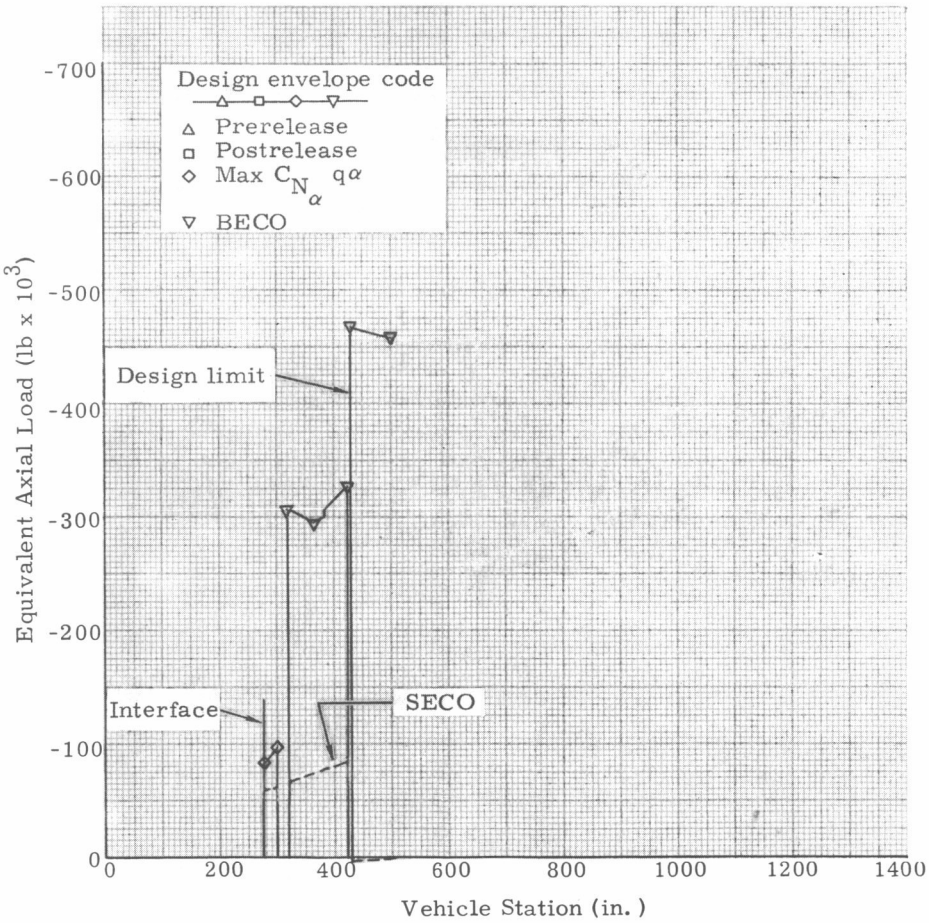

Fig. XII-9. Equivalent Axial Load: SECO

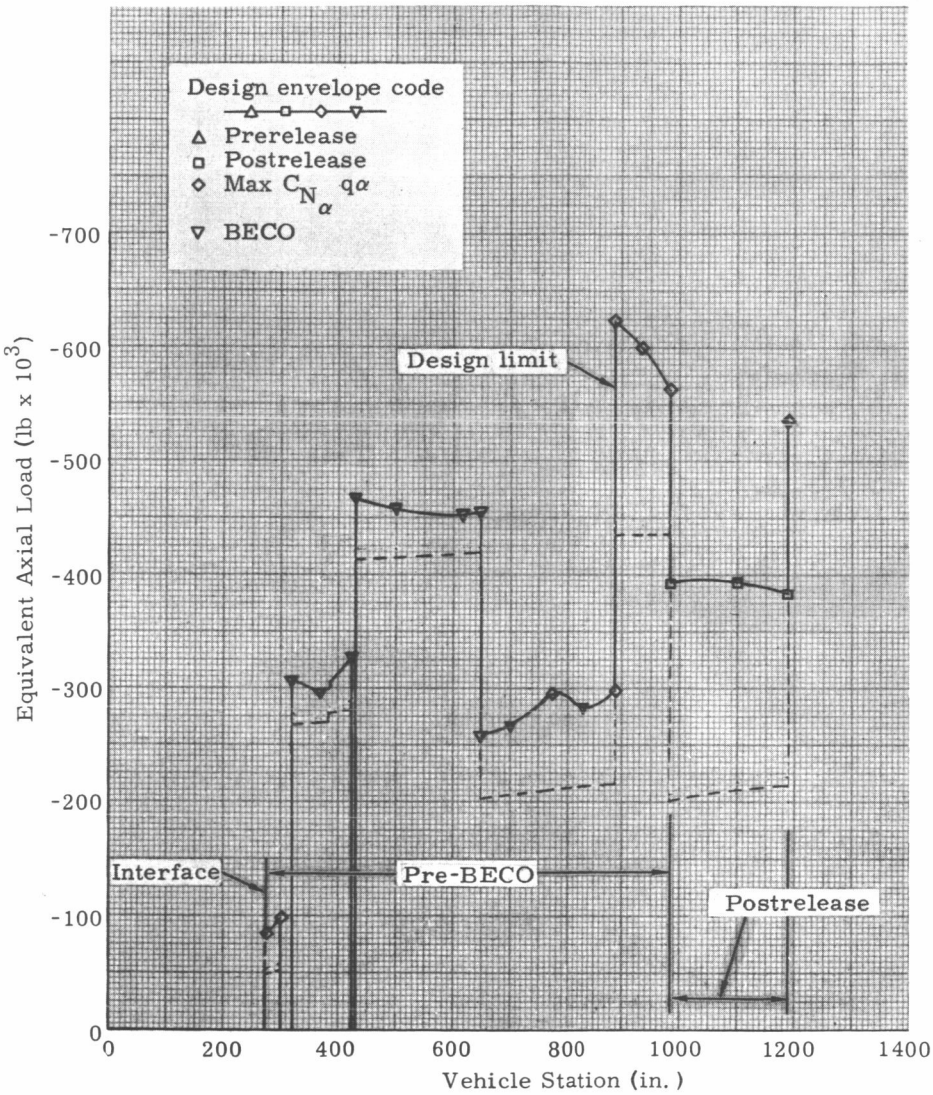

Fig. XII-10. Maximum Structural Load Envelope

oscillation at the spacecraft/launch vehicle interface occurred at LO + 126.1 seconds. The amplitude of these oscillations was 0.140 g zero-to-peak with a response frequency of 11.2 cps, and the oscillations lasted approximately 2-1/2 seconds, well within the maximum acceptable level.

The time history of suppressed POGO response amplitude for Compartments 1 and 5 is shown in Fig. XII-11. Figure XII-12 shows a comparison of longitudinal oscillations for the last four GLV flights. In addition, Table XII-7 shows the comparison of the maximum suppressed POGO response data for all GLV flights.

UNCLASSIFIED

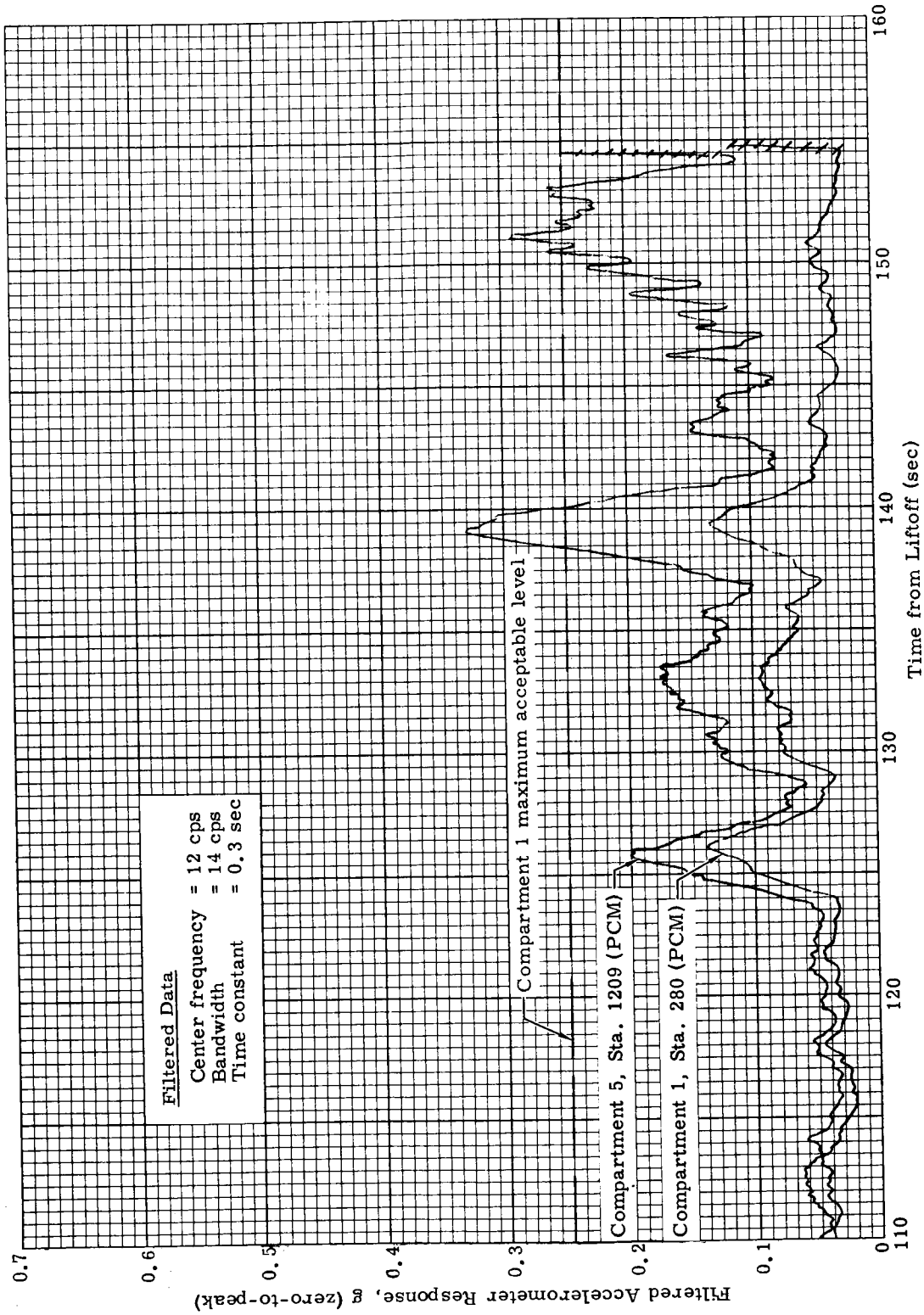

Fig. XII-11. Longitudinal Oscillations

UNCLASSIFIED

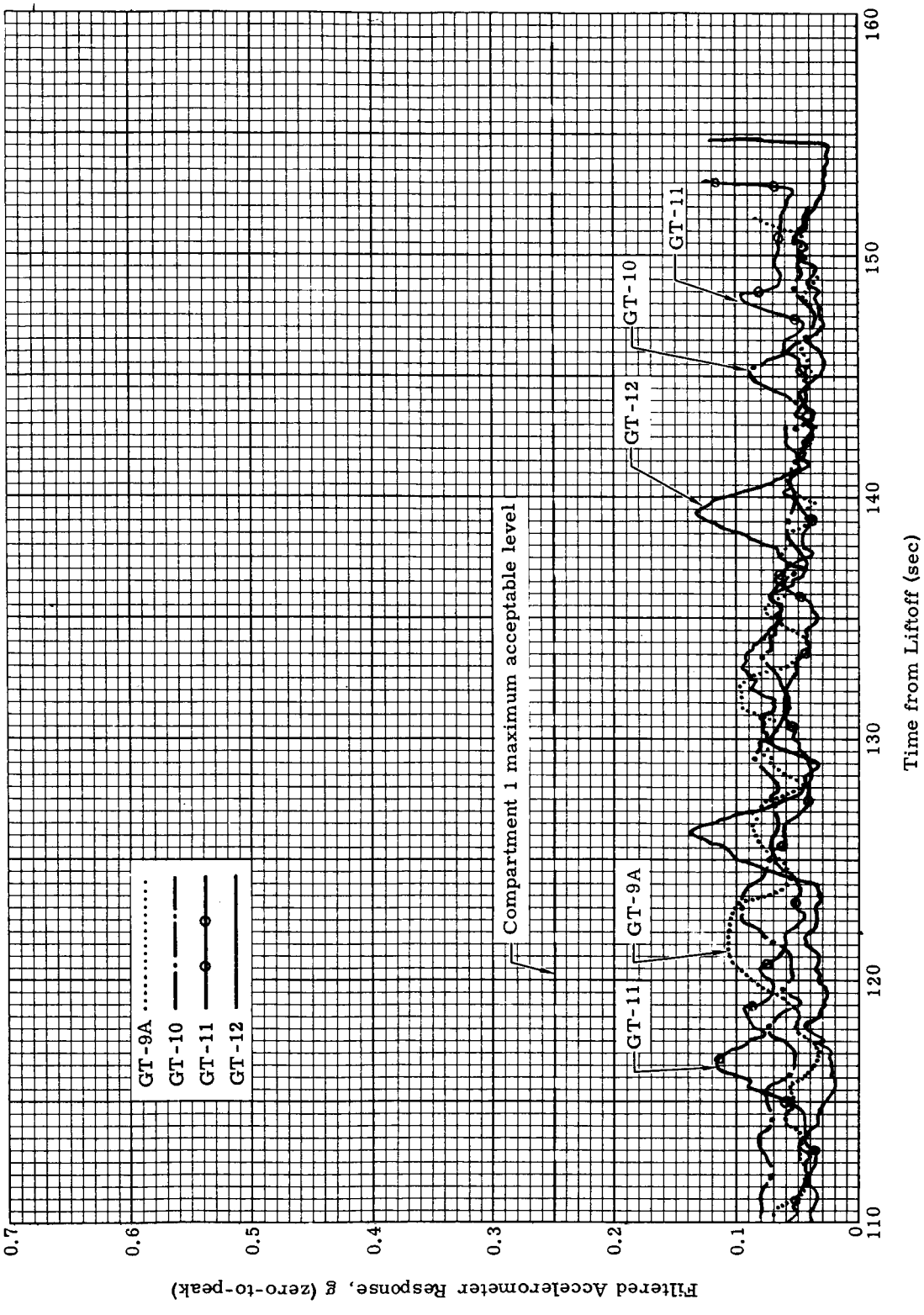

Fig. XII-12. Longitudinal Oscillations, Compartment 1 (Station 280)

UNCLASSIFIED

TABLE XII-7

GLV POGO Comparison (filtered data)

Flight	Time of Peak Response (sec)	Frequency (cps)	Amplitude (zero-to-peak) (g)	Duration of Pulse (sec)	Stage I Fuel Tank Pressure (psia)
GT-1	LO + 136.5	13.4	0.160	2	24.8
GT-2	LO + 127.8	11.5	0.155	2	24.5
GT-3	LO + 140.6	13.5	0.129	4.5	23.8
GT-4	LO + 121.7	11.0	0.220	2	23.4
GT-5	LO + 129.2	11.4	0.380	13	23.0
GT-6A	LO + 146.8 LO + 153.9	13.7 16.8	0.115 0.115	1.5 1	23.2 23.3
GT-7	LO + 133.3	11.8	0.125	2.5	24.5
GT-8	LO + 135.5	12.4	0.215	1.5	23.3
GT-9A	LO + 121.8	10.9	0.110	3	23.5
GT-10	LO + 123.0	10.9	0.100	2	22.9
GT-11	LO + 116.7	10.5	0.120	1	24.0
GT-12	LO + 126.1	11.2	0.140	2.5	23.0

UNCLASSIFIED

XIII. AGE AND FACILITIES

A. MECHANICAL AGE

1. Precount Operations

The mechanical AGE utilized prior to countdown is primarily for transport and erection of Stages I and II. All equipment functioned normally. Both stages of GLV-12 were airlifted to Cape Kennedy by the B377 SG aircraft.

2. Countdown Launch Operations --GT-12

Analysis of magnetic tape recordings of functions carried through the electrical umbilicals and the inspection of film confirm that all electrical launch vehicle umbilicals separated cleanly. The release times of these umbilicals are presented in Table XIII-1.

TABLE XIII-1

Electrical Umbilical Disconnect Sequence

Umbilical Designation	Time of Disconnect (GMT)
3D1M/3D2M	2046:33.404
3D1E	33.641
3D2E	33.818
3B1E	34.071
2B1E	34.217
2B2E	34.238

Film coverage of the spacecraft lower umbilicals (Cables B and C) was off target; therefore, evaluation of this separation was not made. All other flyaway umbilicals separated cleanly.

3. Postlaunch Operations

Mechanical AGE damage was minimal and was directly attributable to blast temperatures and pressures.

B. MASTER OPERATIONS CONTROL SET

Analysis of the MOCS automatic sequence records shows that all functions were properly performed. The automatic countdown sequence was picked up at T-35:00.5 minutes and proceeded on schedule to the programmed hold at T-03:00.2 minutes. After a planned hold the count

was resumed and continued through a successful liftoff. MOCS T-0 occurred at 2046:30.136 GMT, followed by MDTCPS break at T + 0.969 second. Critical functions holdfire E-6 was interrogated for shutdown between T + 2.2 seconds and MDTCPS + 1.8 seconds with a resultant go condition. The following MOCS functions were generated as specified.

MDTCPS+1.6 seconds

MDTCPS+1.8 seconds (holdfire lockout)

MDTCPS+2.0 seconds (launch release signal)

The launch operation through liftoff was completed at 2046:33.419 GMT (T + 3.283 seconds).

The recorders were changed to high speed at T-2 minutes. During the automatic portion of the count, the operation of the sequencer was compared to the real-time trace and patch lift. All traces were checked for time of occurrence and were found to be correct and consistent with the planned operation of the sequencer.

C. FACILITIES

All facility items functioned properly throughout the countdown, and launch damage to facility items caused by engine blast and heat was minor. The most significant damage items follow:

Complete Vehicle Erector

(1) Weather curtains NR-9, NR-35, SR-9, SL-9, SR-15, SL-15 and SC-15 were damaged.

(2) Lights on the underside of the 9 foot 8 inch and 26 foot 7 inch levels were damaged.

Complete Vehicle Umbilical Tower

(1) The hand rail kick plate on the boom 1-1/2 level was blown off. off.

Deck Area

(1) A section of deck grating in front of the west elevator broke loose.

XIV. RELIABILITY

Based on countdown experience through GLV-11, the average number of holds per countdown ($\bar{h}$) was calculated to be 0.067, i.e., one hold per 15 countdowns. The probability of GLV-12 completing the countdown without a hold was predicted to be

$$P_{C/D}(\bar{h} = 0.067) = 0.936$$

Including the GLV-12 countdown, the average number of holds per countdown is shown in Table XIV-1 to be 0.062, i.e., one hold in 16 countdowns. The probability of another GLV completing countdown without a hold would be

$$P_{C/D}(\bar{h} = 0.062) = 0.940$$

$\bar{h}$ is based on countdown experience from T-240 minutes to T-0, except for the GLV-5 attempt, which was scrubbed at T-10 minutes. Spacecraft holds and SCF tests were not considered.

Countdown experience for all GLVs is included in Table XIV-1.

TABLE XIV-1

Countdown Data

Vehicle No.	Number of Countdowns	Number of Holds*	Remarks
GLV-1	1	0	
GLV-2 (attempt)	1	0	3 S/C holds Tandem actuator failed after T-0
GLV-2	1	0	1 S/C hold
GLV-3	1	0	1 hold--not Martin's responsibility (oxidizer leak in Stage I engine transducer)
GLV-4	1	1	Erector stuck during lowering
GLV-5 (attempt)	1	0	1 S/C hold. Incomplete countdown--scrubbed at T-10 due to weather
GLV-5	1	0	

TABLE XIV-1 (continued)

Vehicle No.	Number of Countdowns	Number of Holds*	Remarks
GLV-6 (attempt on 25 Oct 65)	0	0	Incomplete countdown--scrubbed at T-42 due to Agena failure
GLV-7	1	0	
GLV-6 (attempt on 12 Dec 65)	1	0	Umbilical failed (prematurely disconnected), and dust cap left in gas generator line--both after T-0
GLV-6 (launched on 15 Dec 65)	1	0	
GLV-8	1	0	
GLV-9 (attempt on 17 May 66)	0	0	Incomplete countdown--scrubbed at T-84 due to Atlas/Agena failure
GLV-9 (attempt on 1 June 66)	1	0	Recycled at T-1.6 due to spacecraft computer failure to receive its guidance update; subsequently scrubbed
GLV-9 (launched on 3 June 66)	1	0	
GLV-10	1	0	
GLV-11 (attempt on 10 Sept 66)	0	0	Incomplete countdown scrubbed at T-120 due to Atlas control system
GLV-11 (launched on 12 Sept 66)	1	0	
GLV-12	1	0	
Total	16	1	

Note: Prediction for another GLV based on data through GT-12

*Based on Martin holds only.

XV. RANGE DATA

A. LAUNCH DATA DISTRIBUTION

1. Quick-Look Range Data

All available quick-look data were supplied by ETR to Martin-Baltimore as shown in Table XV-1.

TABLE XV-1

Range Supplied Quick-Look Data

Description	Time Requested (hr)	Time Received (ETR) (hr)	Time Received (Baltimore) (hr)
Telemetry magnetic tapes:			
Tel IV, PCM/FM FR600 (6 rolls)	T+1	T+2	T+24
Station 1 formatted final (3 rolls)	T+9	T+5	T+24

The PCM serial magnetic tape was of good quality. The final formatted magnetic tape was of good quality and contained no redundancies. Except for approximately 280 milliseconds of transmission blackout during booster staging, the Tel II formatted tape showed only 11 bad data words from LO - 15 seconds to LO + 396 seconds.

2. Martin Data

Test data and records acquired and generated by Martin at Cape Kennedy were received in Baltimore within two days after launch.

These data consisted of the following items:

(1) One set of quick-look records from RCA tape

(2) High speed records of engine parameters

(3) Landline records (events, Bristol, Multipoint and Sanborn) with associated calibrations

(4) BLH tabulations

(5) CP 2600 records (2612, 2650 and 2660)

(6) Sequencer records with code sheets

(7) Dub of Complex 19 landline magnetic tape

(8) Fuel and oxidizer loading records.

3. Range Data

All data supplied by the ETR are summarized in Table XV-2. The time requested for delivery to Martin-Canaveral (Ref. 6555th ATW Form 1-116, dated 9 November 1966) and the time received at Baltimore are shown in this table.

TABLE XV-2

Range Supplied Data

OD Item No.	Description	Time Requested (Canaveral)	Time Received (Baltimore)
8	Position, velocity, acceleration and special parameters (radar)	4 CD	19 CD
19	Position, velocity and acceleration MISTRAM I	5 CD	7 CD
20	Position, velocity, acceleration and special parameters, MISTRAM I and MISTRAM II	11 WD	17 WD
26	Best estimate of trajectory and special parameters	15 WD	20 WD

TABLE XV-2 (continued)

OD Item No.	Description	Time Requested (Canaveral)	Time Received (Baltimore)
1	Standard orbital parameters	3 hr	2 WD
1	Real-time computer facility selected sources	12 hr	4 CD
236	Quick-look reduction, trajectory parameters, KSC	1 CD	*
114	Weather, Rawinsonde Station 1	6 hr	2 WD
125	Weather, wind profile Station 1	6 hr	2 WD
108	Weather, surface, Station 1	1 WD	2 WD
111	Weather, tower 700/701, Station 1	1 WD	3 WD
113	Weather, triple theodolite, Station 1	3 WD	2 WD
120	Weather, Metroc, Station 1 (200K)	3 WD	7 WD
19.5-12	Magnetic tape, serial PCM FR600 quick-look (Tel IV)	1 hr	2 hr
1.5-2	Magnetic tape, serial PCM FR600 final (Tel IV)	1 WD	*
3.5-2	Magnetic tape, serial PCM FR600 (GBI)	3 CD	4 CD
2	Magnetic tape, formatted PCM quick-look (Tel II)	4 hr	**
3	Magnetic tape, formatted PCM final (Tel II)	9 hr	5 hr

TABLE XV-2 (continued)

OD Item No.	Description	Time Requested (Canaveral)	Time Received (Baltimore)
4	Magnetic tape, formatted PCM (GBI)	1 CD	*
19.5-5	Signal strength, center frequency recording (Tel IV)	1 CD	20 CD
1.5-51	Signal strength, center frequency recording (Tel III)	1 CD	20 CD
3.5-5	Signal strength, center frequency recording (GBI)	3 CD	20 CD
4.5-3	Signal strength, center frequency recording (Eleuthra)	***	*
7.5-3	Signal strength, center frequency recording (Grand Turk)	3 CD	*
91.3-4	Signal strength, center frequency recording (Antigua)	***	7 CD
1.11-1	Command control recording (Station 1)	3 WD	9 WD
1.11-5	Command control recording (Station 1)	3 WD	*
1.11-6	Command control recording (Station 1)	3 WD	*
3.11-1	Command control recording (GBI)	5 WD	12 WD
3.11-3	Command control recording (GBI)	5 WD	12 WD

TABLE XV-2 (continued)

OD Item No.	Description	Time Requested (Canaveral)	Time Received (Baltimore)
7.11-1	Command control recording (Grand Turk)	5 WD	*
7.11-3	Command control recording (Grand Turk)	5 WD	12 WD
1.11-4	Command control operator's log (GBI)	3 WD	5 WD
3.11-2	Command control operator's log (GBI)	3 WD	11 WD
7.11-2	Command control operator's log (Grand Turk)	3 WD	5 WD
1.11-25	Command antenna pointing data (Station 1)	5 CD	7 CD
3.11-25	Command antenna pointing data (GBI)	5 CD	7 CD
7.11-25	Command antenna pointing data (Grand Turk)	5 CD	7 CD
91.11-2	Command antenna pointing data (Antigua)	5 CD	*
1.18	Range safety plotboard charts	4 hr	2 WD
5.4.1.2	Propellant analysis report	2 WD	*
2.4-1	Preliminary test report	2 hr	2 WD
1.6-62	Special FCA log	3 WD	2 WD
229	Vehicle engineering units (KSC NASA)	2 CD	*
243	Vehicle computer words (KSC NASA)	1 CD	*

TABLE XV-2 (continued)

OD Item No.	Description	Time Requested (Canaveral)	Time Received (Baltimore)
225	Vehicle bilevels (KSC NASA)	1 CD	*

CD = Calendar days

WD = Working days

* = Data not received as of 13 December 1966

** = Not required, final received 9 hr

*** = Supplemental data received

4. Agency/Contractor Supplied Data

Table XV-3 presents data received from associated contractors and NASA-MSC.

TABLE XV-3

Agency/Contractor Supplied Data

Description	Supplier	Received (Baltimore)
Mod III radio guidance system	GE-Syracuse	4 CD
Spacecraft ascent mode	IBM-Bethesda	10 CD
Spacecraft bilevel events	NASA	*
GE Mod III MISTRAM plotcharts	GE Cape	10 CD

B. FILM COVERAGE

Photographic coverage (Table XV-4) of the GT-12 launch was excellent throughout the flight.

The C-135 aircraft with the airborne lightweight optical tracking system (ALOTS) was in position to obtain the best view of staging.

Tracking films (Items 1.2-40, RTCB, 1.2-41, RTMB and ALOTS) were reviewed for information pertaining to the staging event. The coverage was excellent. A description of the staging event is contained in Chapter XI.

TABLE XV-4

Film Coverage and Disposition

OD Item No.	Description	Footage (ft)	Time Received (Baltimore)
1.2-9 16mm fixed	Missile centered, movement at launch, 50-ft tower 19-1	180	3 WD
1.2-12 16mm fixed	Spacecraft centered, launch sequence, 50-ft tower 19-2	46	4 WD
1.2-14 16mm fixed	Explosive bolts and first motion, Stage II umbilical	100	3 WD
1.2-15 16mm fixed	Explosive bolts and first motion, 50-ft tower 19-7A	100	3 WD
1.2-16 16mm fixed	Engine area centered, east launch ring	200	3 WD
1.2-17 16mm fixed	Engine area centered, west launch ring	165	3 WD
1.2-18 16mm fixed	Engine bells centered, north launch ring	115	3 WD
1.2-19 16mm fixed	Engine bells centered, south launch ring	160	6 WD
1.2-20 16mm fixed	3D1E and 3D2E umbilical plugs, umbilical tower, first level	100	3 WD
1.2-21 16mm fixed	2DFVT umbilical plug, umbilical tower, second level	80	3 WD
1.2-22 16mm fixed	1DOVT umbilical plug, umbilical tower, fourth level	80	3 WD
1.2-23 16mm fixed	3B1E and associated umbilical plugs, umbilical tower, fifth level	125	3 WD
1.2-24 16mm fixed	2B1E and associated umbilical plugs, umbilical tower, sixth level	130	3 WD
1.2-25 16mm fixed	Umbilical boom 3, "J" bars and lanyards, umbilical tower, sixth level	210	3 WD
1.2-26 16mm fixed	Spacecraft upper umbilical plug, top umbilical tower, level No. 1	130	3 WD
1.2-27 16mm fixed	Spacecraft lower umbilical plug, top umbilical tower, level No. 2	208	3 WD
1.2-34 16mm tracking	Missile centered, LO to LOV, U102R6	336	4 WD
1.2-37 16mm tracking	Engine centered to missile centered, first acquisition to LOV, U29R46	356	9 WD
1.2-40 16mm tracking	Missile centered, first acquisition to LOV (ROTI) RTCB	130	4 WD
1.2-41 16mm tracking	Missile centered, first acquisition to staging (ROTI) RTMB	128	4 WD
1.2-41 70mm tracking	Missile centered, first acquisition to staging (ROTI) RTMB	990	4 WD
ALOTS 16mm tracking	Missile centered to staging (C-135) airborne	125	6 WD
ALOTS 70mm tracking	Missile centered to staging (C-135) airborne		12 WD

*Film not printed due to aircraft availability
WD = Working days

XVI. PRELAUNCH AND COUNTDOWN OPERATIONS

A. PRELAUNCH

1. Simulated Flight Test

The GT-12 simulated flight test (SFT) was successfully performed on 2 November 1966 in accordance with the Martin test (Ref. 13). The countdown for the secondary run was started at T-45 minutes (1015 EST) and was completed successfully at T + 6 minutes. Following recycle, the countdown for the primary run was started at T-3 minutes (1157 EST) and was completed successfully at T + 6 minutes.

2. Precountdown Activities

Final power was applied to the launch vehicle at 0648 EST on 8 November 1966. The precountdown tests were scheduled to start at 1200 EST; however, due to a secondary system 26-volt 800-cycle power failure at 1130 EST, the precount and subsequent launch was delayed 24 hours. The spacecraft remote power up portion (T-770 to T-740) of the precount was performed successfully.

During the troubleshooting operation, the secondary autopilot and secondary Stage I rate gyro packages were removed for failure analysis at Martin-Baltimore. Replacement packages were installed and retested successfully. While applying final power to the launch vehicle at 0831 EST on 9 November 1966, a secondary Stage II rate gyro SMRD no-go was observed for approximately 45 seconds. The secondary autopilot was replaced, and the launch was delayed 24 hours.

On 10 November 1966, the autopilot retest was completed, and final power was applied to the launch vehicle at approximately 0700 EST. The precountdown tests were started at 1200 EST, with the range sequencer at T-740 minutes and counting. The tests were completed successfully, and the range sequencer was secured at T-530 minutes (1530 EST).

Propellant loading started on schedule at 0253 EST on 11 November 1966 and was completed successfully at 0613 EST. The range sequencer was restarted on schedule for the Atlas/Agena countdown at T-530 minutes at 0653 EST.

B. LAUNCH COUNTDOWN SUMMARY

The launch countdown was picked up on schedule at 1143 EST on 11 November 1966. The 240-minute countdown was performed in accordance with the Martin test (Ref. 14). The countdown progressed

smoothly, and flight crew ingress occurred on schedule at T-115 minutes. Atlas/Agena liftoff occurred on schedule at T-95 minutes. The countdown continued without incident, and the programmed hold was initiated automatically as planned at T-3 minutes to adjust for the proper liftoff time of the launch vehicle. The hold was in effect for 3 minutes and 29 seconds. The countdown was resumed at T-3 minutes, and liftoff occurred on schedule at 1546 EST for a successful launch.

The countdown schedule is shown in Fig. XVI-1.

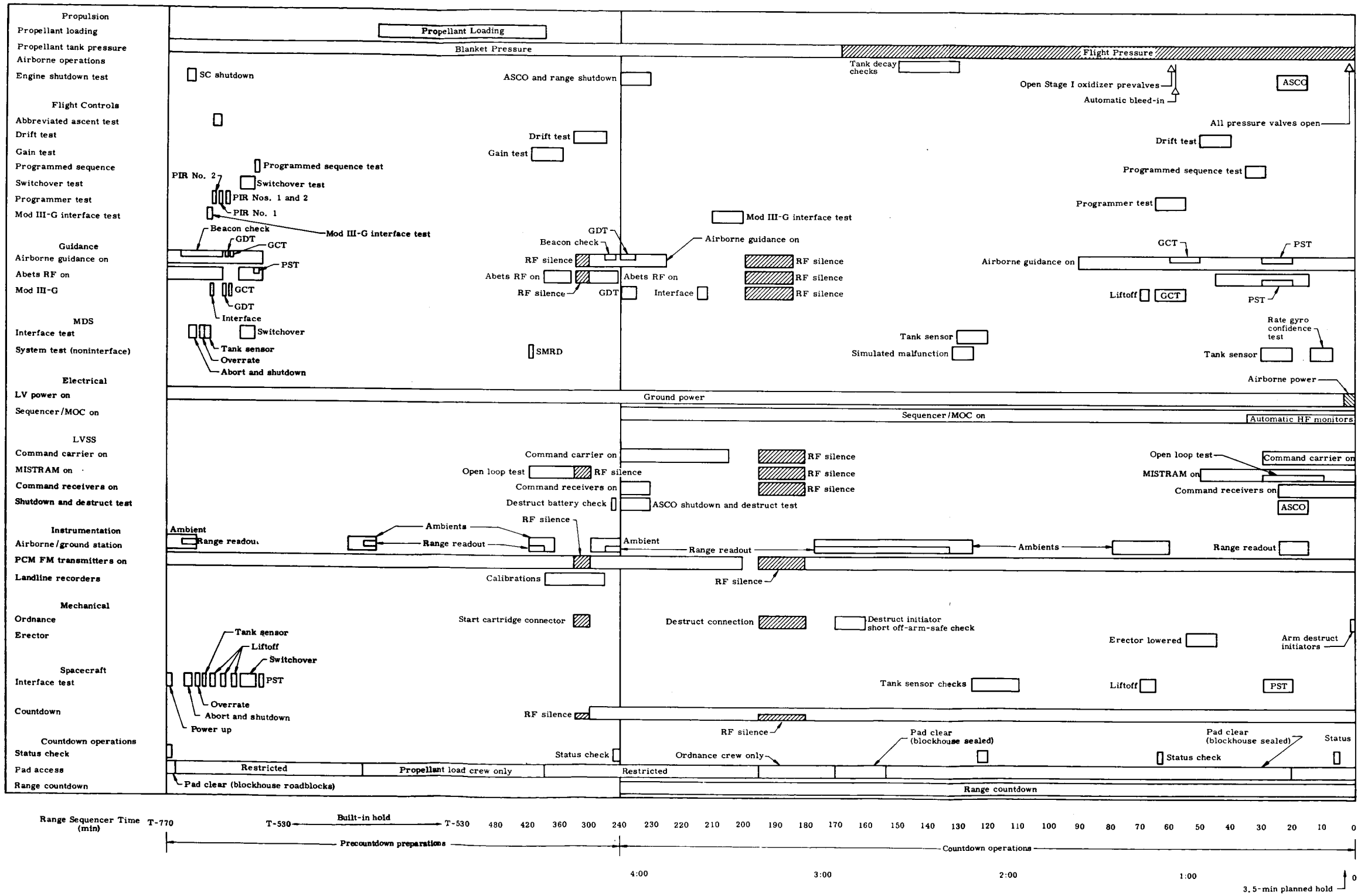

Fig. XVI-1 Countdown Schedule

UNCLASSIFIED

XVII. CONFIGURATION SUMMARY

A. LAUNCH VEHICLE SYSTEMS DESCRIPTION

The Gemini Launch Vehicle (GLV) is a modified two-stage Titan II intercontinental ballistics missile (ICBM) which has been "man rated" for Gemini usage. The propulsion system in each stage uses hypergolic (self-igniting upon mixture) propellants. Modifications to the basic Titan II vehicle to achieve the "man rated" GLV follow:

(1) Addition of a completely redundant malfunction detection system (MDS).

(2) Replacement of the Titan II inertial guidance system (IGS) with the Mod III-G radio guidance system (RGS).

(3) Addition of a three-axis reference system (TARS) to provide attitude reference and open-loop programming to the autopilot.

(4) Addition of a secondary flight control system (FCS).

(5) Addition of a secondary Stage I hydraulic system.

(6) Addition of the capability of switchover to the secondary guidance, flight control, and hydraulic systems.

(7) Provision of redundancy in electrical sequencing by APS and IPS power.

(8) Provision of an engine shutdown capability from the spacecraft.

(9) Provision of a 120-inch diameter cylindrical skirt forward of the Stage II oxidizer tank for mating the spacecraft to the launch vehicle.

(10) Removal of the retrorockets, vernier rockets and associated equipment.

(11) Addition of fuel line spring-piston accumulators and oxidizer line tuned standpipes for suppression of POGO vibrations.

(12) Capability for redundant Stage II engine shutdown (GLV-3 and up).

UNCLASSIFIED

The only significant GLV-12 change from the GLV-11 configuration was the addition of a delay timer (0.5 to 10.0 second) to the flight controls system to change the time of gain change No. 1 from 104.96 to 110.0 seconds.

A detailed description of all GLV systems is presented in Martin Engineering Report, "Launch Vehicle No. 4 Flight Evaluation" (Ref. 8).

B. MAJOR COMPONENTS

The two major GT-12 components were as follows:

(1) Spacecraft

(a) Manufacturer: McDonnell Aircraft Corporation

(b) Serial Number: Spacecraft Number 12

(2) Gemini Launch Vehicle

(a) Manufacturer: Martin Company

(b) Serial Number: GLV-12

(c) Air Force Serial Number: 62-12567

Figure XVII-1 shows the general arrangement of the GLV.

LAUNCH VEHICLE UMBILICAL SYSTEMS INTERFACE

CODE	FUNCTION	SYSTEM	LOCATION
28A	AIR COND	GUIDANCE AIR COND STG II	STA 371.522 QUAD I 85° OFF BL 0
S28OV	OXID. VENT	OXID. STG II	STA 371.522 QUAD II 85° OFF BL 0
28ZE	ELECTRICAL	ELECTRICAL STG II	STA 402.472 QUAD II 65° OFF BL 0
28IE	ELECTRICAL	ELECTRICAL STG II	STA 402.472 QUAD I 65° OFF BL 0
28FVT	FUEL VENT TOPPING	FUEL STAGE II	STA 406.481 QUAD I 30° OFF BL 0
S28FV	FUEL VENT	FUEL STG II	STA 424.473 QUAD I 37½ OFF BL 0
S38H	HYDRAULIC	HYDRAULIC STG II	STA 470.125 QUAD II 15° OFF BL 0
▲ 38A	AIR CONDITIONING	ENGINE AREA STG II	STA 474.879 QUAD II 30° OFF BL 0
S38F	FUEL FILL AND DRAIN	FUEL STG II	STA 492.250 QUAD II 15° OFF BL 0
38FD	FUEL PRESS. SEQ. VALVE DRAIN	FUEL STG II	STA 492.250 QUAD II 30° OFF BL 0
S38O	OXID. FILL AND DRAIN	OXID STG II	STA 492.250 QUAD II 72° OFF BL 0
38IE	ELECTRICAL	ELECTRICAL STG II	STA 492.250 QUAD II 45° OFF BL 0
1CIFD	TUBO-PUMP FUEL DRAIN	FUEL STG I	STA 550.750 QUAD II 17½ OFF BL 0
1COD	TUBO-PUMP OXID. DRAIN	OXID STG I	STA 550.750 QUAD I 17½ OFF BL 0
S1DOV	OXID. VENT	OXID. STG I	STA 553.327 QUAD I WL 60.0
S2DFV	FUEL VENT	FUEL STG I	STA 963.326 QUAD II 40° OFF BL 0
3DIM	MALFUNCTION DETECTION SYS.	MALFUNCTION STG. I	STA 1214.873 QUAD III 34.4° OFF BL 0
302M	MALFUNCTION DETECTION SYS.	MALFUNCTION STG I	STA 1214.873 QUAD III 38.4° OFF BL 0
3DIE	ELECTRICAL	ELECTRICAL STG. I	STA 1216.691 QUAD II 20° OFF BL 0
S3DF	FUEL FILL AND DRAIN	FUEL STG I	STA 1243.560 QUAD I
S3DFD	FUEL DRAIN - PRE-VALVE	FUEL STG I	STA 1244.123 QUAD III
S3DOD	OXID. DRAIN - PRE-VALVE	OXID. STG I	STA 1250.560 QUAD I
S3DIH	HYDRAULIC SUPPLY AND RETURN	HYDRAULIC STG I PRIMARY	STA 1255.835 QUAD I
S3DO	OXID. FILL AND DRAIN	OXID. STG I	STA 1249.560 QUAD III
2BOVT	OXID. VENT TOPPING	OXID. STG II	STA 351.802 QUAD II 4° OFF WL 60
1DOVT	OXID. VENT TOPPING	OXID. STG. I	STA 630.727 QUAD II 60° OFF BL 0
2DFVT	FUEL VENT TOPPING	FUEL STAGE I	STA 963.326 QUAD II 50° OFF BL 0
302E	ELECTRICAL	ELECTRICAL STG. I	STA 1216.691 QUAD II 10° OFF BL 0
S3DIH	HYDRAULIC SUPPLY AND RETURN	HYDRAULIC STG. I SECONDARY	STA 1256.835 QUAD II
▲ 3D10C	OXID. REMOTE CHARGING SYSTEM	OXID. STG. I	STA. 1224.311 QUAD III 22½° OFF BL 0.
▲ 3D20C	OXID. REMOTE CHARGING SYSTEM	OXID. STG. I	STA. 1224.311 QUAD III 17½° OFF BL 0.

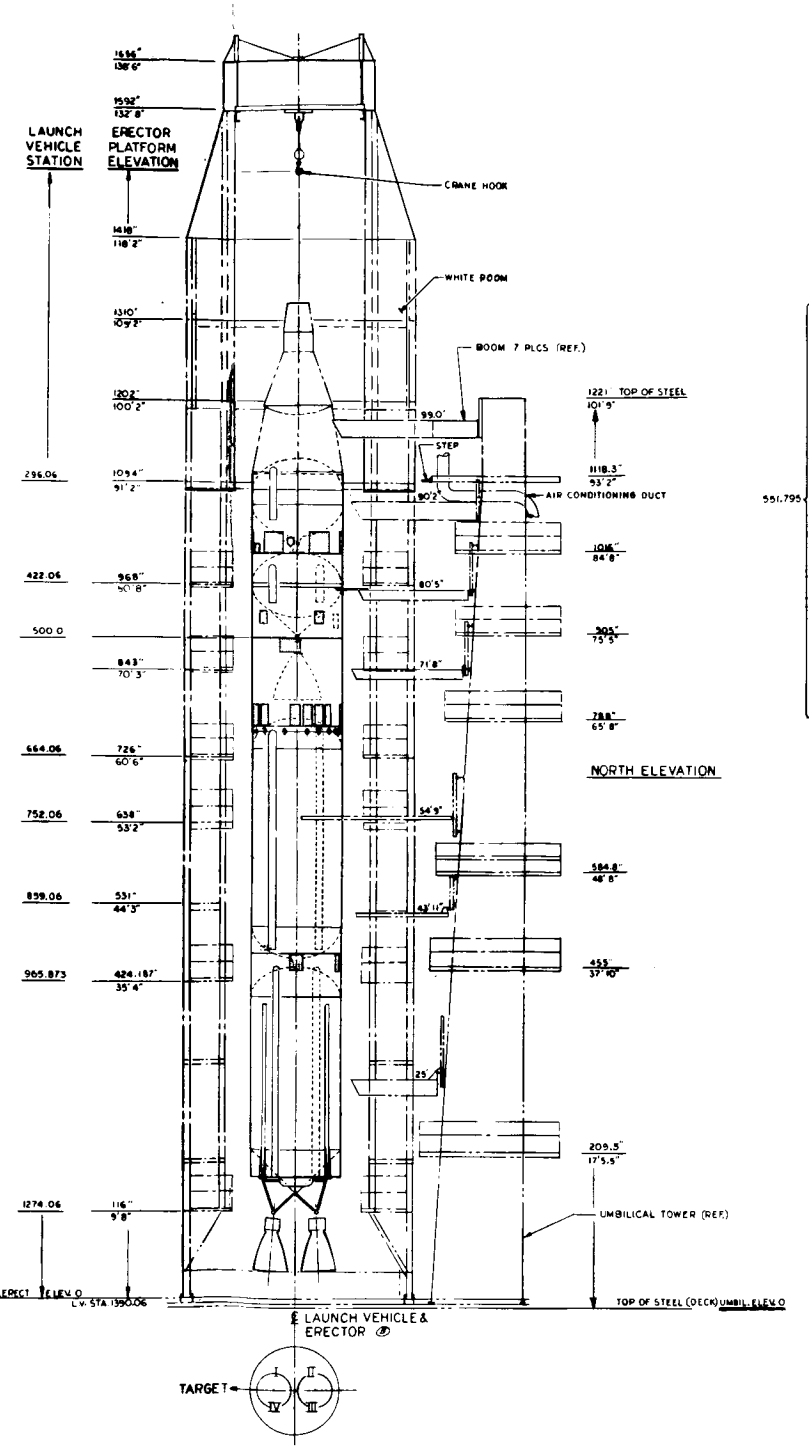

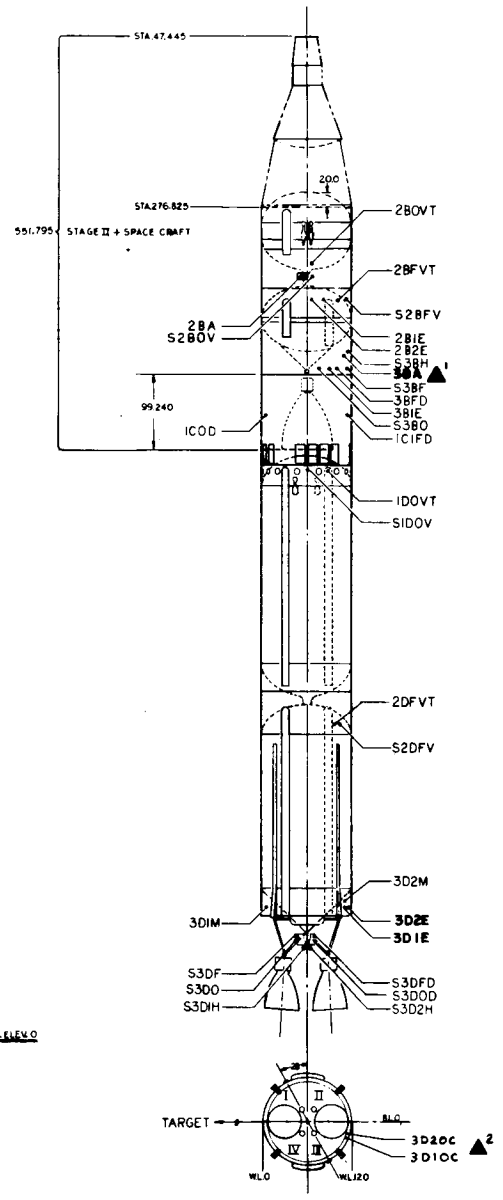

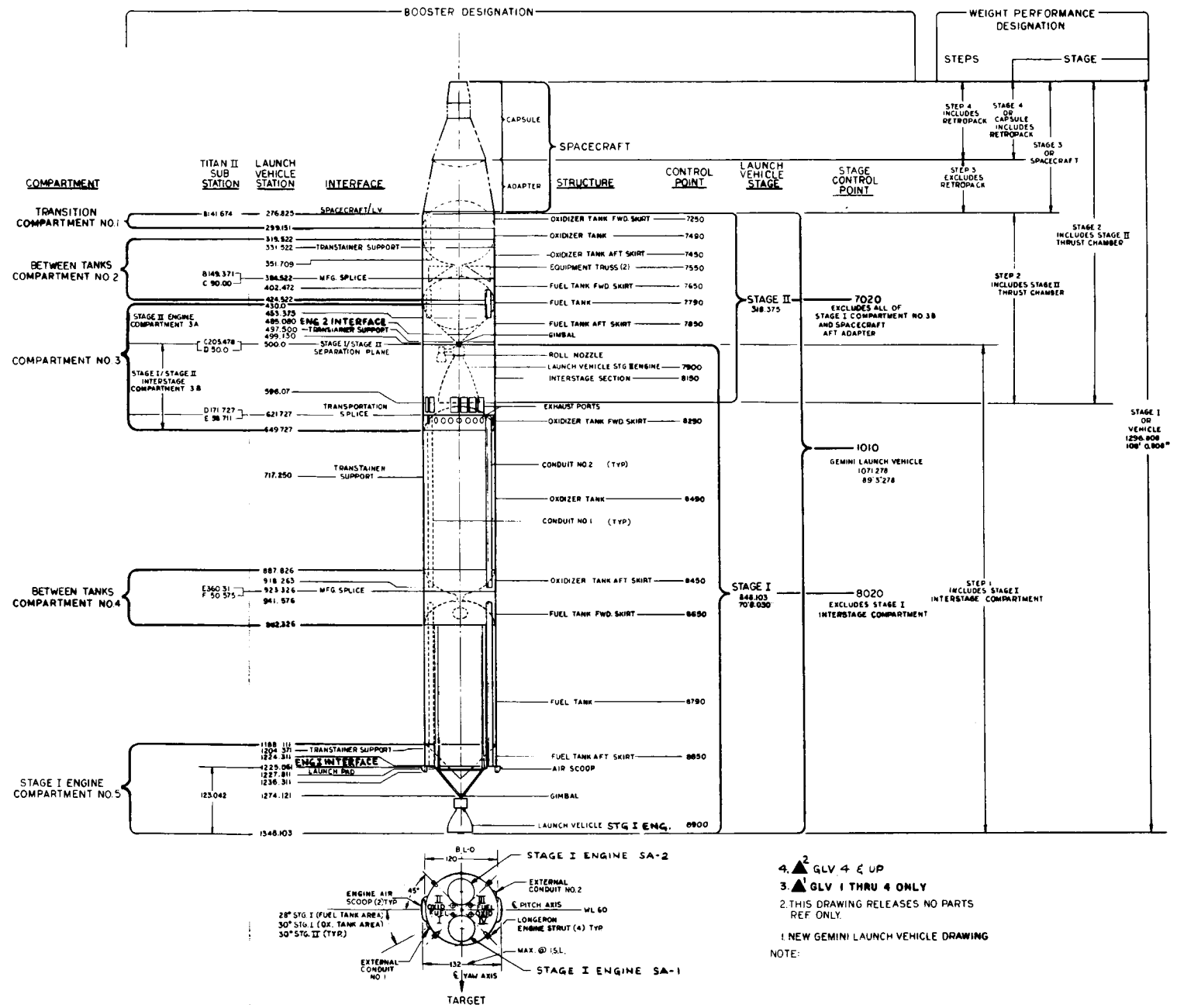

4. ▲2 GLV 4 & UP
3. ▲ GLV 1 THRU 4 ONLY
2. THIS DRAWING RELEASES NO PARTS REF. ONLY.
1. NEW GEMINI LAUNCH VEHICLE DRAWING

NOTE:

Fig. XVII-1. Gemini Launch Vehicle General Arrangement

XVIII. REFERENCES

1. "Launch Vehicle No. 11 Flight Evaluation." Engineering Report 13227-11, Martin Company, Baltimore, Maryland, October 1966. Confidential.

2. "Launch Vehicle No. 10 Flight Evaluation." Engineering Report 13227-10, Martin Company, Baltimore, Maryland, August 1966. Confidential.

3. "Launch Vehicle No. 9 Flight Evaluation." Engineering Report 13227-9, Martin Company, Baltimore, Maryland, July 1966. Confidential.

4. "Launch Vehicle No. 8 Flight Evaluation." Engineering Report 13227-8, Martin Company, Baltimore, Maryland, April 1966. Confidential.

5. "Launch Vehicle No. 6 Flight Evaluation." Engineering Report 13227-6, Martin Company, Baltimore, Maryland, February 1966. Confidential.

6. "Launch Vehicle No. 7 Flight Evaluation." Engineering Report 13227-7, Martin Company, Baltimore, Maryland, January 1966. Confidential.

7. "Launch Vehicle No. 5 Flight Evaluation." Engineering Report 13227-5, Martin Company, Baltimore, Maryland, October 1965. Confidential.

8. "Launch Vehicle No. 4 Flight Evaluation." Engineering Report 13227-4, Martin Company, Baltimore, Maryland, July 1965. Confidential.

9. "Launch Vehicle No. 3 Flight Evaluation." Engineering Report 13227-3, Martin Company, Baltimore, Maryland, May 1965. Confidential.

10. "Launch Vehicle No. 2 Flight Evaluation." Engineering Report 13227-2, Martin Company, Baltimore, Maryland, March 1965. Confidential.

11. "Launch Vehicle No. 2 Launch Attempt Evaluation." Engineering Report 13227-2X, Martin Company, Baltimore, Maryland, January 1965. Confidential.

12. "Launch Vehicle No. 1 Flight Evaluation." Engineering Report 13227-1, Martin Company, Baltimore, Maryland, May 1964. Confidential.

13. "Martin-Canaveral Test Procedure." 424-876-ETR, Revision G.

14. "Martin-Canaveral Test Procedure." 424-875-ETR, Revision S.

15. "GT-12 Preflight Test Report." LV-326-12, Martin Company, Baltimore, Maryland, September 1966. Confidential.

16. "Gemini Launch Vehicle Performance Specification." MB-1046, SCN-PU, Martin Company, Baltimore, Maryland, 10 October 1966. Confidential.

17. Letter from SSD to Martin Company, dated 19 October 1965, subject: "Transmittal of RGS Dispersions for GT-6."

18. "Flight Weight Coordination Report, Postflight Weight, GT-12." LV-165-12B, Martin Company, Baltimore, Maryland, 5 December 1966.

19. "Subsystem Engineering Analysis YLR 87-AJ-5 and YLR 91-AJ-5 Rocket Engines." AGC 521-3.15 Q-15, Aerojet-General Corporation, Sacramento, California, 22 July 1964. Confidential.

20. "Master Measurements List." LV-220, Revision P, Martin Company, Baltimore, Maryland, 30 August 1966.

APPENDIX A

SUMMARY OF GEMINI LAUNCHES

Summary of Gemini Launches

Mission	Launch Date and Time (hr EST)	Launch Vehicle Payload (lb)	Burning Time Stage I (sec)	Burning Time Stage II (sec)	Inertial Velocity (fps) BECO	Inertial Velocity (fps) SECO	Inertial Velocity (fps) SECO + 20 Sec	Altitude (ft) BECO	Altitude (ft) SECO	Altitude (ft) SECO + 20 Sec	Inertial Flight Path Angle (deg) BECO	Inertial Flight Path Angle (deg) SECO	Inertial Flight Path Angle (deg) SECO + 20 Sec	Time in Orbit ③ (hr) Stage II	Time in Orbit ③ (hr) Spacecraft	Orbit (naut mi) Apogee	Orbit (naut mi) Perigee	Launch Evaluation Report Number
GT-1	4-8-64 1100	7029 ①	157.5	185.3	9,752	25,679	25,786	208,262	531,500	528,184	20.00	0.0	-0.03	95.2 ① (64 orbits)	95.2 ① (64 orbits)	173	86.6	ER 13227-1
GT-2	1-19-65 0904	6890 ②	155.1	180.4	9,916	25,611	25,738	229,743	546,960	526,380	26.219	-2.4523	-2.3431	N/A ②	N/A ②	N/A ②	N/A ②	ER 13227-2X ④ ER 13227-2
GT-3	3-23-65 0924	7112	155.8	181.3	9,981	25,587	25,688	224,777	531,477	532,338	21.79	0.0	0.0323	18 (13 orbits)	4.6 (3 orbits)	121	87	ER 13227-3
GT-4	6-3-65 1016	7868	155.7	181.3	9,844	25,670	25,745	214,775	531,522	532,886	18.66	-0.0235	0.059	47.7 (34 orbits)	97.7 (66 orbits)	152.3	87	ER 13227-4
GT-5	8-21-65 0900	7947	156.8	179.7	9,848	25,713	25,806	215,607	531,276	531,118	19.90	-0.0279	-0.0129	72 (51 orbits)	190.9 (127.9 orbits)	189	87	ER 13227-5
GT-7	12-4-65 1430	8085	159.1	181.4	10,049	25,735	25,789	207,088	529,583	529,738	18.66	0.0500	0.0285	66 (46.6 orbits)	330.6 (219.8 orbits)	177.1	87	ER 13227-7
GT-6A	12-15-65 0837	7821	160.4	181.6	9,992	25,634	25,728	202,186	529,891	530,201	17.94	0.08	-0.054	31 (21 orbits)	25.8 (17.1 orbits)	140.4	87	ER 13227-6
GT-8	3-16-66 1141	8351	157.9	182.9	9,917	25,663	25,736	209,005	527,191	526,600	19.34	-0.141	-0.02	29 (21.1 orbits)	10.7 (7 orbits)	148.2	86.9	ER 13227-8
GT-9A	6-3-66 0839	8268	155.6	187.3	9,757	25,630	25,723	210,030	528,828	527,812	19.97	-0.134	-0.269	19.5 (13.4 orbits)	72.3 (48 orbits)	144	87.5	ER 13227-9
GT-10	7-18-66 1720	8294	155.6	188.2	9,745	25,620	25,700	206,554	527,690	527,694	19.16	0.02	0.007	25.6 (16.4 orbits)	70.8 (47 orbits)	145	86.7	ER 13227-10
GT-11	9-12-66 0942	8374	156.5	187.0	9,750	25,615	25,706	207,972	527,352	526,634	19.55	0.025	-0.014	23.9 (16.2 orbits)	71.3 (47 orbits)	143.3	86.9	ER 13227-11
GT-12	11-11-66 1546	8294	157.9	188.8	9,885	25,635	25,710	204,471	526,766	523,703	18.67	0.031	0.025	24.4 (15.1 orbits)	94.6 (63 orbits)	151.5	87.3	ER13227-12

① Spacecraft and Stage II inserted into orbit as a unit.

② Suborbital mission (spacecraft impact 2125 miles downrange).

③ Inertial orbit.

④ Launch attempt report.